

# **Rhodium-mediated Activation and Borylation Reactions of Fluorinated Olefins**

DISSERTATION

zur Erlangung des akademischen Grades

doctor rerum naturalium

(Dr. rer. nat.)

im Fach: Chemie

Spezialisierung: Anorganische und Allgemeine Chemie

eingereicht an der

Mathematisch-Naturwissenschaftlichen Fakultät

der Humboldt-Universität zu Berlin

von

M. Sc. Conghui Xu

Präsidentin der Humboldt-Universität zu Berlin

Prof. Dr.-Ing. Dr. Sabine Kunst

Dekan der Mathematisch-Naturwissenschaftlichen Fakultät

Prof. Dr. Elmar Kulke

Gutachter/innen:

1. Prof. Dr. Thomas Braun
2. Prof. Dr. Christian Müller
3. Prof. Dr. Christian Limberg

Tag der mündlichen Prüfung:

09.11.2020



## Acknowledgement

Deepest gratitude goes first and foremost to my supervisor, Prof. Dr. Thomas Braun, for accepting me as his student and guiding me with his patience for my whole research time in his group. I am extremely lucky to be inspired by his enthusiasm for the project, his prompt response to my questions and his useful suggestions. I appreciate a lot of the opportunity of studying abroad with him and will benefit a lot from this experience.

I would like to extend my sincere gratitude to Prof. Dr. Christian Müller and Prof. Dr. Christian Limberg for agreeing to be my dissertation referee and a member of my defense committee. At the same time, thank you Prof. Dr. Rüdiger Tiemann for being the chairman and Dr. Franziska Emmerling for being a member of my defense committee.

Special thanks should go to HU NMR service department. Thank you Dr. André Dahlmann for measuring the special NMR spectra for me and discussing NMR data with me. I am grateful with the measurement that Frau Pfaff, Frau Thiesies and Jana Hildebrandt provided. Additionally, thank you Dr. Beatrice Cula for analyzing crystallographic data for me.

Many thanks go to my labmate Dr. María Talavera Nevado for her patience in supporting me with her knowledge not only in the lab but also in my daily life.

I am grateful to spend the impressive four years with all the Braun group members. I appreciate Mike a lot for supporting me with the application at the beginning and always being available to help me with the glovebox maintenance. Thank you Hanna and Roy for picking me up from the airport, Cort, María, Nils, Dilcan, Martin and Ruben for measuring the NMR samples, María and Mike for measuring the LIFDI-MS and DFT calculation, María again for correcting my thesis, Philipp for translating the abstract into German, Philipp, Stefan and Simon for being helpful with my “crystals”, Pooja and Yasmin for measuring IR, Clara, Macha, Oscar, Cort and María for experiencing the memorable lunch time and all the other Chinese people Xu Yue, Deng Yuchen, Pan Xinzi and Heyier Linze for chatting in Chinese and having the interesting time after work.

High tribute shall be paid to China Scholarship Council, who support me financially.

最后最后我想感谢我的家人和朋友，他们给了我精神上的鼓励和支持。再者感谢我的祁龙颖先生，这个以男朋友身份出现在我硕士论文致谢的男人在读博期间变成老公，感谢他一路以来的理解和包容，未来的路我们携手向前。感恩。



## Publications

[1] C–H and C–F Bond Activation Reactions of Pentafluorostyrene at Rhodium Complexes

**C. Xu**, M. Talavera, S. Sander, T. Braun, *Dalton Trans.* **2019**, 48, 16258-16267.

[2] Reactivity of 3,3,3-Trifluoropropyne at Rhodium Complexes: Development of Hydroboration Reactions

C. N. von Hahmann, M. Talavera, **C. Xu**, T. Braun, *Chem. Eur. J.* **2018**, 24, 11131-11138.

## Conference presentation

[1] Versatile Reactivities of Rhodium(I) Complexes Towards Pentafluorostyrene

**C. Xu** and T. Braun, 19<sup>th</sup> European Symposium on Fluorine Chemistry, (25-31, August, 2019), Warsaw, Poland. Poster presentation



## Abstract

The dissertation reports on studies on the reactivity of rhodium complexes towards different fluorinated olefins with a focus on C–F activation steps and borylation reactions.

The rhodium(I) hydrido complex  $[\text{Rh}(\text{H})(\text{PEt}_3)_3]$  (**1**) was employed as catalyst in the reactions of HFO-1234yf (2,3,3,3-tetrafluoropropene), HFO-1234ze (*E*-1,3,3,3-tetrafluoropropene), HFO-1225zc (1,1,3,3,3-pentafluoropropene) and HFO-1225ye (*Z*-(*Z*-1,2,3,3,3-pentafluoropropene) with HBpin. A product mixture consisting of borylation products was obtained. Additionally, FBpin was generated, the formation of which can be the driving force of the transformations. When changing the catalyst to  $[\text{Rh}(\mu\text{-Cl})(\text{P}i\text{Pr}_3)_2]_2$  (**14**), the selectivity was enhanced towards the hydroboration of HFO-1234yf and the defluorohydroboration of HFO-1234ze and HFO-1225ye (*Z*). Selective mono and dihydroboration reactions of 3,3,3-trifluoropropyne were achieved by employing complex **1**, complex  $[\text{Rh}(\text{C}\equiv\text{CCF}_3)(\text{PEt}_3)_3]$  (**17**) (together with *fac*- $[\text{Rh}(\text{C}\equiv\text{CCF}_3)_2(\text{H})(\text{PEt}_3)_3]$  (**18**) in a 9:1 ratio), or a mixture of the rhodium(III) complexes **18** and *fac*- $[\text{Rh}\{(E)\text{-CH=CHCF}_3\}(\text{C}\equiv\text{CCF}_3)_2(\text{PEt}_3)_3]$  (**19**) (ratio 5:1) as catalysts. Stoichiometric hydroboration reaction was accomplished on treatment of complex **17** with HBpin to give the Rh(III) complex *fac*- $[\text{Rh}(\text{Bpin})(\text{H})_2(\text{PEt}_3)_3]$  as well as hydroboration compounds  $\text{CF}_3\text{CH}(\text{Bpin})\text{CH}(\text{Bpin})_2$ ,  $\text{CF}_3\text{CH}_2\text{C}(\text{Bpin})_3$  and  $\text{CF}_3\text{CH}_2\text{CH}(\text{Bpin})_2$ .

Similarly, trifluoroethylene was also converted into a mixture of products of the hydroboration product  $\text{CF}_2\text{HCFH}(\text{Bpin})$ , the hydrogenation product  $\text{CF}_2\text{HCFH}_2$ , and traces of defluorohydroboration compounds  $\text{CF}_2\text{HCH}_2(\text{Bpin})$ ,  $\text{CH}_3\text{CH}_2(\text{Bpin})$  and  $\text{CH}_3\text{CH}(\text{Bpin})_2$  by the reaction with HBpin with complex **1** as the catalyst. A stoichiometric reaction of complex **1** resulted in the C–F bond activation as well as a coordination of trifluoroethylene to give complex *trans*- $[\text{Rh}(\text{F})(\eta^2\text{-CF}_2\text{CFH})(\text{PEt}_3)_2]$ . Furthermore, the C–F bond activation was also realized with complex **1** and 1,1,2-trifluorobutene. Mechanistic investigations of the reaction of complex **1** towards 1,1,2-trifluorobutene at variable temperatures indicated the formation of products of coordination, insertion of the olefin and subsequent  $\beta$ -H elimination, C–F oxidative addition as well as HF reductive elimination steps. Reactivity studies of the insertion product  $[\text{Rh}(\text{CF}_2\text{CFHC}_2\text{H}_5)(\text{PEt}_3)_3]$  with CO led to the generation of *cis*- $[\text{Rh}(\text{CF}_2\text{CFHC}_2\text{H}_5)(\text{CO})(\text{PEt}_3)_2]$ .

Furthermore, when utilizing complex **1** or  $[\text{Rh}(\text{Bpin})(\text{P}(\text{Et}_3)_3)_3]$  (**3**) as catalysts, stoichiometric and catalytic hydroboration reactions of pentafluorostyrene occurred with HBpin. The rhodium(I) complexes **1** and **3** were capable of the coordination of the olefin and a C–F bond activation reaction with pentafluorostyrene, while complex  $[\text{Rh}(\text{Me})(\text{P}(\text{Et}_3)_3)_3]$  (**47**) promoted the C–H bond activation. At 333 K, the activation of the fluorinated aromatic ring occurred at the 4-position, while at room temperature, an activation at the 2-position was preferred. The rhodacycle *trans*- $[\text{Rh}(\text{F})(\text{CH}_2\text{CH}_2(2\text{-C}_6\text{F}_4))(\text{P}(\text{Et}_3)_3)_3]$  was identified as an intermediate for the activation at the 2-position. Treatment of CO with the mentioned rhodacycle complex resulted in the formation of the *trans*- $[\text{Rh}(\text{F})(\text{CH}_2\text{CH}_2\text{C}_6\text{F}_4)(\text{CO})(\text{P}(\text{Et}_3)_2)_2]$ .



## Kurzzusammenfassung

Die Dissertation beinhaltet Studien zur Reaktivität von Rhodiumkomplexen gegenüber unterschiedlichen ungesättigten fluorierten Olefinen mit einem Fokus auf C–F Aktivierungs- und Borylierungsreaktionen.

Der Rhodium(I)hydridokomplex  $[\text{Rh}(\text{H})(\text{PEt}_3)_3]$  (**1**) wurde als Katalysator in den Reaktionen von HFO-1234yf (2,3,3,3-Tetrafluorpropen), HFO-1234ze (*E*-1,3,3,3-Tetrafluorpropen), HFO-1225zc (1,1,3,3,3-Pentafluorpropen) bzw. HFO-1225ye (*Z*) (*Z*-1,2,3,3,3-Pentafluorpropen) mit HBpin verwendet. Dabei wurden Produktgemische bestehend aus Borylierungsprodukten erhalten. Weiterhin wurde auch FBpin gebildet, was eine Triebkraft der Reaktionen sein kann. Wenn stattdessen als Katalysator die Verbindung  $[\text{Rh}(\mu\text{-Cl})(\text{P}i\text{Pr}_3)_2]_2$  (**14**) eingesetzt wurde, wurde die Selektivität für HFO-1234yf bezüglich einer Hydroborierung und für HFO-1234ze & HFO-1225ye (*Z*) bezüglich einer Defluorohydroborierung erhöht. Die selektive Mono- und Dihydroborierung von 3,3,3-Trifluorpropin konnte durch Verwendung von Komplex **1**, Verbindung  $[\text{Rh}(\text{C}\equiv\text{CCF}_3)(\text{PEt}_3)_3]$  (**17**) (liegt zusammen mit *fac*- $[\text{Rh}(\text{C}\equiv\text{CCF}_3)_2(\text{H})(\text{PEt}_3)_3]$  (**18**) im Verhältnis 9:1 vor) oder einer Mischung der Komplexe **18** und *fac*- $[\text{Rh}\{(E)\text{-CH=CHCF}_3\}(\text{C}\equiv\text{CCF}_3)_2(\text{PEt}_3)_3]$  (**19**) (Verhältnis 5:1) als Katalysatoren erreicht werden. Eine stöchiometrische Hydroborierung mit HBpin ist möglich bei Verwendung des Komplexes **17** unter Bildung des Rhodium(III)komplexes *fac*- $[\text{Rh}(\text{Bpin})(\text{H})_2(\text{PEt}_3)_3]$ , sowie den Hydroborierungsprodukten  $\text{CF}_3\text{CH}(\text{Bpin})\text{CH}(\text{Bpin})_2$ ,  $\text{CF}_3\text{CH}_2\text{C}(\text{Bpin})_3$  und  $\text{CF}_3\text{CH}_2\text{CH}(\text{Bpin})_2$ .

Trifluorethylen konnte durch die Reaktion mit HBpin und Komplex **1** als Katalysator in ein Produktgemisch aus dem Hydroborierungsprodukt  $\text{CF}_2\text{HCFH}(\text{Bpin})$ , dem Hydrierungsprodukt  $\text{CF}_2\text{HCFH}$  und Spuren der Defluorohydroborierungsprodukte  $\text{CF}_2\text{HCH}_2(\text{Bpin})$ ,  $\text{CH}_3\text{CH}_2(\text{Bpin})$  und  $\text{CH}_3\text{CH}(\text{Bpin})_2$  überführt werden. Stöchiometrische Reaktion zeigen, dass Komplex **1** sowohl unter C–F-Bindungsaktivierung reagiert als auch die Koordination von Trifluorethylen, unter Bildung des Komplexes *trans*- $[\text{Rh}(\text{F})(\eta^2\text{-CF}_2\text{CFH})(\text{PEt}_3)_2]$ , stattfindet.

Im Falle von 1,1,2-Trifluorbuten wurde ebenfalls eine C–F-Bindungsaktivierung durch Komplex **1** beobachtet. Mechanistische Untersuchungen der Reaktion von Komplex **1** und 1,1,2-Trifluorbuten bei unterschiedlichen Temperaturen zeigten Hinweise für Koordination & Insertion des Alkens, sowie anschließende  $\beta$ -H-Eliminierung und

oxidative C–F-Bindungsadditions- und reduktive HF-Eliminierungsschritte. Eine Reaktion von  $[\text{Rh}(\text{CF}_2\text{CFHC}_2\text{H}_5)(\text{PEt}_3)_3]$  mit CO führt zur Bildung von *cis*- $[\text{Rh}(\text{CF}_2\text{CFHC}_2\text{H}_5)(\text{CO})(\text{PEt}_3)_2]$ .

Außerdem konnte durch Verwendung von Komplex **1** oder  $[\text{Rh}(\text{Bpin})(\text{PEt}_3)_3]$  (**3**) als Katalysator eine stöchiometrische und katalytische Hydroborierung von Pentafluorstyren mit HBpin erreicht werden. Die Rhodium(I)komplexe **1** und **3** sind in der Lage das Olefin zu koordinieren und die C–F-Bindung zu aktivieren, während die Verwendung der Verbindung  $[\text{Rh}(\text{Me})(\text{PEt}_3)_3]$  (**47**) die C–H-Bindungsaktivierung fördert. Bei 333 K findet die Aktivierung des fluorierten Aromaten in der 4-Stellung statt, während bei Raumtemperatur die Aktivierung in der 2-Stellung bevorzugt ist. Der Rhodazyklus *trans*- $[\text{Rh}(\text{F})(\text{CH}_2\text{CH}_2(2\text{-C}_6\text{F}_4))(\text{PEt}_3)_3]$  wurde als Zwischenprodukt der Aktivierung in der 2-Stellung identifiziert. Eine Reaktion von CO mit dem genannten Rhodazyklus führte zur Bildung von *trans*- $[\text{Rh}(\text{F})(\text{CH}_2\text{CH}_2\text{C}_6\text{F}_4)(\text{CO})(\text{PEt}_3)_2]$ .

# Table of Contents

<b>1. Introduction.....</b>	<b>1</b>
<b>1.1 Fluorine chemistry and fluorinated compounds .....</b>	<b>1</b>
<b>1.2 Activation of fluorinated compounds at rhodium complexes .....</b>	<b>2</b>
1.2.1 C–F bond activation of aromatic fluorides .....	3
1.2.2 Activation in alkynyl fluorides .....	4
1.2.3 C–F bond activation in alkenyl fluorides .....	5
<b>1.3 Rhodium boryl complexes and borylated compounds.....</b>	<b>7</b>
1.3.1 Reactivity of rhodium boryl complexes .....	7
1.3.2 Catalytic borylation .....	9
1.3.2.1 Hydroboration reactions .....	10
1.3.2.2 Diboration reactions.....	11
1.3.2.3 Dehydroborylation reactions.....	12
<b>1.4 Research objective.....</b>	<b>13</b>
<b>2. Activation and borylation of CF<sub>3</sub>-containing unsaturated compounds towards rhodium(I) complexes.....</b>	<b>15</b>
<b>2.1 Introduction .....</b>	<b>15</b>
<b>2.2 Results and discussion.....</b>	<b>19</b>
2.2.1 Catalytic studies of CF <sub>3</sub> containing olefins with rhodium(I) complexes .....	19
2.2.1.1 HFO-1234yf.....	19
2.2.1.2 HFO-1234ze.....	23
2.2.1.3 Pentafluoroolefins .....	24
2.2.2 Catalytic hydroboration reactions of CF <sub>3</sub> containing olefins with the rhodium complex [Rh( $\mu$ -Cl)(P <i>i</i> Pr <sub>3</sub> ) <sub>2</sub> ] <sub>2</sub> (14) .....	25
2.2.3 Studies on the reactivity of 3,3,3-trifluoropropyne with rhodium complexes .....	27
2.2.3.1 Catalytic hydroboration reactions of 3,3,3-trifluoropropyne.....	27
2.2.3.2 Mechanisms of the catalytic conversions .....	28
2.2.3.3 Catalytic dihydroboration reactions of 3,3,3-trifluoropropyne.....	29
2.2.3.4 Stoichiometric hydroboration reaction of rhodium(I) alkyl complex and HBpin.....	31
<b>3. C–F bond activation of fluorinated olefins towards rhodium(I) complexes.....</b>	<b>35</b>
<b>3.1 Introduction .....</b>	<b>35</b>
<b>3.2 Results and discussion.....</b>	<b>38</b>
3.2.1 Catalytic reactions .....	38
3.2.2 Stoichiometric reactions .....	39

<b>4. Activation and borylation of pentafluorostyrene towards rhodium(I) complexes</b>	<b>51</b>
<b>4.1 Introduction</b>	<b>51</b>
<b>4.2 Results and discussion</b>	<b>53</b>
4.2.1 Catalytic reactions	53
4.2.2 Stoichiometric reactions	54
4.2.2.1 Stoichiometric hydroboration reactions	54
4.2.2.2 Stoichiometric reactions of complex [Rh(H)(PEt <sub>3</sub> ) <sub>3</sub> ] (1) and pentafluorostyrene	56
4.2.2.3 Stoichiometric reactions of complex [Rh(Bpin)(PEt <sub>3</sub> ) <sub>3</sub> ] (3) and pentafluorostyrene	63
4.2.2.4 Stoichiometric reactions of complex [Rh(Me)(PEt <sub>3</sub> ) <sub>3</sub> ] (47) and pentafluorostyrene	68
<b>5. Summary</b>	<b>71</b>
<b>6. Experimental</b>	<b>81</b>
<b>6.1 General</b>	<b>81</b>
6.1.1 Techniques	81
6.1.2 Materials	81
6.1.3 Methods	81
<b>6.2 Instrumentation</b>	<b>81</b>
6.2.1 Nuclear Magnetic Resonance (NMR) Spectroscopy	81
6.2.2 Mass Spectrometry	81
6.2.3 Infrared (IR) Spectroscopy	82
6.2.4 DFT calculations	82
6.2.5 X-ray diffraction analysis	82
<b>6.3 Procedures</b>	<b>83</b>
<b>7. Reference</b>	<b>111</b>
<b>8. Appendix</b>	<b>119</b>
<b>8.1 Abbreviations</b>	<b>119</b>
<b>8.2 Data for <i>mer</i>-[Rh(F)(CH<sub>2</sub>CH<sub>2</sub>(2-C<sub>6</sub>F<sub>4</sub>))(PEt<sub>3</sub>)<sub>3</sub>] (39)</b>	<b>121</b>
<b>8.3 Selbstständigkeitserklärung</b>	<b>122</b>
<b>8.4 List of figures of all complexes</b>	<b>123</b>

# 1. Introduction

## 1.1 Fluorine chemistry and fluorinated compounds

Fluorine has a distinctive position in the periodic table, which specifies it as the most electronegative element (electronegativity 3.98)<sup>[1]</sup> with a high electron affinity (3.448 eV) and extreme ionization energy (17.418 eV).<sup>[2]</sup> The fluoride ion is regarded as the smallest (ion radius 133 pm) and the least polarizable anion.<sup>[2]</sup> Due to these properties, introducing fluorine atoms to organic compounds can change their chemical and physical properties and therefore have an impact on their reactivities.<sup>[3-5]</sup> For example, in the biological field, perfluoroalkanes assume a purely physical function and can be completely neglected by the body.<sup>[2]</sup>

Fluorine is the thirteenth most common element in Earth's crust at 600-700 ppm by mass<sup>[6]</sup> and was recognized as early as 16th century.<sup>[7]</sup> However, the first actual synthesis of an organofluorine compound was published by Dumas *et al.* in 1835 through fluorination of dimethyl sulfate to methyl fluoride.<sup>[8]</sup> Nowadays, owing to the interesting properties, fluorinated compounds are widely investigated in pharmaceuticals, agrochemicals and material science fields.<sup>[3-5]</sup>

As a fluorinated polymer, polytetrafluoroethylene (PTFE) (Figure 1), which is synthesized from tetrafluoroethylene, plays a fundamental role in daily life. Freon<sup>®</sup> was a crucial refrigerant in the past several decades, even though it is facing to be phased out due to its ozone depletion potential (ODP) and the replacement of it is under investigation. Incorporation of fluorine atoms to a drug molecule, in some cases, can increase the lipophilicity and therefore the cell permeability, which results in the enhancement of the bioavailability.<sup>[9-10]</sup> Among them, the gastric acid reducer lansoprazole and the cholesterol drug atorvastatin are two selected top-selling examples in medicine, which contain fluorine atoms (Figure 1).

Consequently, fluorine chemistry is a hot topic and is appealing more and more attention.

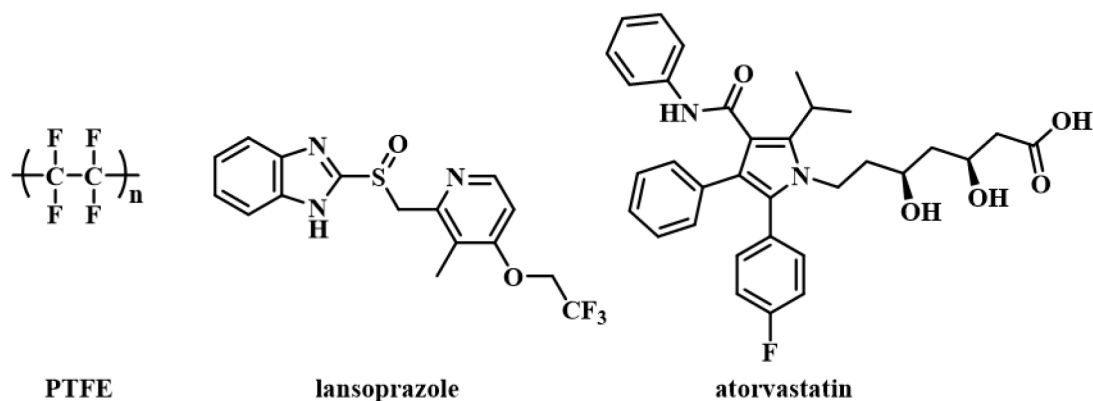
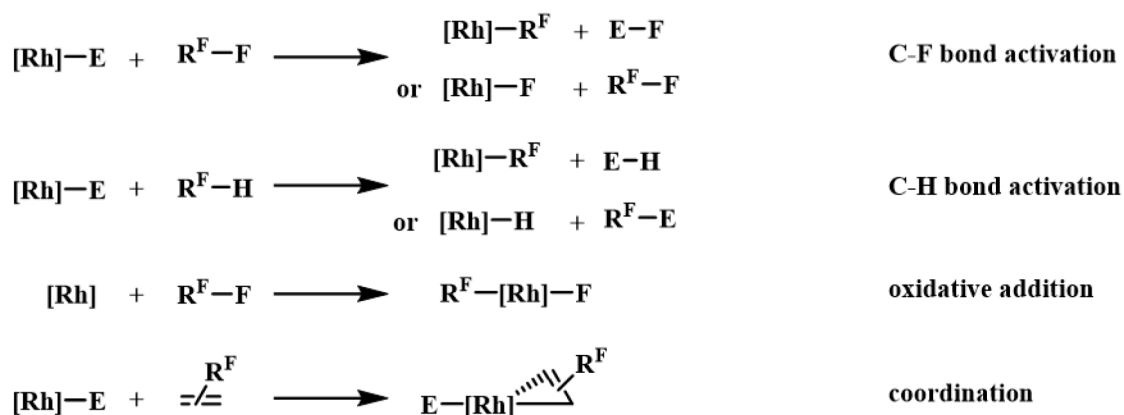


Figure 1. Examples of fluorinated compounds.

## 1.2 Activation of fluorinated compounds at rhodium complexes

Based on the importance of the organofluorine compounds, studies on their synthesis can always be divided into two approaches: one is fluorination and the other one is the C–F activation of fluorinated compounds.<sup>[11]</sup> This section will only focus on the second part. The C–F bond is the strongest single bond among all the other elements that carbon can form<sup>[11]</sup> and is, therefore, often chemically stable.<sup>[12]</sup> This makes it challenging to activate the C–F bond in an effective and selective way. Hence, the formation of strong bonds like Si–F and Ge–F bonds is regarded as the driving force for the cleavage of a C–F bond. Especially, a boron-fluorine bond is even stronger than a Si–F or a Ge–F bond.<sup>[13]</sup> As a result, boron compounds were widely employed. In the last decades, the C–F bond activation of fluorinated compounds was achieved at various complexes, such as iron, copper, palladium, platinum, iridium and rhodium complexes among others.<sup>[12, 14–20]</sup>

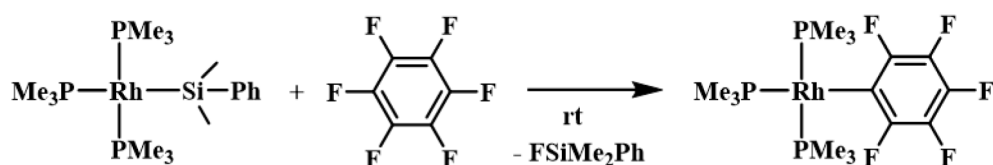
Rhodium complexes can be employed in a lot of reactions including hydroformylation, hydrogenation, C–H bond activation and C–F bond activation among others.<sup>[21]</sup> General reactivity pathways of rhodium complexes towards fluorinated compounds is summarized in Scheme 1. Apparently, rhodium complexes can promote the activation of C–F bonds, which results in the formation of Rh–C and/or Rh–F bonds. Meanwhile, activating the C–H bond of a fluorinated compound is a competitive pathway to the activation of C–F bonds. In addition, coordination of rhodium complexes with fluorinated olefin was also observed as a step prior to the activation. The following sections will only focus on the C–F bond activation of fluorinated aromatics and alkenes as well as activation of fluorinated alkynes.



Scheme 1. General representation of the reactivity of rhodium complexes towards fluorinated compounds.

### 1.2.1 C–F bond activation of aromatic fluorides

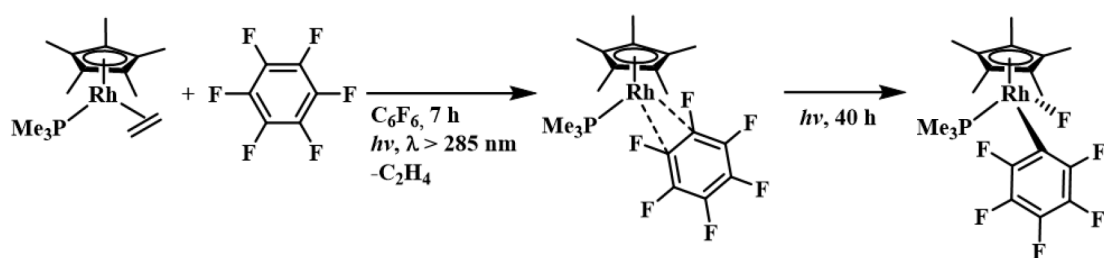
In 1994, Milstein and Aizenberg demonstrated that when treating the Rh(I) silyl complex with perfluorobenzene at room temperature, complex  $[\text{Rh}(\text{C}_6\text{F}_5)(\text{PMe}_3)_3]$  was afforded quantitatively, which was promoted by the formation of fluorosilane (Scheme 2).<sup>[22]</sup>



Scheme 2. C–F bond activation of perfluorobenzene at a rhodium silyl complex.

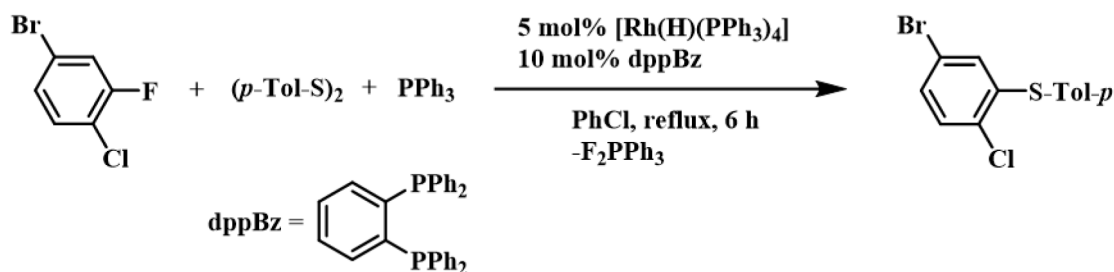
Moreover, when combined with  $\text{HSi}(\text{OEt})_3$ , this reaction can be performed in a catalytic way with high selectivity giving the hydrodefluorination compound  $\text{C}_6\text{F}_5\text{H}$ .<sup>[22]</sup>

Perutz and co-workers published in 1991 that an intramolecular C–F bond oxidative addition product  $[\text{Cp}^*\text{Rh}(\text{C}_6\text{F}_5)(\text{F})(\text{PMe}_3)_3]$  was formed from a 2-step photolytic reaction, in which  $[\text{Cp}^*\text{Rh}(\eta^2\text{-CH}_2\text{CH}_2)(\text{PMe}_3)_3]$  was treated initially with  $\text{C}_6\text{F}_6$  (Scheme 3).<sup>[23–25]</sup> The compound  $[\text{Cp}^*\text{Rh}(\eta^2\text{-C}_6\text{F}_6)(\text{PMe}_3)_3]$  bearing an  $\eta^2$ -coordinated benzene was confirmed to be the initial product. The observation of intramolecular C–F bond oxidative addition is still rare at rhodium complexes at present.



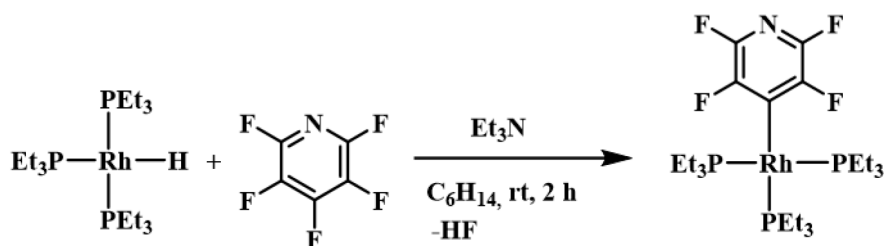
Scheme 3. An intramolecular C–F bond oxidative addition reaction of  $\text{C}_6\text{F}_6$  at a rhodium complex.

In 2008, Yamaguchi *et al.* found that an arylthiolation reaction of aromatic fluoride can be fulfilled by the rhodium hydrido complex  $[\text{Rh}(\text{H})(\text{PPh}_3)_4]$  catalyzed reaction with disulfide (Scheme 4).<sup>[26]</sup> Importantly, the C–F bond activation occurred and the addition of  $\text{PPh}_3$  was used for trapping fluoride to form  $\text{F}_2\text{PPh}_3$ .



Scheme 4. Arylthiolation reaction of aromatic fluoride.

The C–F bond activation of fluorinated pyridines was achieved selectively by the Braun group. Treatment of  $[\text{Rh}(\text{H})(\text{PEt}_3)_3]$  with pentafluoropyridine at room temperature, led to a C–F bond cleavage at the *para* position (Scheme 5).<sup>[27]</sup> The generation of HF facilitated the cleavage of the C–F bond. Additionally, C–F bond activation of pentafluoropyridine and 2,3,5,6-tetrafluoropyridine was also achieved at  $[\text{Rh}(\text{SiPh}_3)(\text{PMe}_3)_3]$ ,  $[\text{Rh}\{\text{Si}(\text{OR})_3\}(\text{PEt}_3)_3]$  ( $\text{R} = \text{Me}, \text{Et}$ ) and  $[\text{Rh}(\text{Bpin})(\text{PEt}_3)_3]$ .<sup>[28-30]</sup>



Scheme 5. C–F bond activation of pentafluoropyridine.

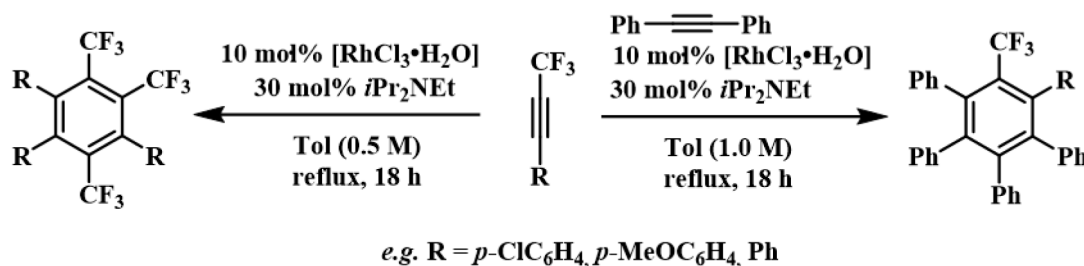
### 1.2.2 Activation in alkynyl fluorides

The activation of terminal and internal alkynes was illustrated to be a fundamental process in chemistry.<sup>[31-34]</sup> Introducing fluorine atom to the alkynes not only altered the reactivity but also provided new building blocks.<sup>[35-37]</sup> Recent studies of fluorinated alkynes at certain W, Co, Pt, Ti, Ru and Rh complexes revealed a variety of reaction pathways such as coordination, insertion, cycloaddition and hydroboration reactions.<sup>[38-46]</sup> Moreover, the hydrogermylation at  $\text{CF}_3$ -containing alkynes has been achieved without the presence of transition metals.<sup>[47]</sup> However, at rhodium complexes, reports on reactivities towards fluorinated alkynes are rare.<sup>[42, 48-50]</sup>



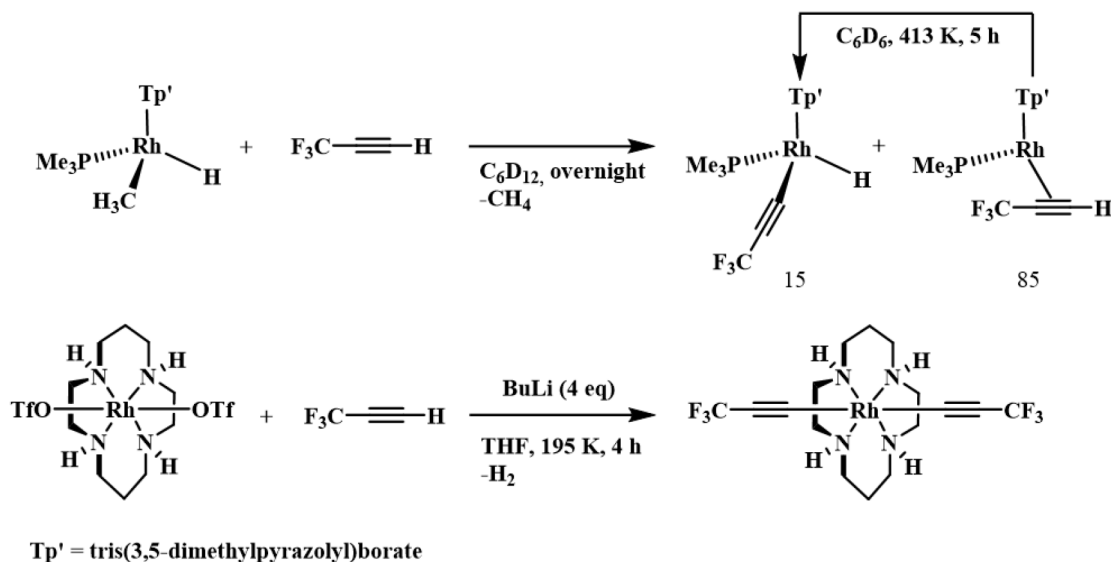
Mague group demonstrated in 1973 that the rhodium(III) complex  $[\text{Rh}(\text{Cl})(\text{C}\equiv\text{CCF}_3)_2(\text{CO})(\text{AsMe}_3)_2]$  was derived from the rhodium(I) complex  $[\text{Rh}(\text{Cl})(\text{CO})(\text{AsMe}_3)_2]$  by conversion with 3,3,3-trifluoropropyne at 373 K.<sup>[48]</sup>

Besides, a novel method of synthesizing multi-substituted fluorinated aromatic compounds through cycloaddition reactions was published by Konno and co-workers in 2010, in which  $\text{RhCl}_3\cdot\text{H}_2\text{O}$  was employed as the pre-catalyst. (Scheme 6).<sup>[42]</sup>



Scheme 6. Cycloaddition reactions of fluorinated alkynes at rhodium.

Other rhodium complexes are capable of inducing C–H bond cleavage of 3,3,3-trifluoropropyne. This process was reported by Jones *et al.* and Wagenknecht *et al.* separately, in which conditions like 413 K or 195 K were needed to fulfill the activation (Scheme 7).<sup>[49-50]</sup>

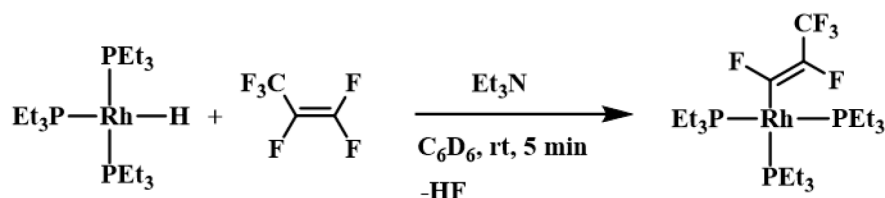


Scheme 7. C–H bond activation of 3,3,3-trifluoropropyne at rhodium complexes. (ratio in mol%)

### 1.2.3 C–F bond activation in alkenyl fluorides

Even though the study of vinyl C–F bond activation was described at other metals such as Ru,<sup>[51-52]</sup> Ta,<sup>[53]</sup> Zr,<sup>[54-55]</sup> Os<sup>[56]</sup> and lanthanoid reagents,<sup>[57]</sup> the amount of rhodium-mediated C–F bond activation studies in olefins is limited.<sup>[21, 58]</sup> The first example of

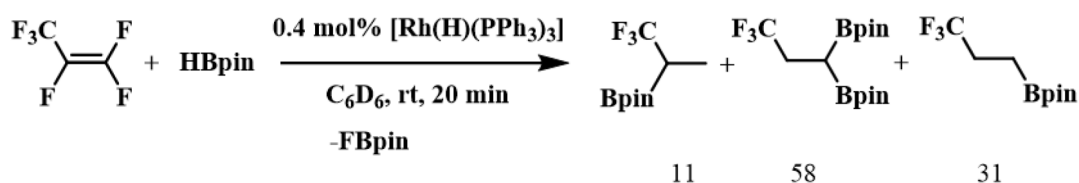
selective vinyl C–F bond activation was reported by Braun and co-workers in 2002, in which the rhodium hydrido complex  $[\text{Rh}(\text{H})(\text{PEt}_3)_3]$  was employed to react with hexafluoropropene giving  $[\text{Rh}\{(Z)\text{-CF}=\text{CFCF}_3\}(\text{PEt}_3)_3]$  regioselectively (Scheme 8).<sup>[59]</sup> This reaction provided a new method for activating fluorinated olefins and was applied to other substrates in the following years.<sup>[21]</sup>



Scheme 8. C–F bond activation of hexafluoropropene at a rhodium hydrido complex.

Additionally, Whittlesey *et al.* reported the reaction of *cis/trans*- $[\text{Rh}(\text{F})(6\text{-NHC})(\text{PPh}_3)_2]$  (6-NHC = 1,3-dialkyltetrahydropyrimidin-2-ylidene; alkyl = Me, Et, *i*Pr) being treated with hexafluoropropene to give the corresponding mixtures of *cis/trans*-rhodium(I) fluorido complexes and the hydrodefluorination compound *E*-CFH=CFCF<sub>3</sub>.<sup>[60]</sup>

Furthermore, catalytic reactions of hexafluoropropene were accomplished *via* defluorohydroboration reactions to give Bpin (Bpin = 4,4,5,5-tetramethyl-1,3,2-dioxaboryl) derivatives of trifluoropropane, when being treated with HBpin (Scheme 9).<sup>[61]</sup> Importantly, the formation of the F–B bond, which is even stronger than the C–F bond was the key point of the reaction and it facilitated the cleavage of C–F bond. The formation of the rhodium(III) complex *fac*- $[\text{Rh}(\text{Bpin})(\text{H})_2(\text{PEt}_3)_3]$  through the oxidative addition reaction of rhodium hydrido complex and HBpin was regarded as the catalytic resting state. The complex  $[\text{Rh}(\text{Bpin})(\text{PEt}_3)_3]$ , which derived from the reductive elimination reaction of the former mentioned rhodium(III) boryl complex was proved in the last years to be an active complex in the C–F bond activation step.<sup>[62–65]</sup>



Scheme 9. Catalytic borylation of hexafluoropropene (ratio in mol%).

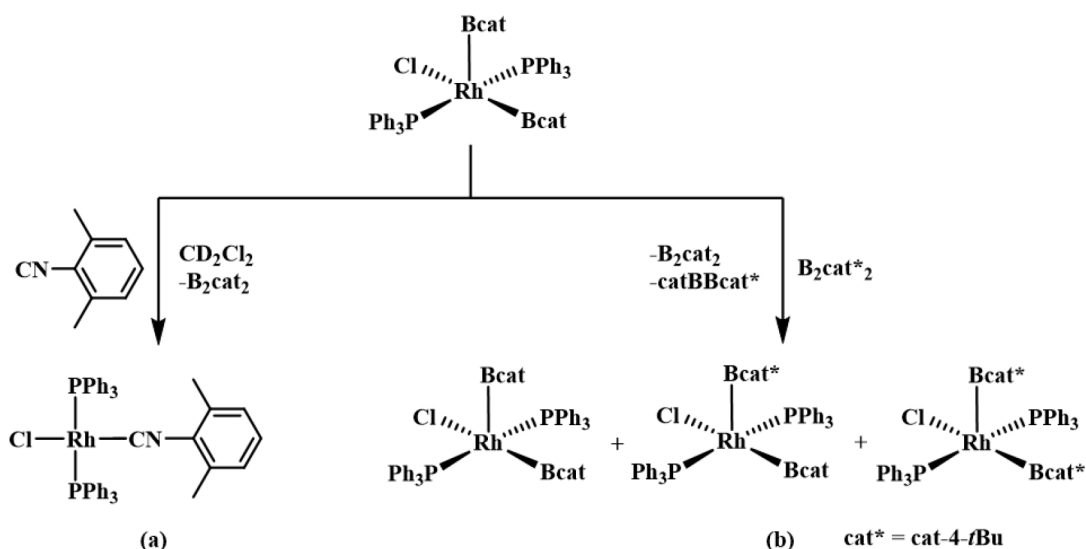
## 1.3 Rhodium boryl complexes and borylated compounds

### 1.3.1 Reactivity of rhodium boryl complexes

The special structure of a rhodium boryl complex is the existence of a covalent two-center, two-electron bond between the rhodium center and a three-coordinate,  $sp^2$ -hybridized boron atom.<sup>[62]</sup>

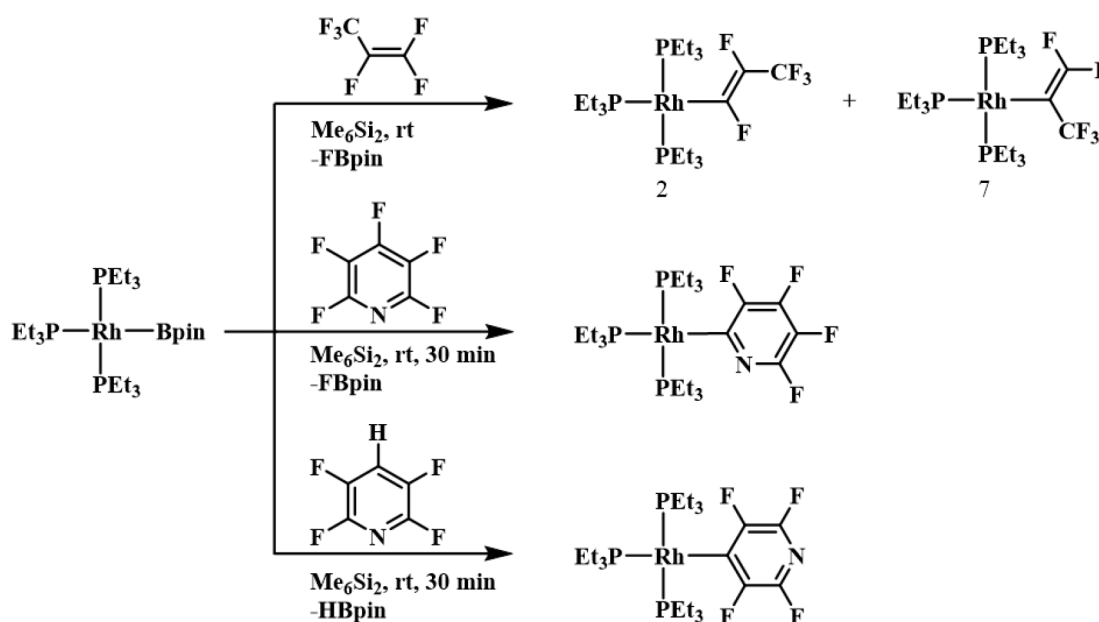
Reactions at rhodium boryl complexes can be classified mainly into (i) reactions involving breaking the Rh–B bond<sup>[30, 62, 66-73]</sup> and (ii) reactions occurring at the rhodium center with the retention of Rh–B bond.<sup>[62, 67, 70, 74]</sup>

Regarding the reactions involving breaking Rh–B bond, a rhodium(III) complex  $[\text{Rh}(\text{Bcat})_2(\text{Cl})(\text{PPh}_3)_2]$  (Bcat = 1,3,2-benzodioxaboryl) was reported to undergo reductive elimination reaction and metathesis reactions (Scheme 10).<sup>[67-68]</sup> Baker, Marder and co-workers demonstrated the feasibility of the rapid reductive elimination of  $\text{B}_2\text{cat}_2$  resulting in the formation of the monovalent rhodium complex *trans*- $[\text{Rh}(\text{Cl})(\text{CNAr})(\text{PPh}_3)_2]$  in the presence of CNAr (Ar = 2,6-Me<sub>2</sub>C<sub>6</sub>H<sub>3</sub>) in 1993 (Scheme 10a).<sup>[67]</sup> Afterwards, Marder and Norman *et al.* investigated the same rhodium(III) complex being treated with diborane  $\text{B}_2\text{cat}^*_2$  (Scheme 10b).<sup>[68]</sup> Metathesis reactions took place affording again rhodium(III) boryl complexes. Importantly, this reaction showed the complexity of the mechanisms involving rhodium boryl complex and diborane.



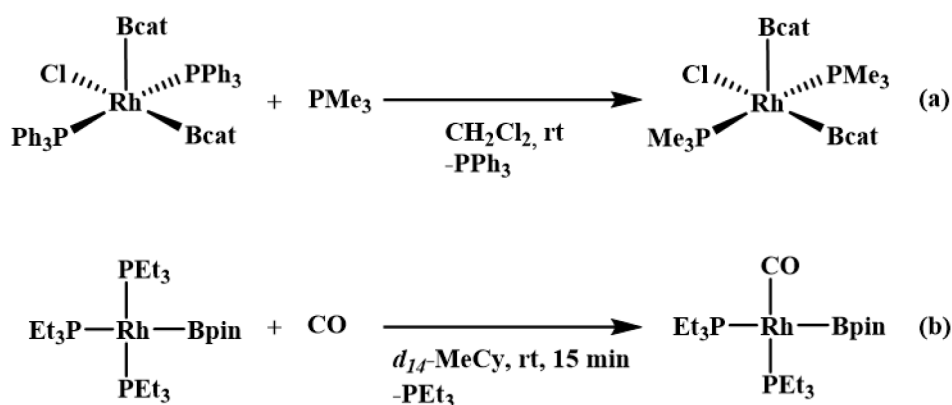
Scheme 10. Selected examples of reactivity investigation of rhodium(III) complex.

Moreover, the rhodium(I) boryl complex  $[\text{Rh}(\text{Bpin})(\text{PEt}_3)_3]$  facilitated the C–F bond activation of pentafluoropyridine (Scheme 11) *via* a boryl assisted four-member transition state.<sup>[30]</sup> Additionally, the C–F bond activation of hexafluoropropene and the C–H bond activation of 2,3,5,6-tetrafluoropyridine were also accomplished with this rhodium(I) boryl complex. The release of FBpin or HBpin in the reaction was considered as the driving force (Scheme 11).



Scheme 11. The reactivity of rhodium(I) boryl complex towards fluorinated compounds.

Until recently, only a few reactions were reported at rhodium boryl complexes with the retention of Rh–B bond and they mainly impart phosphine ligand substitution.<sup>[62, 67, 70, 74]</sup> The phosphine ligand substitution was carried out on the more readily dissociating ligands. Marder and Norman *et al.* published in 1998 that with an excess amount of  $\text{PMe}_3$ , a phosphine exchange was observed at a rhodium(III) boryl complex (Scheme 12a).<sup>[74]</sup> Besides, Braun group exhibited that the phosphine ligand of a rhodium(I) boryl complex can be easily substituted by carbon monoxide giving *cis*- $[\text{Rh}(\text{Bpin})(\text{CO})(\text{PEt}_3)_2]$  along with the formation of free phosphine (Scheme 12b).<sup>[70]</sup>

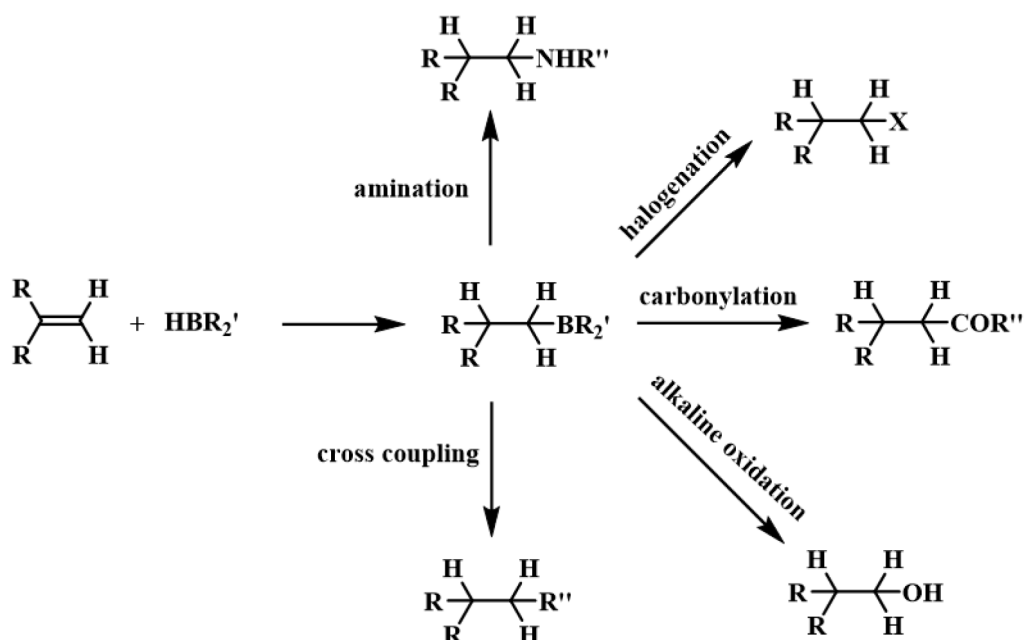


Scheme 12. The reactivity of rhodium boryl complex with the retention of Rh–B bond.

### 1.3.2 Catalytic borylation

Not only rhodium boryl complexes but also boron containing compounds are appealing more and more attention over the past several years, which is on the basis that organoboron compound could be employed as a fundamental building block in versatile reactions.<sup>[75-79]</sup>

Borylated compounds can be further derived by amination, halogenation, carbonylation, alkaline oxidation and cross coupling reactions. Organoboron compounds were therefore investigated widely in the pharmaceutical and agricultural chemistry (Scheme 13).<sup>[75-79]</sup>



Scheme 13. Transformations of organoboron compounds.

The catalytic formation of organoboron compounds can be mainly achieved through (i) hydroboration reactions; (ii) diborylation reactions and (iii) dehydroborylation reactions.

### 1.3.2.1 Hydroboration reactions

In hydroboration reactions a boron-hydrogen moiety is added to a multiple bond of an unsaturated compound.<sup>[80]</sup> Generally, hydroboration reaction can take place at unsaturated compounds including C=C, C≡C, C=O, C≡N or N=N bonds among others.

Mechanistically, a hydroboration reaction is initiated *via* a coordination of the electron rich double bond or triple bond to the electron deficient boron atom giving a four-center transition state structure (Figure 2).<sup>[75, 80-82]</sup> The hydride prefers to bind the more substituted carbon atom, where the carbocation type intermediate can be best stabilized while the boryl moiety goes to the less substituted carbon atom.<sup>[75]</sup> Finally, the corresponding organoboron product is afforded.

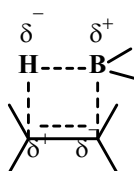


Figure 2. Four-center transition state.

Diborane (BH<sub>3</sub>-BH<sub>3</sub>) was studied as the first hydroboration reagent in 1948. It has a structure in which each boron atom forms a 2-center 2-electron bond with the terminal hydrogen atoms and forms a 3-center 2-electron bond with the bridging hydrogen atoms (Figure 3).<sup>[83]</sup> Hurd reported several reactions of diborane and olefins at high temperature giving trialkylboranes, in which the BH<sub>3</sub> molecule was proposed as the active reagent.<sup>[84]</sup>

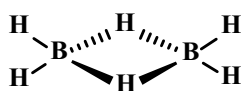
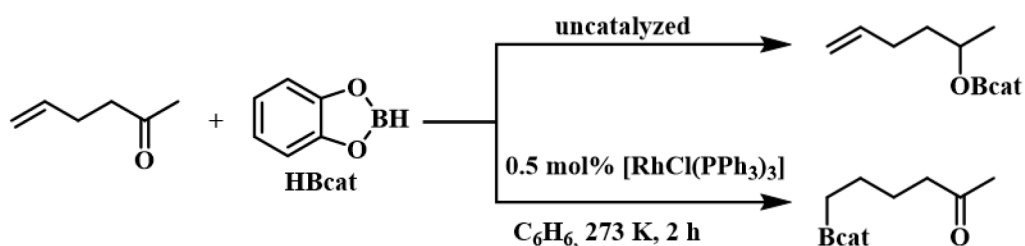


Figure 3. Structure of diborane.

Besides BH<sub>3</sub>, other borane derivatives like mono- and dialkylboranes were also employed as the hydroboration reagents.

Furthermore, the hydroboration reaction process was reported to be mediated by transition metals.<sup>[70, 75, 85-89]</sup> Männig and Nöth first demonstrated in 1985 that the chemoselectivity of a hydroboration reaction, in which a substrate containing both a C=O and a C=C bond was involved, was different in the catalyzed compared to the uncatalyzed reaction (Scheme 14).<sup>[90]</sup> In the catalyzed reaction, the addition occurred to the C=C bond, while without any catalyst the C=O bond was activated.



Scheme 14. Catalyzed and uncatalyzed hydroboration reaction of 5-hexen-2-one with HBcat.

Subsequently, a number of investigations were carried out revealing the possibilities of the regio-, enantio- and diastereoselectivity of the transition metals catalyzed hydroboration reactions.<sup>[70, 75, 85-86]</sup>

Regarding to the reagents employed in the metal catalyzed hydroboration reactions, the boronic esters HBcat (catechol borane) and HBpin (pinacol borane) attracted a lot of attention in the last decades. The introduction of the oxygen atom into the boron source leads to a decrease in the rate of uncatalyzed reaction.<sup>[77, 91]</sup>

Compared with HBcat, HBpin is more stable to air, water and in column chromatography purification.<sup>[77, 91]</sup> Besides alkenes, catalyzed hydroboration reaction of alkynes was also achieved with HBpin at Fe, Co or Rh complexes among others.<sup>[44, 92-95]</sup> Most importantly, the reaction can be controlled to result in monohydroboration.

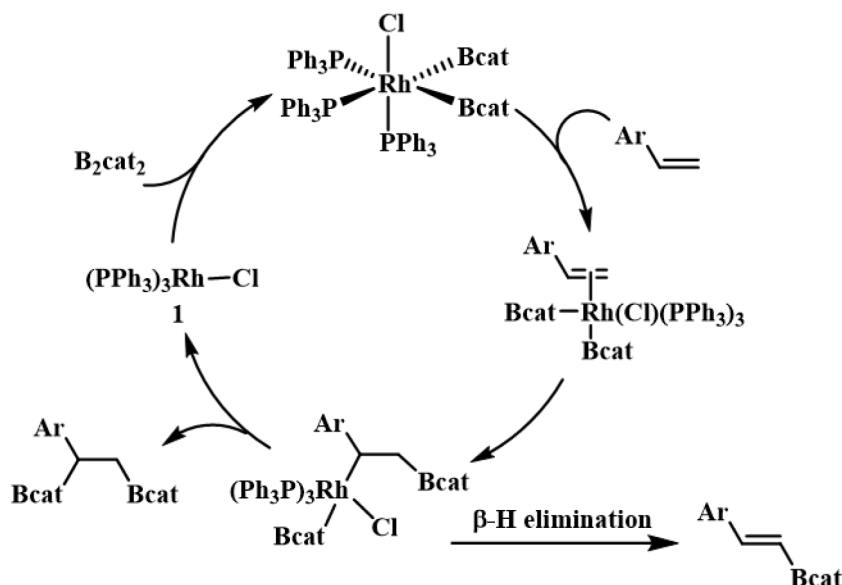
### 1.3.2.2 Diboration reactions

A diboration is a reaction in which diboron compounds are treated with unsaturated compounds affording diborylated products. It is noteworthy that both C–B bonds might be further transformed. The conversions can be mediated by transition metals to lower the reaction energy barrier.<sup>[96-101]</sup>

The first *syn*-selective diboration reaction under metal catalysis was realized at the platinum(0) complex  $[\text{Pt}(\text{PPh}_3)_4]$  by investigating reactivity towards alkynes in 1993<sup>[96]</sup> to yield a diborylated alkene. A conceivable mechanism was proposed in which initially an oxidative addition of the B–B bond occurs at the platinum(0) complex, followed by the insertion of the alkyne into the Pt–B bond. The final product is formed after the reductive elimination.

The achievement of an oxidative addition at the rhodium complex  $[\text{Rh}(\text{Cl})(\text{PPh}_3)_3]$  with  $\text{B}_2\text{cat}_2$ <sup>[102]</sup> opened up the possibility of breaking the B–B bond and promoted further investigations of the diboration reaction at the rhodium complex. Marder, Baker, and Westcott published the addition of B–B bond to C=C bond at a rhodium center.<sup>[103]</sup>

However, instead of the diboration product, the hydroboration product were reported to be the main products in this reaction. Considering the mechanism, after the oxidative addition and olefin insertion into the Rh–B bond, the formation of another new C–B bond is not preferred over a the  $\beta$ -H elimination (Scheme 15).<sup>[70]</sup> Subsequent studies to achieve diboration reactions ended up with higher selectivity,<sup>[99-100, 103-105]</sup> and even when chiral rhodium complexes or ligands were employed, the diboration product was generated with high enantioselectivity.<sup>[99-100]</sup>



Scheme 15. Proposed mechanism for a rhodium catalyzed diboration and the competing  $\beta$ -H elimination.

### 1.3.2.3 Dehydroborylation reactions

Besides hydroboration and diboration reactions, another fundamental way to form borylated compound is direct C–H bond functionalization.

Hartwig *et al.* disclosed in 2000 the first regiospecific catalytic C–H bond functionalization of linear alkanes when utilizing  $[\text{Re}(\text{Cp}^*)(\text{CO})_3]$  as the catalyst and  $\text{B}_2\text{pin}_2$  as the boron source.<sup>[106]</sup> Afterwards, dehydroborylation was achieved at Ru, Rh and Ir complexes among others.<sup>[70, 107]</sup> Additionally, besides  $\text{B}_2\text{pin}_2$ ,  $\text{HBpin}$ ,  $\text{HBcat}$  and  $\text{B}_2\text{cat}_2$  *etc.* were proved to be efficient boron sources. Meanwhile, the substrate scope was spread to benzene, heteroaromatics and fluorinated alkanes among others.



## 1.4 Research objective

Rhodium catalyzed C–F bond activation as well as C–E (E = Rh, B, H *etc.*) bond formation is an important tool to access fluorinated building blocks. Rhodium complexes and especially  $[\text{Rh}(\text{H})(\text{PEt}_3)_3]$  were reported to be effective catalysts in the activation and borylation reactions of hexafluoropropene and 3,3,3-trifluoropropene. However, those reactions were often not accomplished with high selectivity. Additionally, the substrates which have been used were very limited. Therefore, goals of this thesis are to develop routes for the activation of a variety of fluorinated olefins such as HFO-1234yf (2,3,3,3-tetrafluoropropene), HFO-1234ze (*E*-1,3,3,3-tetrafluoropropene), HFO-1225zc (1,1,3,3,3-pentafluoropropene), HFO-1225ye (*Z*) (*Z*-1,2,3,3,3-pentafluoropropene), 3,3,3-trifluoropropyne, trifluoroethylene, 1,1,2-trifluorobutene and pentafluorostyrene. Another focus is on catalytic and selective borylation processes.

The formation of F–E bond is one of the driving forces of the transformations. Consequently, different boron sources (HBpin and B<sub>2</sub>pin<sub>2</sub>), rhodium catalysts ( $[\text{Rh}(\text{H})(\text{PEt}_3)_3]$ ,  $[\text{Rh}(\text{Cl})(\text{PEt}_3)_3]$ ,  $[\text{Rh}(\text{Bpin})(\text{PEt}_3)_3]$   $[\text{Rh}(\mu\text{-Cl})(\text{P}i\text{Pr}_3)_2]_2$  and  $[\text{Rh}(\text{Me})(\text{PEt}_3)_3]$ ) and solvents should also be tested. For understanding catalytic processes, stoichiometric activation and borylation reactions were studied. It was envisaged that the identification of the intermediates will give an insight into possible mechanistic pathways.

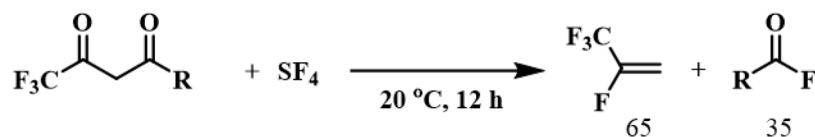


## 2. Activation and borylation of CF<sub>3</sub>-containing unsaturated compounds towards rhodium(I) complexes

### 2.1 Introduction

Climate engineering technologies, which mainly contain two categories: greenhouse gas removal and solar radiation management, are appealing more and more attention because of their attempts for a sustainable environment.<sup>[108-109]</sup> In this regards, refrigeration is a significant source of greenhouse gas. Thanks to the low ozone depleting potential (ODP), hydrofluorocarbons (HFCs) such as HFC-134a (1,1,1,2-tetrafluoroethane)<sup>[110]</sup> were widely used in the refrigeration and air-conditioning industry. However, while considering the high global warming potential (GWP),<sup>[110]</sup> they are facing to be phased out. Therefore, an increasing interest on the development of new refrigerants appeared. Hydrofluoroolefins (HFOs) came into public eyes as the alternative. Among them, HFO-1234yf (2,3,3,3-tetrafluoropropene), which has high efficiency, low pressure and low flammability, attracts a large global concern.<sup>[111]</sup>

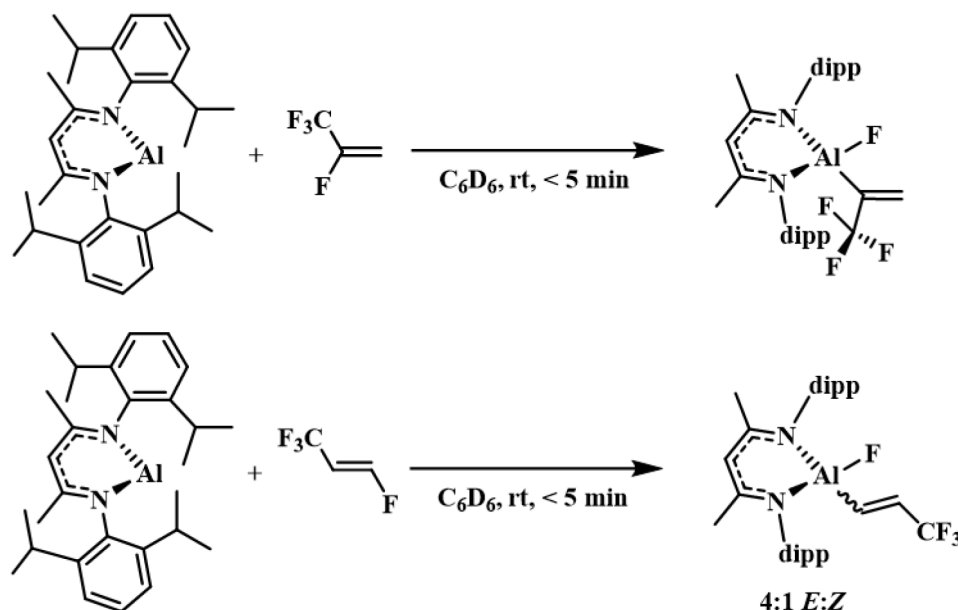
In 1983, Stepanov *et al.* first published the synthesis of HFO-1234yf in which 1,1,1-trifluorinated  $\beta$ -diketones were treated with an excess amount of SF<sub>4</sub> providing the target compound and the corresponding alkanoyl fluoride in a 65:35 ratio (Scheme 16).<sup>[112]</sup> Inspired by this strategy, a numerous explorations were conducted to make it a successful synthesizing protocol in industry.<sup>[113-115]</sup>



Scheme 16. The formation of HFO-1234yf through  $\beta$ -diketones (ratio in mol%).

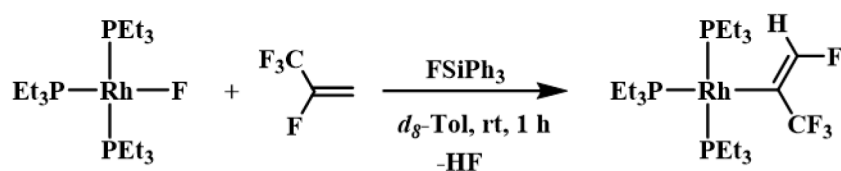
Apart from the advantages as a refrigerant, HFO-1234yf can be a substrate for new building blocks.<sup>[116-120]</sup> Comparably, the analogues of HFO-1234yf such as HFO-1234ze (*E*-1,3,3,3-tetrafluoropropene), HFO-1225zc (1,1,3,3,3-pentafluoropropene) and HFO-1225ye (*Z*) (*Z*-1,2,3,3,3-pentafluoropropene) behave similarly to HFO-1234yf not only as refrigerants but also in reactivity. In this regard, Crimmin *et al.* published a stoichiometric methodology for activating HFO-1234yf and HFO-1234ze to synthesize

fluorinated organoaluminium compounds through oxidative addition reaction at Al(I) center (Scheme 17).<sup>[119]</sup>



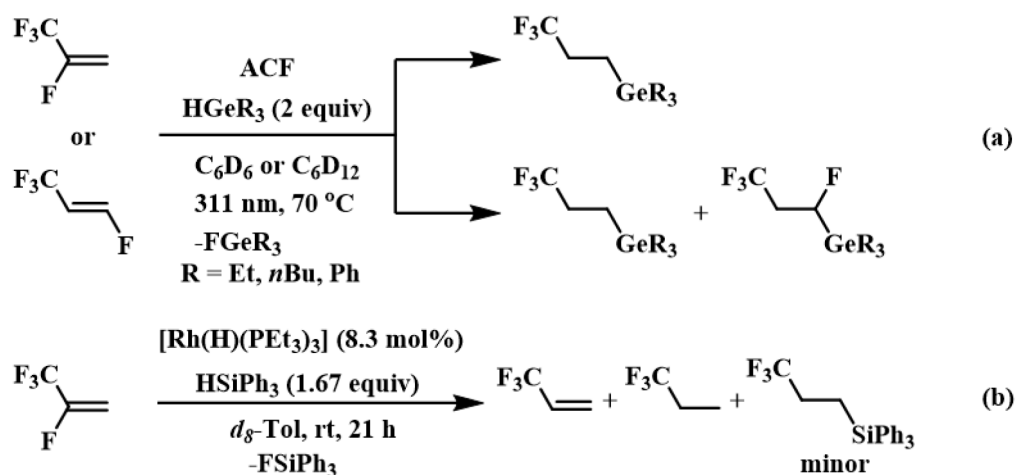
Scheme 17. Stoichiometric reaction of an aluminium complex with HFO-1234yf and HFO-1234ze.

Contrasted to this work, in 2019, the Braun group reported a system in which a C–H bond activation reaction occurred on using a rhodium fluoro complex and HFO-1234yf in the presence of FSiPh<sub>3</sub>. The compound FSiPh<sub>3</sub> was evidenced to be critical in the reaction (Scheme 18).<sup>[120]</sup>



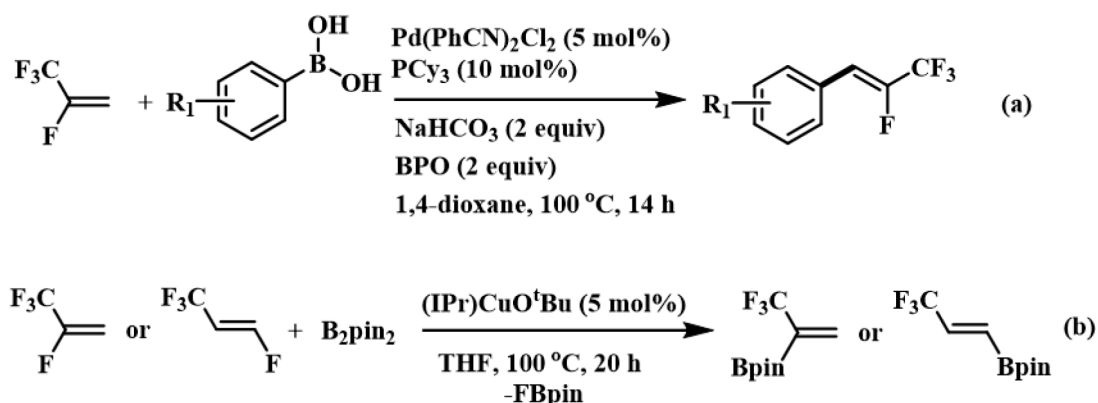
Scheme 18. Stoichiometric reaction of rhodium fluoro complex with HFO-1234yf.

Additionally, in the previous work, hydrogermylation or defluorohydrogermylation has been achieved on HFO-1234yf and HFO-1234ze giving the related fluorine-containing frameworks when using tertiary germanes as hydrogen sources and nanoscopic aluminum chlorofluoride AlCl<sub>x</sub>F<sub>3-x</sub> (ACF, x ≈ 0.05-0.3) as the catalyst (Scheme 19a).<sup>[118]</sup> Besides, HFO-1234yf could be transformed to the corresponding defluorohydrosilylation product slowly under mild conditions using HSiPh<sub>3</sub> and rhodium hydrido complex (Scheme 19b).<sup>[120]</sup>



Scheme 19. Hydrogermylation or hydrosilylation reactions of HFO-1234yf and HFO-1234ze.

In addition, Lu's group first gave examples of oxidative Heck reaction to form fluorinated compounds when dealing with HFO-1234yf and arylboronic acids in 2015,<sup>[116]</sup> which brings the further interest in the study of borylated fluorine-containing compounds formation (Scheme 20a). Moreover, the strategy has a considerable tolerance of arylboronic acids and presents a direct routine to synthesize the *Z*-isomer stereoselectively. Meanwhile in 2017, Ogoshi and co-workers published a practical method in which the polyfluorinated alkene HFO-1234yf or HFO-1234ze was treated with B<sub>2</sub>pin<sub>2</sub> (bis(pinacolato)diboron) to afford the borylated alkene regioselectively *via* monodefluoroboration reaction using a copper catalyst (Scheme 20b).<sup>[117]</sup> However, borylation reactions of fluoroolefins are rare and hydroboration reactions of HFO-1234yf and analogues have not been explored, yet.



Scheme 20. Derivatization of HFO-1234yf and HFO-1234ze.

Besides olefins, alkynes are also fundamental precursors of borylated building blocks. The hydroboration reaction of alkynes has been achieved in the last decades.<sup>[44-45, 92-94]</sup> Fe, Co and Rh complexes were tested yielding the corresponding anti-Markovnikov selective borylated olefins.

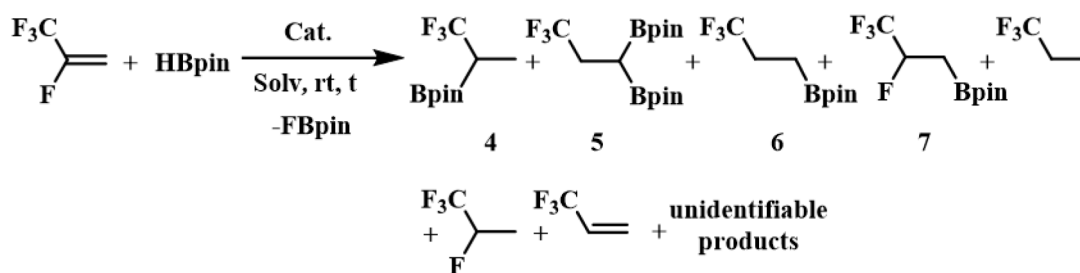
However, the investigation among fluorinated alkynes is rare.<sup>[38-45]</sup> When highlighting 3,3,3-trifluoropropyne, the HX (X = F, Cl, Br, I, CN, OMe, OEt, NEt<sub>2</sub>) addition explored before suggest that a formation of fluorinated alkenes might be conceivable. The addition of another equivalent of HX needed to be conducted under harsh condition.<sup>[121]</sup> Nonetheless, the hydroboration reaction of trifluorinated propyne remains to be explored.

## 2.2 Results and discussion

### 2.2.1 Catalytic studies of CF<sub>3</sub> containing olefins with rhodium(I) complexes

#### 2.2.1.1 HFO-1234yf

The catalytic functionalization of HFO-1234yf (2,3,3,3-tetrafluoropropene) was initiated using HBpin (pinacol borane) as boron source. A reaction was run at room temperature with HBpin and an excess amount of HFO-1234yf using a 5 mol% (based on the amount of HBpin) of [Rh(H)(PEt<sub>3</sub>)<sub>3</sub>] (**1**) as a catalyst in C<sub>6</sub>D<sub>6</sub>. With a full conversion of HBpin, a mixture of products CF<sub>3</sub>CH(Bpin)CH<sub>3</sub> (**4**),<sup>[61]</sup> CF<sub>3</sub>CH<sub>2</sub>CH(Bpin)<sub>2</sub> (**5**),<sup>[61]</sup> CF<sub>3</sub>CH<sub>2</sub>CH<sub>2</sub>Bpin (**6**),<sup>[61]</sup> CF<sub>3</sub>CFHCH<sub>2</sub>Bpin (**7**), 1,1,1-trifluoropropane,<sup>[122]</sup> 1,1,1,2-tetrafluoropropane,<sup>[123]</sup> 3,3,3-trifluoropropene<sup>[124]</sup> and a small amount of unidentifiable products in a 17:15:22:19:13:4:5:5 ratio was observed after 1 h, as well as the release of FBpin (Scheme 21) (Table 1, entry 1).



Scheme 21. Catalytic reaction of HFO-1234yf with HBpin.

Table 1. Comparison of catalytic reactions of HFO-1234yf with HBpin (ratio in mol%).

Entry	Excess	Solv.	Cat.	mol%	Time	Ratio
1	HFO-1234yf	C <sub>6</sub> D <sub>6</sub>	<b>1</b>	5	1 h	17:15:22:19:13:4:5:5
2	HBpin	C <sub>6</sub> D <sub>6</sub>	<b>1</b>	8.6	10 min	23:20:24:17:7:9:--:--
3	HBpin	<i>d</i> <sub>8</sub> -THF	<b>1</b>	8.6	20 min	27:21:29:9:7:7:--:--
4	HBpin	Me <sub>6</sub> Si <sub>2</sub>	<b>3</b>	4.6	30 min	23:23:22:20:3:9:--:--

--: Not detected.

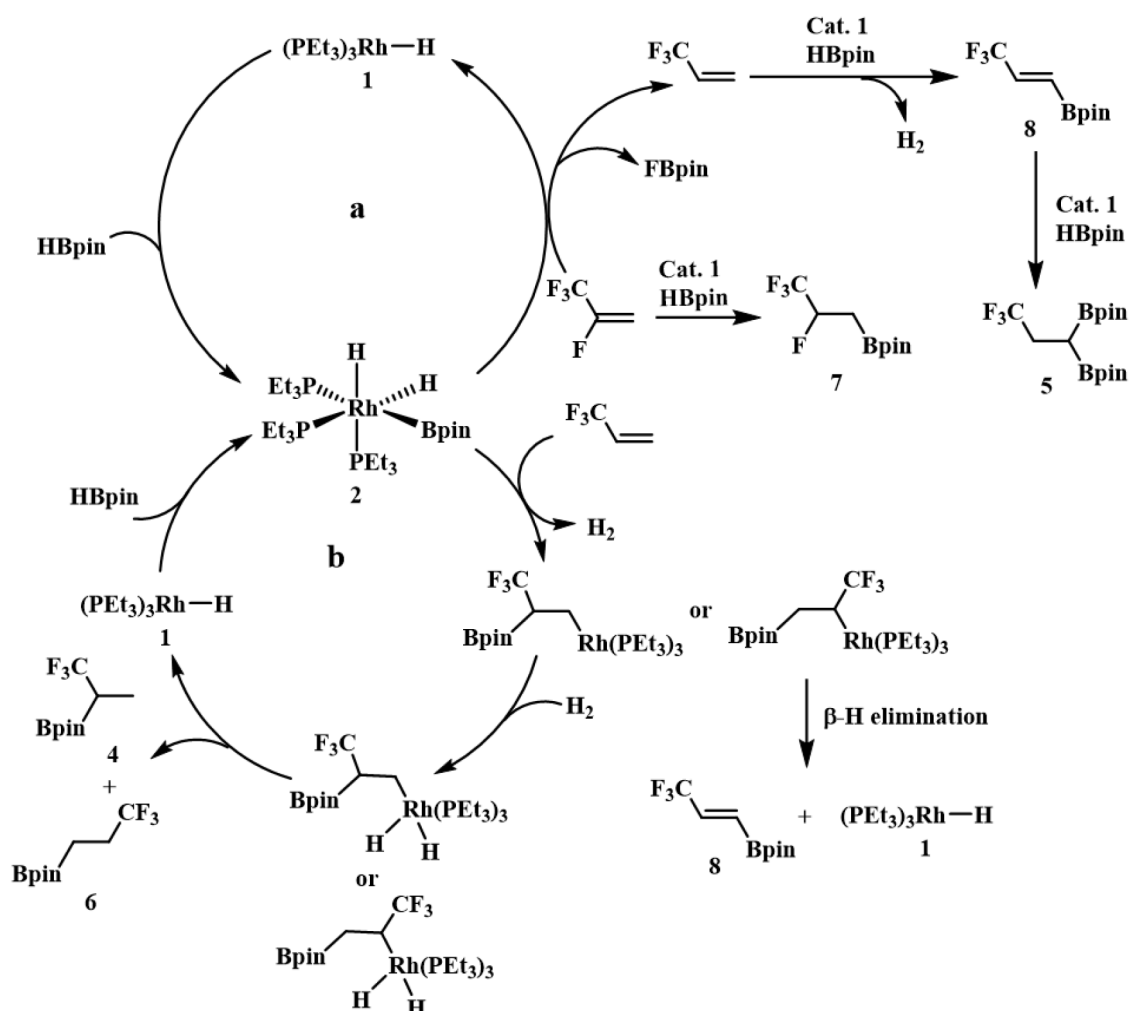
As it has been previously reported, complex **1** catalyzed the hydroboration of hexafluoropropene and 3,3,3-trifluoropropene yielding respective ratio of 11:58:31 and 4:14:82 for products **4**, **5** and **6** by hydrodefluorination-hydroboration and dehydrogenative borylation- hydroboration reactions.<sup>[61]</sup> However, in contrast to hexafluoropropene, hydroboration and hydrogenation reactions of HFO-1234yf without prior C–F bond activation were also observed allowing different regio and chemoselectivity. The presence of 1,1,1,2-tetrafluoropropane and the fluorinated boryl-containing propane **7** suggests that the hydrodefluorination could be less favored than in the activation of hexafluoropropene. Furthermore, compound **7** was characterized by NMR and GC-MS. In the  $^{19}\text{F}$  NMR spectrum, a doublet of doublets at -81.6 ppm was assigned to the  $\text{CF}_3$  group, due to the coupling with the fluorine and the hydrogen atoms of the CFH moiety with a  $^3J$  of 11 Hz and 6 Hz, respectively. Additionally, the multiplet at -191.5 ppm belongs to the fluorine of the CFH moiety which in the  $^{19}\text{F}\{^1\text{H}\}$  NMR spectrum simplified to a quartet due to the fluorine-fluorine coupling. In the  $^1\text{H}$  spectrum, a doublet of multiplets appeared at 5.05 ppm with a proton-fluorine coupling constant of 46.0 Hz typical for a *geminal* arrangement corresponding to the hydrogen of the CFH group. The correlated resonance for the  $\text{CH}_2$  moiety was observed at 1.36 ppm in the  $^1\text{H}$ - $^1\text{H}$  COSY NMR spectrum. The GC-MS spectrum revealed a peak at  $m/z$  242, confirming the structure proposed for **7**.

In an attempt to obtain a higher selectivity, HBpin was added in excess in respect to the olefin. Thus, the unidentifiable products were not formed and 3,3,3-trifluoropropene was fully reacted leading to the formation of the hydroborated compounds **4**, **5**, **6**, **7**, 1,1,1-trifluoropropane and 1,1,1,2-tetrafluoropropane in a 23:20:24:17:7:9 ratio after 10 min (Table 1, entry 2). In order to study a possible solvent effect,  $d_8$ -THF was employed instead of  $\text{C}_6\text{D}_6$  affording the same products with a similar ratio of 27:21:29:9:7:7 in 20 min (Table 1, entry 3). Thus, this result indicates that  $d_8$ -THF is not better than  $\text{C}_6\text{D}_6$ . Consequently,  $\text{C}_6\text{D}_6$  was still employed as the solvent for the following reactions. Note that no reaction took place at room temperature or under 311 nm UV light in the absence of the catalyst.

Regarding a plausible mechanism, several pathways are proposed (Scheme 22). As it is known, complex *fac*- $[\text{Rh}(\text{Bpin})(\text{H})_2(\text{PET}_3)_3]$  (**2**) is formed immediately after mixing the complex  $[\text{Rh}(\text{H})(\text{PET}_3)_3]$  (**1**) and HBpin.<sup>[61]</sup> Then the hydrodefluorination reaction between complex **2** and HFO-1234yf driven by the formation of FBpin occurs. The hydrodefluorination reaction is rare for fluoroolefins, but observed in some transition

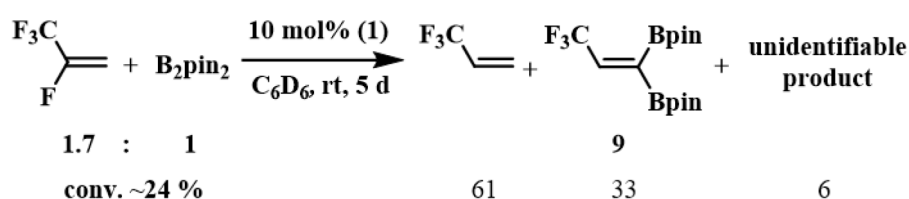


metal catalyzed processes.<sup>[120, 125-126]</sup> As a result, 3,3,3-trifluoropropene is afforded as well as the regeneration of complex **1** (Scheme 22a). Tentatively, compound  $\text{CF}_3\text{CH}=\text{CHBpin}$  (**8**)<sup>[117]</sup> is formed from 3,3,3-trifluoropropene *via* dehydroboration reaction. Afterwards, a competitive hydroboration might take place. In terms of the hydroboration reaction of 3,3,3-trifluoropropene, the insertion reaction of HFO-1234yf into a Rh–B bond of complex **2** is accompanied by the release of  $\text{H}_2$ . After the oxidative addition of  $\text{H}_2$  and reduction elimination, the compounds **4** and **6** are formed along with the regeneration of complex **1** (Scheme 22b). Compounds **5** and **7** which stem from HFO-1234yf and compound **8**, respectively, are also furnished through similar hydroboration reaction pathway (Scheme 22). With the presence of  $\text{H}_2$ , hydrogenation reactions take place giving compound 1,1,1-trifluoropropane and 1,1,1,2-tetrafluoropropane.



Scheme 22. Plausible mechanism of the catalytic activation of HFO-1234yf.

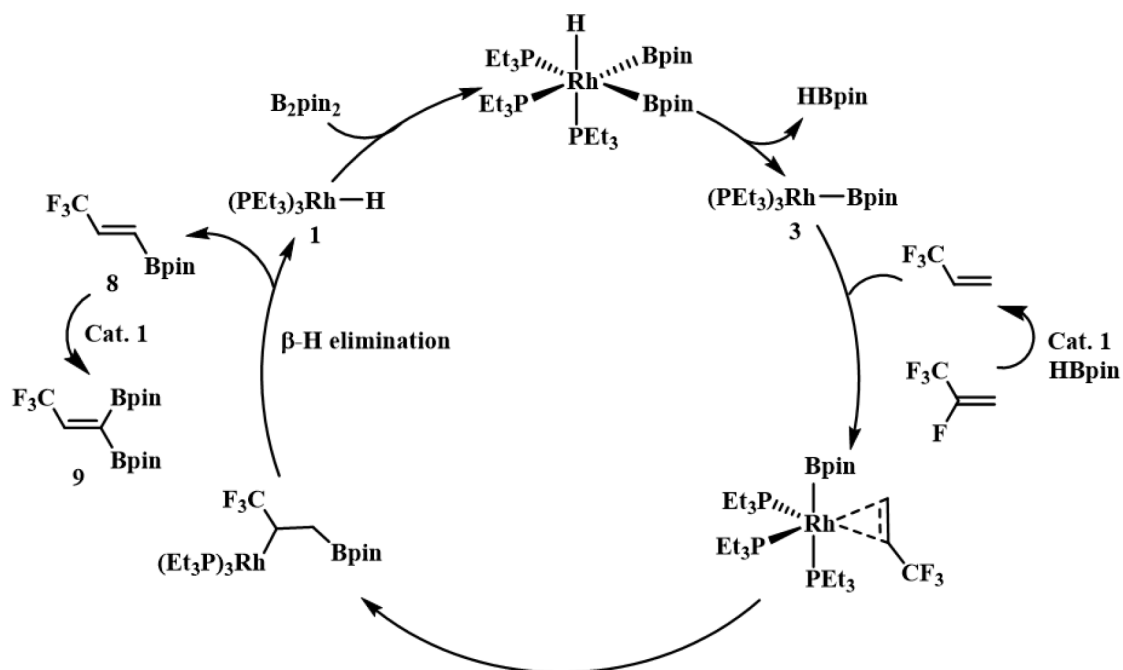
Realizing that the boron source may affect the reactivity and selectivity, B<sub>2</sub>pin<sub>2</sub> was examined in the reaction with HFO-1234yf with complex **1** as catalyst giving 3,3,3-trifluoropropene, CF<sub>3</sub>CH=C(Bpin)<sub>2</sub> (**9**) and an unidentified product in a 61:33:6 ratio (Scheme 23) in 5 d with a *ca.* 24 % conversion of HFO-1234yf based on the <sup>19</sup>F NMR spectrum. For compound **9**, the doublet with a fluorine-proton coupling constant of 7 Hz at -64.6 ppm in the <sup>19</sup>F NMR spectrum was assigned to the CF<sub>3</sub> group. The <sup>1</sup>H NMR spectrum showed a quartet with a fluorine-hydrogen coupling of 7.1 Hz at 6.85 ppm for the proton on the CH moiety. A peak at *m/z* 348 was shown in the GC-MS spectrum illustrating the presence of compound **9**.



Scheme 23. Catalytic hydroboration reaction of HFO-1234yf with B<sub>2</sub>pin<sub>2</sub> (ratio in mol%).

The rhodium(III) complex *fac*-[Rh(Bpin)<sub>2</sub>(H)(PEt<sub>3</sub>)<sub>3</sub>]<sup>[30]</sup> is regarded as an intermediate for the transformation on complex **1** and the rhodium boryl complex [Rh(Bpin)(PEt<sub>3</sub>)<sub>3</sub>] (**3**).<sup>[30]</sup> A conceivable mechanistic pathway for the formation of compound **9** is proposed. Initially, [Rh(Bpin)(PEt<sub>3</sub>)<sub>3</sub>] (**3**) is formed through oxidative addition and reductive elimination reaction releasing HBpin. After that, coordination of 3,3,3-trifluoropropene, which stems from HFO-1234yf under catalyst **1**, would take place followed by insertion reaction into the Rh–B bond. Then β-H elimination occurs giving compound **8** and the regeneration of the rhodium hydrido complex **1**. Finally, compound **8** would be activated through the same mechanism than 3,3,3-trifluoropropene affording compound **9** (Scheme 24).

Additionally, complex **3** was first synthesized in an independent reaction by the Braun group<sup>[30]</sup> and employed as a significant species in C–F bond activation, C–H bond activation, C–F bond borylation and N–H bond activation reactions of aromatics as well as hexafluoropropene and 3,3,3-trifluoropropene.<sup>[30, 127-129]</sup> Due to the interesting results, the same protocol with complex **1** was applied to complex **3**. With an excess amount of HBpin, the same products were produced in a 23:23:22:20:3:9 ratio in 30 min with a full conversion of HFO-1234yf (Table 1, entry 4).



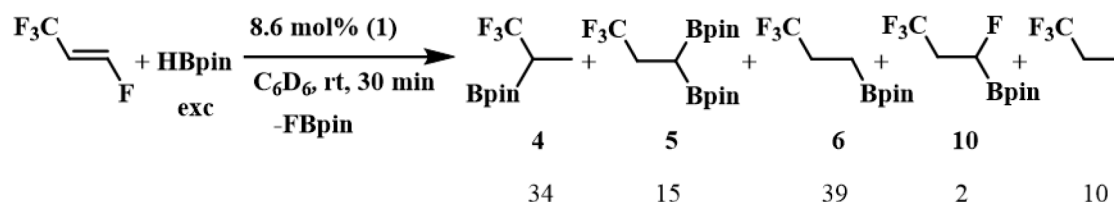
Scheme 24. Plausible mechanism for the formation of compound 9.

Taking every factor such as the reactivity, the selectivity and economy into account, the best reaction conditions so far are the use of complex **1** as catalyst, C<sub>6</sub>D<sub>6</sub> as solvent and an excess amount of HBpin as boron source. Keeping in mind that not only HFO-1234yf but also analogous fluoroolefins may be capable of transformations such as hydroboration and defluorohydroboration. The optimized conditions mentioned above will be applied to other substrates.

### 2.2.1.2 HFO-1234ze

According to a Honeywell report, when taking the balance of performance, cost effectiveness, environmental impact and safety into account, HFO-1234ze (*E*-1,3,3,3-tetrafluoropropene) is agreed to be the best medium pressure, low GWP refrigerant on the market.<sup>[130]</sup> Because of this general interest, the functionalization of HFO-1234ze was also studied. The optimized condition provided a full conversion of HFO-1234ze, with a 34:15:39:2:10 ratio of compounds **4**, **5**, **6**, CF<sub>3</sub>CH<sub>2</sub>CFHBpin (**10**) and 1,1,1-trifluoropropane as well as the formation of FBpin in 30 min (Scheme 25). The <sup>19</sup>F NMR spectrum of compound **10** displayed at -64.6 ppm a triplet of doublets, which simplified to a doublet in the <sup>19</sup>F{<sup>1</sup>H} NMR spectrum, with a <sup>3</sup>*J* fluorine-proton coupling of 10 Hz and <sup>4</sup>*J* fluorine-fluorine coupling constant of 7 Hz for the CF<sub>3</sub> group. The corresponding fluorine signal of the CFH moiety appeared as in **7** at higher field as multiplet, which was supported by the <sup>19</sup>F-<sup>19</sup>F COSY NMR spectrum. It was displayed at -224.5 ppm. A

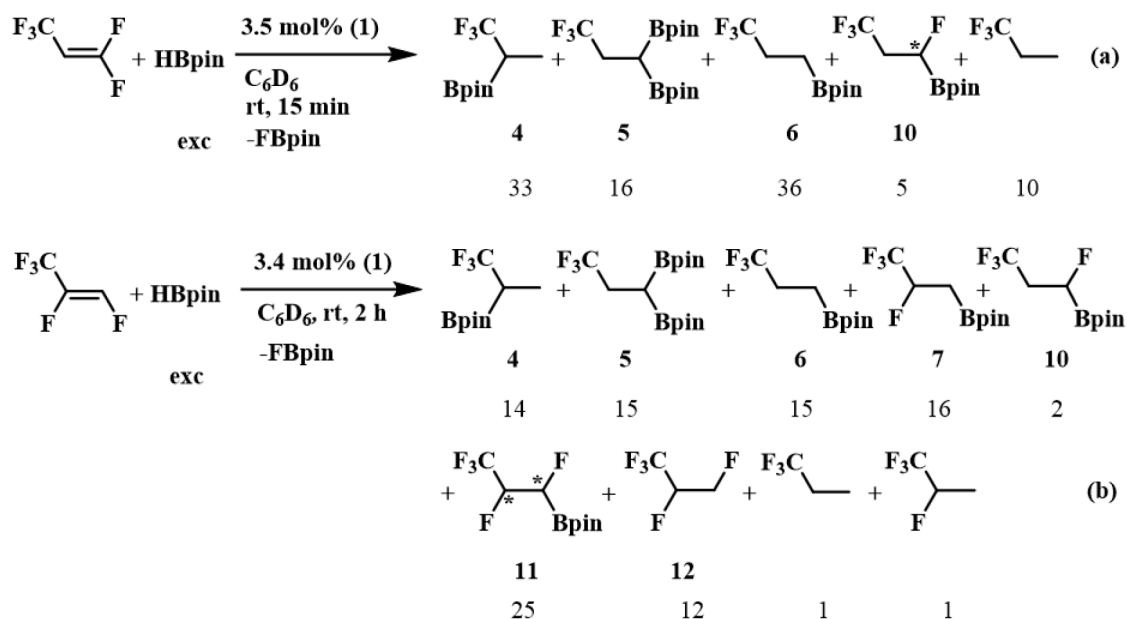
doublet of triplets depicted at 4.02 ppm in the  $^1\text{H}$  NMR spectrum was assigned to the proton on the CFH moiety. The coupling constants of 46.7 and 5.5 Hz were due to the coupling with the *geminal* fluorine and the  $\text{CH}_2$  group, respectively. The proton signal of the  $\text{CH}_2$  moiety was detected at 1.80 ppm by  $^1\text{H}$ - $^1\text{H}$  COSY NMR spectrum. In addition, a peak at  $m/z$  242 in the GC-MS spectrum supported the formation of compound **10**.



Scheme 25. Catalytic reaction of HFO-1234ze and HBpin (ratio in mol%).

### 2.2.1.3 Pentafluoroolefins

The pentafluoropropene, HFO-1225zc (1,1,3,3,3-pentafluoropropene) and HFO-1225ye (Z) (Z-1,2,3,3,3-pentafluoropropene) were suitable as precursors for the formation of tetrafluoroallene.<sup>[131-133]</sup> Apart from that, they are crucial compositions of refrigerants. Therefore, the generality of the optimized catalytic conditions was also investigated on HFO-1225zc and HFO-1225ye (Z). Both reactions with complex **1** as the catalyst and HBpin as the boron source gave a full conversion of the fluorinated olefins after a specific reaction time at room temperature. The reaction with HFO-1225zc afforded in 15 min mixture of products **4**, **5**, **6**, **10** and 1,1,1-trifluoropropane in a 33:16:36:5:10 ratio along with the formation of FBpin (Scheme 26a); while **4**, **5**, **6**, **7**, **10**,  $\text{CF}_3\text{CFHCFH}(\text{Bpin})$  (**11**),  $\text{CF}_3\text{CFHCFH}_2$  (**12**),<sup>[123]</sup> 1,1,1-trifluoropropane and 1,1,1,2-tetrafluoropropane were observed in a ratio of 14:15:15:16:2:25:12:1:1 as well as the production of FBpin after 2 h for HFO-1225ye (Z) (Scheme 26b). Note that structure of compound **11** was proposed tentatively. The  $^{19}\text{F}$  NMR spectrum of compound **11** displayed a triplet of doublets, which simplified as triplet in the  $^{19}\text{F}\{^1\text{H}\}$  NMR spectrum, at -75.7 ppm with a fluorine-fluorine coupling constant of 10 Hz and a fluorine-proton coupling constant of 6 Hz for  $\text{CF}_3$  group. According to the  $^{19}\text{F}$ - $^{19}\text{F}$  NMR spectrum, the corresponding signals for CFH and CFH(Bpin) moieties were observed at -207.2 and -241.8 ppm as pseudo triplet of multiplets and multiplet, respectively. The resonance at -207.2 ppm had a coupling constant of 41 Hz to the *geminal* proton and the proton of the CFH(Bpin) moiety and it simplified in the  $^{19}\text{F}\{^1\text{H}\}$  NMR spectrum to a quartet of doublets with coupling constants of 10 and 7 Hz to fluorine atoms of  $\text{CF}_3$  and CFH(Bpin) groups, respectively. A peak of  $m/z$  245 in the GC-MS spectrum indicated the presence of compound **11**.



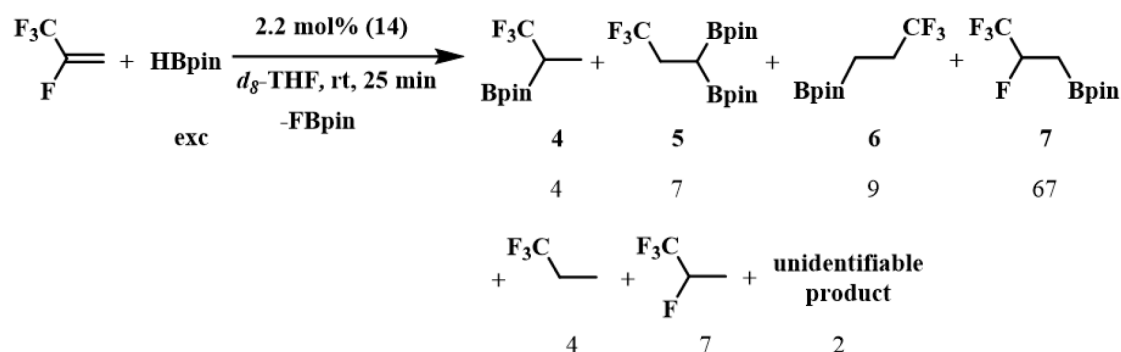
Scheme 26. Catalytic reaction of HFO-1225zc (a) or HFO-1225ye (Z) (b) and HBpin (ratio in mol%).

### 2.2.2 Catalytic hydroboration reactions of $CF_3$ containing olefins with the rhodium complex $[Rh(\mu-Cl)(P^iPr_3)_2]_2$ (**14**)

Different attempts such as changing of the rhodium(I) catalysts, solvents and boron sources were examined above to try to improve the selectivity of the catalytic reaction of HFO-1234yf. Unfortunately, neither of them provided better selectivity. Besides, one of the rhodium(I) precursors of complex **1**— $[Rh(Cl)(PEt_3)_3]$  was tested showing the same selectivity but worse reactivity when compared with complex **1**. According to Iwasawa and coworkers, a C–H bond activation was involved in the catalytic direct carboxylation of aromatic compounds.<sup>[134]</sup> They proposed the dimeric complex,  $[Rh(\mu-Cl)(PCy_3)_2]_2$ , as the active catalyst which was formed *in situ* from the precursor rhodium complex  $[Rh(\mu-Cl)(COE)_2]_2$  (**13**) and the bulky phosphine co-ligand  $PCy_3$ .<sup>[134]</sup> Thus, the *in situ* formation of a dimeric rhodium phosphine complex from  $[Rh(\mu-Cl)(COE)_2]_2$  (**13**) and  $P^iPr_3$  was tested in the catalytic reactions of  $CF_3$  containing olefins.

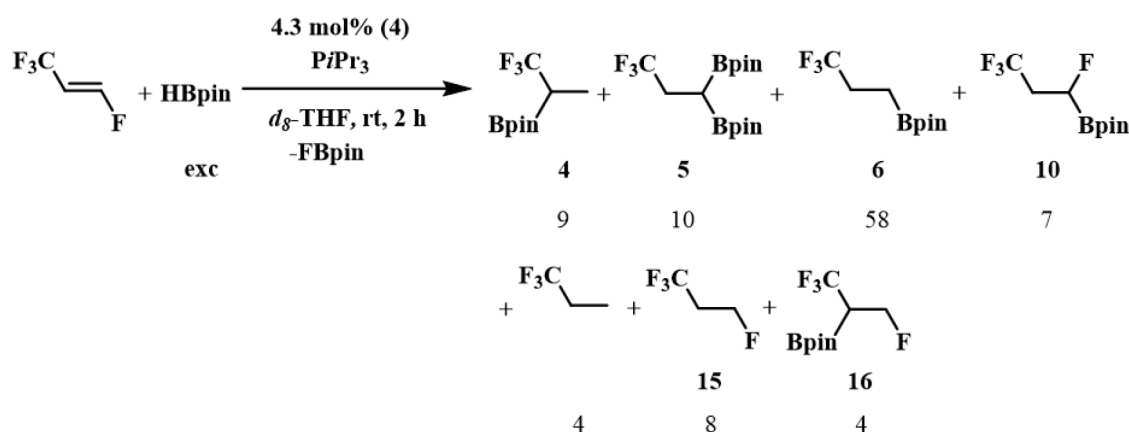
As a result, complex  $[Rh(\mu-Cl)(P^iPr_3)_2]_2$  (**14**) was generated. Then reaction of HFO-1234yf with an excess amount of HBpin in  $d_8$ -THF employing the *in situ* formed complex **14** as the catalyst was initiated affording the same products mixture as before (ratio 4:7:9:67:4:7) as well as an unidentified product (2 %) with a full conversion of HFO-1234yf in 25 min (Scheme 27). Unfortunately, only a doublet at -65.1 ppm with a fluorine-proton coupling constant of 11 Hz in the  $^{19}F$  NMR spectrum can be assigned to the unidentified product. Importantly, compared with the previous reactions of the same

substrate, the amount of product **7** (67 %) increased and an improvement of the selectivity was observed.



Scheme 27. Catalytic reaction of HFO-1234yf using rhodium dimer **14** as the catalyst (ratio in mol%).

Inspired by the result, the strategy was applied to HFO-1234ze, HFO-1225zc and HFO-1225ye (Z). For the reaction with HFO-1234ze, besides the same products mixture when employing rhodium hydrido complex **1** as catalyst, new compounds CF<sub>3</sub>CH<sub>2</sub>CFH<sub>2</sub> (**15**)<sup>[135]</sup> and CF<sub>3</sub>CH(Bpin)CFH<sub>2</sub> (**16**) were afforded (Scheme 28). Among them, the amount of compound CF<sub>3</sub>CH<sub>2</sub>CH<sub>2</sub>(Bpin) (**6**) was enhanced from 39 % to 58 %. The structure of **16** was proposed only based on the <sup>19</sup>F NMR spectrum. Two signals that appeared at -62.8 and -217.9 ppm as doublet of doublets and multiplet, respectively, could be assigned to the CF<sub>3</sub> and CFH<sub>2</sub> moiety of this compound. The resonance at -62.8 ppm showed a <sup>3</sup>J fluorine-proton coupling constant of 11 Hz and <sup>4</sup>J fluorine-fluorine coupling constant of 7 Hz and simplified to doublet in the <sup>19</sup>F{<sup>1</sup>H} NMR spectrum.



Scheme 28. Catalytic reaction of HFO-1234ze using rhodium dimer **5** as the catalyst (ratio in mol%).

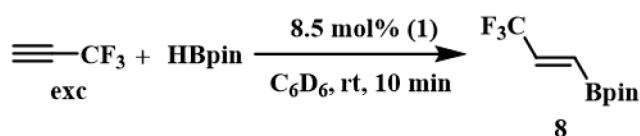
When using HFO-1225zc as the starting material, **4**, **5**, **6**, **10**, 1,1,1-trifluoropropane and a new compound **15** were generated in a 8:28:32:5:14:13 ratio as well as the formation of FBpin. The selectivity changed but the main product was still the defluorohydroboration compound **6**. With the treatment of HFO-1225ye (Z), the same products mixture except

**10** as the reaction with complex **1** were generated. Interestingly, the ratio of the defluorohydroboration compound **7** increased to 49 %. However, catalyst  $[\text{Rh}(\mu\text{-Cl})(\text{P}i\text{Pr}_3)_2]_2$  (**14**) is not as effective as catalyst **1**. The NMR spectra showed the full conversion of HFO-1234ze, HFO-1225zc and HFO-1225ye in 2 h, 20 h and 20 h when employing complex  $[\text{Rh}(\mu\text{-Cl})(\text{P}i\text{Pr}_3)_2]_2$  (**14**) as the catalyst.

### 2.2.3 Studies on the reactivity of 3,3,3-trifluoropropyne with rhodium complexes

#### 2.2.3.1 Catalytic hydroboration reactions of 3,3,3-trifluoropropyne

Even though hydroboration of alkynes has been investigated in the last decade,<sup>[44-45, 92-94]</sup> 3,3,3-trifluoropropyne has never been tested. Aiming to expand the scope with the catalytic system HBpin as boron source and  $[\text{Rh}(\text{H})(\text{P}Et_3)_3]$  (**1**) as the catalyst, the 3,3,3-trifluoropropyne as substrate was explored. This substrate can undoubtedly lead to new building blocks. Treatment of an excess of 3,3,3-trifluoropropyne with HBpin gave the anti-Markovnikov hydroboration product  $\text{CF}_3\text{CH}=\text{CHBpin}$  (**8**) with high selectivity at room temperature in 10 min when 8.5 % of the catalyst **1** was employed (Scheme 29). When 5 % of complex **1** was used, the reaction time increased to 4 h with the same outcome. In contrast to a reported copper-catalyzed defluoroboration reaction,<sup>[117]</sup> these studies resulted in a milder and higher efficient protocol to synthesize compound **8**.



Scheme 29. Catalytic hydroboration reaction of trifluoropropyne and HBpin.

The stoichiometric reactions between the rhodium hydrido complex  $[\text{Rh}(\text{H})(\text{P}Et_3)_3]$  (**1**) and 3,3,3-trifluoropropyne were studied by the Braun group.<sup>[72]</sup> The result showed that based on the ratio of the starting materials, complex  $[\text{Rh}(\text{C}\equiv\text{CCF}_3)(\text{P}Et_3)_3]$  (**17**) (together with *fac*- $[\text{Rh}(\text{C}\equiv\text{CCF}_3)_2(\text{H})(\text{P}Et_3)_3]$  (**18**) with a 9:1 ratio) or a mixture of the rhodium(III) complexes **18** and *fac*- $[\text{Rh}\{(E)\text{-CH}=\text{CHCF}_3\}(\text{C}\equiv\text{CCF}_3)_2(\text{P}Et_3)_3]$  (**19**) (ratio 5:1) can be formed separately.

The catalytic reactivity of these complex mixtures towards 3,3,3-trifluoropropyne was also studied. The complex **17** (together with **18**, ratio 9:1) and the mixture of **18** and **19**

(ratio 5:1) were used separately affording the same product mixtures in a full consumption of HBpin. A comparison among all catalysts is depicted in Table 2.

Table 2. Catalytic hydroboration reaction of 3,3,3-trifluoropropyne with rhodium complexes.

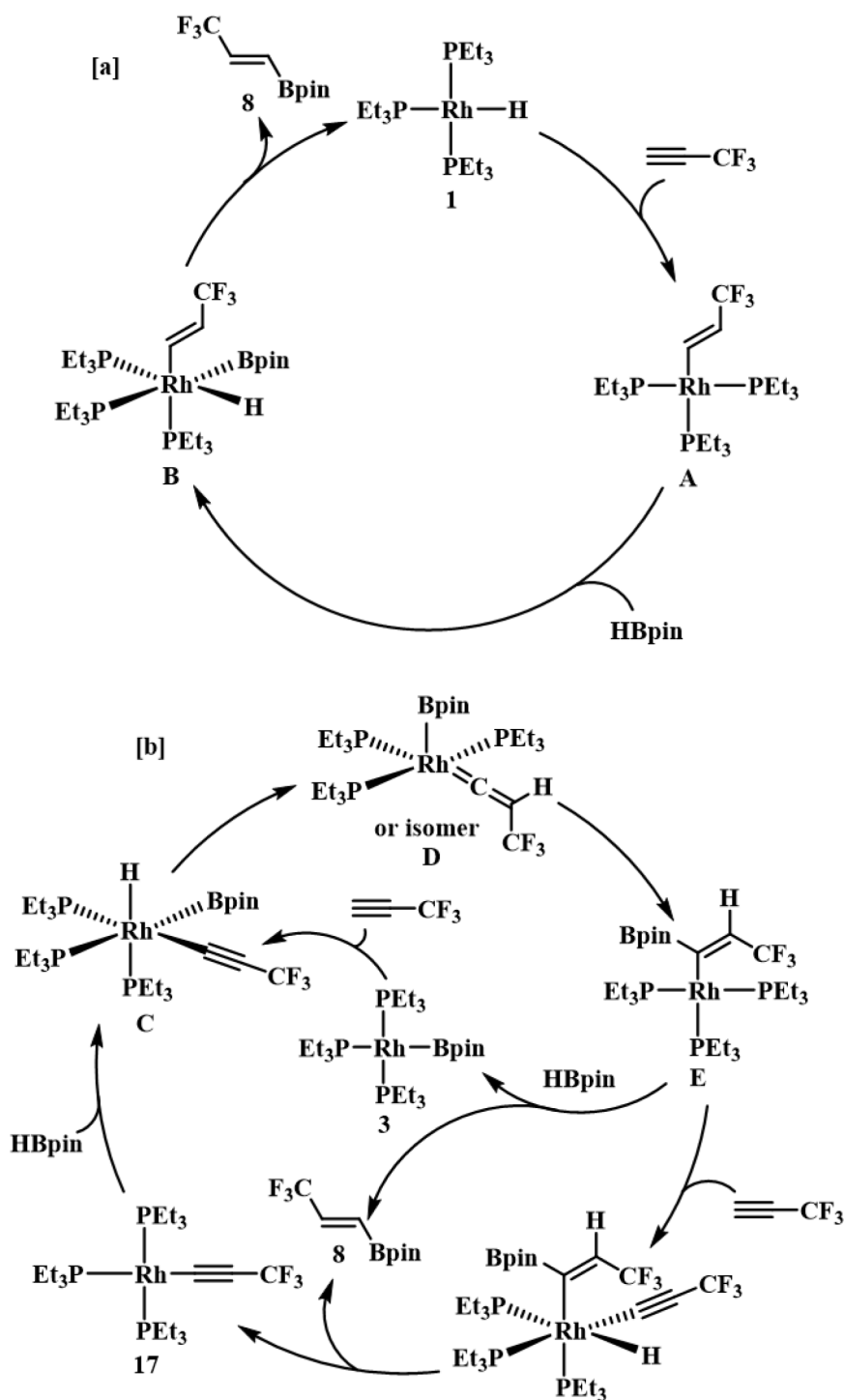
Catalyst	mol %	Reaction time	Yield (%) <sup>a</sup>
<b>1</b>	8.5	10 min	94
<b>1</b>	5.0	4 h	96
<b>17</b> and <b>18</b> (ratio 9:1)	5.0	3 h	96
<b>18</b> and <b>19</b> (ratio 5:1)	5.6	5 h	94

a) Based on the <sup>19</sup>F NMR spectrum.

### 2.2.3.2 Mechanisms of the catalytic conversions

Several different conceivable mechanisms are proposed for the catalytic conversions. For the rhodium hydrido complex **1**, an insertion reaction at Rh–H bond is initiated to afford the  $\beta$ -CF<sub>3</sub>-vinyl complex [Rh(CH=CHCF<sub>3</sub>)(PEt<sub>3</sub>)<sub>3</sub>] (**A**) and followed by an oxidative addition reaction of HBpin to form the rhodium(III) complex *fac*-[Rh(Bpin)(CH=CHCF<sub>3</sub>)(H)(PEt<sub>3</sub>)<sub>3</sub>] (**B**). Complex **1** is regained as well as the release of **8** through the reductive elimination reaction at complex **B** (Scheme 30a). Regarding complex **17** as the catalyst, an initial oxidative addition of HBpin gives a rhodium(III) complex *fac*-[Rh(Bpin)(C $\equiv$ CCF<sub>3</sub>)(H)(PEt<sub>3</sub>)<sub>3</sub>] (**C**), which undergoes a further rearrangement to form the vinylidene complex [Rh(Bpin)(=C=CHCF<sub>3</sub>)(PEt<sub>3</sub>)<sub>3</sub>] (**D**). Bpin ligand migration leads to the generation of the vinyl complex [Rh((Bpin)C=CHCF<sub>3</sub>)(PEt<sub>3</sub>)<sub>3</sub>] (**E**). At this point, oxidative addition of HBpin or the fluorinated alkyne can take place. Complex **3** is formed in the presence of HBpin while complex **17** is regenerated under 3,3,3-trifluoropropyne. In both cases **8** would be released. Note that complex **3** can be transformed to the oxidative addition complex **C** when treated with 3,3,3-trifluoropropyne (Scheme 30b). As it is reported by the Braun group, complex *fac*-[Rh(C $\equiv$ CCF<sub>3</sub>)<sub>2</sub>(H)(PEt<sub>3</sub>)<sub>3</sub>] (**18**) may play a role of being a source of alkynyl complex [Rh(C $\equiv$ CCF<sub>3</sub>)(PEt<sub>3</sub>)<sub>3</sub>] (**17**) by releasing 3,3,3-trifluoropropyne.



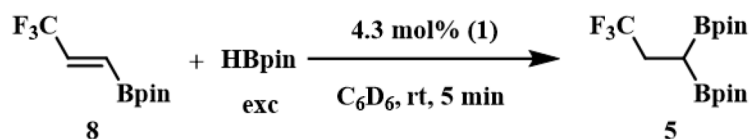


Scheme 30. Possible mechanisms for the catalytic hydroboration of 3,3,3-trifluoropropyne.

### 2.2.3.3 Catalytic dihydroboration reactions of 3,3,3-trifluoropropyne

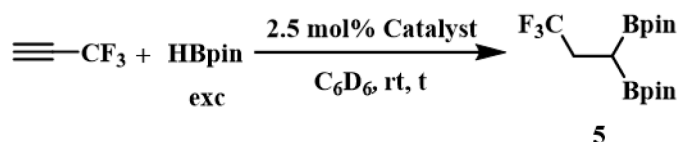
Apart from the mentioned substrates HFO-1234yf and its analogues, other alkenes are reported to achieve hydroboration products easily.<sup>[61, 136-139]</sup> Therefore, the reactivity of compound **8** and  $\text{HBpin}$  was tested in an independent reaction. After the isolation of the monoborylated olefin **8**, it was fully converted into the dihydroborated compound **5** by

its treatment with an excess amount of HBpin employing the rhodium hydrido complex **1** as the catalyst (Scheme 31).



*Scheme 31. Independent catalytic hydroboration reaction of **8** with an excess of HBpin.*

Encouraged by this result, the reaction of 3,3,3-trifluoropropyne and an excess amount of HBpin was attempted (Scheme 32). Similar to the studies of the formation of the monoborylated olefin **8**, complex **1**, complex mixture **17** and **18** and complex mixture **18** and **19** were tested demonstrating that compound **5** can be generated in high regioselectivity and 3,3,3-trifluoropropyne was converted completely (Table 3).



*Scheme 32. Catalytic dihydroboration reactions of 3,3,3-trifluoropropyne with an excess amount of HBpin.*

Interestingly, NMR spectroscopy showed the appearance of 91 % of compound **8** and conversion of 94 % of the alkyne after 25 min when using the complex mixture of **18** and **19** as the catalyst. Afterwards, the signals of compound **5** were slowly increasing until the complete conversion was reached within 3 h (Table 3).

*Table 3. Catalyst comparison of catalytic dihydroboration reactions of 3,3,3-trifluoropropyne and an excess amount of HBpin.*

Catalyst (2.5 mol%)	Reaction time (t)	Yield (%) <sup>a</sup>
<b>1</b>	20 min	96
<b>17</b> and <b>18</b> (ratio 9:1)	10 min	95
<b>18</b> and <b>19</b> (ratio 5:1)	3 h	97

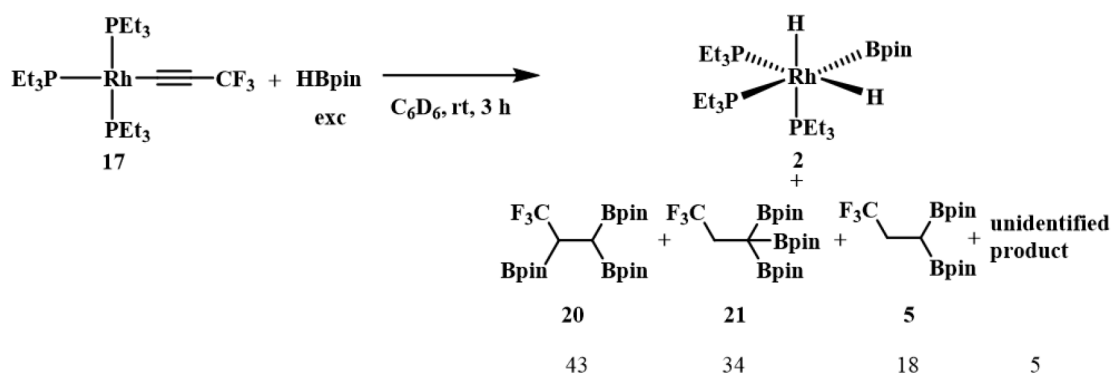
a) Based on the <sup>19</sup>F NMR spectrum.

The borylated alkane **5** was generated in a less selective way in the previous investigations with hexafluoropropene, 3,3,3-trifluoropropene, HFO-1234yf, HFO-1234ze and their analogues as starting compounds, in which defluoroboration or dehydroboration

accompanied by hydroboration occurred to form the corresponding compound.<sup>[61]</sup> In contrast, the same compound **5** can be formed selectively in the protocol with 3,3,3-trifluoropropyne. This is the first protocol of synthesizing compound **5** in a high selective and efficient way, according to Scifinder.<sup>[140]</sup>

#### 2.2.3.4 Stoichiometric hydroboration reaction of rhodium(I) alkyl complex and HBpin

Because of the close electronic system to the cyano ligand, the trifluoropropynyl group was previously studied as a surrogate for the cyano ligand.<sup>[49]</sup> Additionally, a C–H bond activation reaction was achieved by  $[\text{RhTp}'(\text{PMe}_3)]$  ( $\text{Tp}' = \text{Tris-(3,5-dimethylpyrazolyl)borate}$ ) on 3,3,3-trifluoropropyne yielding a trifluoropropynyl bonded rhodium complex  $[\text{Rh}(\text{Tp}')(\text{H})(\text{C}\equiv\text{CCF}_3)(\text{PMe}_3)]$ .<sup>[50]</sup> Noteworthy is that a further reactivity investigation of trifluoroalkynyl complexes has not been explored yet. Besides, to further investigate the catalytic reaction and to explore the reactivity of trifluoroalkynyl complex, 2.1 equivalents of HBpin was added to a  $\text{C}_6\text{D}_6$  solution of complex **17**. Consequently, the rhodium(III) complex *fac*- $[\text{Rh}(\text{Bpin})(\text{H})_2(\text{PEt}_3)_3]$  (**2**) as well as hydroboration compounds  $\text{CF}_3\text{CH}(\text{Bpin})\text{CH}(\text{Bpin})_2$  (**20**),  $\text{CF}_3\text{CH}_2\text{C}(\text{Bpin})_3$  (**21**) and compound **5** as main organic products were obtained in a ratio of 43:34:18 in 3 h. In addition, one product, which was unidentified was observed (Scheme 33).

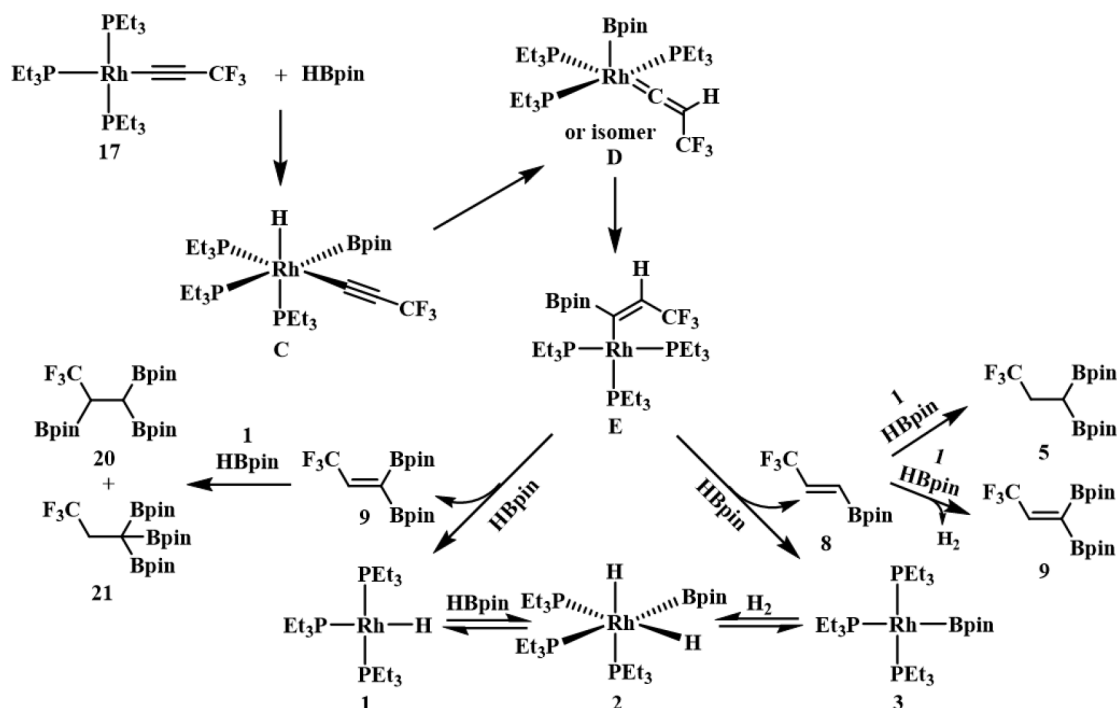


Scheme 33. Stoichiometric hydroboration reaction of rhodium(I) alkynyl complex **17**.

In the  $^{19}\text{F}$  NMR spectrum, the doublet at -63.4 ppm with a  $^3J$  fluorine-proton coupling constant of 12 Hz was due to the  $\text{CF}_3$  group of compound **20** while the triplet shown at -63.5 ppm with same  $^3J$  fluorine-proton value belongs to the  $\text{CF}_3$  group of compound **21**. The quartet of doublets exhibited at 2.54 ppm in the  $^1\text{H}$  NMR spectrum with a coupling constant of 12.2 Hz to fluorine atoms and 8.9 Hz to proton atom was assigned to the proton on the  $\text{CF}_3\text{CH}$  moiety of compound **20**. Based on the  $^1\text{H}$ - $^1\text{H}$  COSY NMR spectrum, the corresponding signal for the proton of the  $\text{CH}(\text{Bpin})_2$  fragment appeared at

1.43 ppm as a multiplet. On the other hand, a signal at 2.94 ppm displayed as quartet was attributed to the CH<sub>2</sub> moiety of compound **21**. The GC-MS data confirmed the presence of [20-CH<sub>3</sub>]<sup>+</sup> and **21** with their peaks at *m/z* 461 and 476, respectively.

For the formation of compounds **20**, **21** and **5**, a conceivable mechanism is proposed with the initial formation of *fac*-[Rh(Bpin)(C≡CCF<sub>3</sub>)(H)(PEt<sub>3</sub>)<sub>3</sub>] (**C**) through oxidative addition reaction. Afterwards, the rhodium vinylidene complex [Rh(Bpin)(=C=CHCF<sub>3</sub>)(PEt<sub>3</sub>)<sub>3</sub>] (**D**) is generated and followed by the migration of boryl group yielding the vinyl complex **E**, as afore mentioned.



Scheme 34. Plausible mechanism for the reaction of **17** and HBpin.

Then in the presence of HBpin, borylated olefin **8** or a diborylated alkene is released together with the formation of rhodium boryl complex **3** or rhodium hydrido complex **1**, respectively. Alternatively, the diborylated alkene can be formed by dehydrogenative borylation of **8** releasing H<sub>2</sub>. The appearance of borylated alkanes **20** and **21** are attributed to the subsequent hydroboration reaction of the diborylated alkene and the formation of **5** is due to the hydroboration reaction of borylated olefin **8** catalyzed by rhodium complexes as shown before. In contrast to the stoichiometric reaction, compounds **20** and **21** were achieved just in traces in the catalytic reaction with HBpin added in excess. The rhodium(III) complex *fac*-[Rh(Bpin)(H)<sub>2</sub>(PEt<sub>3</sub>)<sub>3</sub>] (**2**) can be generated easily through oxidative addition reaction of H<sub>2</sub> or HBpin to complex **3** or **1**, respectively (Scheme 34).<sup>[30, 61, 129]</sup>

In conclusion, HFO-1234yf, HFO-1234ze, HFO-1225zc and HFO-1225ye (Z) were transformed into the corresponding defluorohydroboration, hydroboration, defluorohydrogenation and defluoroboration-hydroboration products efficiently but not selectively using rhodium hydrido complex **1** as the catalyst, C<sub>6</sub>D<sub>6</sub> as the solvent and HBpin as the boron source. However, 3,3,3-trifluoropropyne was converted efficiently and selectively to the hydroboration product CF<sub>3</sub>CH=CHBpin (**8**) or dihydroboration product CF<sub>3</sub>CH<sub>2</sub>CH(Bpin)<sub>2</sub> (**5**) under the same conditions. When [Rh( $\mu$ -Cl)(P*t*Pr<sub>3</sub>)<sub>2</sub>]<sub>2</sub> (**14**) was employed in the reaction of HFO-1234yf, HFO-1234ze and HFO-1225ye (Z), the amount of hydroboration, defluorohydroboration and monodefluorohydroboration products were enhanced, respectively. Further research could investigate olefins without CF<sub>3</sub> group or with other fluorinated moiety.



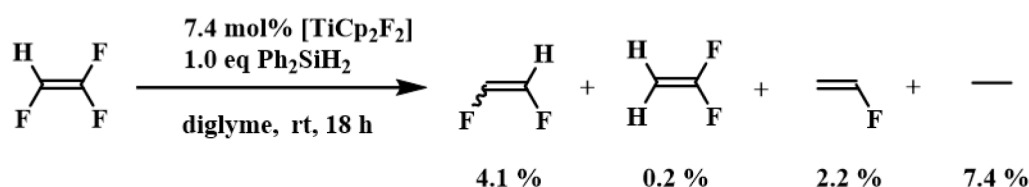
## 3. C–F bond activation of fluorinated olefins towards rhodium(I) complexes

### 3.1 Introduction

Fluorinated polymers exhibit a combination of properties and are, therefore, widely used. Fluorinated ethylenes are the fundamental monomers for the synthesis of several fluorinated polymers.<sup>[141]</sup> Hence, the study of the fluorinated ethylenes is valuable. Reactivities of tetrafluoroethylene have been well explored. Regarding reactions involving boron containing compounds, C<sub>2</sub>F<sub>4</sub> was employed mainly as a starting material to construct new building blocks through three or more components coupling reactions.<sup>[142-143]</sup> Nevertheless, the defluoroboration reaction was achieved at the copper complex catalyst [Cu(IPr)(OtBu)] (IPr = 1,3-bis(2,6-diisopropylphenyl)-imidazol-2-ylidene).<sup>[117]</sup>

Regarding 1,1,2-trifluorobutene and trifluoroethylene, derivatization of 1,1,2-trifluorobutene was accomplished through alkylation of tetrafluoroethylene in the presence of a lithium salt.<sup>[144]</sup> Reactivity investigation of 1,1,2-trifluorobutene are rare at transition metals or main group elements,<sup>[145]</sup> while studies with trifluoroethylene have been more conducted.

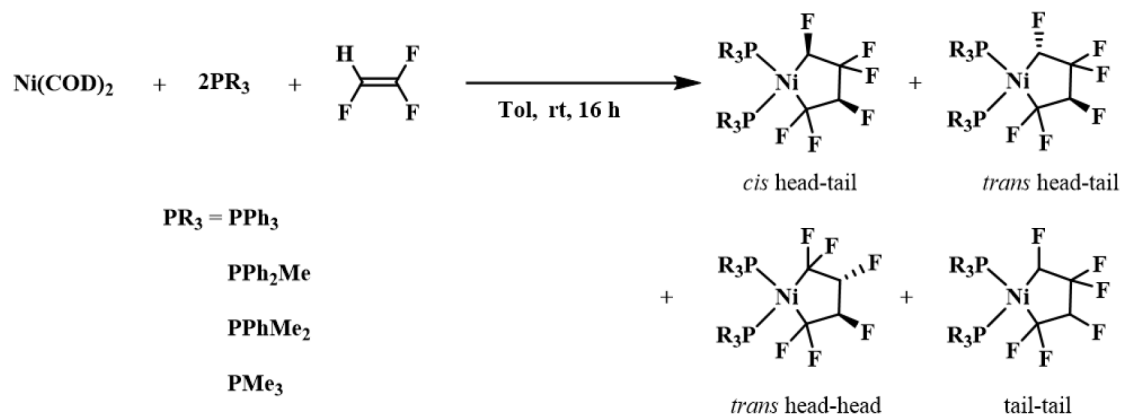
In 2012, Lentz and coworkers published a catalytic hydrodefluorination reaction in which trifluoroethylene was treated with the precatalyst titanocene difluoride and a secondary silane affording several hydrodefluorination products and an additional hydrogenation product (Scheme 35).<sup>[146]</sup>



*Scheme 35. Titanium catalyzed hydrodefluorination of trifluoroethylene.*

Apart from the exploration of catalytic reactivities, stoichiometric studies exhibited outstanding outcomes. It is known that the generation of metallacyclic intermediates through the oxidative cyclization of unsaturated substrates at low valent metal centers is an efficient process for atom economical C–C bond formation.<sup>[147-148]</sup> Stone *et al.* reported

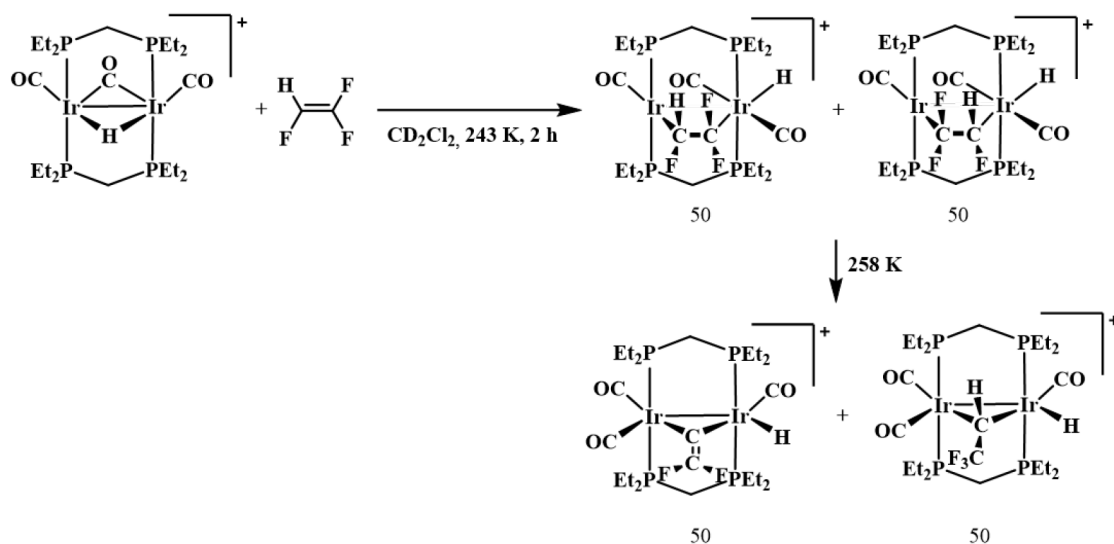
in 1970 the first investigations on the reactivity of trifluoroethylene at  $[\text{Ni}(\text{PPh}_2\text{Me})_4]$  and  $[\text{Ni}(\text{C}_2\text{H}_4)(\text{PPh}_3)_2]$  where a 5-membered nickelacycles  $[\text{Ni}(\text{C}_4\text{F}_6\text{H}_2)\text{L}_2]$  ( $\text{L} = \text{PPh}_2\text{Me}$  or  $\text{PPh}_3$ ) were generated.<sup>[147, 149]</sup> Afterwards, Baker and coworkers investigated the ligand effects on the regio- and stereoselectivity in the reaction of Ni complexes and trifluoroethylene (Scheme 36).<sup>[148]</sup> Even though whether the steric or the electronic properties of the ligands give a bigger effect was not figured out, the ratio among the four generated isomers changed along with the used ligands.



Scheme 36. The formation of hydrofluoronickelacyclopentanes.

Apart from the investigation of the above mentioned transition metals, treatment of the diiridium complex  $[\text{Ir}_2(\mu\text{-H})(\text{CO})_3(\text{depm})_2][\text{BAr}^{\text{F}}_4]$  ( $\text{depm} = \text{Bis}(\text{diethylphosphino})\text{methane}$ ) ( $\text{BAr}^{\text{F}}_4 = \text{B}(3,5\text{-(CF}_3)_2\text{C}_6\text{H}_3)_4$ ) with trifluoroethylene was conducted by Cowie and coworkers. Two isomers of  $[\text{Ir}_2(\text{H})(\mu\text{-CFHCF}_2)(\text{CO})_3(\text{depm})_2][\text{BAr}^{\text{F}}_4]$  were formed at 243 K. While warming up the mixture to 258 K, the complex  $[\text{Ir}_2(\text{H})(\mu\text{-C}=\text{CF}_2)(\text{CO})_3(\text{depm})_2][\text{BAr}^{\text{F}}_4]$  and complex  $[\text{Ir}_2(\text{H})(\mu\text{-CHCF}_3)(\text{CO})_3(\text{depm})_2][\text{BAr}^{\text{F}}_4]$  were afforded by C–F/C–H bond activation or a [1,2]-fluoride shift, respectively (Scheme 37).<sup>[150]</sup>





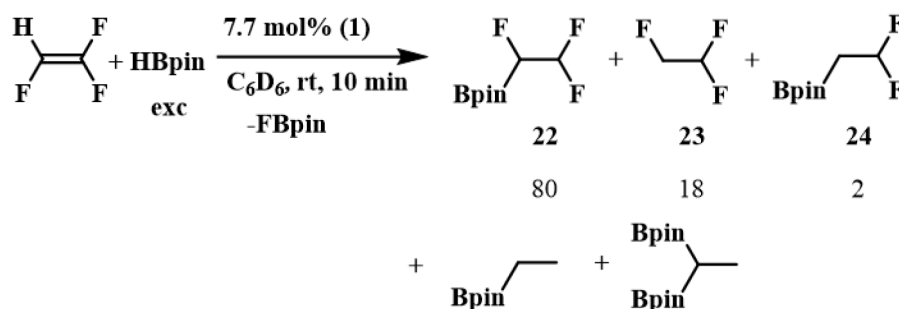
Scheme 37. Activation of trifluoroethylene at diiridium complex (ratio in mol%).

However, the reactivity of trifluoroethylene towards rhodium complex was not explored yet. Therefore, the study of 1,1,2-trifluorobutene and trifluoroethylene at rhodium complex will be interesting.

## 3.2 Results and discussion

### 3.2.1 Catalytic reactions

In the previous chapter, HFO-1234yf and analogues were transformed into the corresponding defluorohydroboration, hydroboration, defluorohydrogenation and defluoroboration-hydroboration products when using rhodium hydrido complex  $[\text{Rh}(\text{H})(\text{PEt}_3)_3]$  (**1**) as the catalyst and an excess amount of HBpin as the boron source. Thus, it is interesting to apply the same reaction conditions to trifluoroethylene. As a result, the hydroboration compound  $\text{CF}_2\text{HCFH}(\text{Bpin})$  (**22**), hydrogenation product  $\text{CF}_2\text{HCFH}_2$  (**23**)<sup>[151]</sup> and traces of defluorohydroboration compounds  $\text{CF}_2\text{HCH}_2(\text{Bpin})$  (**24**),  $\text{CH}_3\text{CH}_2(\text{Bpin})$ <sup>[152-153]</sup> and  $\text{CH}_3\text{CH}(\text{Bpin})_2$ <sup>[154]</sup> were afforded with a full conversion of trifluoroethylene in 10 min at room temperature in  $\text{C}_6\text{D}_6$  (Scheme 38). The  $^{19}\text{F}$  NMR spectrum showed a ratio of 80:18:2 among the fluorinated compounds **22**:**23**:**24**, while the rest of the proposed products were confirmed by GC-MS.



Scheme 38. Catalytic reaction of trifluoroethylene with HBpin (ratio in mol%).

In the  $^{19}\text{F}$  NMR spectrum of **22**, two groups of doublet of triplets which can be assigned to the  $\text{CF}_2\text{H}$  moiety appeared at -126.4 and -126.5 ppm with a coupling constant of 54 Hz or 53 Hz to the *geminal* proton and 15 Hz or 17 Hz to the proton and the fluorine atom of the  $\text{CFH}$  moiety. The difference of the two fluorine atoms of the  $\text{CF}_2\text{H}$  moiety can be explained by the existence of the adjacent chiral center and was also observed for other compounds<sup>[155-157]</sup>. The corresponding fluorine of the  $\text{CFH}$  moiety exhibited at -242.7 ppm as a broad signal. The resonance of the proton of the  $\text{CF}_2\text{H}$  moiety was shown at 5.72 ppm as pseudo triplet of doublet of doublets with a  $^2J$  proton-fluorine coupling constant of 54.3 Hz,  $^3J$  proton-fluorine coupling constant of 11.8 Hz and  $^3J$  proton-proton coupling constant of 2.8 Hz in the  $^1\text{H}$  NMR spectrum. The doublet of doublet of doublet of doublets at 4.32 ppm with a coupling constant of 45.8 Hz to the *geminal* fluorine, 18.8 and 16.2 Hz to the  $\text{CF}_2$  moiety and 2.8 Hz to the proton was due

to the proton of the CFH moiety. In the GC-MS spectrum, a peak of  $m/z$  210 confirmed the presence of compound **22**.

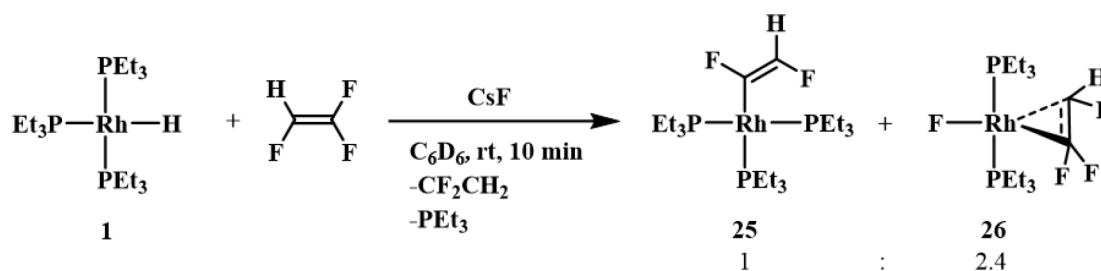
For compound **23**, a doublet of doublet of triplets which simplified to a doublet in the  $^{19}\text{F}\{^1\text{H}\}$  NMR spectrum was observed at -129.8 ppm in the  $^{19}\text{F}$  NMR spectrum. The splitting is assigned to the  $\text{CF}_2\text{H}$  moiety with coupling constants of 54 Hz, 18 Hz and 13 Hz, which were attributed to the *geminal* proton, fluorine atom of the  $\text{CFH}_2$  moiety and protons of the  $\text{CFH}_2$  moiety. The signal of the other fluorine atom at -240.8 ppm appeared as triplet of triplet of doublets and simplified to triplet in the  $^{19}\text{F}\{^1\text{H}\}$  NMR spectrum. It has a coupling constant of 46 Hz to the *geminal* proton, 18 Hz to the fluorine of the  $\text{CF}_2\text{H}$  moiety and 7 Hz to the proton of the  $\text{CF}_2\text{H}$  moiety. The  $^1\text{H}$  NMR data are consistent with the literature.<sup>[151]</sup>

The structure of compound **24** was proposed only based on the signal in the  $^{19}\text{F}$  NMR spectrum, in which a signal was observed as a doublet of triplet at -106.0 ppm. The signal showed a coupling constant of 58 Hz to the *geminal* proton and 20 Hz to the adjacent protons and simplified to a singlet in the  $^{19}\text{F}\{^1\text{H}\}$  NMR spectrum.

The same reaction conditions (HBpin as the boron source and rhodium hydrido complex  $[\text{Rh}(\text{H})(\text{PEt}_3)_3]$  (**1**) as the catalyst) were also applied to 1,1,2-trifluorobutene. However, only traces of products were produced based on the  $^{19}\text{F}$  NMR spectrum, which were not characterized further.

### 3.2.2 Stoichiometric reactions

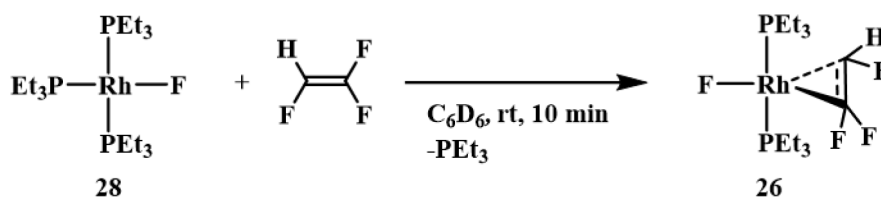
To investigate the reactivity of the rhodium hydrido complex  $[\text{Rh}(\text{H})(\text{PEt}_3)_3]$  (**1**) towards trifluoroethylene, treatment of complex **1** with trifluoroethylene (ratio 1:2.8) was conducted in the presence of CsF at room temperature affording the C–F bond activation complex  $[\text{Rh}((Z)\text{-CFCFH})(\text{PEt}_3)_3]$  (**25**), complex *trans*- $[\text{Rh}(\text{F})(\eta^2\text{-CF}_2\text{CFH})(\text{PEt}_3)_2]$  (**26**) and 1,1-difluoroethylene as well as free phosphine in 10 min (Scheme 39). Note that, when reacting complex **1** and trifluoroethylene in a 1:1 ratio without CsF, complex **25** and rhodium fluoro complex  $[\text{Rh}(\text{F})(\text{PEt}_3)_3]$  (**28**)<sup>[59]</sup> were formed in 10 min. Unfortunately, complex **25** cannot be isolated. Therefore, its further investigation with HBpin cannot be conducted.



Scheme 39. Stoichiometric reaction of rhodium complex **1** with trifluoroethylene.

The formation of complex **25** resembles the formation of  $[\text{Rh}((Z)\text{-CF}=\text{CFCH}_3)(\text{PEt}_3)_3]$  when complex **1** reacted with 1,1,2,3,3,3-hexafluoropropene.<sup>[59]</sup> For complex **25**, two signals appeared in the  $^{31}\text{P}\{^1\text{H}\}$  NMR spectrum at 20.3 and 17.3 ppm in a 1:2 ratio as doublet of apparent quartets and doublet of doublet of multiplets, respectively. The former signal showed a coupling constant of 122.1 Hz to rhodium atom and 36.3 Hz to the fluorine atom at the  $\alpha$ -carbon and the two *cis* phosphorus atoms, assigning this resonance to the *trans* phosphine ligand. The signal for the two equivalent phosphine ligands depicted a coupling constant of 147.4 Hz to rhodium atom, giving evidence of the existence of Rh(I) complex, and 37.1 Hz to the inequivalent phosphorus atoms. In the  $^{19}\text{F}$  NMR spectrum, two resonances were assigned to complex **25**. A doublet of multiplets with a fluorine-fluorine coupling constant of 109 Hz was observed at -128.5 ppm, which simplified to a doublet of doublet of doublet of triplets in the  $^{19}\text{F}\{^1\text{H}\}$  NMR spectrum with additional coupling of 35 Hz to the phosphine ligand *trans* to the fluorinated moiety, 8 Hz to the rhodium atom and 4 Hz to the two phosphine ligands in the mutual *trans* position. The signal is due to the fluorine atom bound at the  $\alpha$ -carbon. The resonance for the fluorine on the CFH moiety emerged at -183.1 ppm as doublet of doublet of multiplets with a fluorine-fluorine coupling constant of 109 Hz and fluorine-proton coupling constant of 90 Hz. The proton on the CFH fragment appeared at 8.21 ppm as doublet of doublet of multiplets in the  $^1\text{H}$  NMR spectrum and simplified to doublet of doublets in the  $^1\text{H}\{^{31}\text{P}\}$  NMR spectrum. The signal showed a coupling of 89.6 Hz to the *geminal* fluorine atom and 12.7 Hz to the fluorine atom at the  $\alpha$ -position.

An independent reaction in which rhodium fluoro complex  $[\text{Rh}(\text{F})(\text{PEt}_3)_3]$  (**28**)<sup>[59]</sup> was treated with trifluoroethylene confirmed the formation of complex **26** due to the coordination of the olefin at rhodium and the loss of one equivalent of triethylphosphine (Scheme 40).



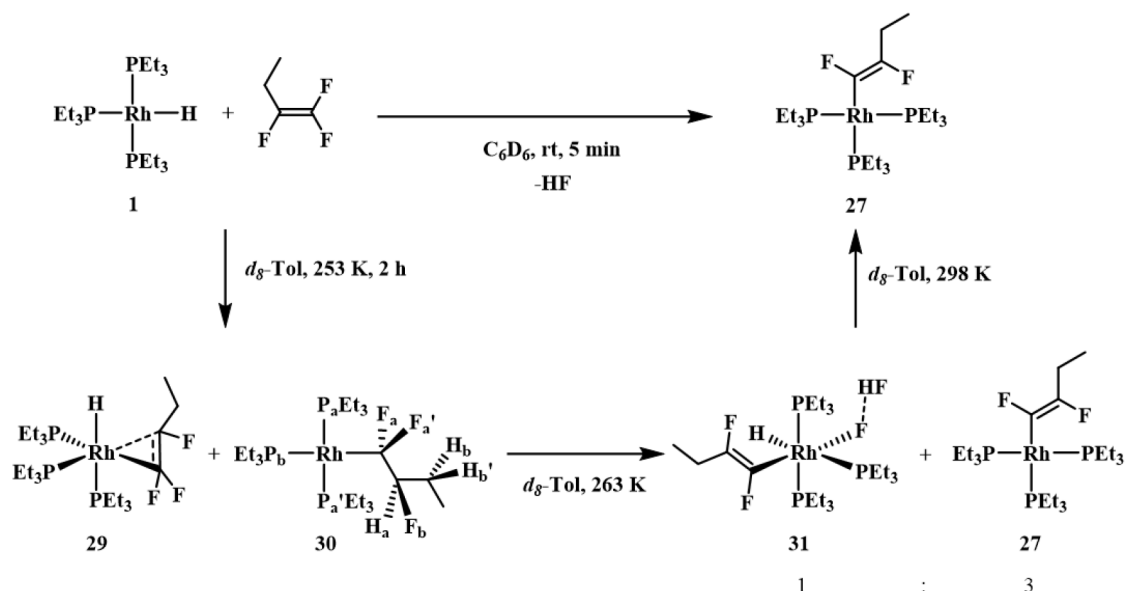
Scheme 40. The independent reaction of the rhodium fluorido complex **28** and trifluoroethylene.

The rhodium(I) complex **26** bears 2 inequivalent phosphine ligands with a AA' pattern at 32.3 and 25.9 ppm in the  $^{31}\text{P}\{^1\text{H}\}$  NMR spectrum. The doublet of doublet of triplet of doublet at 32.3 ppm revealed a coupling constant of 368.2 Hz, 138.9 Hz, 47.9 Hz and 27.5 Hz to the phosphorus atom in a mutual *trans* position, the rhodium atom, one fluorine atom of the CF<sub>2</sub> moiety and the fluorine atom of the CFH moiety and the fluoride. While the other signal at 25.9 ppm was observed as doublet of doublet of doublet of doublet of doublets ( $^2J_{(\text{P},\text{P})} = 368.5$  Hz,  $^1J_{(\text{P},\text{Rh})} = 133.3$  Hz,  $^3J_{(\text{P},\text{F})} = 44.2$  Hz,  $^2J_{(\text{P},\text{F})} = 28.6$  Hz, 14.8 Hz). The coupling constant of 368.2 Hz resulted from the coupling of the phosphine ligands in a mutual *trans* position, which is consistent with the literature.<sup>[158-160]</sup> The phosphorus-rhodium atom coupling constants demonstrate the presence of a Rh(I) complex.<sup>[29-30, 161-162]</sup> In the  $^{19}\text{F}$  NMR spectrum, the CF<sub>2</sub>-CFH moiety can be disclosed due to signals at -89.4 ppm, -90.8 ppm and -194.9 ppm. The signal at -89.4 ppm exhibited as a doublet of doublet of doublets with a fluorine-fluorine coupling constant of 109 Hz, fluorine-phosphorus coupling constant of 47 Hz and additional coupling constants 33 Hz and 13 Hz for one fluorine of the CF<sub>2</sub> moiety. The other fluorine signal of the CF<sub>2</sub> moiety was detected at -90.8 ppm as doublet of doublet of doublet of multiplets, which simplified to doublet of doublet of doublet of doublet of doublets ( $^2J_{(\text{F},\text{F})} = 109$  Hz,  $^3J_{(\text{F},\text{F})} = 69$  Hz,  $^3J_{(\text{F},\text{P})} = 44$  Hz,  $J = 7$  and 4 Hz) in the  $^{19}\text{F}\{^1\text{H}\}$  NMR spectrum. The resonance of the CFH occurred at -194.9 ppm as multiplet. Based on the  $^{19}\text{F}$ - $^{19}\text{F}$  COSY NMR spectrum, another fluorine atom at -218.3 ppm belongs to the structure, which was assigned to the fluoride. The signal was observed as multiplet. The  $^1\text{H}$  NMR showed a broad doublet of doublets for CFH moiety at 5.50 ppm with  $^2J$  proton-fluorine coupling constant of 73.3 Hz and proton-phosphorus coupling constant of 9.1 Hz.

The rhodium hydrido complex  $[\text{Rh}(\text{H})(\text{PEt}_3)_3]$  (**1**) was also reacted with 1,1,2-trifluorobutene to compare with the trifluoroethylene reaction. Treatment was run in a 1:2.1 ratio of complex **1** and 1,1,2-trifluorobutene in C<sub>6</sub>D<sub>6</sub> giving the C–F bond activation complex  $[\text{Rh}((Z)\text{-CFCFC}_2\text{H}_5)(\text{PEt}_3)_3]$  (**27**) selectively after 5 min at room temperature (Scheme 41). Furthermore, the formation of rhodium fluorido complex  $[\text{Rh}(\text{F})(\text{PEt}_3)_3]$  (**28**)<sup>[59]</sup> was observed over time due to the presence of HF which reacted with **27** as also

observed in the reaction with the rhodium hydrido complexes *cis/trans*-[Rh(H)(6-NHC)(PPh<sub>3</sub>)<sub>2</sub>] (6-NHC = 1,3-dialkyltetrahydropyrimidin-2-ylidene; alkyl = Me, Et, *i*Pr) with fluorinated olefins.<sup>[60]</sup>

Moreover, the reaction in which complex **1** was employed in an excess amount towards 1,1,2-trifluorobutene (1:1.25) gave a consistent result at room temperature.



Scheme 41. Stoichiometric reaction of rhodium complex **1** with 1,1,2-trifluorobutene at different temperatures.

The <sup>31</sup>P{<sup>1</sup>H} NMR spectrum of complex **27** (Figure 4) showed two groups of signals in a 1:2 ratio.

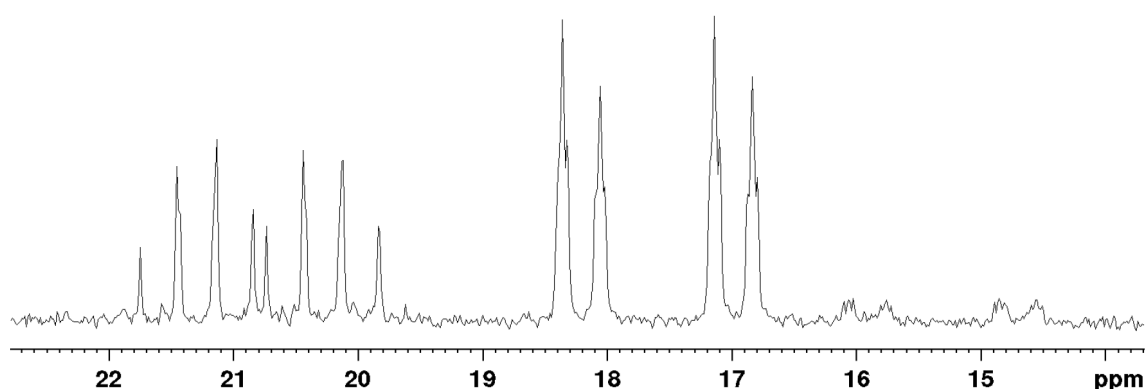


Figure 4. The <sup>31</sup>P{<sup>1</sup>H} NMR spectrum of complex **27**.

The doublet of apparent quartets at 20.8 ppm with a phosphorus-rhodium coupling constant of 123.1 Hz, a phosphorus-fluorine and a phosphorus-phosphorus coupling constant of 36.5 Hz was assigned to the phosphine ligand in the *trans* position to the fluorinated moiety. The resonance at 17.5 ppm was observed as doublet of doublet of

multiplets ( $^1J_{(P,Rh)} = 148.5$ ,  $^2J_{(P,P)} = 37.0$  Hz) and was attributed to the two phosphine ligands in a mutual *trans* position. These NMR data coincide with the ones observed for **25** and as in that complex, the coupling constant of phosphorus and rhodium indicates the presence of a Rh(I) complex.<sup>[29-30, 161-162]</sup> The structure of complex **27** with selected coupling constants is depicted in Figure 5.

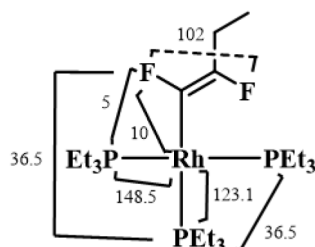


Figure 5. The structure of **27** with coupling constants, which are obtained first from  $^{31}P\{^1H\}$  NMR spectrum then from  $^{19}F$  NMR spectrum. The couplings with proton are not shown.

Two resonances were revealed in the  $^{19}F$  NMR spectrum (Figure 6) at -120.5 and -155.1 ppm as doublet of doublet of multiplets and doublet of triplet of multiplets, respectively. The signal at -120.5 ppm for the fluorine at the  $\alpha$ -carbon showed a coupling constant of 102 Hz to a fluorine nucleus, which is typical for fluorine atoms in *trans* positions,<sup>[59]</sup> and 36 Hz to a phosphorus atom. Apart from the coupling with fluorine, the pattern at -155.1 ppm showed additional coupling constant of 22 Hz to the adjacent  $CH_2$  moiety. These patterns simplified in the  $^{19}F\{^1H\}$  NMR spectrum revealing an additional coupling for the former signal to rhodium (10 Hz) and to the two *cis* phosphine ligands (5 Hz). In the  $^1H$  NMR spectrum, a doublet of multiplets for  $CFCH_2$  moiety appeared at 2.69 ppm with a coupling constant of 21.7 Hz to the  $^3J$  fluorine atom. It simplified to a quartet in the  $^1H\{^{19}F\}$  NMR spectrum with a coupling constant of 7.3 Hz to the proton of  $CH_3$  group. However, the signal for  $CH_3$  group overlapped by signals of  $PEt_3$  moiety.

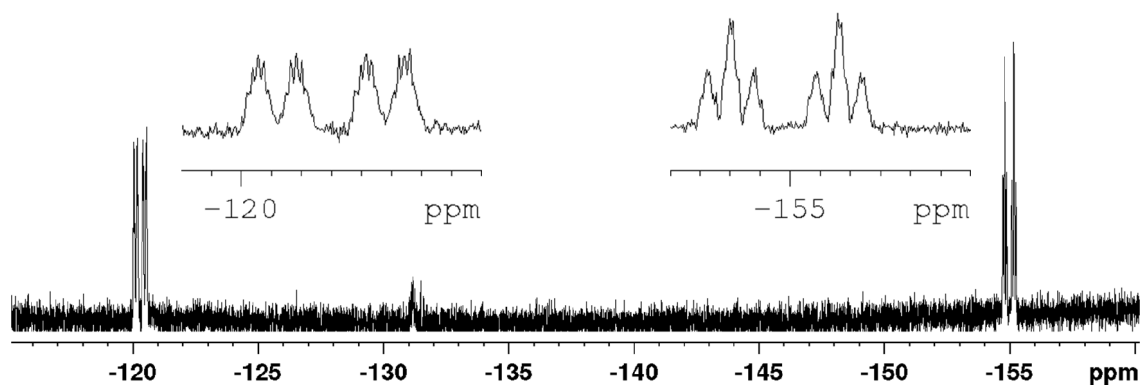


Figure 6. The  $^{19}F$  NMR spectrum of complex **27**.

The coordination of fluoroolefins such as 3,3,3-trifluoropropene, HFO-1234yf and HFO-1234ze at the rhodium complex **1** has been previously described at low temperature as the first step for the C–F bond activation of those olefins.<sup>[120, 162–163]</sup> Therefore, the reaction of complex **1** with 1,1,2-trifluorobutene was also monitored by NMR spectroscopy at variable temperatures. Thus, the reaction was performed in *d*<sub>8</sub>-toluene at 77 K and the sample was warmed up to 233 K. The complexes *fac*-[Rh(H)( $\eta^2$ -CF<sub>2</sub>CFC<sub>2</sub>H<sub>5</sub>)(PEt<sub>3</sub>)<sub>3</sub>] (**29**) and complex [Rh(CF<sub>2</sub>CFHC<sub>2</sub>H<sub>5</sub>)(PEt<sub>3</sub>)<sub>3</sub>] (**30**) were detected at the same time. After 2 h at 253 K the NMR spectra revealed the full conversion of complex **1** into **30** (Scheme 41). Continuing to increase the reaction temperature to 263 K immediately gave *mer*-[Rh(H)(FHF)((*Z*)-CFCFC<sub>2</sub>H<sub>5</sub>)(PEt<sub>3</sub>)<sub>3</sub>] (**31**) and [Rh((*Z*)-CFCFC<sub>2</sub>H<sub>5</sub>)(PEt<sub>3</sub>)<sub>3</sub>] (**27**) in a 1:3 ratio. Finally, only complex **27** was obtained after warming up the reaction to 298 K (Scheme 41).

The proposed structure of **29** is based on the <sup>19</sup>F NMR and <sup>1</sup>H NMR spectra. In the <sup>19</sup>F NMR spectrum, three signals appeared at -95.3 ppm, -102.1 ppm and -174.9 ppm as multiplet, doublet of doublet of multiplets (*J* = 145, 67 Hz) and multiplet, respectively. The resonance of hydride at Rh appeared as a doublet of multiplets at -13.36 ppm in the <sup>1</sup>H NMR spectrum with a coupling constant of 149.7 Hz to the phosphorus atom in the *trans* position. The signal simplified to a doublet of triplet of doublets in the <sup>1</sup>H{<sup>19</sup>F} NMR spectrum with additional couplings of 23.7 Hz to the two phosphine ligands in the *cis* position to the hydride, 17.3 Hz to the rhodium atom. A broad pseudo triplet appeared in the <sup>1</sup>H{<sup>31</sup>P} NMR spectrum.

The <sup>31</sup>P{<sup>1</sup>H} NMR spectrum of complex **30** at 253 K showed broad resonances, while at 193 K, the signal resolved to three patterns at 15.5, 11.7 and 8.4 ppm as doublet of doublet of doublet of multiplets, doublet of apparent pentet of doublet of multiplets and doublet of doublet of doublet of triplet of doublet of multiplets, respectively. The resonances at 15.5 and 8.4 ppm were due to the mutually *trans* phosphine ligands and observed as AA' pattern. The signal of P<sub>a</sub> showed coupling constants of 291.0 Hz to P<sub>a</sub>', 175.2 Hz to rhodium, 96.1 Hz to F<sub>a</sub>' and 38.1 Hz to P<sub>b</sub>. While for the latter signal, apart from the same coupling with the phosphorus in the mutual *trans* position, coupling constants of 166.7 Hz to rhodium, 36.1 Hz to P<sub>b</sub>, 17.6 Hz to the CF<sub>2</sub> moiety and 6.2 Hz to the F<sub>b</sub> atom were assigned. The coupling constant of <sup>1</sup>*J* phosphorus-rhodium indicates the presence of a Rh(I) complex.<sup>[29–30, 161–162]</sup> For the signal at 11.7 ppm, besides the coupling with the other two phosphine ligands, the splitting arose also from coupling to rhodium, the CF<sub>2</sub> moiety and F<sub>b</sub> of 111.3 Hz, 37.3 Hz and 10.2 Hz, respectively.



Regarding the complicated splitting, a simulation was conducted using gNMR software<sup>[164]</sup> and it is depicted in Figure 7 confirming the values described.

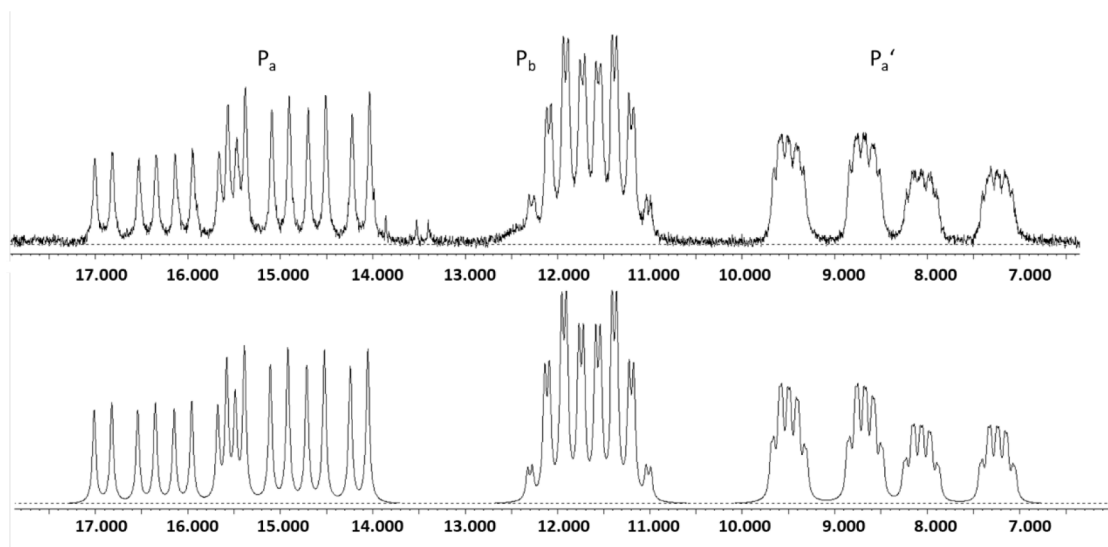


Figure 7. The  $^{31}\text{P}\{^1\text{H}\}$  NMR spectrum of complex **30**; simulated (below) observed (above) using the following coupling constants (Hz):  $^2J_{(\text{Pa},\text{Pa}')} = 291.0$ ,  $^1J_{(\text{Pa},\text{Rh})} = 175.2$ ,  $^2J_{(\text{Pa},\text{Pb})} = 38.1$ ,  $^3J_{(\text{Pa},\text{Fa}')} = 96.1$ ,  $^3J_{(\text{Pa}',\text{Pb})} = 36.1$ ;  $^1J_{(\text{Pb},\text{Rh})} = 111.3$ ,  $^3J_{(\text{Pb},\text{Fa})} = 37.3$ ,  $^3J_{(\text{Pb},\text{Fa}')} = 37.3$ ,  $^4J_{(\text{Pb},\text{Fb})} = 10.2$ ,  $^1J_{(\text{Pa}',\text{Rh})} = 166.7$ ,  $^3J_{(\text{Pa}',\text{Fa})} = 17.6$ ,  $^3J_{(\text{Pa}',\text{Fa}')} = 17.6$ ,  $^4J_{(\text{Pa}',\text{Fb})} = 6.2$ .

The structure of complex **30** with coupling constants is depicted in Figure 8, which is obtained from  $^{31}\text{P}\{^1\text{H}\}$  NMR spectrum (left) and  $^{19}\text{F}$  NMR spectrum and  $^1\text{H}$  NMR spectrum (right).

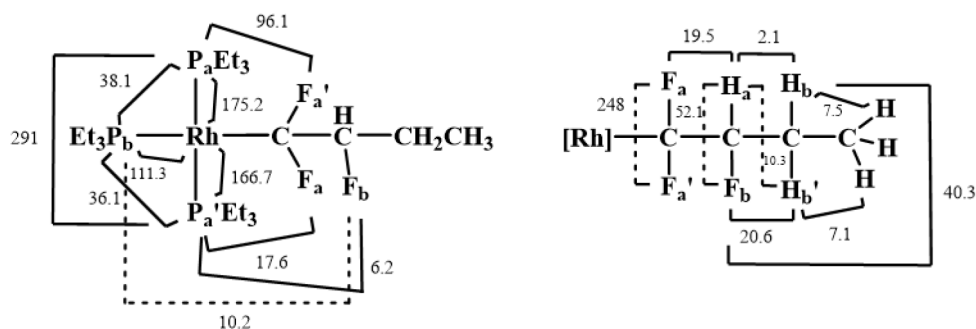


Figure 8. The structure of complex **30** with coupling constants.

In the  $^{19}\text{F}$  NMR spectrum, two broad doublet of multiplets at -75.6 and -82.2 ppm with a  $^2J$  fluorine-fluorine coupling constant of 248 Hz were assigned to the  $\text{CF}_2$  moiety. The inequivalent fluorine atoms can be explained by the presence of the adjacent chiral center. A broad resonance at -186.9 ppm was due to the  $\text{CFH}$  moiety. The simulation of the spectrum is depicted in Figure 9. The  $^{19}\text{F}$ - $^{19}\text{F}$  COSY NMR spectrum confirmed that the three signals stemmed from the same complex.

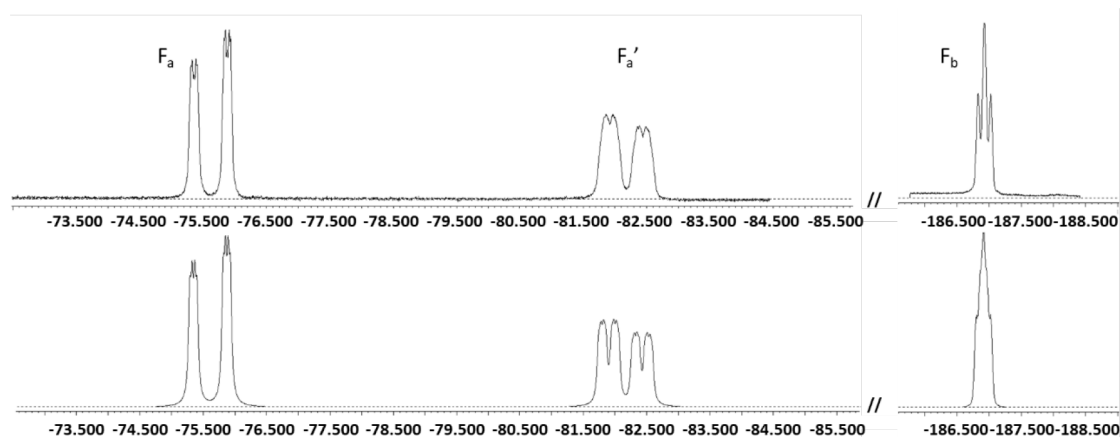


Figure 9. The  $^{19}\text{F}$  NMR spectrum of complex **30**; simulated (below) observed (above) using the following coupling constants (Hz):  $^2J_{(\text{Fa},\text{Fa}')} = 248.0$ ,  $^3J_{(\text{Fa},\text{Fb})} = 7.0$ ,  $^3J_{(\text{Fa}',\text{Pa})} = 96.1$ ,  $^3J_{(\text{Fa},\text{Pb})} = 37.3$ ,  $^3J_{(\text{Fa}',\text{Pb})} = 37.3$ ,  $^4J_{(\text{Fb},\text{Pb})} = 10.2$ ,  $^3J_{(\text{Fa},\text{Pa}')} = 17.6$ ,  $^3J_{(\text{Fa}',\text{Pa}')} = 17.6$ ,  $^4J_{(\text{Fb},\text{Pa}')} = 6.2$ ,  $^2J_{(\text{Fb},\text{Ha})} = 52.1$ ,  $^3J_{(\text{Fa}',\text{Ha})} = 19.5$ ,  $^3J_{(\text{Fb},\text{Hb})} = 40.3$ ,  $^3J_{(\text{Fb},\text{Hb}')} = 20.6$ .

Four signals in the  $^1\text{H}$  NMR belonged to complex **30** and the simulation is displayed in Figure 10.

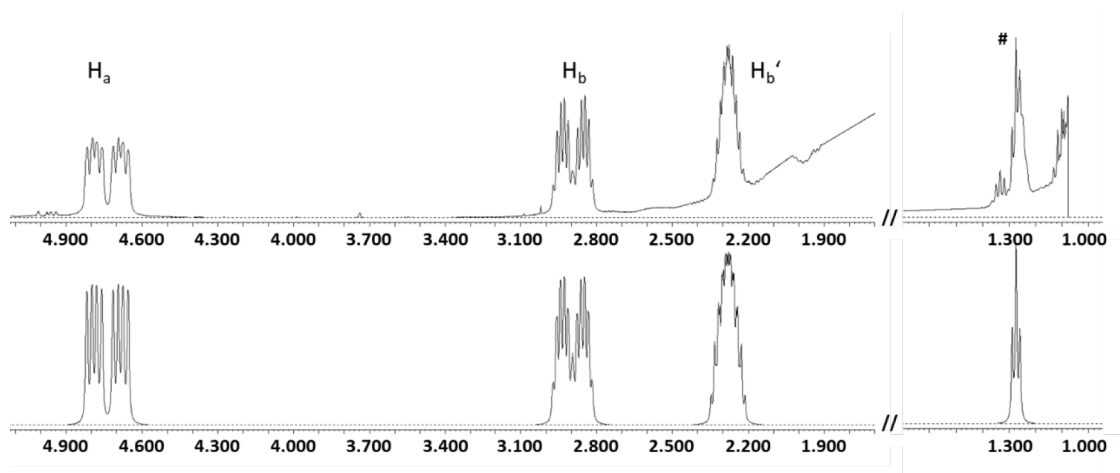


Figure 10. The  $^1\text{H}$  NMR spectrum of complex **30**; simulated (below) observed (above) using the following coupling constants (Hz):  $^2J_{(\text{Ha},\text{Fb})} = 52.1$ ,  $^3J_{(\text{Ha},\text{Fa}')} = 19.5$ ,  $^3J_{(\text{Hb},\text{Fb})} = 40.3$ ,  $^3J_{(\text{Hb}',\text{Fb})} = 20.6$ ,  $^3J_{(\text{Ha},\text{Hb})} = 2.1$ ,  $^3J_{(\text{Ha},\text{Hb}')} = 10.3$ ,  $^2J_{(\text{Hb},\text{Hb}')} = 15.0$ ,  $^3J_{(\text{Hb},\text{H})} = 7.5$ ,  $^3J_{(\text{Hb}',\text{H})} = 7.1$ . Note that there is overlapping in the 1.3 ppm region (#).

A doublet of doublet of doublet of doublets at 4.74 ppm with a coupling constant of 52.1 Hz to the *geminal* fluorine, 19.5 Hz to a  $^3J$  fluorine atom, 10.3 Hz to one proton of the  $\text{CH}_2$  moiety and 2.1 Hz to the other proton of the  $\text{CH}_2$  moiety was attributed to the proton of the CFH moiety. The signal at 2.89 ppm as doublet of doublet of quartets was assigned to one proton of  $\text{CH}_2$  moiety, in which the coupling constants of 40.3, 15.0 and 7.5 Hz were due to the fluorine of the CFH moiety,  $^2J$  proton and  $^3J$  protons of the  $\text{CH}_3$  group. For the other proton of the  $\text{CH}_2$  moiety, a doublet of multiplets appeared at 2.28 ppm with coupling constants of 20.6 Hz to the fluorine of the CFH moiety and simplified to doublet of doublet of quartets in the  $^1\text{H}\{^{19}\text{F}\}$  NMR spectrum showing a

coupling constant of 15.0 Hz to the *geminal* proton, 10.3 Hz to the proton of the CFH moiety and 7.1 Hz to the protons of the CH<sub>3</sub> moiety. Finally, a triplet with a coupling constant of 7.4 Hz to the CH<sub>2</sub> moiety was observed at 1.27 ppm for the proton of the CH<sub>3</sub> moiety, which overlapped with other signals, but was confirmed by a <sup>1</sup>H-<sup>1</sup>H COSY NMR spectrum.

For complex **31**, two signals with a integration of 2:1 were observed in the <sup>31</sup>P{<sup>1</sup>H} NMR spectrum. The doublet of doublet of doublet of doublets at 20.1 ppm with a coupling constant of 102.8 Hz to the rhodium(III) atom, 23.2 Hz to the phosphine ligand, 15.4 Hz to the fluorido ligand<sup>[165]</sup> and 2.7 Hz to a fluorine atom on the fluorinated moiety was due to the two phosphine ligands in a mutual *trans* position. The other signal was visible from 2.2 ppm to 0.0 ppm as multiplet and it was assigned to the phosphine ligand *trans* to the hydrido ligand. The coupling constant of phosphorus-rhodium gives evidence for a rhodium(III) complex.<sup>[30, 166]</sup> The structure of complex **31** with coupling constants, which are observed in the <sup>31</sup>P{<sup>1</sup>H} NMR, <sup>19</sup>F NMR and <sup>1</sup>H NMR spectra, is shown in Figure 11.

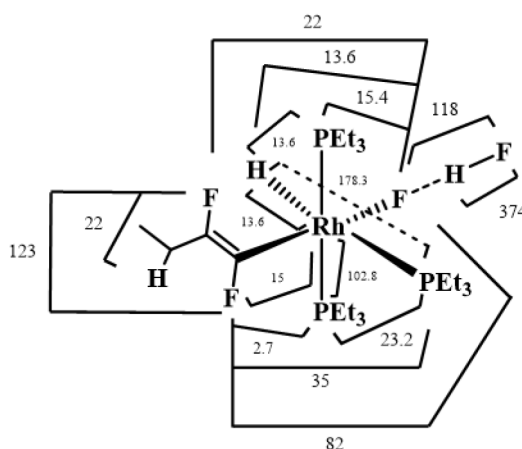
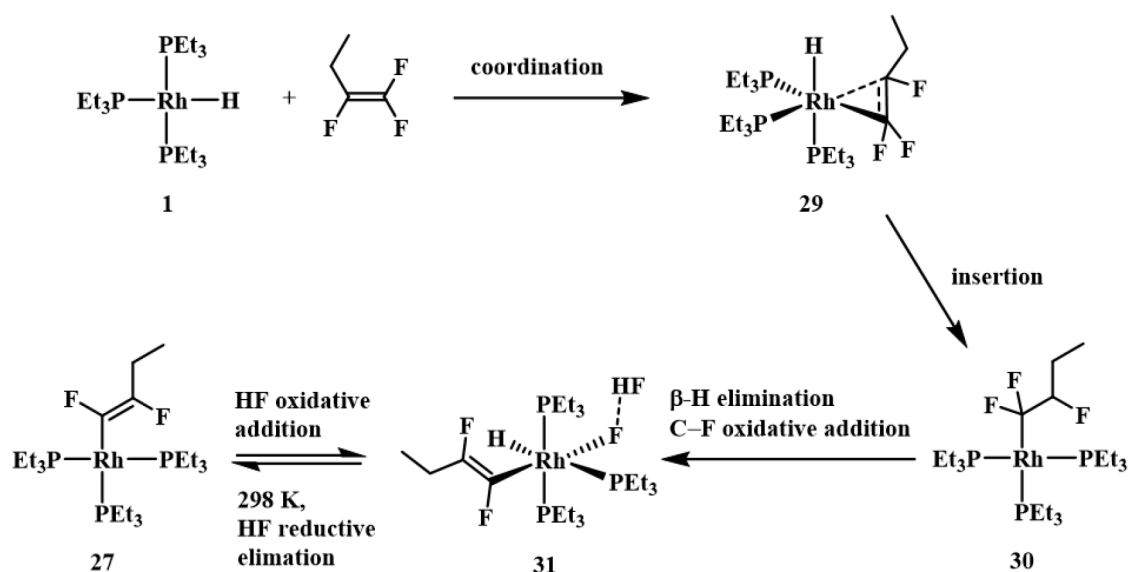


Figure 11. The structure of complex **31** with coupling constants.

Two signals were observed at -91.0 and -146.9 ppm in the <sup>19</sup>F NMR spectrum as doublet of doublet of doublet of multiplets (<sup>3</sup>J<sub>(F,F)</sub> = 123 Hz, <sup>3</sup>J<sub>(F,F)</sub> = 82 Hz, <sup>3</sup>J<sub>(F,P)</sub> = 35 Hz) and doublet of quartet of multiplets (<sup>3</sup>J<sub>(F,F)</sub> = 123 Hz, <sup>3</sup>J<sub>(F,H)</sub> ≈ <sup>4</sup>J<sub>(F,F)</sub> = 22 Hz). The two signals for the fluorine atoms of the RhCF and CFCH<sub>2</sub> moieties simplified to doublet of doublet of doublet of doublets (additional <sup>2</sup>J<sub>(F,Rh)</sub> = 15 Hz) and doublet of doublet of multiplets in the <sup>19</sup>F{<sup>1</sup>H} NMR spectrum, respectively. For the rhodium bound FHF moiety, a broad doublet of doublet at -177.0 ppm with a coupling constant of *ca.* 374 Hz to a proton and 118 Hz to a fluorine atom was assigned to the distal fluorine; while the appearance of a broad signal at -357.2 ppm was due to the proximal fluorine. The data of the FHF moiety

are consistent with the ones for complex  $[\text{Rh}(\text{F})(\text{FHF})(\text{PEt}_3)_3]$ .<sup>[167]</sup> Similar to the  $\text{CFCH}_2$  moiety of complex **27**, in the  $^1\text{H}$  NMR spectrum, a doublet of multiplets was present at 2.36 ppm with the same coupling constants to the  $^3J$  fluorine and the protons of the  $\text{CH}_3$  group. For the rhodium bound hydrido ligand, a doublet of multiplets was apparent at -9.27 ppm, which simplified to a broad triplet in the  $^1\text{H}\{^{31}\text{P}\}$  NMR spectrum with a coupling constant of 13.6 Hz to rhodium and fluorido ligand and to clear doublet of quartets in the  $^1\text{H}\{^{19}\text{F}\}$  NMR spectrum with, apart from the coupling to rhodium, 178.3 Hz to phosphorus in the *trans* position and 13.6 Hz to the two phosphorus in the *cis* position. The coupling constants of proton-phosphorus are comparable to the ones observed in the complex  $[\text{Rh}(\text{H})(\text{PEt}_3)_3]$  (**1**). The proton of the FHF moiety appeared at 12.91 ppm as broad doublet with a coupling constant of *ca.* 381 Hz to the distal fluorine.<sup>[167]</sup> Unfortunately, the resonance of the  $\text{CH}_3$  moiety is overlapped with other signals. The NMR data are comparable to these of the literature known complex *cis-mer*- $[\text{Rh}(\text{H})_2((Z)\text{-CFCFCF}_3)(\text{PEt}_3)_3]$ <sup>[59]</sup> and the data of the FHF moiety is consistent with the complex  $[\text{Rh}(\text{F})(\text{FHF})(\text{PEt}_3)_3]$ <sup>[167]</sup>.

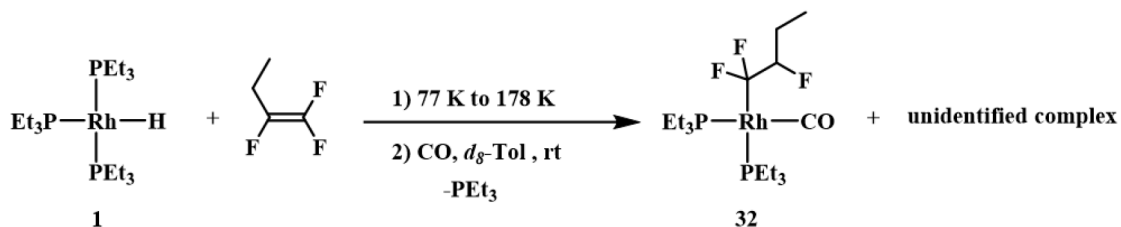


Scheme 42. The proposed mechanism for the formation of complex **27**.

A mechanism for the formation of complex **27** is proposed. Initially, coordination occurs between complex **1** and 1,1,2-trifluorobutene affording complex *fac*- $[\text{Rh}(\text{H})(\eta^2\text{-CF}_2\text{CFC}_2\text{H}_5)(\text{PEt}_3)_3]$  (**29**). The latter converts by insertion into the complex  $[\text{Rh}(\text{CF}_2\text{CFHC}_2\text{H}_5)(\text{PEt}_3)_3]$  (**30**). Note that a similar complex was never observed in the reactions of complex **1** with  $\text{CF}_3$ -containing olefins. Then presumably  $\beta$ -H elimination and subsequent C-F bond oxidative addition would take place yielding complex *mer*- $[\text{Rh}(\text{H})(\text{FHF})((Z)\text{-CFCFC}_2\text{H}_5)(\text{PEt}_3)_3]$  (**31**). With temperature rising up, HF reductive

elimination at the complex **31** occurs along with the generation of complex  $[\text{Rh}((Z)\text{-CFCFC}_2\text{H}_5)(\text{PEt}_3)_3]$  (**27**) (Scheme 42).

The structure of complex **30** was further explored through the introduction of CO to the mixture after the reaction of rhodium hydrido complex  $[\text{Rh}(\text{H})(\text{PEt}_3)_3]$  (**1**) and 1,1,2-trifluorobutene at low temperature, in which complex **1** was partially converted. Complex *cis*- $[\text{Rh}(\text{CF}_2\text{CFHC}_2\text{H}_5)(\text{CO})(\text{PEt}_3)_2]$  (**32**) and an unidentified complex were generated along with the release of  $\text{PEt}_3$  after warming up to room temperature (Scheme 43). Note that the unidentified complex showed a resonance at 5.0 ppm with a  $^2J$  phosphorus-rhodium coupling constant of 158.9 Hz in the  $^{31}\text{P}\{^1\text{H}\}$  NMR spectrum and was also observed in the independent reaction of complex **1** and CO.



Scheme 43. Stoichiometric reaction of rhodium complex **1** with 1,1,2-trifluorobutene under CO atmosphere.

A broad signal was revealed at 14.5 ppm in the  $^{31}\text{P}\{^1\text{H}\}$  NMR spectrum at room temperature for complex **32**, which indicates the existence of a dynamic process. While at 243 K, two resonances were observed at 21.9 and 8.6 ppm as doublet of triplet of doublets ( $^1J_{(\text{P,Rh})} = 73.1$  Hz,  $^3J_{(\text{P,F})} = 47.8$  Hz,  $^2J_{(\text{P,P})} = 24.0$  Hz) and doublet of multiplets ( $^1J_{(\text{P,Rh})} = 124.8$  Hz) with an integral of 1:1 illustrating the existence of *cis* isomer. The coupling constant of 73.1 Hz may be due to the phosphine ligand in the *cis* position to the CO ligand, while the coupling of 124.8 Hz may be attributed to the phosphine ligand in the *trans* position to the CO ligand.<sup>[168-169]</sup> The structure of complex **32** with coupling constants is shown in Figure 12. The coupling constants are obtained first from the  $^{31}\text{P}\{^1\text{H}\}$  NMR then the  $^{19}\text{F}$  NMR and  $^1\text{H}$  NMR spectra.

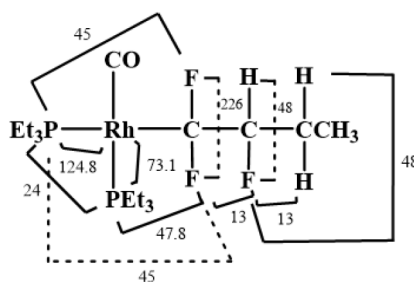


Figure 12. The structure of complex **32** with coupling constants.

In the  $^{19}\text{F}$  NMR spectrum, two groups of broad doublet of triplet of multiplets were shown at -59.5 ppm ( $^2J_{(\text{F},\text{F})} = 226$  Hz,  $^3J_{(\text{F},\text{P})} = 45$  Hz) and -60.9 ppm ( $^2J_{(\text{F},\text{F})} = 226$  Hz,  $^3J_{(\text{F},\text{P})} = 45$  Hz) for  $\text{CF}_2$  moiety at 243 K. A broad triplet of multiplets at -183.5 ppm was assigned for the CFH moiety. The same signal was observed as pseudo triplet of quartets in the room temperature spectrum with a coupling of 48 Hz to the *geminal* proton and one proton of the  $\text{CH}_2$  moiety, 13 Hz to the fluorine atoms of  $\text{CF}_2$  moiety and the other proton of the  $\text{CH}_2$  moiety. A doublet of multiplets at 4.52 ppm with a coupling constant of 47.7 Hz resulting from *geminal* proton and fluorine was detected in the  $^1\text{H}$  NMR spectrum, which belonged to the proton of the CFH moiety. This signal correlated to two resonances, which were overlapped with other signals at 2.18 and 2.09 ppm in the  $^1\text{H}$ - $^1\text{H}$  COSY NMR spectrum. Based on it, the triplet at 1.09 ppm with a coupling of 7.3 Hz to proton for the  $\text{CH}_3$  moiety also belonged to complex **32**.

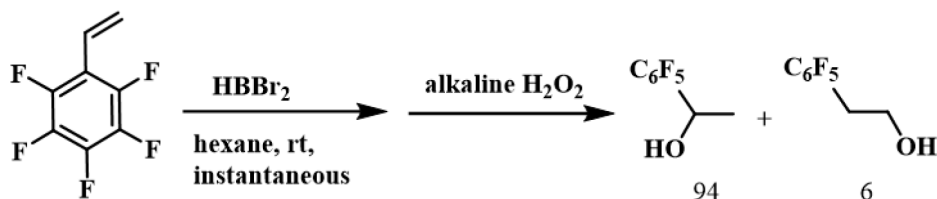
Overall, a catalytic reaction of trifluoroethylene was conducted with an excess amount of HBpin under the catalyst  $[\text{Rh}(\text{H})(\text{PEt}_3)_3]$  (**1**) affording the corresponding hydroboration compound, hydrogenation compound and defluorohydroboration compounds. When complex **1** was treated with trifluoroethylene stoichiometrically, the C–F bond activation complex  $[\text{Rh}((Z)\text{-CFCFH})(\text{PEt}_3)_3]$  (**25**) was furnished. Similarly, treatment of complex **1** with 1,1,2-trifluorobutene at room temperature gave the corresponding C–F bond activation complex  $[\text{Rh}((Z)\text{-CFCFC}_2\text{H}_5)(\text{PEt}_3)_3]$  (**27**). Monitoring the reaction by NMR spectroscopy at variable temperatures, the coordination product *fac*- $[\text{Rh}(\text{H})(\eta^2\text{-CF}_2\text{CFC}_2\text{H}_5)(\text{PEt}_3)_3]$  (**29**) and the Rh–H insertion complex  $[\text{Rh}(\text{CF}_2\text{CFHC}_2\text{H}_5)(\text{PEt}_3)_3]$  (**30**) were detected at 233 K. Subsequently,  $\beta$ -H elimination and subsequent C–F bond oxidative addition complex *mer*- $[\text{Rh}(\text{H})(\text{FHF})((Z)\text{-CFCFC}_2\text{H}_5)(\text{PEt}_3)_3]$  (**31**) was observed at 263 K. The HF reductive elimination of **31** occurred at 298 K along with the formation of complex **27**.

## 4. Activation and borylation of pentafluorostyrene towards rhodium(I) complexes

### 4.1 Introduction

Substituent effects which can change the electronic properties of a compound is well-investigated in chemistry.<sup>[170-171]</sup> It is known that the electron withdrawing ability of C<sub>6</sub>F<sub>5</sub> group is weaker than CF<sub>3</sub> group but stronger than that of a F atom.<sup>[172-173]</sup> Ethylene derivatized by a CF<sub>3</sub> group (such as in 3,3,3-trifluoropropene),<sup>[120, 162]</sup> a CF<sub>3</sub> and a F moiety (such as in HFO-1234yf,<sup>[120]</sup> HFO-1234ze<sup>[163]</sup> and all the other olefins that were used in chapter 2) and a F atom alone (such as in 1,1,2-trifluoroethylene and all the other olefins that were employed in chapter 3) were also investigated in the last decades. However, of particular interest is in addition the reactivity of pentafluorostyrene towards rhodium complexes.

Being regarded as a fundamental fluorinated building block, pentafluorostyrene was involved in a lot of reactions, such as arylation,<sup>[174]</sup> C–C coupling,<sup>[175]</sup> epoxidation,<sup>[176]</sup> hydrogenation,<sup>[177-178]</sup> hydroformylation<sup>[179]</sup> and hydroboration reactions<sup>[180-187]</sup>. Indeed, various hydroboration reactions of pentafluorostyrene were achieved by rhodium complexes affording Markovnikov or anti-Markovnikov products.<sup>[181-185]</sup> In 1999, the first literature known Markovnikov hydroboration at pentafluorostyrene was reported by Brown *et al.*, in which HBBBr<sub>2</sub> was employed as boron source to give after addition and oxidation reaction the Markovnikov and anti-Markovnikov products in a 94:6 ratio (Scheme 44).<sup>[180]</sup> Particularly, no metal was involved.

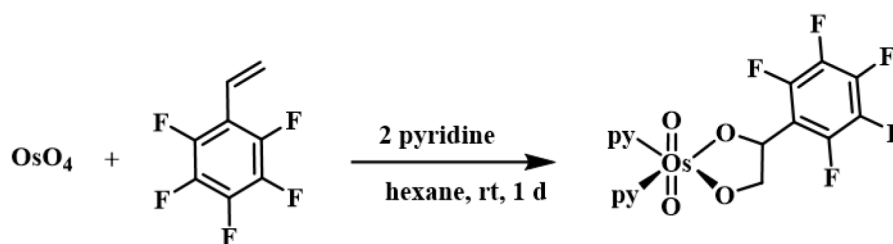


Scheme 44. Hydroboration and oxidation reaction of pentafluorostyrene using HBBBr<sub>2</sub> as boron source (ratio in mol%).

HBpin (pinacol borane) and HBcat (catechol borane) are also useful organoboron compounds, and because of the oxygen atoms bound at the boron atom, the risk of the background reaction was decreased.<sup>[77, 91]</sup> Interestingly, both compounds were utilized by Ramachandran *et al.* in 1999 in rhodium catalyzed reactions giving anti-Markovnikov

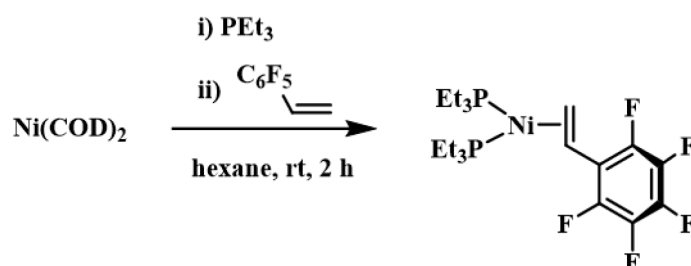
and Markovnikov products. Importantly, anti-Markovnikov products were generated at the neutral rhodium complex  $[\text{Rh}(\text{Cl})(\text{PPh}_3)_3]$  with HBpin, while Markovnikov products were furnished at the cationic  $[\text{Rh}(\text{COD})(\text{dppb})]\text{BF}_4$  (dppb = 1,4-bis(diphenylphosphino)butane) complex with HBcat.<sup>[181]</sup> Note that for all the published hydroboration reactions of pentafluorostyrene, the boron source is crucial. Among all the publications, there is only one example from Westcott and co-workers indicating that HBpin yields a mixture including Markovnikov addition product when treated with the neutral complex  $[\text{Rh}(\text{acac})(\kappa^2\text{-}o\text{-Ph}_2\text{PC}_6\text{H}_4\text{CH}=\text{N-}2,6\text{-}i\text{Pr}_2\text{C}_6\text{H}_3)]$  as the catalyst.<sup>[184]</sup> However, the mixture of products resulted in a low selectivity. Hence, it is interesting to have a further investigation on the combination of HBpin and rhodium complexes to achieve Markovnikov addition products.

Regarding stoichiometric conversions of pentafluorostyrene, a fluorinated osmate ester was obtained quantitatively by a cycloaddition reaction of osmium tetroxide and pentafluorostyrene by Herrmann's group (Scheme 45).<sup>[188]</sup>



Scheme 45. Stoichiometric reaction of osmium tetroxide and pentafluorostyrene.

Additionally, a coordination was accomplished by Perutz and coworkers when treating  $[\text{Ni}(\text{COD})_2]$  with pentafluorostyrene (Scheme 46).<sup>[189]</sup>



Scheme 46. Stoichiometric reaction of  $[\text{Ni}(\text{COD})_2]$  with pentafluorostyrene.

Stoichiometric reactions of pentafluorostyrene towards rhodium complexes are still unknown.



## 4.2 Results and discussion

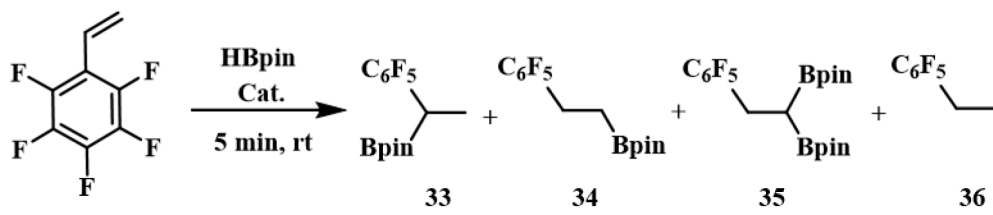
### 4.2.1 Catalytic reactions

In consistence with above mentioned strategy (HBpin as the boron source and rhodium hydrido complex  $[\text{Rh}(\text{H})(\text{PEt}_3)_3]$  (**1**) as the catalyst), a reaction of pentafluorostyrene was performed initially at room temperature with HBpin (ratio 1:1.5) in  $\text{C}_6\text{D}_6$  using complex  $[\text{Rh}(\text{H})(\text{PEt}_3)_3]$  (**1**) (3 mol% based on the amount of pentafluorostyrene) as the catalyst. The  $^{19}\text{F}$  and  $^1\text{H}$  NMR spectra demonstrated the full conversion of pentafluorostyrene in 5 min yielding the Markovnikov hydroboration product  $\text{C}_6\text{F}_5\text{CH}(\text{Bpin})\text{CH}_3$  (**33**),<sup>[184]</sup> the anti-Markovnikov hydroboration product  $\text{C}_6\text{F}_5\text{CH}_2\text{CH}_2\text{Bpin}$  (**34**),<sup>[184]</sup> small amounts of the diborylated derivative  $\text{C}_6\text{F}_5\text{CH}_2\text{CH}(\text{Bpin})_2$  (**35**)<sup>[184]</sup> along with the hydrogenation product  $\text{C}_6\text{F}_5\text{CH}_2\text{CH}_3$  (**36**)<sup>[190]</sup> in a 91:6:1:2 ratio (Table 4, entry 1). In the  $^{19}\text{F}$  NMR spectrum of compound **33**, three groups of resonances appeared at -144.8, -160.3 and -164.4 ppm as doublet of multiplets, triplet and triplet of multiplets, respectively. The coupling constant of 22 Hz is due to a  $^3J$  fluorine-fluorine coupling. The  $^1\text{H}$  NMR spectrum displayed a quartet with a coupling constant of 7.7 Hz to proton at 2.63 ppm and a doublet with the same proton-proton coupling at 1.28 ppm. In addition, a peak of  $m/z$  320 in the GC-MS implied the presence of **33**.

The rhodium boryl complex  $[\text{Rh}(\text{Bpin})(\text{PEt}_3)_3]$  (**3**)<sup>[30, 127-129]</sup> shows a versatile catalytic reactivity towards fluorinated aromatics, anilines and  $\text{SCF}_3$ -functionalized arenes. It was also utilized as catalyst (3.7 mol%) towards pentafluorostyrene. With a full conversion of pentafluorostyrene, the same products were gained in a ratio of 81:9:3:3 in 5 min, which suggests a decrease in the formation of Markovnikov addition product (Table 4, entry 2). In addition, an unidentified product was formed in a 4 % yield.

The emergence of the concept of green chemistry is appealing the attention world widely.<sup>[191]</sup> Eliminating the use of solvent fits one of the basic principles of green chemistry proposed by Paul T. Anastas.<sup>[192]</sup> Therefore, the reaction was carried out under neat condition with a full conversion of pentafluorostyrene in 5 min when employing 1.5 mol% of complex **1** as the catalyst affording the same products. Among them, compound **33** is the main product with a comparable yield of 75 % (Table 4, entry 3).

Table 4. Catalytic hydroboration reactions of pentafluorostyrene.

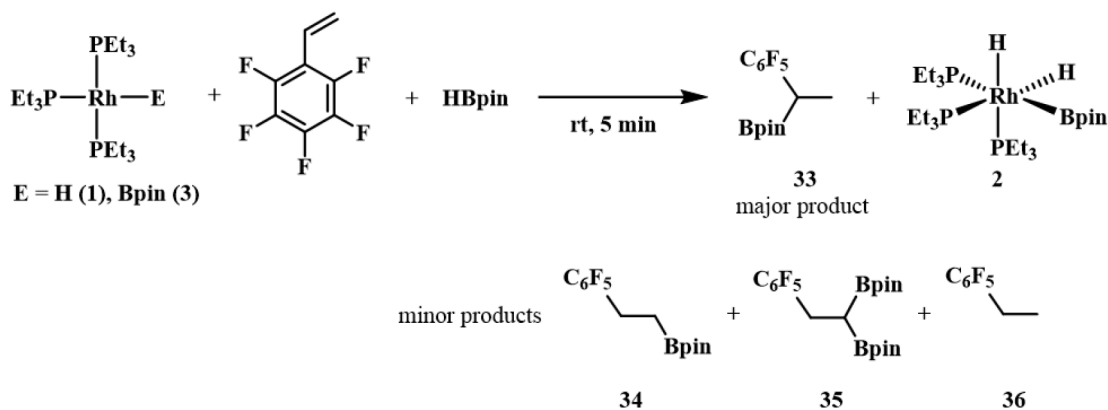
				
Catalyst	mol%	Solvent	Conversion (%) <sup>a</sup>	Ratio (%) <sup>b</sup>
				<b>33:34:35:36</b>
<b>1</b>	3	C <sub>6</sub> D <sub>6</sub>	> 99	91:6:1:2
<b>3</b>	3.7	Me <sub>6</sub> Si <sub>2</sub>	> 99	81:9:3:3
<b>1</b>	1.5	neat	> 99	75:13:4:8

a) Based on the consumption of pentafluorostyrene. b) Based on the <sup>19</sup>F NMR spectrum.

## 4.2.2 Stoichiometric reactions

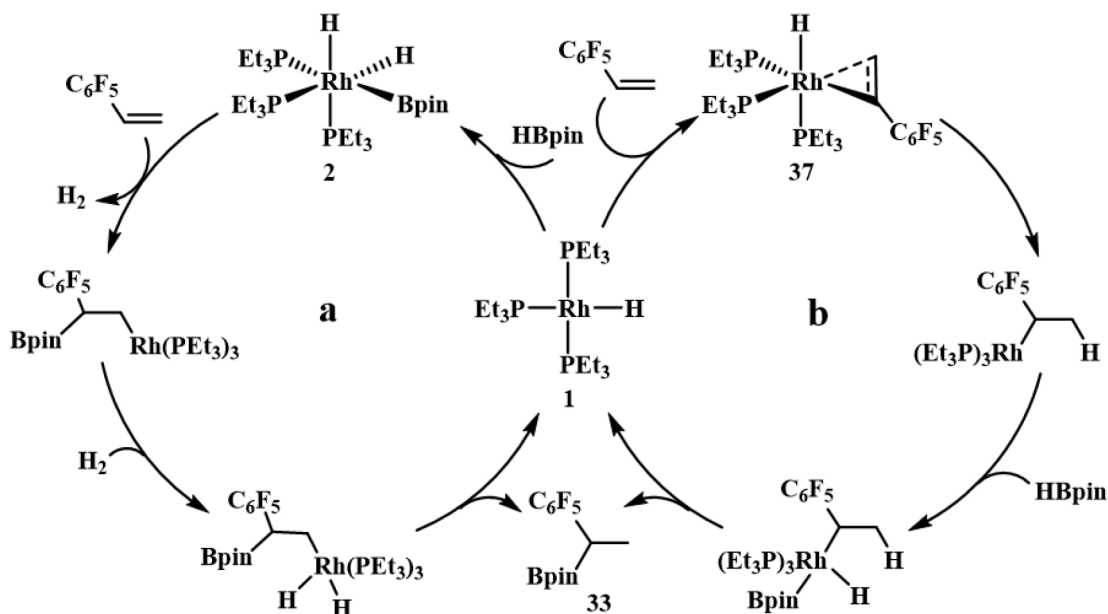
### 4.2.2.1 Stoichiometric hydroboration reactions

To further investigate and get an understanding of the catalytic hydroboration reaction cycle, the hydroboration reactions were conducted in a stoichiometric way. Indeed, [Rh(H)(PEt<sub>3</sub>)<sub>3</sub>] (**1**), pentafluorostyrene and HBpin were employed in a 1:1:2.5 ratio in *d*<sub>8</sub>-toluene. As a result, the same organic products as in the catalytic reaction **33**, **34**, **35** and **36** were obtained in a ratio of 92:2:4:2 at room temperature in 5 min together with rhodium(III) complex *fac*-[Rh(Bpin)(H)<sub>2</sub>(PEt<sub>3</sub>)<sub>3</sub>](**2**)<sup>[61]</sup> as the only rhodium species (Scheme 47). In fact, the order of HBpin and pentafluorostyrene addition had no influence in the reaction outcome. When the complex [Rh(Bpin)(PEt<sub>3</sub>)<sub>3</sub>] (**3**) was used instead of complex **1** in *d*<sub>14</sub>-methylcyclohexane, the same organic compounds were produced in a 49:14:22:15 ratio as well as complex **2** at room temperature in 5 min.



Scheme 47. Stoichiometric hydroboration reactions of complex **1** or **3**.

Two plausible mechanisms for the hydroboration reaction are given in Scheme 48 regarding complex **1**, which resemble mechanisms proposed for Ti or other Rh complexes.<sup>[137, 193-194]</sup>



Scheme 48. Two plausible pathways for the formation of the main hydroboration product **33**.

After the initial formation of the oxidative addition product **2** from complex **1** and HBpin, an insertion reaction of pentafluorostyrene occurs with concomitant elimination of H<sub>2</sub> or dissociation of a phosphine ligand. Followed by oxidative addition of H<sub>2</sub> or rebinding of the phosphine ligand and reductive elimination reaction, the hydroboration product **33** is generated together with complex **1** (Scheme 48a). Note that the behavior of 3,3,3-trifluoropropene, HFO-1234yf or HFO-1234ze towards the rhodium hydrido complex **1** were studied by the Braun group affording activation or coordination products.<sup>[120, 162-163]</sup> Alternatively, complex **37** is generated by the coordination of complex **1** and pentafluorostyrene, which undergoes the insertion of the olefin into Rh–H bond. A

subsequent oxidative addition of HBpin followed by reductive elimination gives the final product **33** as well as the regeneration of complex **1** (Scheme 48b).

#### 4.2.2.2 Stoichiometric reactions of complex $[\text{Rh}(\text{H})(\text{PEt}_3)_3]$ (**1**) and pentafluorostyrene

To confirm the proposed pathway, the reactivity between complex **1** and pentafluorostyrene was tested independently. Subsequently, treatment of complex **1** and pentafluorostyrene (ratio 1.4:1) in *d*<sub>8</sub>-toluene afforded *fac*- $[\text{Rh}(\text{H})(\eta^2\text{-CH}_2\text{CHC}_6\text{F}_5)(\text{PEt}_3)_3]$  (**37**) quantitatively at room temperature in 5 min (Scheme 49). Note that complex **37** is only stable in solution at low temperature for a long period. And similar to the reported rhodium complexes *fac*- $[\text{Rh}(\text{H})(\eta^2\text{-CH}_2\text{CHCF}_3)(\text{PEt}_3)_3]$ <sup>[162]</sup> and *fac*- $[\text{Rh}(\text{H})(\eta^2\text{-CH}_2\text{CFCF}_3)(\text{PEt}_3)_3]$ <sup>[120]</sup>, complex **37** was therefore characterized at 213 K after the preparation.

The  $^{31}\text{P}\{^1\text{H}\}$  NMR spectrum depicted three broad signals at 19.7, 13.3 and 4.6 ppm indicating the presence of dynamic process at room temperature, which may be caused by the rotation about the olefinic bond. However, three signals with splitting were observed at 20.3, 13.7 and 5.8 ppm with a ratio of 1:1:1 in the  $^{31}\text{P}\{^1\text{H}\}$  NMR spectrum at 213 K (Figure 13), suggesting a structure with a *fac*-arrangement.<sup>[120, 162]</sup> The doublet of doublets at 20.3 ppm with a coupling constant of 139.8 Hz to rhodium, 42.6 and 24.2 Hz to the other two phosphorus atoms and the doublet of doublet of doublets ( $^1J_{(\text{P,Rh})} = 134.0$  Hz,  $^2J_{(\text{P,P})} = 42.9$  Hz,  $^2J_{(\text{P,P})} = 28.8$  Hz) at 13.7 ppm belonged to the phosphine ligands *trans* to the  $\text{CHC}_6\text{F}_5$  and  $\text{CH}_2$  moieties. The coupling constant of  $^1J$  phosphorus-rhodium gives the evidence of a Rh(I) species.<sup>[29-30, 161-162]</sup> The doublet of multiplets at 5.8 ppm with a  $^1J$  phosphorus-rhodium coupling constant of 95.8 Hz was assigned to the phosphine ligand *trans* to the hydrido ligand. The smaller coupling constant was attributed to the large *trans* influence of the hydrido ligand.<sup>[162, 195-196]</sup>

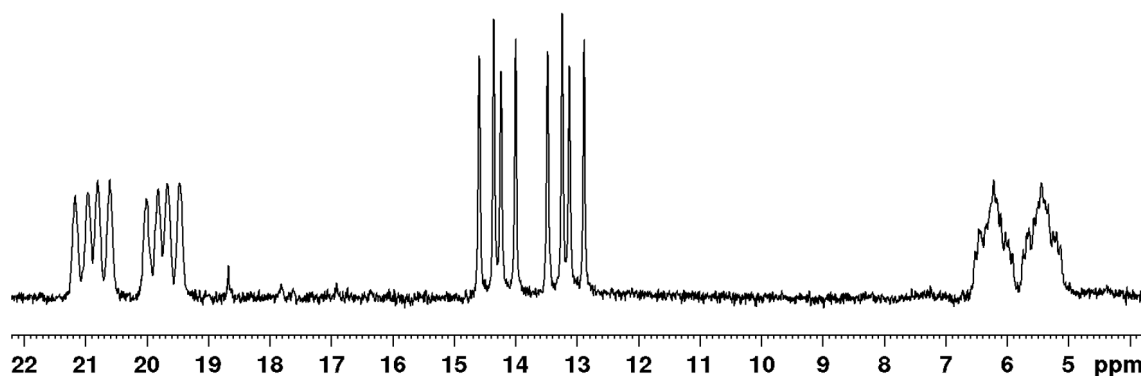
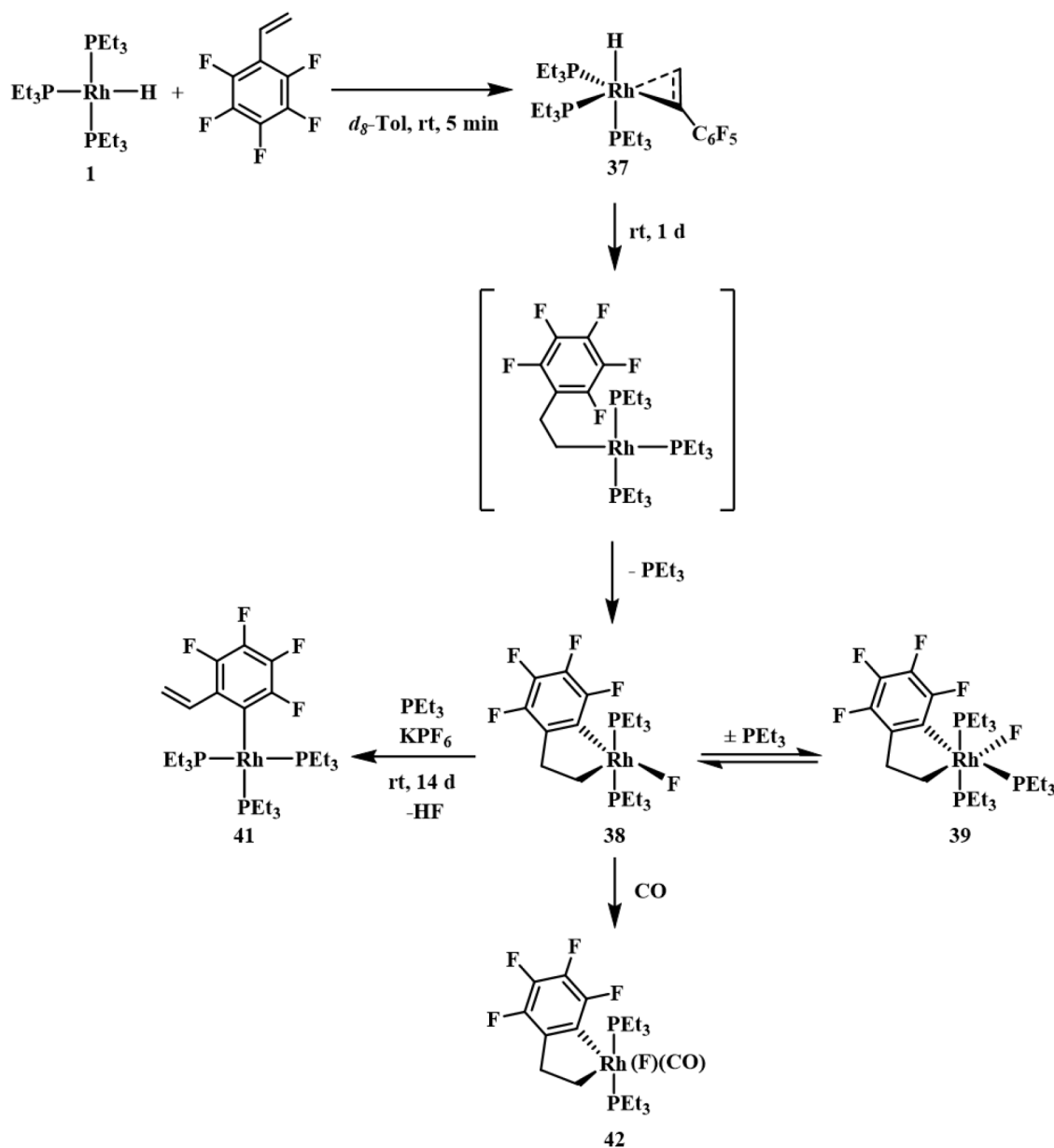


Figure 13.  $^{31}\text{P}\{^1\text{H}\}$  NMR spectrum of complex **37**.

In accordance with the dynamic process shown in the  $^{31}\text{P}\{^1\text{H}\}$  NMR spectrum, three broad signals with a 2:2:1 ratio were also observed in the room temperature  $^{19}\text{F}$  NMR spectrum, while at 213 K, five resonances appeared in a 1:1:1:1:1 ratio. It is supposed that signals at -146.0 and -146.7 ppm belonged to the two fluorine atoms in the *ortho* position, while the two *meta* fluorine atoms emerged at -166.3 and -167.0 ppm and the signal at -170.9 ppm was due to the *para* fluorine atom.<sup>[197-200]</sup> The  $^1\text{H}$  NMR spectrum at 213 K displayed three broad signals at 3.32, 3.05, 1.83 ppm for the olefinic protons, which is consistent with data for the previously reported complex *fac*-[Rh(H)( $\eta^2$ -CH<sub>2</sub>CHCF<sub>3</sub>)(PEt<sub>3</sub>)<sub>3</sub>]<sup>[162]</sup>. The  $^1\text{H}\{^{31}\text{P}\}$  NMR spectrum showed at 3.32 ppm a broad pseudo triplet for the proton on the CHC<sub>6</sub>F<sub>5</sub> moiety with a coupling constant of approximately 8 Hz to the two inequivalent protons of the CH<sub>2</sub> group. The broad doublets at 3.05 ppm and at 1.83 ppm for the protons on the CH<sub>2</sub> moiety revealed a coupling constant of 9.5 Hz and 8.1 Hz, respectively, to the proton on the CHC<sub>6</sub>F<sub>5</sub> moiety. For the rhodium-bound hydrido ligand, a signal appeared at -14.64 ppm in the  $^1\text{H}$  NMR spectrum as doublet of triplet of doublets, which simplified to a doublet in the  $^1\text{H}\{^{31}\text{P}\}$  NMR spectrum. The coupling constant of 161.8 Hz and 9.2 Hz were attributed to the phosphine ligand in the *trans* position and the rhodium atom, respectively. The *cis* phosphine ligands gave a coupling constant of 19.8 Hz.

Furthermore, keeping **37** or the reaction of complex **1** and pentafluorostyrene at room temperature for 1 d, the rhodaindane complex *trans*-[Rh(F)(CH<sub>2</sub>CH<sub>2</sub>(2-C<sub>6</sub>F<sub>4</sub>))(PEt<sub>3</sub>)<sub>2</sub>] (**38**) was formed through a cyclometallation and C–F bond activation reaction with a 64% conversion of complex **37** (Scheme 49). Apart from complex **38**, free PEt<sub>3</sub>, traces of complex *mer*-[Rh(F)(CH<sub>2</sub>CH<sub>2</sub>(2-C<sub>6</sub>F<sub>4</sub>))(PEt<sub>3</sub>)<sub>3</sub>] (**39**) and minor amounts of the C–H bond activation complex [Rh(*E*-CHCHC<sub>6</sub>F<sub>5</sub>)(PEt<sub>3</sub>)<sub>3</sub>] (**40**) as well as the hydrogenation product

ethylpentafluorobenzene **36** (**40** and **36** were not shown in the scheme) were also generated.



Scheme 49. Stoichiometric reactions of complex **1** and pentafluorostyrene.

Presumably the formation of compound **36** was promoted by the production of before mentioned C–H bond activation, in which hydrogen was produced. Interestingly, after cooling down the solution temperature to 233 K, complex **38** was transformed into complex **39** completely in the presence of free  $\text{PEt}_3$  indicating the equilibrium between complex **38**, free  $\text{PEt}_3$  and complex **39**. A ratio of 1:0.07:0.18 among **39**:**40**:**36** was found in the low temperature  $^{19}\text{F}$  NMR spectrum. Furthermore, after removing the solvent and some free phosphine under vacuum, complex **38** cannot be converted into complex **39** completely.

The C–F bond activation complex  $[\text{Rh}(\text{2-C}_6\text{F}_4\text{CHCH}_2)(\text{PEt}_3)_3]$  (**41**), which was synthesized independently (see Scheme 54), was afforded slowly through transformation of complex **38**. This is presumably accompanied by the formation of HF (Scheme 49). However, this transformation can be accelerated by the presence of  $\text{KPF}_6$  and within 14 d **38** can be converted completely. Moreover, the generation of *ortho* position C–F bond activation complex **41** are in accordance with the formation of the rhodacycle structures.

The  $^{31}\text{P}\{^1\text{H}\}$  NMR spectrum of complex **38** depicted a broad doublet of doublets at 18.4 ppm. The coupling constant of 114.2 Hz was due to the  $^1J$  coupling with rhodium while the 16.6 Hz was caused by the  $^2J$  coupling with the fluorido ligand. In the  $^{19}\text{F}$  NMR spectrum, five signals appeared at -130.6, -142.0, -162.5, -167.3 and -290.6 ppm. The signal at -290.6 ppm belonged to the metal bound fluorido ligand.<sup>[59]</sup> Two broad signals shown at 3.20 and 2.45 ppm in the  $^1\text{H}$  NMR spectrum were assigned to the protons on the  $\text{C}_6\text{F}_4\text{CH}_2\text{CH}_2$  moiety. In the  $^{13}\text{C}\{^1\text{H}\}$  NMR spectrum, a singlet and a broad doublet of multiplets with a carbon-rhodium coupling constant of 32.6 Hz appeared at 37.3 and 23.2 ppm, respectively. The two signals were attributed to the  $\beta$  and  $\alpha$  carbon atoms, respectively. The APT  $^{13}\text{C}$  NMR spectrum proved the presence of the two  $\text{CH}_2$  moieties. DFT calculations (BP86/def2-SVP) revealed for the optimized geometry the fluorido ligand in a *trans* position to the aromatic ring (Figure 14).

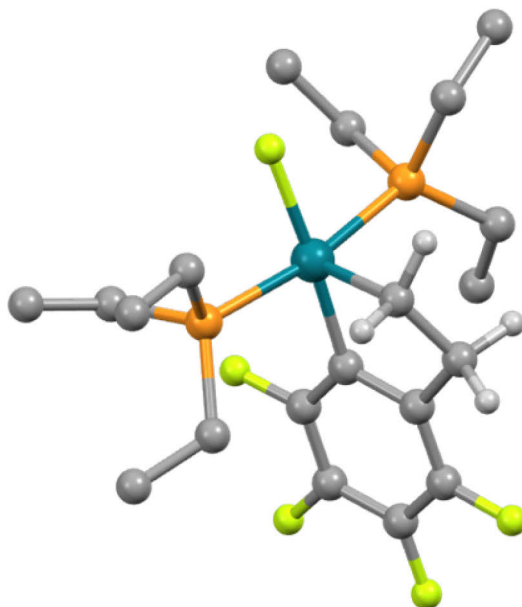


Figure 14. DFT optimized structure of complex **38**. Hydrogen atoms of the phosphine ligands are omitted for clarity.

In terms of complex **39**, two signals appeared at 7.9 and -2.8 ppm in the  $^{31}\text{P}\{^1\text{H}\}$  NMR spectrum with a 2:1 ratio as a doublet of doublet of doublets and a doublet of multiplets,

respectively. The resonance at 7.9 ppm was assigned to the phosphine ligands *trans* to each other and the coupling constant of 103.8 Hz was due to the rhodium atom, which is consistent with the existence of rhodium(III) complex.<sup>[30, 166]</sup> The coupling constants of 29.7 and 17.9 Hz were associated with the phosphine and fluorido ligand, respectively. The other resonance at -2.8 ppm revealed a coupling constant of approximately 90 Hz to the rhodium atom. Four signals that exhibited at -122.6, -140.6, -161.2 and -165.7 ppm in the  $^{19}\text{F}$  NMR spectrum were attributed to fluorine atoms at aromatic ring and one signal which appeared at -385.1 ppm is typical for the rhodium(III) bound fluorido ligand.<sup>[201-203]</sup> Consistent with complex **38**, the  $^1\text{H}$  NMR spectrum also displayed two signals at 3.04 and 1.42 ppm belonging to the  $\text{C}_6\text{F}_4\text{CH}_2\text{CH}_2$  group of complex **39**. The assignment of the signal at 1.42 ppm was based on the  $^1\text{H}$ - $^1\text{H}$  COSY NMR spectrum. In the  $^{13}\text{C}\{^1\text{H}\}$  NMR spectrum the resonance at 37.8 ppm as multiplet was assigned to the  $\beta$ -carbon atom and the resonance at 23.7 ppm as doublet of multiplets with a carbon-rhodium coupling constant of 16.4 Hz to the  $\alpha$ -carbon atom, which is in accordance to the  $^{13}\text{C}$  NMR data of complex **38**.

Fortunately, by slowly warming up a concentrated solution of complex **39** in hexane from 193 K to 278 K, single crystals of complex **39** were obtained and X-ray crystallography confirmed the structure proposed (Figure 15). The molecular structure displays a distorted octahedral geometry with a fluorido ligand *trans* to the  $\text{CH}_2$  moiety.

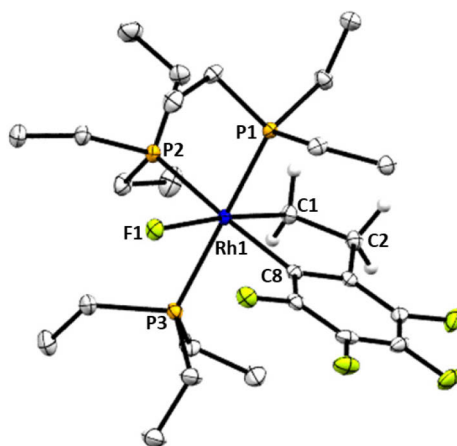


Figure 15. ORTEP diagram of complex **39**. Ellipsoids are drawn at the 50% probability. Hydrogen atoms of the phosphine ligands are omitted for clarity. Selected distances [ $\text{\AA}$ ] and bond angles [ $^\circ$ ]: Rh1–C1 2.0775(15), Rh1–C8 2.0828(15), Rh1–F1 2.1360(9), Rh1–P3 2.3470(4), Rh1–P1 2.3502(4), Rh1–P2 2.3836(4), C1–C2 1.539(2), C1–Rh1–F1 173.53(5), C8–Rh1–F1 96.96(5), C1–Rh1–P3 93.56(4), C8–Rh1–P3 87.01(4), F1–Rh1–P3 92.84(3), P3–Rh1–P1 168.314(15), C1–Rh1–P2 90.47(4), C8–Rh1–P2 172.89(4), F1–Rh1–P2 90.08(3), P3–Rh1–P2 93.662(15), P1–Rh1–P2 92.732(16).



Furthermore, it was also shown by DFT calculations (BP86/def2-SVP) that this structure is 12 kJ/mol lower in energy than its isomer with the fluorido ligand in the *trans* position to the aromatic ring. A comparison among literature known rhodium(III) fluorido complexes<sup>[202, 204]</sup> and complex **39** suggested that the 2.1360(9) Å distance of Rh1–F1 for complex **39** is slightly longer than others.

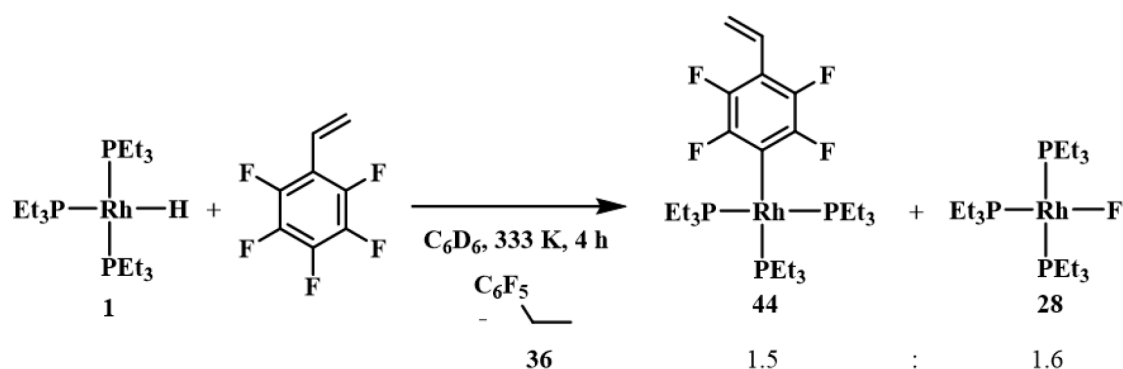
The possible mechanism for the formation of complex **38** from complex **37** is initiated by an insertion reaction of the rhodium-bound olefin into the rhodium-hydrogen bond followed by an intramolecular oxidative addition of the C–F bond (Scheme 49). In the past years, the generation of group 10 metallaindanes such as platinacycles, nickellacycles and palladacycles were carried out with non-fluorinated compounds, in which a C–H orthometallation reaction was involved.<sup>[205-207]</sup> In contrast, C–F bond oxidative addition steps at rhodium are very rare and are limited to cyclopentadienyl or trispyrazolylborate complexes.<sup>[23, 25, 201]</sup> In the presence of free  $\text{PEt}_3$ , complex **41** is afforded through  $\beta$ -hydride elimination and a subsequent HF elimination. The HF elimination reaction can be promoted by  $\text{KPF}_6$  because of the initial generation of KF. Furthermore, HF can be trapped by KF through the formation of a bifluoride.

The 5-coordinate 16-electron complex **38** might react easily because of the existence of the unoccupied vacant site. Therefore, to confirm and stabilize the structure, the reaction of **38** and carbon monoxide was conducted affording the 18-electron product *trans*- $[\text{Rh}(\text{F})(\text{CH}_2\text{CH}_2\text{C}_6\text{F}_4)(\text{CO})(\text{PEt}_3)_2]$  (**42**) quantitatively (Scheme 49). On treatment of **38** with  $^{13}\text{CO}$ , the isotopologue *trans*- $[\text{Rh}(\text{F})(\text{CH}_2\text{CH}_2\text{C}_6\text{F}_4)(^{13}\text{CO})(\text{PEt}_3)_2]$  (**42'**) was furnished. Notice that, the NMR spectra also indicated the formation of  $[\text{Rh}(\text{H})(\text{CO})(\text{PEt}_3)_3]$  (**43**)<sup>[208]</sup> (or the isotopologue  $[\text{Rh}(\text{H})(^{13}\text{CO})(\text{PEt}_3)_3]$  (**43'**)), which could stem from the reaction of rhodium hydrido complex **1** and CO (or  $^{13}\text{CO}$ ) directly.

In the  $^{31}\text{P}\{^1\text{H}\}$  NMR spectrum of **42**, a doublet of doublets with a phosphorus-rhodium coupling constant of 98.5 Hz and phosphorus-fluorine coupling constant of 17.3 Hz appeared at 16.9 ppm. For complex **42'**, the labelled carbon gave an additional coupling of 10.9 Hz, which is in agreement with a *cis*-arrangement of phosphine and CO ligands.<sup>[72, 209]</sup> The  $^{19}\text{F}$  NMR spectrum revealed a broad resonance at -425.3 and -418.2 ppm for rhodium-bound fluorido ligand of the complexes **42** and **42'**, respectively.<sup>[203]</sup> A broad triplet ( $J = 7.5$  Hz), which simplified to a triplet of pseudo triplets in the  $^1\text{H}\{^{19}\text{F}\}$  NMR spectrum shown at 3.15 ppm in the  $^1\text{H}$  NMR spectrum corresponded to the  $\beta$ -carbon atom observed at 33.4 ppm in the  $^{13}\text{C}$  domain of the  $^1\text{H}$ - $^{13}\text{C}$  HMQC NMR spectrum. A multiplet

at 2.56 ppm in the  $^1\text{H}$  domain that simplified to a triplet of triplet of doublets in the  $^1\text{H}\{^{19}\text{F}\}$  NMR spectrum was correlated with the carbon atom at the  $\alpha$ -position. The signal for the carbon atom was detected at 24.0 ppm as doublet of quartets ( $J = 19.9, 6.6$  Hz) in the  $^{13}\text{C}\{^1\text{H}\}$  NMR spectrum. Additional coupling constants of 1.9 and 2.1 Hz of the  $\beta$ - and  $\alpha$ -proton atoms to the labelled carbon were observed for complex **42'**. These coupling constants might indicate a *trans* arrangement of carbonyl ligand to the  $\text{CH}_2\text{CH}_2$  moiety, which is comparable with the configuration proposed for complex **38**. A doublet of doublet of triplets at 189.5 ppm in the APT  $^{13}\text{C}$  NMR spectrum for complex **42'** was due to the carbonyl ligand. The coupling constants of 41.3, 14.8 and 10.9 Hz were attributed to the rhodium atom, the metal-bound fluorido ligand and the two phosphorus atoms, respectively. An absorption band observed at  $2056\text{ cm}^{-1}$  in the IR spectrum was assigned to the carbonyl ligand of complex **42** and it is consistent with other rhodium(III) carbonyl complexes.<sup>[27, 210]</sup> In addition, the absorption band for the carbonyl ligand in complex **42'** appeared at  $2002\text{ cm}^{-1}$ , whose isotopic shift is in agreement with the data reported in the literature.<sup>[72]</sup>

In contrast to the room temperature reaction, when treating the rhodium hydrido complex **1** with pentafluorostyrene in a 1:1.3 ratio at 333 K for 4 h, the C–F bond at the 4-position was activated to yield complex  $[\text{Rh}(4\text{-C}_6\text{F}_4\text{CHCH}_2)(\text{PEt}_3)_3]$  (**44**) and rhodium fluorido complex  $[\text{Rh}(\text{F})(\text{PEt}_3)_3]$  (**28**)<sup>[59]</sup> as well as the hydrogenation product ethylpentafluorobenzene **36** in a ratio of 1.5:1.6:1 (based on the  $^{19}\text{F}$  NMR spectroscopy) (Scheme 50).



Scheme 50. Stoichiometric reaction of complex **1** and pentafluorostyrene at 333 K.

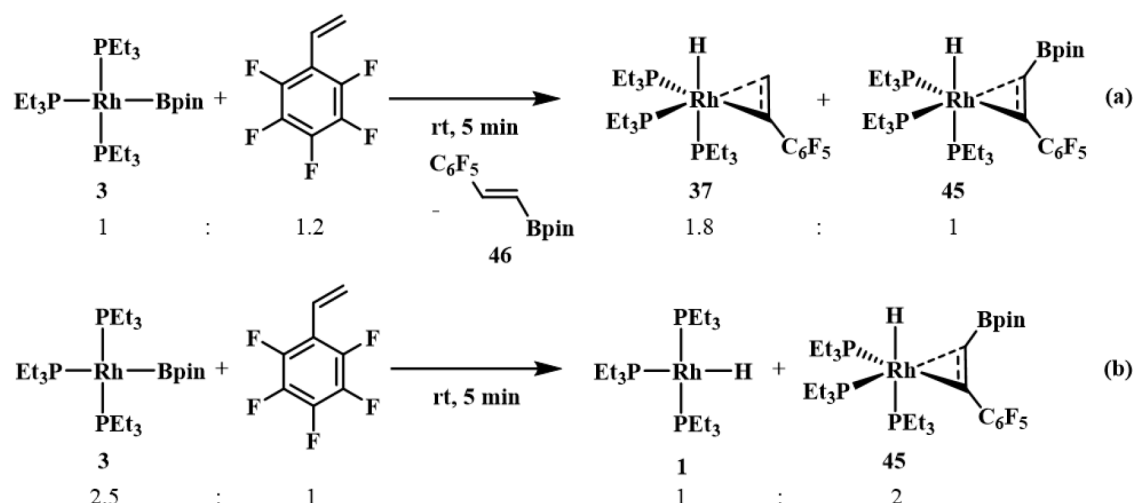
Mechanistically, the formation of Rh–C bond would imply the release of HF, which resembles a reaction pathway observed for other substrates.<sup>[29, 129, 161]</sup> HF can react further with complex **1** affording the rhodium fluorido complex **28** and  $\text{H}_2$  or also a dihydrido

fluorido complex.<sup>[59]</sup> Consequently, in the presence of H<sub>2</sub>, complex **36** is generated as the hydrogenation product of pentafluorostyrene.

A doublet of multiplets displayed at 18.4 ppm in the <sup>31</sup>P{<sup>1</sup>H} NMR spectrum of complex **44** with a phosphorus-rhodium coupling constant of 138.1 Hz was assigned to the phosphine ligand *trans* to the fluorinated fragment. The second resonance appeared at 14.0 ppm with a phosphorus-rhodium coupling constant of 141.1 Hz and phosphorus-phosphorus coupling constant of 40.1 Hz as doublet of doublets due to the two phosphine ligands in a mutual *trans* position. The <sup>19</sup>F NMR spectrum showed two signals at -110.7 and -147.3 ppm as multiplets in a 1:1 ratio, which gives evidence for the C–F bond activation at the 4-position.<sup>[28-29, 129, 200, 211]</sup> Finally, three resonances were observed in the <sup>1</sup>H NMR spectrum as a doublet of doublets (<sup>3</sup>J<sub>(H,H)</sub> = 18.1, <sup>3</sup>J<sub>(H,H)</sub> = 12.1 Hz), a doublet (<sup>3</sup>J<sub>(H,H)</sub> = 18.1 Hz) and a doublet (<sup>3</sup>J<sub>(H,H)</sub> = 12.1 Hz) at 6.98, 6.20 and 5.33 ppm, respectively, for the olefinic moiety. The coupling constant of 18.1 Hz is typical for protons in a *trans* arrangement and 12.1 Hz is attributed to the protons in the *cis* position.<sup>[212-214]</sup>

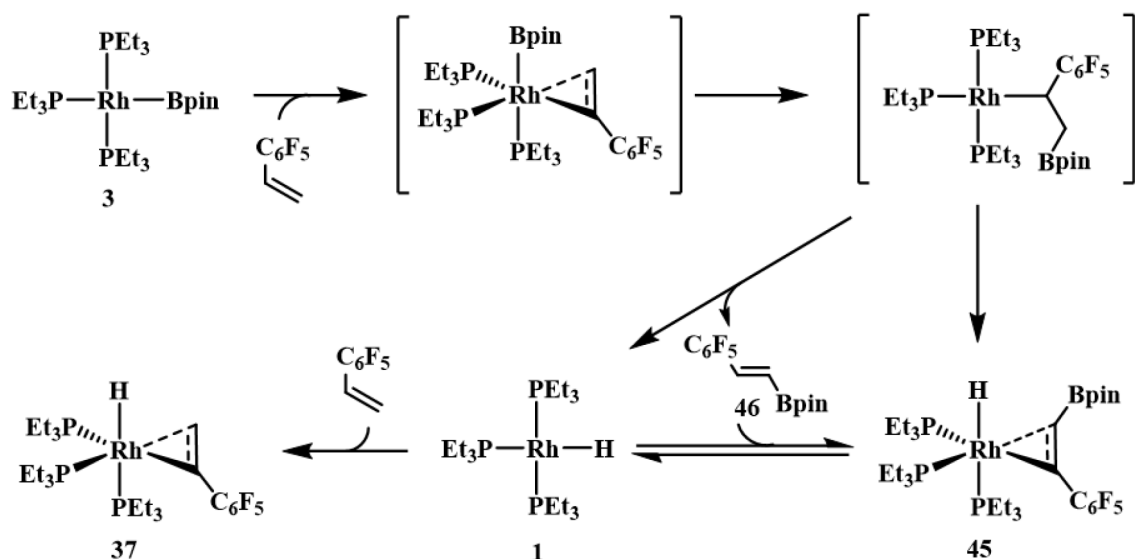
#### 4.2.2.3 Stoichiometric reactions of complex [Rh(Bpin)(PEt<sub>3</sub>)<sub>3</sub>] (**3**) and pentafluorostyrene

Considering the interesting stoichiometric reactivity of benzene, 1,1,2,3,3,3-hexfluoropropene, ketones, imines and fluorinated aromatics towards complex [Rh(Bpin)(PEt<sub>3</sub>)<sub>3</sub>] (**3**),<sup>[30, 128-129, 209]</sup> it was therefore treated with pentafluorostyrene. With an excess amount of pentafluorostyrene (ratio 1:1.2), besides complex **37**, which stemmed from the reaction of complex **1** and pentafluorostyrene, compound *fac*-[Rh(H)(η<sup>2</sup>-CH(Bpin)CHC<sub>6</sub>F<sub>5</sub>)(PEt<sub>3</sub>)<sub>3</sub>] (**45**) as well as the borylated olefin *E*-BpinCH=CHC<sub>6</sub>F<sub>5</sub> (**46**) were afforded in a 1.8:1:0.6 ratio (based on the <sup>19</sup>F NMR spectrum) at room temperature in 5 min in *d*<sub>14</sub>-methylcyclohexane (Scheme 51a). In contrast, when the ratio between complex **3** and pentafluorostyrene was enhanced to 2.5:1, only complex **45** and the rhodium hydrido complex **1** were formed (Scheme 51b). As it is described above, complex **37** was characterized at 213 K because it could evolve to other derivatives after a long time at room temperature. As with complex **37** and other literature known complexes *fac*-[Rh(H)(η<sup>2</sup>-CH<sub>2</sub>CHCF<sub>3</sub>)(PEt<sub>3</sub>)<sub>3</sub>]<sup>[162]</sup> and *fac*-[Rh(η<sup>2</sup>-CH<sub>2</sub>CFCF<sub>3</sub>)(H)(PEt<sub>3</sub>)<sub>3</sub>]<sup>[120]</sup>, the characterization of complex **45** was also conducted at 213 K.



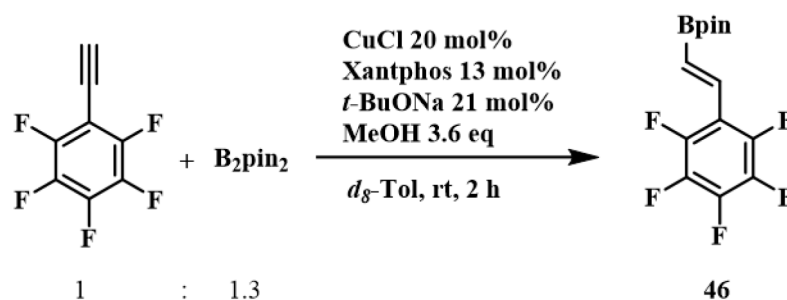
Scheme 51. Stoichiometric reactions of complex **3** with pentafluorostyrene.

Mechanistically, a direct coordination would take place between pentafluorostyrene and complex **3** followed by the insertion reaction of the olefin into Rh–B bond. Then, a  $\beta$ -hydride elimination reaction results in the formation of complex **45**, which may undergo a further disassociation reaction releasing complex **1** and compound **46**. Alternatively, complex **1** and compound **46** are generated initially and **45** is furnished after coordination. The presence of an excess amount of pentafluorostyrene results in coordination at complex **1** to give complex **37** (Scheme 52). A comparable stoichiometric reaction was reported employing complex **3** and styrene as substrates.<sup>[209]</sup>



Scheme 52. Conceivable mechanism for the formation of complexes **37** and **45**.

Compound **46** could be synthesized in an independent reaction in which pentafluorophenylacetylene was employed to undergo a monohydroboration reaction based on a similar reported procedure<sup>[215]</sup> (Scheme 53).



Scheme 53. Independent synthesis of borylated pentafluorostyrene **46**.

Three signals for **46** were observed as multiplets at -144.0, -155.5 and -163.5 ppm, respectively, in a 2:1:2 ratio in the  $^{19}\text{F}$  NMR spectrum. The two doublets with  $^3J$  proton-proton coupling constant of 18.8 Hz appeared at 7.48 and 6.70 ppm in the  $^1\text{H}$  NMR spectrum due to the olefinic moiety. A singlet at 1.08 ppm was assigned to the  $\text{CH}_3$  moiety on Bpin group. Note that a value of 18.8 Hz is a typical coupling constant of a *trans* arrangement.<sup>[72]</sup> A peak of  $m/z$  320 in the GC-MS indicates the presence of compound **46**.

With the independently synthesized boryl derivative **46** in hand, an independent reaction was designed between **46** and rhodium hydrido complex  $[\text{Rh}(\text{H})(\text{PET}_3)_3]$  (**1**) to confirm the proposed structure of complex **45** and the mechanism. As a consequence, *fac*- $[\text{Rh}(\text{H})(\eta^2\text{-CH}(\text{Bpin})\text{CHC}_6\text{F}_5)(\text{PET}_3)_3]$  (**45**) was afforded in  $d_8$ -toluene at 213 K after 5 min treating complex **1** with compound **46** (ratio 1.7:1).

The  $^{31}\text{P}\{^1\text{H}\}$  NMR spectrum of **45** at 213 K was comparable to the one for complex **37**. It revealed three signals at 18.2, 15.3 and 3.3 ppm. Five signals appeared at -144.2, -145.0, -166.5, -167.1 and -170.4 ppm in the  $^{19}\text{F}$  NMR spectrum. However, in the  $^1\text{H}$  NMR spectrum, only two broad signals were observed at 3.97 and 3.10 ppm. The  $^1\text{H}\{^{31}\text{P}\}$  NMR spectrum showed two doublets with a proton-proton coupling constant of 12.0 Hz. These signals were attributed to the protons of the coordinated olefinic moiety. A doublet of triplet of doublets at -14.87 ppm with a proton-*trans* phosphorus coupling constant of 163.0 Hz, proton-*cis* phosphorus of 18.2 Hz and proton-rhodium of 5.5 Hz was assigned to the hydrido ligand. DFT calculations (BP86/def2-SVP) of **45** revealed that the isomer with the Bpin group and hydrido ligand orientated on the same side of a plane defined by rhodium and the rhodium-bound olefin, and the fluorinated moiety positioned on the other side, was favored by 21.2 kJ/mol over the other rotational isomer (Figure 16).

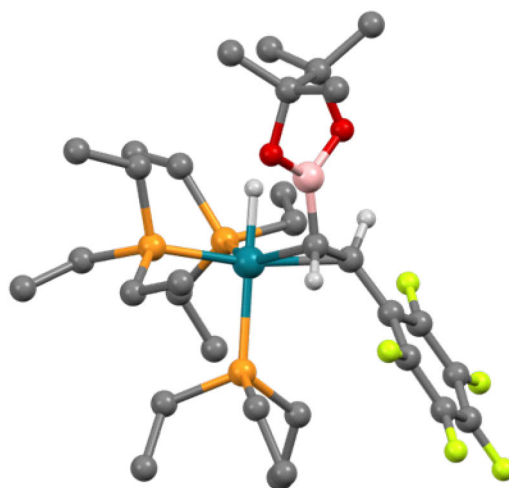
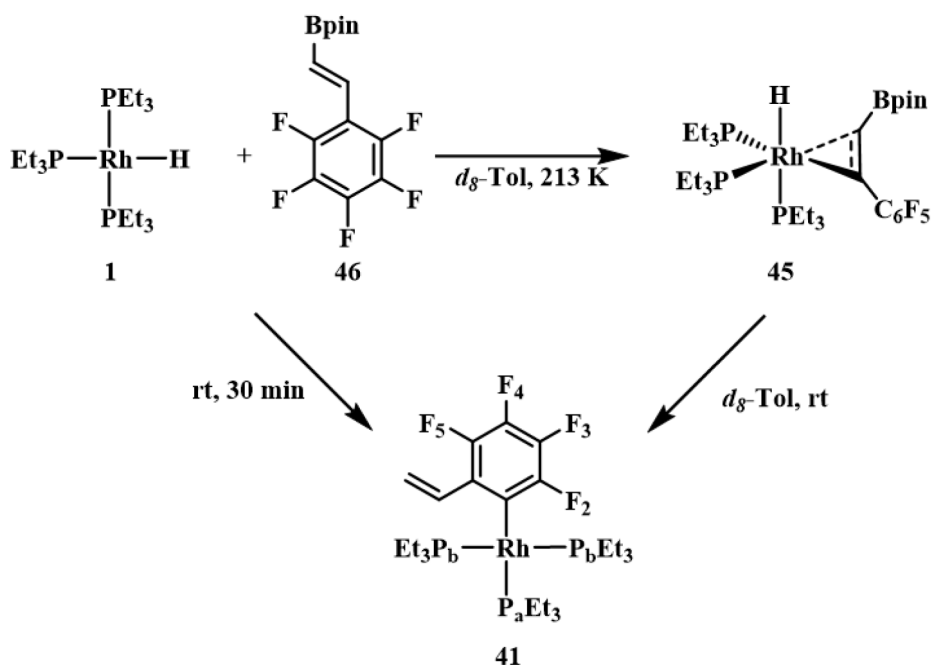


Figure 16. DFT optimized structure of complex **45**. Hydrogens of the phosphine ligands are omitted for clarity.

Inspired by the room temperature reaction of complex **1** and pentafluorostyrene, the same reaction solution in which complex **1** and compound **46** were involved was also warmed up or performed directly at room temperature (ratio 1:1.4). Interestingly, the *ortho* position to the olefin moiety C–F bond was activated giving  $[\text{Rh}(\text{2-C}_6\text{F}_4\text{CHCH}_2)(\text{PEt}_3)_3]$  (**41**) and another unidentified complex in a 13.5:1 ratio (based on the  $^{31}\text{P}\{^1\text{H}\}$  NMR spectrum) (Scheme 54).



Scheme 54. Independent stoichiometric reaction of complex **1** and compound **46**.

Presumably, the formation of **41** is accompanied by the formation of fluoroboronates, which are generated by the deborylation reaction of the olefinic moiety of complex **45**

and HF. Considering the *ortho*-directing effect, similar behaviors were observed before at the  $\{\text{Rh}(\text{PET}_3)_3\}$  fragment in the C–H bond and C–F bond activation reactions of aromatic  $\text{SCF}_3$  compounds and fluorinated pyridines, respectively.<sup>[29-30, 128, 162, 211]</sup>

Two groups of signals appeared at 15.8 and 10.5 ppm in the  $^{31}\text{P}\{^1\text{H}\}$  NMR spectrum, which were assigned to complex **41**. The doublet of triplet of doublet of doublet of doublets at 15.8 ppm with a coupling constant of 123.3 Hz to rhodium, 38.0 Hz to phosphorus, 14.6 Hz to F<sub>2</sub>, 9.8 Hz to F<sub>5</sub> and 6.6 Hz to F<sub>3</sub> was assigned to the phosphine ligand *trans* to the fluorinated moiety (P<sub>a</sub>). For the two *cis*-phosphine ligands (P<sub>b</sub>), a doublet of doublets at 10.5 ppm with a coupling of 143.3 Hz to rhodium, a coupling of 38.0 Hz to the phosphorus atoms was observed. The  $^1J$  coupling constant of phosphorus and rhodium indicates the presence of Rh(I) complex.<sup>[29-30, 161-162]</sup> In order to facilitate the assignment, the spectrum was simulated<sup>[164]</sup> and is shown in Figure 17.

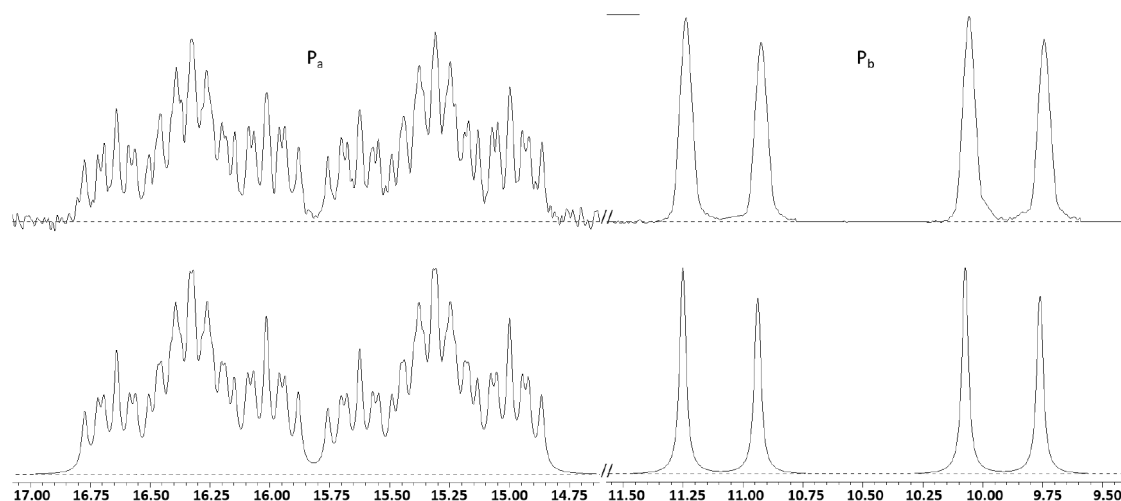


Figure 17. The  $^{31}\text{P}\{^1\text{H}\}$  NMR spectrum of complex **41**; simulated (below) observed (above) using the following coupling constants (Hz):  $^1J_{(\text{P}_a, \text{Rh})} = 123.3$ ,  $^2J_{(\text{P}_a, \text{P}_b)} = 38.0$ ,  $^4J_{(\text{P}_a, \text{F}_2)} = 14.6$ ,  $^5J_{(\text{P}_a, \text{F}_5)} = 9.8$ ,  $^5J_{(\text{P}_a, \text{F}_3)} = 6.6$ ;  $^1J_{(\text{P}_b, \text{Rh})} = 143.3$ .

Four signals that were observed in the  $^{19}\text{F}$  NMR spectrum at -105.7, -143.4, -160.5 and -165.7 ppm were also simulated and the spectrum is depicted in Figure 18. The fluorine resonances were assigned based on the literature known complexes<sup>[29-30, 129, 216-217]</sup> and coupling was confirmed by the  $^{19}\text{F}$ - $^{19}\text{F}$  COSY NMR spectrum. The chemical shifts are similar to the ones found for complex *trans*- $[\text{Ni}(2,3,4,5\text{-C}_6\text{F}_4\text{H})(\text{F})(\text{PET}_3)_2]$ .<sup>[200]</sup> In the  $^1\text{H}$  NMR spectrum, three resonances were found at 8.16, 6.38 and 5.40 ppm as a doublet of doublets ( $^3J_{(\text{H}, \text{H})} = 18.4$ ,  $^3J_{(\text{H}, \text{H})} = 11.8$  Hz), a doublet ( $^3J_{(\text{H}, \text{H})} = 18.1$  Hz) and a doublet ( $^3J_{(\text{H}, \text{H})} = 11.5$  Hz), respectively. The coupling constants resemble these reported for **44** and are due to the olefinic pattern. Moreover, a peak at  $m/z$  632 revealed in the liquid

injection field desorption ionization mass spectrometry (LIFDI MS) further proved the existence of complex **41**.

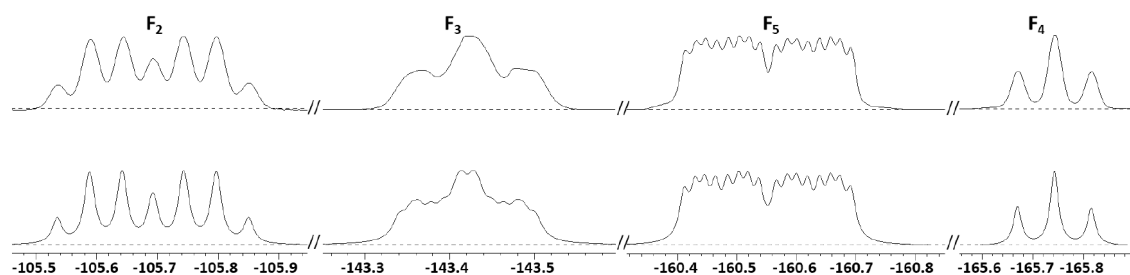
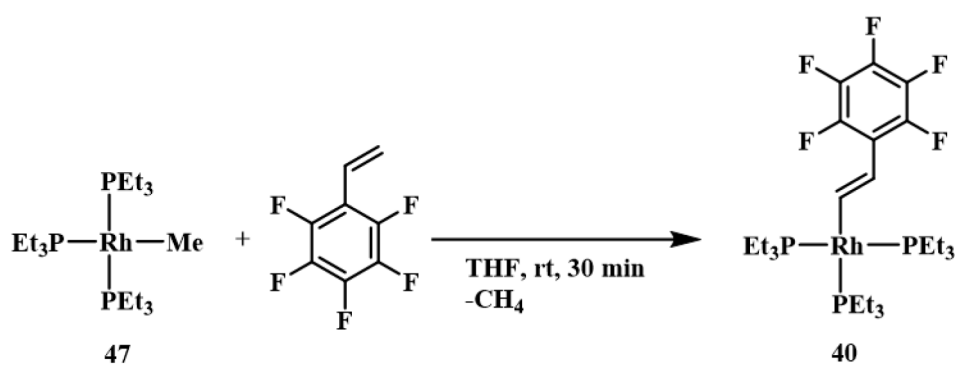


Figure 18. The  $^{19}\text{F}$  NMR spectrum of complex **41**; simulated (below) observed (above) using the following coupling constants (Hz):  $^5J_{(\text{F}_2, \text{F}_5)} = 43.8$ ,  $^3J_{(\text{F}_2, \text{F}_3)} = 14.6$ ,  $^4J_{(\text{F}_2, \text{P}_a)} = 14.6$ ,  $^3J_{(\text{F}_2, \text{Rh})} = 14.6$ ,  $^3J_{(\text{F}_3, \text{F}_4)} = 20.3$ ,  $^5J_{(\text{F}_3, \text{P}_a)} = 6.6$ ,  $^4J_{(\text{F}_3, \text{Rh})} = 4.0$ ,  $^3J_{(\text{F}_5, \text{F}_4)} = 20.3$ ,  $^5J_{(\text{F}_5, \text{P}_a)} = 9.8$ ,  $^4J_{(\text{F}_5, \text{Rh})} = 5.2$ .

#### 4.2.2.4 Stoichiometric reactions of complex $[\text{Rh}(\text{Me})(\text{PEt}_3)_3]$ (**47**) and pentafluorostyrene

The rhodium methyl complex  $[\text{Rh}(\text{Me})(\text{PEt}_3)_3]$  (**47**)<sup>[218]</sup> was investigated as a useful precursor to C–H bond activation reactions.<sup>[29, 120, 161, 211]</sup> In order to fulfill a C–H bond activation instead of the C–F bond activation, complex **47** was therefore treated with pentafluorostyrene (ratio 1:1.1). Indeed, the C–H bond activation complex  $[\text{Rh}(\text{E-CHCHC}_6\text{F}_5)(\text{PEt}_3)_3]$  (**40**) was produced after 30 min at room temperature in THF as a brown oil (Scheme 55).



Scheme 55. Stoichiometric reaction of complex **47** with pentafluorostyrene.

In the  $^{31}\text{P}\{^1\text{H}\}$  NMR spectrum, a doublet of triplets with  $^1J$  phosphorus-rhodium coupling constant of 115.7 Hz and  $^2J$  phosphorus-phosphorus coupling constant of 36.1 Hz and a doublet of doublets with  $^1J$  phosphorus-rhodium of 156.7 Hz and same phosphorus-phosphorus coupling constant appeared at 19.4 and 16.6 ppm, respectively, in a 1:2 ratio. Three resonances were observed in the  $^{19}\text{F}$  NMR spectrum at -155.3, -171.0 and -172.1 ppm with a ratio of 2:2:1. Finally, a doublet of multiplets and a doublet of



doublet of quartets, which simplified to two broad doublets in the  $^1\text{H}\{^{31}\text{P}\}$  NMR spectrum, were observed at 9.18 and 6.42 ppm in the  $^1\text{H}$  NMR spectrum. Similar to complex **41** and **44**, the coupling constant of 18.6 Hz illustrates a *trans* arrangement at the double bond. On the basis of the assignment of complex  $[\text{Rh}(\textit{E}\text{-CHCHCF}_3)(\text{PEt}_3)_3]$ ,<sup>[120]</sup> the signal at 9.18 ppm belonged to the proton at the  $\alpha$ -position to the rhodium atom and the  $\beta$ -position proton displayed a coupling to the *trans* phosphine ligand for 6.7 Hz. In addition, a peak with  $m/z$  650 shown in the LIFDI MS data proved the presence of complex **40**.

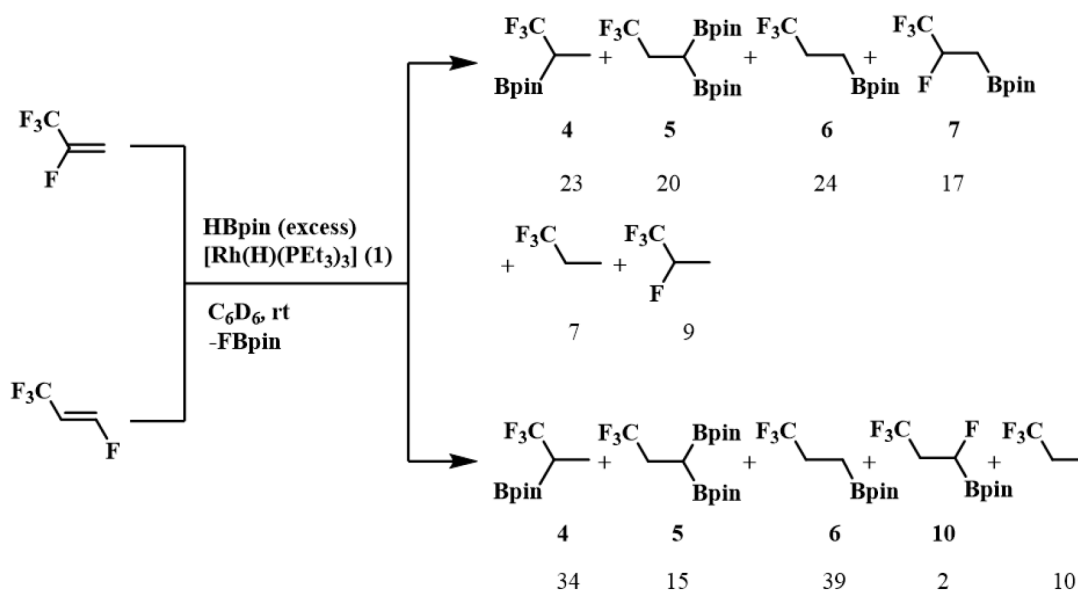


## 5. Summary

Introducing fluorine atoms to organic compounds changes their chemical and physical properties and therefore their reactivities, which results in the exploration of them in different fields including pharmaceuticals, agrochemicals and material science. The employment of boron sources facilitates the activation of the fluorinated molecules by the formation of F–B bonds. This work focuses on the investigation of rhodium-mediated activation reactions of fluorinated olefins as well as possible borylation reactions.

Because of the low ozone depleting potential and short lifetime, hydrofluoroolefins (HFOs) especially HFO-1234yf (2,3,3,3-tetrafluoropropene) and HFO-1234ze (*E*-1,3,3,3-tetrafluoropropene) find more and more attention as cooling and foaming agents.

Reactivity investigations were conducted towards HFO-1234yf and HFO-1234ze, in which HBpin was employed as the boron source and the rhodium hydrido complex [Rh(H)(PEt<sub>3</sub>)<sub>3</sub>] (**1**) as the catalyst. With an excess amount of HBpin, CF<sub>3</sub>CH(Bpin)CH<sub>3</sub> (**4**), CF<sub>3</sub>CH<sub>2</sub>CH(Bpin)<sub>2</sub> (**5**), CF<sub>3</sub>CH<sub>2</sub>CH<sub>2</sub>Bpin (**6**), CF<sub>3</sub>CFHCH<sub>2</sub>Bpin (**7**), 1,1,1-trifluoropropane and 1,1,1,2-tetrafluoropropane were generated in a ratio of 23:20:24:17:7:9 for HFO-1234yf, while the compounds **4**, **5**, **6**, CF<sub>3</sub>CH<sub>2</sub>CFHBpin (**10**) and 1,1,1-trifluoropropane were afforded in a 34:15:39:2:10 ratio in the catalytic reaction of HFO-1234ze (Scheme 56).

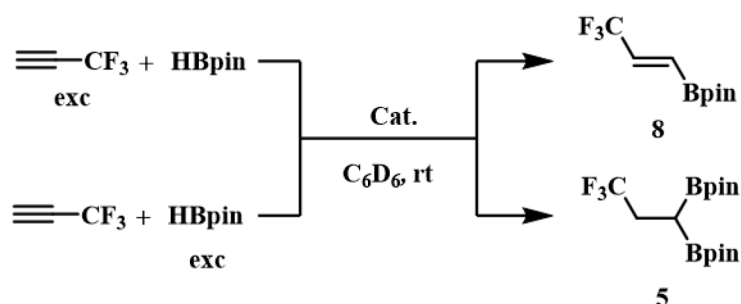


Scheme 56. Catalytic reaction of HFO-1234yf and HFO-1234ze with an excess amount of HBpin (ratio in mol%).

The same catalytic reaction conditions were applied to the pentafluoropropenes, HFO-1225zc (1,1,3,3,3-pentafluoropropene) and HFO-1225ye (*Z*) (*Z*-1,2,3,3,3-pentafluoropropene). Compounds **4**, **5**, **6**, **10** and 1,1,1-trifluoropropane in a 33:16:36:5:10 ratio were generated with the former substrate and compounds **4**, **5**, **6**, **7**, **10**, CF<sub>3</sub>CFHCFH(Bpin) (**11**), CF<sub>3</sub>CFHCFH<sub>2</sub> (**12**), 1,1,1-trifluoropropane and 1,1,1,2-tetrafluoropropane were observed in a ratio of 14:15:15:16:2:25:12:1:1 in the reaction with the latter substrate.

Different attempts such as employing complex [Rh(Cl)(PEt<sub>3</sub>)<sub>3</sub>] as the catalyst or B<sub>2</sub>pin<sub>2</sub> as the boron source or *d*<sub>8</sub>-THF as the solvent were examined to try to improve the selectivity. However, none of the variations provided a better selectivity. Subsequently, the *in situ* formed rhodium phosphine complex [Rh( $\mu$ -Cl)(PiPr<sub>3</sub>)<sub>2</sub>]<sub>2</sub> (**14**) was employed instead of complex **1**. Even though the same products mixture were generated, the yield of the hydroboration product CF<sub>3</sub>CFHCH<sub>2</sub>Bpin (**7**) was enhanced significantly from 17 % to 67 %. Similarly, in the reaction with HFO-1234ze, the defluorohydroboration product **6** was formed as the main product in a 58 %. For the substrate HFO-1225zc, the selectivity was not improved. While the ratio of the defluorohydroboration product of HFO-1225ye (*Z*), **7**, was increased from 16 % to 49 %.

Aiming to expand the substrate scope of the catalytic conditions involving HBpin as the boron source and complex **1** as the catalyst, 3,3,3-trifluoropropyne was then investigated. The highly selective monohydroboration product CF<sub>3</sub>CH=CHBpin (**8**) when introducing an excess amount of 3,3,3-trifluoropropyne to the reaction was observed; in contrast, the dihydroboration product CF<sub>3</sub>CH<sub>2</sub>CH(Bpin)<sub>2</sub> (**5**) was formed selectively in the presence of an excess amount of HBpin. Studying of complex [Rh(C $\equiv$ CCF<sub>3</sub>)(PEt<sub>3</sub>)<sub>3</sub>] (**17**) (together with *fac*-[Rh(C $\equiv$ CCF<sub>3</sub>)<sub>2</sub>(H)(PEt<sub>3</sub>)<sub>3</sub>] (**18**) in a 9:1 ratio) or the mixture of the rhodium(III) complexes **18** and *fac*-[Rh{(E)-CH=CHCF<sub>3</sub>}(C $\equiv$ CCF<sub>3</sub>)<sub>2</sub>(PEt<sub>3</sub>)<sub>3</sub>] (**19**) (ratio 5:1) as the catalytic precursor in the borylation reactions of 3,3,3-trifluoropropyne gave the same result when employing complex **1** as the catalyst (Scheme 57).



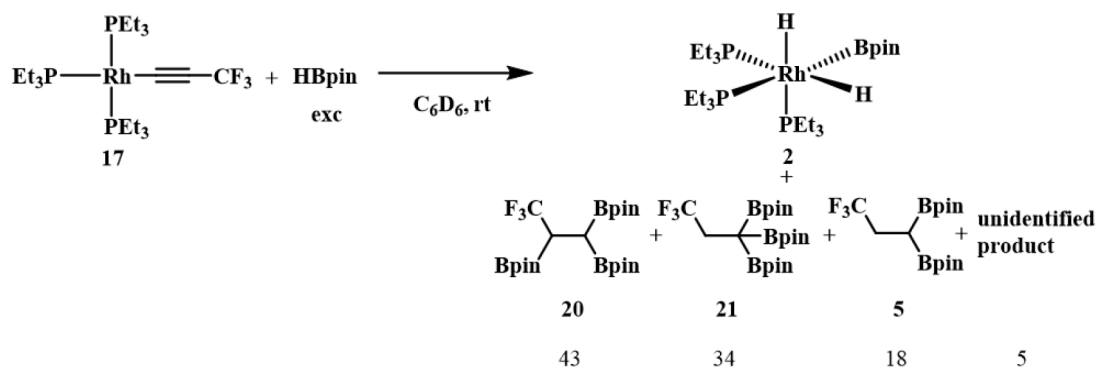
Cat. =  $[\text{Rh}(\text{H})(\text{P}(\text{Et}_3)_3)]$  (**1**)

$[\text{Rh}(\text{C}\equiv\text{CCF}_3)(\text{P}(\text{Et}_3)_3)]$  (**17**) : *fac*- $[\text{Rh}(\text{C}\equiv\text{CCF}_3)_2(\text{H})(\text{P}(\text{Et}_3)_3)]$  (**18**) 9:1

*fac*- $[\text{Rh}(\text{C}\equiv\text{CCF}_3)_2(\text{H})(\text{P}(\text{Et}_3)_3)]$  (**18**) : *fac*- $[\text{Rh}\{(E)\text{-CH=CHCF}_3\}(\text{C}\equiv\text{CCF}_3)_2(\text{P}(\text{Et}_3)_3)]$  (**19**) 5:1

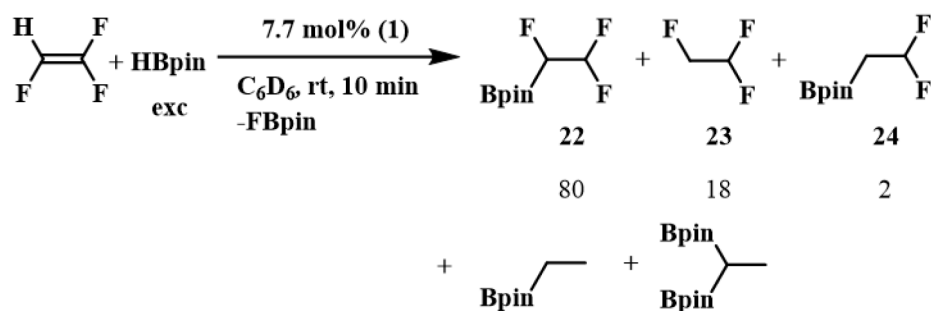
Scheme 57. Catalytic hydroboration of 3,3,3-trifluoropropyne with HBpin.

To better understand the catalytic processes, complex **17** was therefore treated with 2.1 equivalents of HBpin. Apart from an unidentified compound (5 %), only the rhodium(III) complex *fac*- $[\text{Rh}(\text{Bpin})(\text{H})_2(\text{P}(\text{Et}_3)_3)]$  (**2**) as well as hydroboration compounds  $\text{CF}_3\text{CH}(\text{Bpin})\text{CH}(\text{Bpin})_2$  (**20**),  $\text{CF}_3\text{CH}_2\text{C}(\text{Bpin})_3$  (**21**) and compound **5** as main organic products were obtained (Scheme 58).



Scheme 58. Stoichiometric hydroboration reaction of rhodium(I) complex **17**.

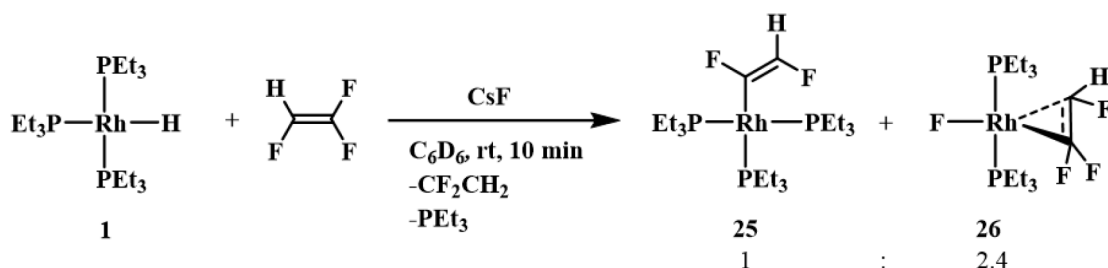
Encouraged by the results in which the activation and borylation of the  $\text{C}(\text{sp}^2)\text{-F}$  or the  $\text{C}(\text{sp})\text{-H}$  bond was achieved in the above mentioned substrates at the rhodium complex **1** in the presence of boron sources, olefins that only contain  $\text{C}(\text{sp}^2)\text{-F}$  bond were subsequently studied. Treatment of trifluoroethylene with an excess amount of HBpin using rhodium hydrido complex  $[\text{Rh}(\text{H})(\text{P}(\text{Et}_3)_3)]$  (**1**) as the catalyst afforded the compounds  $\text{CF}_2\text{HCFH}(\text{Bpin})$  (**22**),  $\text{CF}_2\text{HCFH}_2$  (**23**), traces of  $\text{CF}_2\text{HCH}_2(\text{Bpin})$  (**24**),  $\text{CH}_3\text{CH}_2(\text{Bpin})$  and  $\text{CH}_3\text{CH}(\text{Bpin})_2$ , in which the ratio with **22:23:24** was 80:18:2 (Scheme 59).



Scheme 59. Catalytic reaction of trifluoroethylene with HBpin (ratio in mol%).

However, when applying the same conditions to 1,1,2-trifluorobutene, only traces of products were formed, which were not characterized further.

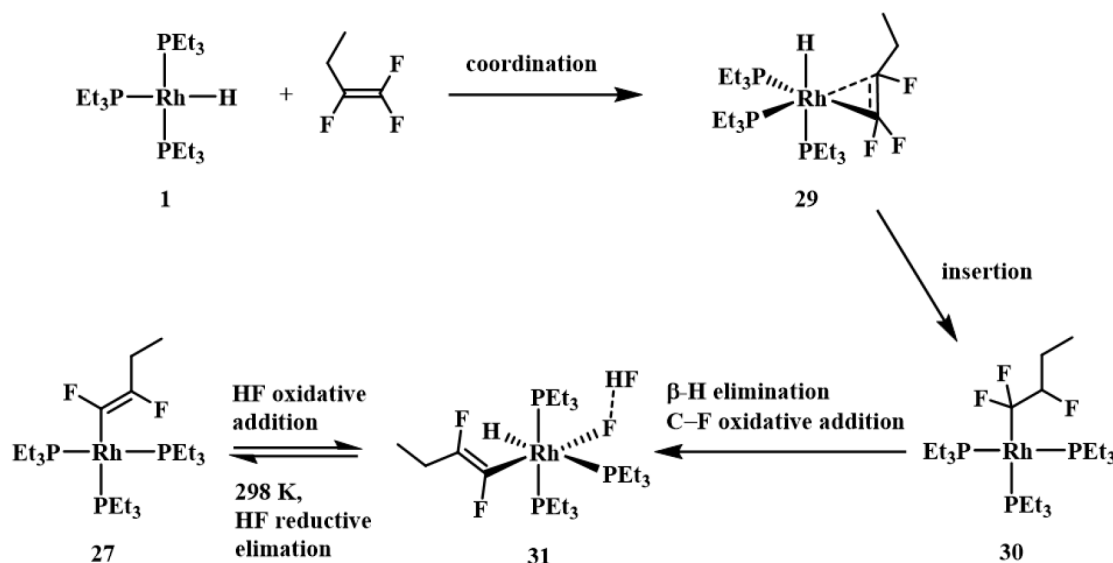
Reactivity studies between complex **1** and trifluoroethylene (ratio 1:2.8) in the presence of CsF showed that the C–F bond activation product  $[\text{Rh}((Z)\text{-CFCFH})(\text{PEt}_3)_3]$  (**25**), complex *trans*- $[\text{Rh}(\text{F})(\eta^2\text{-CF}_2\text{CFH})(\text{PEt}_3)_2]$  (**26**) and 1,1-difluoroethylene as well as free phosphine were generated (Scheme 60). Moreover, an independent reaction of  $[\text{Rh}(\text{F})(\text{PEt}_3)_3]$  (**28**) and trifluoroethylene confirmed the formation of complex **26**.



Scheme 60. Stoichiometric reaction of the rhodium hydrido complex **1** with trifluoroethylene.

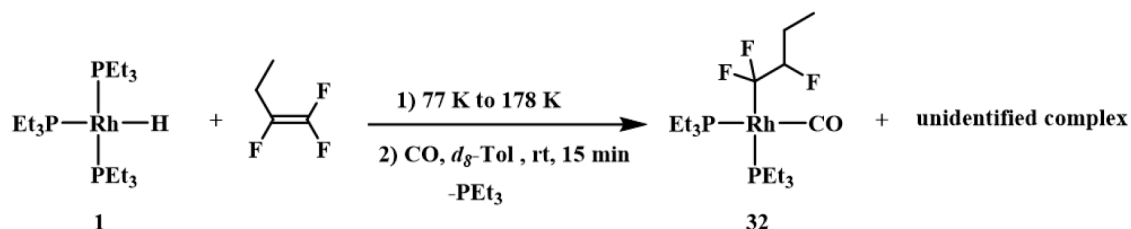
Similarly, treatment of complex **1** with 1,1,2-trifluorobutene (ratio 1:2.1) also led to a C–F bond activation to give  $[\text{Rh}((Z)\text{-CFCFC}_2\text{H}_5)(\text{PEt}_3)_3]$  (**27**) selectively at room temperature. Furthermore, the rhodium fluoro complex  $[\text{Rh}(\text{F})(\text{PEt}_3)_3]$  (**28**) was formed over time. A mechanism was proposed for the formation of complex **27**. It is based on the reaction, which was monitored by NMR spectroscopy, of complex **1** and 1,1,2-trifluorobutene at variable temperatures. Initially, coordination of 1,1,2-trifluorobutene occurred at complex **1** generating complex *fac*- $[\text{Rh}(\text{H})(\eta^2\text{-CF}_2\text{CFC}_2\text{H}_5)(\text{PEt}_3)_3]$  (**29**), which was followed by a insertion reaction to yield complex  $[\text{Rh}(\text{CF}_2\text{CFHC}_2\text{H}_5)(\text{PEt}_3)_3]$  (**30**) at 233 K. After 2 h at 253 K, the NMR spectra revealed the full conversion of complex **1** into **30**. Then  $\beta$ -H elimination and subsequent C–F bond oxidative addition took place affording complex *mer*- $[\text{Rh}(\text{H})(\text{FHF})((Z)\text{-CFCFC}_2\text{H}_5)(\text{PEt}_3)_3]$  (**31**) at 263 K. When increasing the temperature to 298 K, HF reductive elimination at the complex **31**

occurred along with the formation of complex  $[\text{Rh}((Z)\text{-CFCFC}_2\text{H}_5)(\text{PEt}_3)_3]$  (**27**) (Scheme 61).



Scheme 61. Stoichiometric reaction of the rhodium complex **1** with 1,1,2-trifluorobutene.

In order to trap the insertion product **30**, a reaction was conducted through introducing CO to the mixture after the reaction of complex **1** with 1,1,2-trifluorobutene at low temperature. This afforded complex  $[\text{Rh}(\text{CF}_2\text{CFHC}_2\text{H}_5)(\text{CO})(\text{PEt}_3)_2]$  (**32**) (Scheme 62).

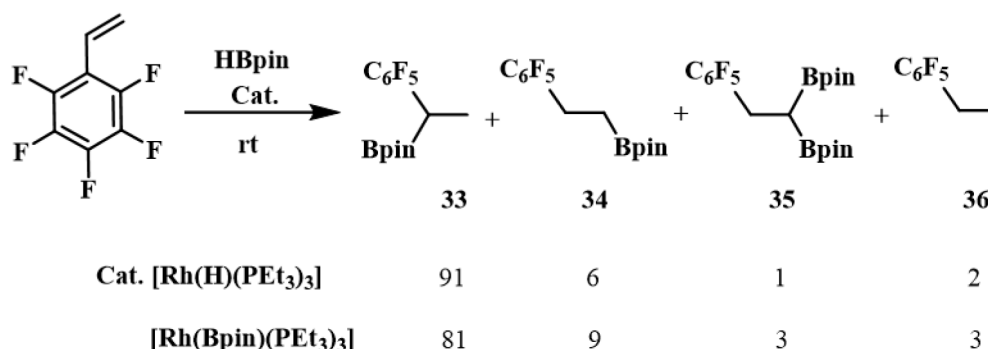


Scheme 62. Stoichiometric reaction of rhodium complex **1** with 1,1,2-trifluorobutene and subsequently CO.

As it is known, the electron withdrawing ability of  $\text{C}_6\text{F}_5$  group is weaker than that of the  $\text{CF}_3$  group, but stronger than that of an F atom. Therefore, investigations on the reactivity of pentafluorostyrene was also of particular interest.

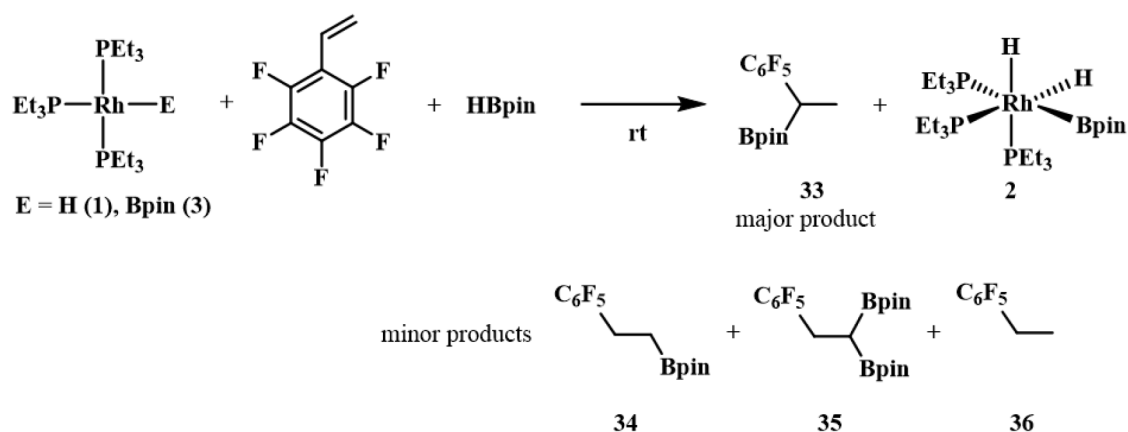
Following the above mentioned strategy, a reaction of pentafluorostyrene was performed with HBpin using complex  $[\text{Rh}(\text{H})(\text{PEt}_3)_3]$  (**1**) as the catalyst. As a result, the Markovnikov hydroboration product  $\text{C}_6\text{F}_5\text{CH}(\text{Bpin})\text{CH}_3$  (**33**), the anti-Markovnikov hydroboration product  $\text{C}_6\text{F}_5\text{CH}_2\text{CH}_2\text{Bpin}$  (**34**), small amounts of the diborylated derivative  $\text{C}_6\text{F}_5\text{CH}_2\text{CH}(\text{Bpin})_2$  (**35**) along with the hydrogenation product  $\text{C}_6\text{F}_5\text{CH}_2\text{CH}_3$  (**36**) in a 91:6:1:2 ratio were furnished. Instead of complex **1**, the rhodium boryl complex  $[\text{Rh}(\text{Bpin})(\text{PEt}_3)_3]$  (**3**) was also employed to the same reaction giving the same products

in a ratio of 81:9:3:3 (Scheme 63). Interestingly, when complex **1** was utilized as the catalyst under neat condition, the NMR spectrum still revealed the formation of **33:34:35:36** in a 75:13:4:8 ratio.



Scheme 63. Catalytic hydroboration reactions of pentafluorostyrene with HBpin at rhodium complexes.

Running the catalytic reaction in a stoichiometric provides a better understanding of a catalytic process. Indeed, treatment of complex **1** with pentafluorostyrene and HBpin stepwisely or with HBpin and pentafluorostyrene stepwisely resulted in the same rhodium(III) complex *fac*-[Rh(Bpin)(H)<sub>2</sub>(PEt<sub>3</sub>)<sub>3</sub>] (**2**) and **33**, **34**, **35** and **36** (ratio: 92:2:4:2). When complex **3** was treated, the same mixture of products was obtained in a ratio of 49:14:22:15 (Scheme 64).

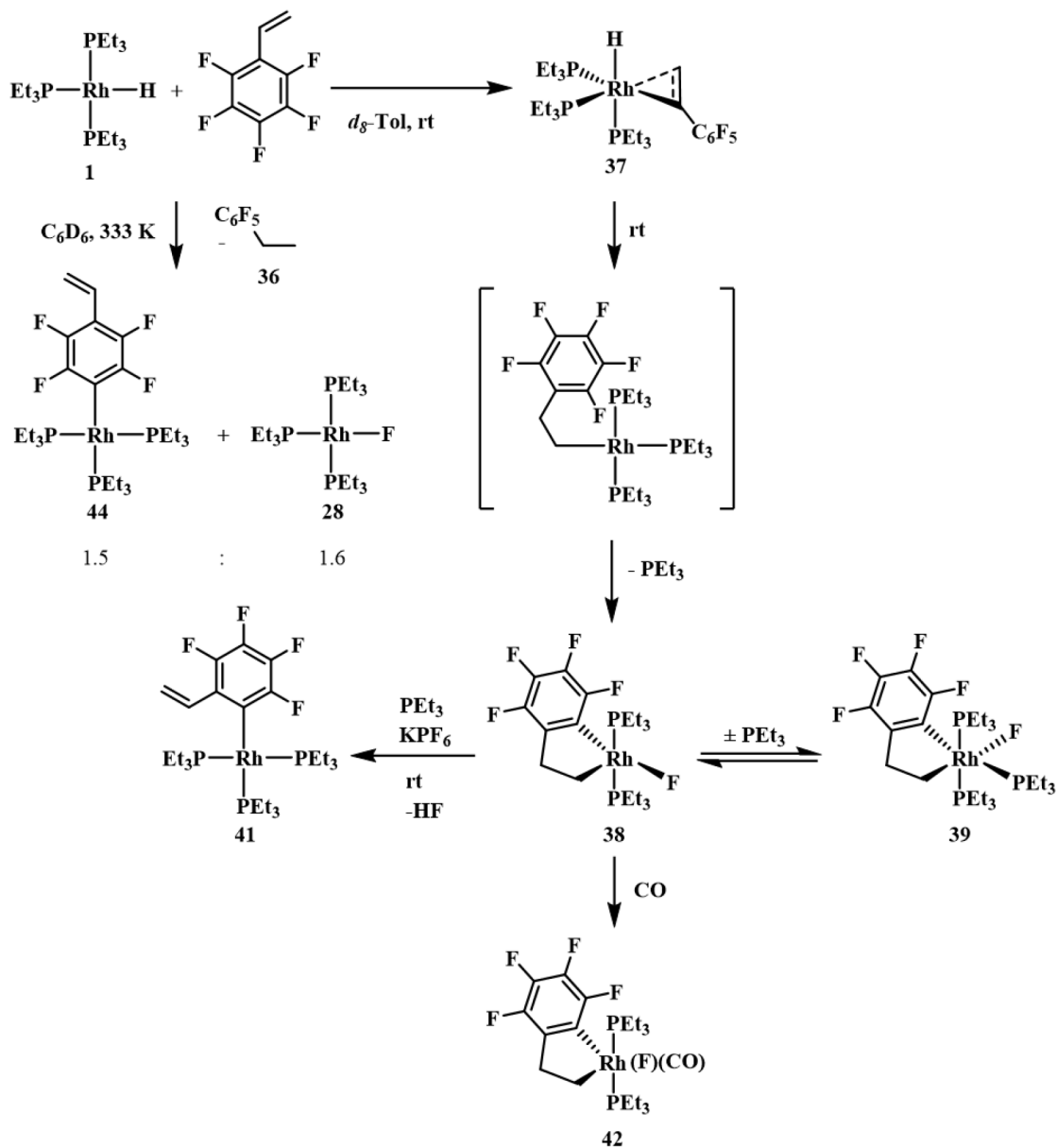


Scheme 64. Stoichiometric hydroboration reactions of complex **1** or **3**.

The independent stoichiometric reaction of complex **1** and pentafluorostyrene resulted in a coordination of olefin giving *fac*-[Rh(H)( $\eta^2$ -CH<sub>2</sub>CHC<sub>6</sub>F<sub>5</sub>)(PEt<sub>3</sub>)<sub>3</sub>] (**37**), which was only stable in solution at low temperature for a longer period and therefore characterized at 213 K. After 1 d at room temperature, the rhodaindane complex *trans*-[Rh(F)(CH<sub>2</sub>CH<sub>2</sub>(2-C<sub>6</sub>F<sub>4</sub>))(PEt<sub>3</sub>)<sub>2</sub>] (**38**) was formed through a cyclometallation and C–F bond activation reaction. Apart from **38**, free PEt<sub>3</sub>, traces of complex *mer*-[Rh(F)(CH<sub>2</sub>CH<sub>2</sub>(2-C<sub>6</sub>F<sub>4</sub>))(PEt<sub>3</sub>)<sub>3</sub>] (**39**) and minor amounts of the C–H bond activation complex [Rh(E-



$\text{CHCHC}_6\text{F}_5)(\text{PEt}_3)_3]$  (**40**) as well as the hydrogenation product ethylpentafluorobenzene **36** were also generated (Scheme 65).

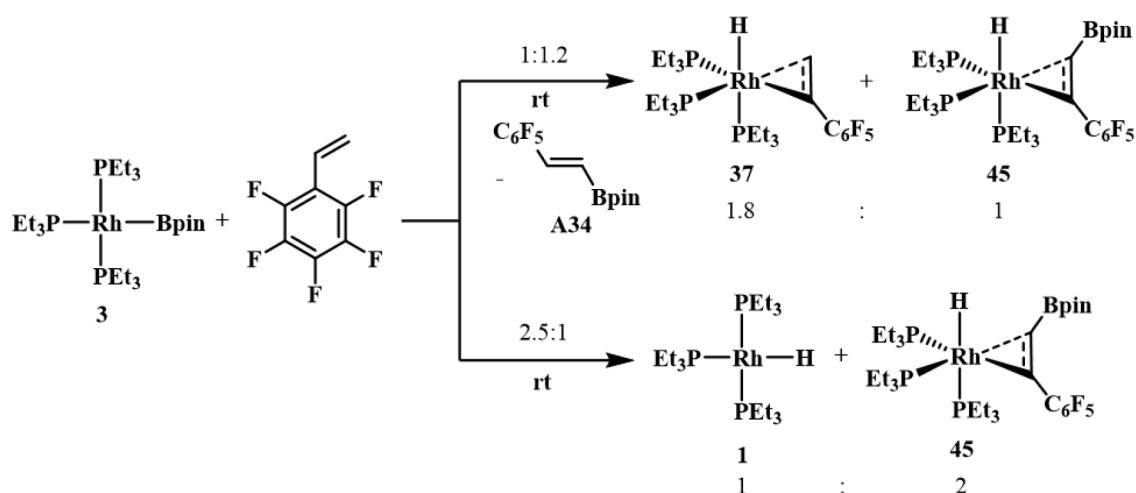


Scheme 65. Stoichiometric reactions of complex **1** and pentafluorostyrene.

Complex **38** can be transformed to complex **39** in the presence of free  $\text{PEt}_3$  at 233 K. Single crystals of complex **39** were obtained and X-ray crystallography confirmed the proposed structure. Furthermore, the C–F bond activation complex  $[\text{Rh}(2\text{-C}_6\text{F}_4\text{CHCH}_2)(\text{PEt}_3)_3]$  (**41**) was generated slowly from complex **38** and the conversion can be accelerated by  $\text{KPF}_6$ . Because of the existence of the unoccupied vacant site at complex **38**, it was then treated with  $\text{CO}$  (or  $^{13}\text{CO}$ ) to confirm and stabilize the structure. Consequently,  $\text{trans}-[\text{Rh}(\text{F})(\text{CH}_2\text{CH}_2\text{C}_6\text{F}_4)(\text{CO})(\text{PEt}_3)_2]$  (**42**) (or the corresponding isotopologue) was furnished quantitatively (Scheme 65).

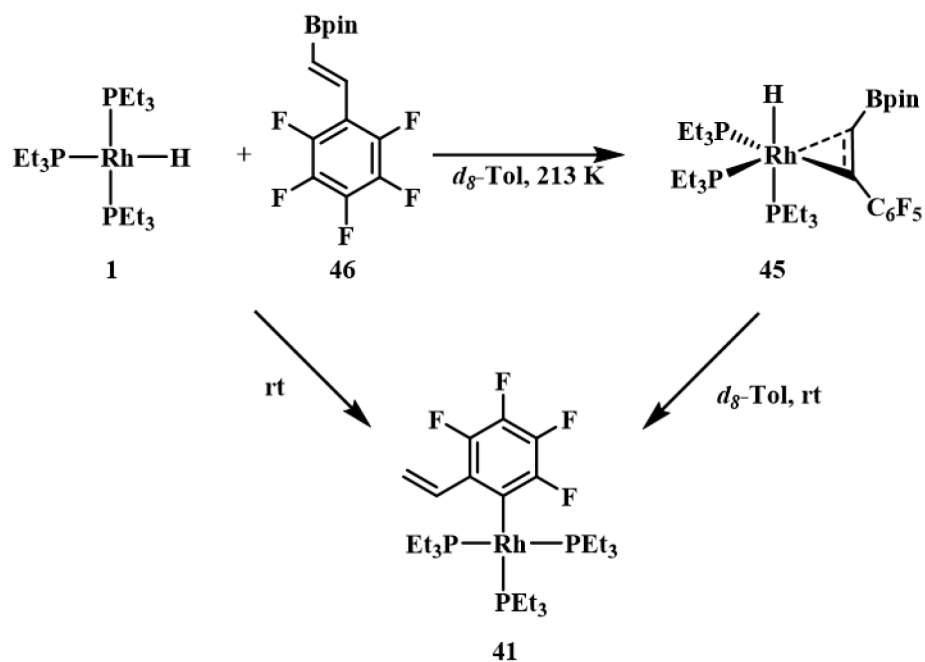
In contrast to the room temperature reaction, C–F activation at the 4-position to give  $[\text{Rh}(4\text{-C}_6\text{F}_4\text{CHCH}_2)(\text{PEt}_3)_3]$  (**44**) along with rhodium fluoro complex  $[\text{Rh}(\text{F})(\text{PEt}_3)_3]$  (**28**) and ethylpentafluorobenzene **36** was observed in the reaction of complex  $[\text{Rh}(\text{H})(\text{PEt}_3)_3]$  (**1**) and pentafluorostyrene at 333 K (Scheme 65).

Subsequently, the rhodium boryl complex  $[\text{Rh}(\text{Bpin})(\text{PEt}_3)_3]$  (**3**) was also treated with pentafluorostyrene. The results varied by the ratio between the starting materials. With an excess amount of pentafluorostyrene, complex *fac*- $[\text{Rh}(\text{H})(\eta^2\text{-CH}_2\text{CHC}_6\text{F}_5)(\text{PEt}_3)_3]$  (**37**), *fac*- $[\text{Rh}(\text{H})(\eta^2\text{-CH}(\text{Bpin})\text{CHC}_6\text{F}_5)(\text{PEt}_3)_3]$  (**45**) as well as the borylated olefin *E*- $\text{BpinCH}=\text{CHC}_6\text{F}_5$  (**46**) were afforded; while enhancing the ratio to have an excess amount of complex **3**, only complex **45** and the rhodium hydrido complex **1** were formed (Scheme 66).



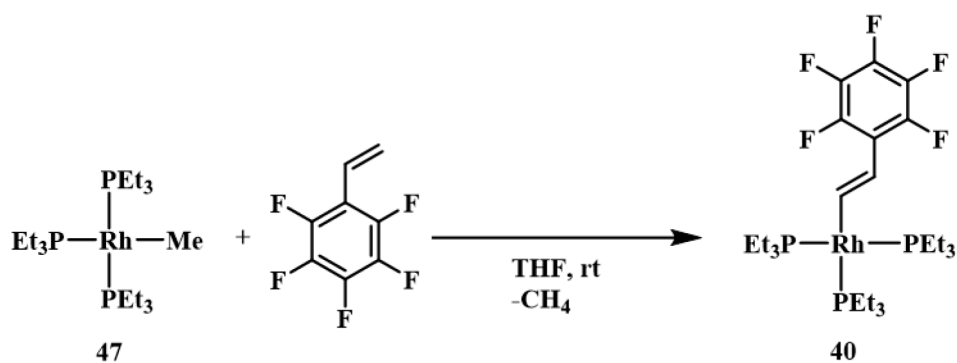
Scheme 66. Stoichiometric reactions of complex **3** with pentafluorostyrene.

To confirm the structure of complex **45**, an independent reaction was designed between **46** and rhodium hydrido complex  $[\text{Rh}(\text{H})(\text{PEt}_3)_3]$  (**1**). Indeed, *fac*- $[\text{Rh}(\text{H})(\eta^2\text{-CH}(\text{Bpin})\text{CHC}_6\text{F}_5)(\text{PEt}_3)_3]$  (**45**) was furnished at 213 K. Inspired by the behavior of complex **37** at room temperature, complex **45** was therefore warmed up to room temperature to result in a C–F bond activation at the 2-position to give complex  $[\text{Rh}(2\text{-C}_6\text{F}_4\text{CHCH}_2)(\text{PEt}_3)_3]$  (**41**) and another unidentified complex in a 13.5:1 ratio (Scheme 67). Treatment of complex **1** and **46** gave directly in 30 min complex **41** at room temperature.



Scheme 67. Independent stoichiometric reaction of complex **1** and compound **46**.

Given the significant role of complex  $[\text{Rh}(\text{Me})(\text{PEt}_3)_3]$  (**47**) played in C–H bond activation reactions, complex **47** was also treated with pentafluorostyrene. Indeed, the C–H bond activation was observed and complex  $[\text{Rh}(\text{E-CHCHC}_6\text{F}_5)(\text{PEt}_3)_3]$  (**40**) was produced (Scheme 68).



Scheme 68. Stoichiometric reaction of complex **4** with pentafluorostyrene.

In conclusion, reactivities of several rhodium(I) complexes towards fluorinated alkenes and 3,3,3-trifluoropropyne were studied in the presense of boron compounds. C–F bond activation or C–H bond activation as well as borylation were observed.



## 6. Experimental

### 6.1 General

#### 6.1.1 Techniques

Unless otherwise noted, all experiments were carried out under an atmosphere of argon by Schlenk techniques or inside an Ar-filled MBraun glovebox with oxygen level below 0.1 ppm. Glassware was pre-dried using heat and vacuum.

#### 6.1.2 Materials

All solvents, except hexane and diethyl ether used for eluting, were purified and dried by conventional methods and distilled under argon before use.

#### 6.1.3 Methods

The rhodium complexes  $[\text{Rh}(\text{H})(\text{PEt}_3)_3]$  (**1**),<sup>[219]</sup>  $[\text{Rh}(\text{Cl})(\text{PEt}_3)_3]$ ,<sup>[220]</sup>  $[\text{Rh}(\text{Bpin})(\text{PEt}_3)_3]$  (**3**),<sup>[127]</sup>  $[\text{Rh}(\text{Me})(\text{PEt}_3)_3]$  (**47**)<sup>[218]</sup> and  $[\text{Rh}(\text{F})(\text{PEt}_3)_3]$  (**28**)<sup>[59, 120]</sup> were prepared as reported in the literature. All reagents used were commercially available

### 6.2 Instrumentation

#### 6.2.1 Nuclear Magnetic Resonance (NMR) Spectroscopy

Unless stated, NMR spectra were recorded at room temperature on a Bruker DPX 300 or a Bruker Advance 300 spectrometer using the solvent as an internal lock.  $^1\text{H}$  and  $^{13}\text{C}$  signals are referred to residual solvent peaks, those of  $^{31}\text{P}\{^1\text{H}\}$  to 85%  $\text{H}_3\text{PO}_4$ , the  $^{19}\text{F}$  NMR spectra to external  $\text{CFCl}_3$ . NMR assignments were supported by  $^1\text{H}$ - $^1\text{H}$  COSY,  $^1\text{H}$ - $^{13}\text{C}$  HMQC,  $^1\text{H}$ - $^{13}\text{C}$  HMBC,  $^1\text{H}\{^{19}\text{F}\}$ ,  $^1\text{H}\{^{31}\text{P}\}$   $^{13}\text{C}$ - $^{19}\text{F}$  HMQC,  $^{19}\text{F}$ - $^1\text{H}$  COSY and  $^{19}\text{F}$ - $^{19}\text{F}$  COSY experiments.

#### 6.2.2 Mass Spectrometry

**Liquid Injection Field Desorption Ionization:** Mass spectra were measured with a Micromass Q-ToF-2 instrument equipped with a Linden LIFDI source (Linden CMS GmbH).

**Gas Chromatography/Mass Spectrometry:** GC-MS analyses were performed with an Agilent 6890N gas-phase chromatograph equipped with an Agilent 5973 Network mass selective detector at 70eV.

### 6.2.3 Infrared (IR) Spectroscopy

Infrared spectra were recorded with a Bruker Vertex 70 spectrometer equipped with an ATR unit (diamond).

### 6.2.4 DFT calculations

Calculations were run using the Gaussian 09 (Revision D.01) program package<sup>[221]</sup> and the BP86 functional. Rhodium was described with RECPs and the associated def2-SVP basis sets.<sup>[222-223]</sup> All the other atoms were described with def2-SVP basis sets. A Grimme D3 dispersion correction with Becke-Johnson damping was included.<sup>[224-225]</sup> All calculated structures were identified as minima (no negative eigenvalues).

### 6.2.5 X-ray diffraction analysis

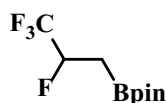
Crystallographic data of **39** were collected on a Bruker D8 Venture diffractometer at 100 K. The structures were solved by intrinsic phasing (SHELXT-2014)<sup>[226]</sup> and refined by full matrix least-squares procedures based on  $F^2$  with all measured reflections (SHELXL-2016).<sup>[227]</sup> The SADABS program<sup>[228]</sup> was used for multi-scan absorption corrections. All non-hydrogen atoms were refined with anisotropic displacement parameters. Hydrogen atoms were included in idealized positions and refined using a riding model.

## 6.3 Procedures

### Catalytic conversion of an excess amount of HFO-1234yf with HBpin

In a Young NMR tube  $[\text{Rh}(\text{H})(\text{PET}_3)_3]$  (**1**) (5.0 mg, 0.011 mmol, 5 mol% based on the amount of HBpin) was dissolved in  $\text{C}_6\text{D}_6$  (0.5 mL) and HBpin (35.0  $\mu\text{L}$ , 0.23 mmol) was added to the solution. The solution was cooled to 77 K, degassed *in vacuo*, and pressurized with HFO-1234yf to 0.7 bar (105 mg, 0.92 mmol). After warming up to room temperature the reaction was monitored by NMR spectroscopy. After 1 h at room temperature the  $^1\text{H}$  and  $^{19}\text{F}$  NMR spectroscopic data revealed the complete conversion of HBpin as well as the formation of  $\text{CF}_3\text{CH}(\text{Bpin})\text{CH}_3$  (**4**),  $\text{CF}_3\text{CH}_2\text{CH}(\text{Bpin})_2$  (**5**),  $\text{CF}_3\text{CH}_2\text{CH}_2(\text{Bpin})$  (**6**),  $\text{CF}_3\text{CFHCH}_2\text{Bpin}$  (**7**), 1,1,1-trifluoropropane, 1,1,1,2-tetrafluoropropane, 3,3,3-trifluoropropene and a small amount of unidentifiable products in a 17:15:22:19:13:4:5:5 ratio. Additionally, FBpin was obtained. Compounds **4**, **5**, **6**, 1,1,1-trifluoropropane, 1,1,1,2-tetrafluoropropane and 3,3,3-trifluoropropene were identified by comparison of their data with the corresponding literature.<sup>[61, 122-124]</sup>

Analytical data for **7**:



**$^{19}\text{F}$  NMR** (282.4 MHz,  $d_8$ -THF):  $\delta$  = -81.6 (dd, d in the  $^{19}\text{F}\{^1\text{H}\}$  NMR,  $^3J(\text{F},\text{F}) = 11$ ,  $^3J(\text{F},\text{H}) = 6$  Hz,  $\text{CF}_3$ ); -191.5 (m, q in the  $^{19}\text{F}\{^1\text{H}\}$  NMR,  $^3J(\text{F},\text{F}) = 11$ ,  $\text{CFH}$ ) ppm.

**$^1\text{H}$  NMR** (300.1 MHz,  $d_8$ -THF):  $\delta$  = 5.05 (dm,  $^2J(\text{H},\text{F}) = 46.0$ ,  $\text{CFH}$ ); 1.36 (m, based on the  $^1\text{H}$ - $^1\text{H}$  COSY NMR spectrum, the signal is overlapped with signals of the other products,  $\text{CH}_2\text{Bpin}$ ) ppm. The signals of Bpin ligand cannot be identified because of the mixture of products.

**GC/MS** ( $\text{C}_6\text{D}_6$ ): Calculated ( $m/z$ ) for  $[\text{C}_9\text{H}_{15}\text{BF}_4\text{O}_2]^+$ : 242; found: 242.

### General catalytic conversion of hydrofluoroolefins with an excess amount of HBpin using $[\text{Rh}(\text{H})(\text{PET}_3)_3]$ (**1**) as the catalyst

In a Young NMR tube  $[\text{Rh}(\text{H})(\text{PET}_3)_3]$  (**1**) was dissolved in  $\text{C}_6\text{D}_6$  (0.5 mL) and HBpin was added to the solution. The solution was cooled to 77 K, degassed *in vacuo*, and pressurized with the corresponding hydrofluoroolefin to 0.3 bar. After warming up to room temperature the reaction was monitored by NMR spectroscopy.

**HFO-1234yf**

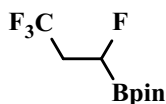
[Rh(H)(PEt<sub>3</sub>)<sub>3</sub>] (**1**) (10.0 mg, 0.022 mmol, 8.6 mol% based on the amount of HFO-1234yf) and HBpin (70  $\mu$ l, 0.46 mmol) was added. After 10 min at room temperature the <sup>1</sup>H and <sup>19</sup>F NMR spectroscopic data revealed the complete conversion of HFO-1234yf as well as the formation of compounds **4**, **5**, **6**, **7**, 1,1,1-trifluoropropane and 1,1,1,2-tetrafluoropropane in a ratio of 23:20:24:17:7:9.

When *d*<sub>8</sub>-THF was employed as solvent instead of C<sub>6</sub>D<sub>6</sub>, the same products in a 27:21:29:9:7:7 ratio after 20 min were afforded.

**HFO-1234ze**

[Rh(H)(PEt<sub>3</sub>)<sub>3</sub>] (**1**) (10.0 mg, 0.022 mmol, 8.6 mol% based on the amount of HFO-1234ze) and HBpin (70  $\mu$ l, 0.46 mmol) was added. After 30 min at room temperature the <sup>1</sup>H and <sup>19</sup>F NMR spectroscopic data revealed the complete conversion of HFO-1234ze as well as the formation of **4**, **5**, **6**, CF<sub>3</sub>CH<sub>2</sub>CFHBpin (**10**) and 1,1,1-trifluoropropane in a ratio of 34:15:39:2:10.

Analytical data for **10**:



<sup>19</sup>F NMR (282.4 MHz, C<sub>6</sub>D<sub>6</sub>):  $\delta$  = -64.6 (td, d in <sup>19</sup>F{<sup>1</sup>H} NMR, <sup>3</sup>*J*(F,H) = 10, <sup>4</sup>*J*(F,F) = 7 Hz, CF<sub>3</sub>); -224.5 (m, CFH) ppm.

<sup>1</sup>H NMR (300.1 MHz, C<sub>6</sub>D<sub>6</sub>):  $\delta$  = 4.02 (dt, <sup>2</sup>*J*(H,F) = 46.7, <sup>3</sup>*J*(H,H) = 5.5 Hz, CFH); 1.80 (observed in the <sup>1</sup>H-<sup>1</sup>H COSY NMR spectrum, overlapped with signals of other products, CH<sub>2</sub>) ppm. The signal of Bpin ligand cannot be identified because of the mixture of products.

GC/MS (C<sub>6</sub>D<sub>6</sub>): Calculated (*m/z*) for [C<sub>9</sub>H<sub>15</sub>BF<sub>4</sub>O<sub>2</sub>]<sup>+</sup>: 242; found: 242.

**HFO-1225zc**

[Rh(H)(PEt<sub>3</sub>)<sub>3</sub>] (**1**) (5.7 mg, 0.013 mmol, 3.5 mol% based on the amount of HFO-1225zc) and HBpin (70  $\mu$ l, 0.46 mmol) was added. After 15 min at room temperature the <sup>1</sup>H and <sup>19</sup>F NMR spectroscopic data revealed the complete conversion of HFO-1225zc as well as the formation of **4**, **5**, **6**, **10** and 1,1,1-trifluoropropane in a ratio of 33:16:36:5:10.



**HFO-1225ye (Z)**

[Rh(H)(PEt<sub>3</sub>)<sub>3</sub>] (**1**) (5.0 mg, 0.011 mmol, 3.4 mol% based on the amount of HFO-1225ye) and HBpin (70  $\mu$ l, 0.46 mmol) was added. After 2 h at room temperature the <sup>1</sup>H and <sup>19</sup>F NMR spectroscopic data revealed the complete conversion of HFO-1225ye (**Z**) as well as the formation of **4**, **5**, **6**, **7**, **10**, **11**, **12**, 1,1,1-trifluoropropane and 1,1,1,2-tetrafluoropropane in a ratio of 14:15:15:16:2:25:12:1:1.

Analytical data for **11**:



<sup>19</sup>F NMR (282.4 MHz, C<sub>6</sub>D<sub>6</sub>):  $\delta$  = -75.7 (td, t in <sup>19</sup>F{<sup>1</sup>H} NMR, <sup>3</sup>J(F,F)  $\approx$  <sup>4</sup>J(F,F) = 10, <sup>3</sup>J(F,H) = 6 Hz, CF<sub>3</sub>); -207.2 (pseudo tm, qd in <sup>19</sup>F{<sup>1</sup>H} NMR, <sup>2</sup>J(F,H)  $\approx$  <sup>3</sup>J(F,H) = 41, <sup>3</sup>J(F,F) = 10, <sup>3</sup>J(F,F) = 7 Hz, CFH); -241.8 (m, CFH(Bpin)) ppm.

<sup>1</sup>H NMR (300.1 MHz, C<sub>6</sub>D<sub>6</sub>):  $\delta$  = 4.69-4.52 (m, observed by <sup>19</sup>F-<sup>1</sup>H COSY NMR spectrum, overlapped with other signals)

GC/MS (C<sub>6</sub>D<sub>6</sub>): Calculated (*m/z*) for [C<sub>9</sub>H<sub>14</sub>BF<sub>5</sub>O<sub>2</sub>]<sup>+</sup>: 245; found: 245.

**Catalytic conversion of HFO-1234yf using rhodium boryl complex [Rh(Bpin)(PEt<sub>3</sub>)<sub>3</sub>] (**3**) as the catalyst**

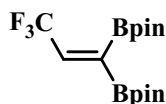
In a Young NMR tube equipped with a PFA inliner [Rh(Bpin)(PEt<sub>3</sub>)<sub>3</sub>] (**3**) (10.5 mg, 0.018 mmol, 4.6 mol% based on the amount of HFO-1234yf) was dissolved in Me<sub>6</sub>Si<sub>2</sub> (0.3 mL) and HBpin (100  $\mu$ l, 0.66 mmol) was added to the solution. The solution was cooled to 77 K, degassed *in vacuo*, and pressurized with HFO-1234yf to 0.3 bar (45 mg, 0.39 mmol). After warming up to room temperature the reaction was monitored by NMR spectroscopy using C<sub>6</sub>D<sub>6</sub>. After 30 min at room temperature the <sup>1</sup>H and <sup>19</sup>F NMR spectroscopic data revealed the complete conversion of HFO-1234yf as well as the formation of **4**, **5**, **6**, **7**, 1,1,1-trifluoropropane and 1,1,1,2-tetrafluoropropane in a ratio of 23:23:22:20:3:9.

**Catalytic conversion of HFO-1234yf with B<sub>2</sub>pin<sub>2</sub> as boron source**

In a Young NMR tube [Rh(H)(PEt<sub>3</sub>)<sub>3</sub>] (**1**) (10.0 mg, 0.022 mmol, 8.5 mol% based on the amount of B<sub>2</sub>pin<sub>2</sub>) was dissolved in C<sub>6</sub>D<sub>6</sub> (0.5 mL) and B<sub>2</sub>pin<sub>2</sub> (58 mg, 0.23 mmol) was added to the solution. The solution was cooled to 77 K, degassed *in vacuo*, and

pressurized with HFO-1234yf to 0.3 bar (45 mg, 0.39 mmol). After warming up to room temperature the reaction was monitored by NMR spectroscopy. After 5 d at room temperature the  $^1\text{H}$  and  $^{19}\text{F}$  NMR spectroscopic data revealed a *ca.* 24 % conversion of HFO-1234yf as well as the formation of 3,3,3-trifluoropropene,  $\text{CF}_3\text{CH}=\text{C}(\text{Bpin})_2$  (**9**) and an unidentified product in a ratio of 61:33:6.

Analytical data for **9**:



$^{19}\text{F}$  NMR (282.4 MHz,  $\text{C}_6\text{D}_6$ ):  $\delta = -64.6$  (d,  $^3J(\text{F},\text{H}) = 7$  Hz,  $\text{CF}_3$ ) ppm.

$^1\text{H}$  NMR (300.1 MHz,  $\text{C}_6\text{D}_6$ ):  $\delta = 6.85$  (q,  $^3J(\text{H},\text{F}) = 7.1$  Hz,  $\text{CH}$ ) ppm. The signal of Bpin ligand cannot be identified because of the mixture of products.

GC/MS ( $\text{C}_6\text{D}_6$ ): Calculated ( $m/z$ ) for  $[\text{C}_{15}\text{H}_{25}\text{B}_2\text{F}_3\text{O}_4]^+$ : 348; found: 348.

#### General catalytic conversion of HFO-1234yf with an excess amount of HBpin using *in situ* formed rhodium complex $[\text{Rh}(\mu\text{-Cl})(\text{PiPr}_3)_2]_2$ (**14**) as catalyst

In a Young NMR tube  $[\text{Rh}(\mu\text{-Cl})(\text{COE})_2]_2$  (**13**) and  $\text{PiPr}_3$  were dissolved in  $d_8$ -THF (0.5 mL). After 5 min at room temperature, the complex  $[\text{Rh}(\mu\text{-Cl})(\text{PiPr}_3)_2]_2$  (**14**) was formed *in situ* and the solvent was removed under vacuum. A solution of HBpin (70  $\mu\text{L}$ , 0.46 mmol) in 0.5 mL  $d_8$ -THF was then transferred into the Young NMR tube. The solution was cooled to 77 K, degassed *in vacuo*, and pressurized with HFOs to 0.3 bar. After warming up to room temperature the reaction was monitored by NMR spectroscopy.

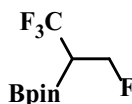
#### HFO-1234yf

$[\text{Rh}(\mu\text{-Cl})(\text{COE})_2]_2$  (**13**) (6.0 mg, 0.0084 mmol, 2.2 mol% based on the amount of HFO-1234yf) and  $\text{PiPr}_3$  (5.4 mg, 0.034 mmol) were added. After 25 min at room temperature the  $^1\text{H}$  and  $^{19}\text{F}$  NMR spectroscopic data revealed the full conversion of HFO-1234yf as well as the formation of **4**, **5**, **6**, **7**, 1,1,1-trifluoropropane and 1,1,1,2-tetrafluoropropane in a ratio of 4:7:9:67:4:7. Additionally, a 2 % of unidentified product and FBpin were formed.

**HFO-1234ze**

[Rh( $\mu$ -Cl)(COE)<sub>2</sub>]<sub>2</sub> (**13**) (12.0 mg, 0.0168 mmol, 4.3 mol% based on the amount of HFO-1234ze) and  $\text{P}i\text{Pr}_3$  (10.3 mg, 0.065 mmol) were added. After 2 h at room temperature the  $^1\text{H}$  and  $^{19}\text{F}$  NMR spectroscopic data revealed the full conversion of HFO-1234ze as well as the formation of **4**, **5**, **6**, **10**, 1,1,1-trifluoropropane,  $\text{CF}_3\text{CH}_2\text{CFH}_2$  (**15**) and  $\text{CF}_3\text{CH}(\text{Bpin})\text{CFH}_2$  (**16**) in a ratio of 9:10:58:7:4:8:4. Additionally, FBpin was formed.

Analytical data for **16**:



$^{19}\text{F}$  NMR (282.4 MHz,  $d_8$ -THF):  $\delta = -62.8$  (dd, d in  $^{19}\text{F}\{^1\text{H}\}$  NMR,  $^3J(\text{F},\text{H}) = 11$ ,  $^4J(\text{F},\text{F}) = 7$  Hz,  $\text{CF}_3$ );  $-217.9$  (m,  $\text{CFH}_2$ ) ppm.

**HFO-1225zc**

[Rh( $\mu$ -Cl)(COE)<sub>2</sub>]<sub>2</sub> (**13**) (12.3 mg, 0.0172 mmol, 4.7 mol% based on the amount of HFO-1225zc) and  $\text{P}i\text{Pr}_3$  (10.3 mg, 0.065 mmol) were added. After 20 h at room temperature the  $^1\text{H}$  and  $^{19}\text{F}$  NMR spectroscopic data revealed the full conversion of HFO-1225zc as well as the formation of **4**, **5**, **6**, **10**, 1,1,1-trifluoropropane and **15** in a ratio of 8:28:32:5:14:13. Additionally, FBpin was formed.

**HFO-1225ye (Z)**

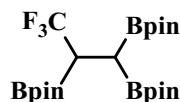
[Rh( $\mu$ -Cl)(COE)<sub>2</sub>]<sub>2</sub> (**13**) (12.0 mg, 0.0168 mmol, 5.1 mol% based on the amount of HFO-1225ye (Z)) and  $\text{P}i\text{Pr}_3$  (10.8 mg, 0.068 mmol) were added. After 20 h at room temperature the  $^1\text{H}$  and  $^{19}\text{F}$  NMR spectroscopic data revealed the full conversion of HFO-1225ye (Z) as well as the formation of **4**, **5**, **6**, **7**, **11**, **12**, 1,1,1-trifluoropropane and 1,1,1,2-tetrafluoropropane in a ratio of 4:11:13:49:4:10:2:4. Additionally, a 3 % of unidentified product and FBpin were formed.

**Reactivity of [Rh(C $\equiv$ CCF<sub>3</sub>)(PEt<sub>3</sub>)<sub>3</sub>] (**17**) towards HBpin**

In a Young NMR tube [Rh(C $\equiv$ CCF<sub>3</sub>)(PEt<sub>3</sub>)<sub>3</sub>] (**17**) (80 mg of a mixture of **17** and **18** (ratio 9:1) which equals to 0.13 mmol of **17**) was dissolved in  $\text{C}_6\text{D}_6$  (0.5 mL), and HBpin (40  $\mu\text{L}$ , 0.27 mmol) was added to the solution. The reaction was monitored by NMR spectroscopy. After 3 h at room temperature the  $^1\text{H}$  and  $^{19}\text{F}$  NMR spectroscopic data revealed the complete conversion of complex **17** into *fac*-[Rh(Bpin)(H)<sub>2</sub>(PEt<sub>3</sub>)<sub>3</sub>] (**2**)

as well as the formation of  $\text{CF}_3\text{CH}(\text{Bpin})\text{CH}(\text{Bpin})_2$  (**20**),  $\text{CF}_3\text{CH}_2\text{C}(\text{Bpin})_3$  (**21**),  $\text{CF}_3\text{CH}_2\text{CH}(\text{Bpin})_2$  (**5**) and an unidentifiable product in a 43:34:18:5 ratio.

Selected analytical data for **20**:



**$^{19}\text{F}$  NMR** (282.4 MHz,  $\text{C}_6\text{D}_6$ ):  $\delta = -63.4$  (d,  $^3J(\text{F},\text{H}) = 12$  Hz,  $\text{CF}_3$ ) ppm.

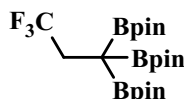
**$^1\text{H}$  NMR** (300.1 MHz,  $\text{C}_6\text{D}_6$ ):  $\delta = 2.54$  (qd,  $^3J(\text{H},\text{F}) = 12.2$  Hz,  $^3J(\text{H},\text{H}) = 8.9$  Hz,  $\text{CF}_3\text{CH}$ ); 1.43 (m, the assignment has been confirmed by a  $^1\text{H}$ - $^1\text{H}$  COSY NMR spectrum, because of overlapping of signals,  $\text{CH}(\text{Bpin})_2$ ) ppm. Signals of Bpin group cannot be assigned due to the mixture of products.

**$^{11}\text{B}$  NMR** (96.3 MHz,  $\text{C}_6\text{D}_6$ ):  $\delta = 29.0$  (s br) ppm.

**$^{13}\text{C}\{^1\text{H}\}$  NMR** (75.4 MHz,  $\text{C}_6\text{D}_6$ ):  $\delta = 129.8$  (q,  $^1J(\text{C},\text{F}) = 282$  Hz, observed by  $^1\text{H}$ - $^{13}\text{C}$  HMBC NMR spectrum,  $\text{CF}_3$ ); 28.5 (m, observed by  $^1\text{H}$ - $^{13}\text{C}$  HMBC NMR spectrum,  $\text{CF}_3\text{CH}$ ); 24.4 (m, observed by  $^1\text{H}$ - $^{13}\text{C}$  HMBC NMR spectrum,  $\text{CH}(\text{Bpin})_2$ ) ppm.

**GC/MS** ( $\text{C}_6\text{D}_6$ ): Calculated ( $m/z$ ) for  $[\text{C}_{21}\text{H}_{38}\text{B}_3\text{F}_3\text{O}_6]^+$ : 476; calculated ( $m/z$ ) for  $[\text{M}-\text{CH}_3]^+$ : 461; found: 461.

Selected analytical data for **21**:



**$^{19}\text{F}$  NMR** (282.4 MHz,  $\text{C}_6\text{D}_6$ ):  $\delta = -63.5$  (t,  $^3J(\text{F},\text{H}) = 12$  Hz,  $\text{CF}_3$ ) ppm.

**$^1\text{H}$  NMR** (300.1 MHz,  $\text{C}_6\text{D}_6$ ):  $\delta = 2.94$  (q,  $^3J(\text{H},\text{F}) = 11.5$  Hz,  $\text{CH}_2$ ) ppm.

**$^{11}\text{B}$  NMR** (96.3 MHz,  $\text{C}_6\text{D}_6$ ):  $\delta = 29.0$  (s br) ppm.

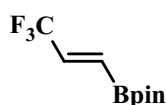
**$^{13}\text{C}\{^1\text{H}\}$  NMR** (75.4 MHz,  $\text{C}_6\text{D}_6$ ):  $\delta = 129.0$  (q, observed by  $^1\text{H}$ - $^{13}\text{C}$  HMBC NMR spectrum,  $^1J(\text{C},\text{F}) = 276$  Hz,  $\text{CF}_3$ ); 33.7 (q,  $^2J(\text{C},\text{F}) = 28.7$  Hz,  $\text{CF}_3\text{CH}_2$ ); 24.2 (m, observed by  $^1\text{H}$ - $^{13}\text{C}$  HMBC NMR spectrum,  $\text{C}(\text{Bpin})_3$ ) ppm.

**GC/MS** ( $\text{C}_6\text{D}_6$ ): Calculated ( $m/z$ ) for  $[\text{C}_{21}\text{H}_{38}\text{B}_3\text{F}_3\text{O}_6]^+$ : 476; found: 476.

**Catalytic conversion of 3,3,3-trifluoropropyne into  $\text{CF}_3\text{CH}=\text{CHBpin}$  (**8**)**

In a Young NMR tube the catalyst (mol% based on the amount of HBpin) was dissolved in C<sub>6</sub>D<sub>6</sub> (0.5 mL), and HBpin was added to the solution. The solution was cooled to 77 K, degassed *in vacuo*, and pressurized with 3,3,3-trifluoropropyne to 0.3 bar. After warming up to room temperature the reaction was monitored by NMR spectroscopy. After the reaction time at room temperature the <sup>1</sup>H and <sup>19</sup>F NMR spectroscopic data revealed full conversion of HBpin as well as the formation of (*E*)-CF<sub>3</sub>CH=CHBpin (**8**). Compound **8** was identified by comparison with the literature.<sup>[117]</sup>

Analytical data for **8**:



**<sup>19</sup>F NMR** (282.4 MHz, C<sub>6</sub>D<sub>6</sub>): δ = −67.2 (dm, <sup>3</sup>*J* (F,H) = 6 Hz, 3F, CF<sub>3</sub>) ppm.

**<sup>1</sup>H NMR** (300.1 MHz, C<sub>6</sub>D<sub>6</sub>): δ = 6.51 (dq, <sup>3</sup>*J*(H,H) = 18.2 Hz, <sup>3</sup>*J*(H,F) = 6.1 Hz, 1H, CF<sub>3</sub>CH=); 6.30 (dq, <sup>3</sup>*J*(H,H) = 18.2 Hz, <sup>3</sup>*J*(H,F) = 1.9 Hz, 1H, =CHBpin); 1.0 (s, 12H, Bpin) ppm.

**<sup>11</sup>B NMR** (96.3 MHz, C<sub>6</sub>D<sub>6</sub>): δ = 29.0 (s br) ppm.

**<sup>13</sup>C{<sup>1</sup>H} NMR** (75.4 MHz, C<sub>6</sub>D<sub>6</sub>): δ = 135.6 (q, <sup>2</sup>*J*(C,F) = 34.6 Hz, CF<sub>3</sub>CH=); 127.6 (m, observed by <sup>1</sup>H-<sup>13</sup>C HMQC NMR spectrum, =CHBpin); 122.6 (q, <sup>1</sup>*J*(C,F) = 270.3 Hz, CF<sub>3</sub>); 84.2 (s, C<sub>q</sub> Bpin); 24.7 (s, CH<sub>3</sub> Bpin) ppm.

**Method A:** [RhH(PEt<sub>3</sub>)<sub>3</sub>] (**1**) (5 mg, 0.011 mmol, 8.4 mol%) and HBpin (20 μl, 0.13 mmol) were used and compound **8** was obtained in a 94% yield after 10 min.

**Method B:** Complexes **17** and **18** (9:1 ratio, 4.5 mg, 0.008 mmol, 5 mol%) and HBpin (24 μl, 0.16 mmol) were used and compound **8** was obtained in 96% yield after 3 h.

**Method C:** Complexes **18** and **19** (5:1 ratio, 6 mg, 0.009 mmol, 5.6 mol%) and HBpin (24 μl, 0.16 mmol) were used and compound **8** was obtained in 94% yield after 5 h.

#### **Independent catalytic conversion of CF<sub>3</sub>CH=CHBpin (**8**) into CF<sub>3</sub>CH<sub>2</sub>CH(Bpin)<sub>2</sub> (**5**)**

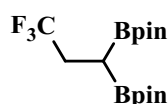
In a NMR tube compound **8** (51.1 mg, 0.23 mmol) and complex **1** (4.5 mg, 0.01 mmol, 4.3 mol% based on the amount of **8**) was dissolved in C<sub>6</sub>D<sub>6</sub> (0.5 mL), and HBpin (80 μl, 0.53 mmol) was added to the solution. After 5 min at room temperature the <sup>1</sup>H and

$^{19}\text{F}$  NMR spectroscopic data revealed the complete conversion of **8** into  $\text{CF}_3\text{CH}_2\text{CH}(\text{Bpin})_2$  (**5**). Compound **5** was identified by comparison with the literature.<sup>[61]</sup>

#### Catalytic conversion of 3,3,3-trifluoropropyne into $\text{CF}_3\text{CH}_2\text{CH}(\text{Bpin})_2$ (**5**)

In a Young NMR tube the catalyst (2.5 mol% based on the amount of gas) was dissolved in  $\text{C}_6\text{D}_6$  (0.5 mL), and HBpin (140  $\mu\text{L}$ , 0.93 mmol) was added to the solution. The solution was cooled to 77 K, degassed *in vacuo*, and pressurized with 3,3,3-trifluoropropyne. After warming up to room temperature the reaction was monitored by NMR spectroscopy. After the reaction time at room temperature the  $^1\text{H}$  and  $^{19}\text{F}$  NMR spectroscopic data revealed the complete conversion of 3,3,3-trifluoropropyne into  $\text{CF}_3\text{CH}_2\text{CH}(\text{Bpin})_2$  (**5**). Compound **5** was identified by comparison with the literature.<sup>[61]</sup>

Additional analytical data for **5**:



$^{13}\text{C}\{^1\text{H}\}$  NMR (75.4 MHz,  $\text{C}_6\text{D}_6$ ):  $\delta$  = 128.3 (q,  $^1J(\text{C},\text{F}) = 276.4$  Hz,  $\text{CF}_3$ ); 83.6 (s,  $\text{C}_q$  Bpin); 30.5 (q,  $^2J(\text{C},\text{F}) = 29.0$  Hz,  $\text{CF}_3\text{CH}_2$ ); 24.8 (overlapping with HBpin,  $\text{CH}_3$  Bpin); 23.0 (m, observed by  $^1\text{H}$ - $^{13}\text{C}$  HMQC NMR spectrum,  $\text{CH}(\text{Bpin})_2$ ) ppm.

*Method A:*  $[\text{RhH}(\text{PEt}_3)_3]$  (**1**) (5 mg, 0.011 mmol) and 3,3,3-trifluoropropyne (40 mg, 0.42 mmol) were used to form compound **5** in 96% yield after 20 min.

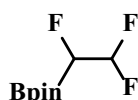
*Method B:* Complexes **17** and **18** (9:1 ratio, 7 mg, 0.013 mmol) and 3,3,3-trifluoropropyne (50 mg, 0.53 mmol) were used to form compound **5** in 95% yield after 10 min.

*Method C:* Complexes **18** and **19** (5:1 ratio, 9 mg, 0.013 mmol) and 3,3,3-trifluoropropyne (51 mg, 0.54 mmol) were used to generate compound **5** in 97% yield after 3 h.

### Catalytic conversion of trifluoroethylene with an excess amount of HBpin using $[\text{Rh}(\text{H})(\text{PEt}_3)_3]$ (**1**) as the catalyst

In a Young NMR tube  $[\text{Rh}(\text{H})(\text{PEt}_3)_3]$  (**1**) (9.0 mg, 0.020 mmol, 7.7 mol% based on the amount of trifluoroethylene) was dissolved in  $\text{C}_6\text{D}_6$  (0.5 mL) and HBpin (70  $\mu\text{L}$ , 0.46 mmol) was added to the solution. The solution was cooled to 77 K, degassed *in vacuo*, and pressurized with trifluoroethylene to 0.3 bar (21 mg, 0.26 mmol). After 10 min at room temperature the  $^1\text{H}$  and  $^{19}\text{F}$  NMR spectroscopic data revealed the complete conversion of trifluoroethylene as well as the formation of compounds  $\text{CF}_2\text{HCFH}(\text{Bpin})$  (**22**),  $\text{CF}_2\text{HCFH}_2$  (**23**),  $\text{CF}_2\text{HCH}_2(\text{Bpin})$  (**24**),  $\text{CH}_3\text{CH}_2(\text{Bpin})$  and  $\text{CH}_3\text{CH}(\text{Bpin})_2$ . Additionally, FBpin was obtained. The ratio among **22:23:24** is 80:18:2. The non-fluorinated compounds were only confirmed by GC-MS.

Analytical data for **22**:



$^{19}\text{F}$  NMR (470.6 MHz,  $\text{C}_6\text{D}_6$ ):  $\delta = -126.4$  (dt,  $^2J(\text{F},\text{H}) = 54$  Hz,  $^3J(\text{F},\text{H}) \approx ^3J(\text{F},\text{F}) = 15$  Hz, d in the  $^{19}\text{F}\{^1\text{H}\}$  NMR spectrum, CFF);  $-126.5$  (dt,  $^2J(\text{F},\text{H}) = 53$  Hz,  $^3J(\text{F},\text{H}) \approx ^3J(\text{F},\text{F}) = 17$  Hz, d in the  $^{19}\text{F}\{^1\text{H}\}$  NMR spectrum, CFF);  $-242.7$  (br, CFH) ppm.

$^1\text{H}$  NMR data (500.1 MHz,  $\text{C}_6\text{D}_6$ ):  $\delta = 5.72$  (tdd,  $^2J(\text{H},\text{F}) = 54.3$  Hz,  $^3J(\text{H},\text{F}) = 11.8$  Hz,  $^3J(\text{H},\text{H}) = 2.8$  Hz,  $\text{CF}_2\text{H}$ );  $4.32$  (dddd,  $^2J(\text{H},\text{F}) = 45.8$  Hz,  $^3J(\text{H},\text{F}) = 18.8$  Hz,  $^3J(\text{H},\text{F}) = 16.2$  Hz,  $^3J(\text{H},\text{H}) = 2.8$  Hz, CFH) ppm.

GC-MS ( $\text{C}_6\text{D}_6$ ): Calculated ( $m/z$ ) for  $[\text{C}_8\text{H}_{14}\text{BF}_3\text{O}_2]^+$ : 210; found: 210.

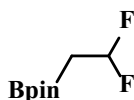
Analytical data for **23**:



$^{19}\text{F}$  NMR (470.6 MHz,  $\text{C}_6\text{D}_6$ ):  $\delta = -129.8$  (ddt,  $^2J(\text{F},\text{H}) = 54$  Hz,  $^3J(\text{F},\text{F}) = 18$  Hz,  $^3J(\text{F},\text{H}) = 13$  Hz, d in the  $^{19}\text{F}\{^1\text{H}\}$  NMR spectrum,  $\text{CF}_2$ );  $-240.8$  (ttd,  $^2J(\text{F},\text{H}) = 46$  Hz,  $^3J(\text{F},\text{F}) = 18$  Hz,  $^3J(\text{F},\text{H}) = 7$  Hz, t in the  $^{19}\text{F}\{^1\text{H}\}$  NMR spectrum,  $\text{CFH}_2$ ) ppm.

**$^1\text{H}$  NMR** data (500.1 MHz,  $\text{C}_6\text{D}_6$ ):  $\delta = 5.06$  (tdt,  $^2J(\text{H},\text{F}) = 54.3$  Hz,  $^3J(\text{H},\text{F}) = 7.2$  Hz,  $^3J(\text{H},\text{H}) = 3.6$  Hz,  $\text{CF}_2\text{H}$ );  $3.58$  (dtd,  $^2J(\text{H},\text{F}) = 46.2$  Hz,  $^3J(\text{H},\text{F}) = 13.5$  Hz,  $^3J(\text{H},\text{H}) = 3.7$  Hz,  $\text{CFH}_2$ ) ppm.

Analytical data for **24**:



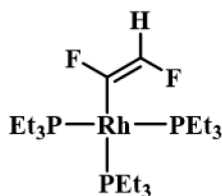
**$^{19}\text{F}$  NMR** (470.6 MHz,  $\text{C}_6\text{D}_6$ ):  $\delta = -106.0$  (dt,  $^2J(\text{F},\text{H}) = 58$  Hz,  $^3J(\text{F},\text{H}) = 20$  Hz, s in the  $^{19}\text{F}\{^1\text{H}\}$  NMR spectrum,  $\text{CF}_2\text{H}$ ) ppm.

**$^1\text{H}$  NMR** data (500.1 MHz,  $\text{C}_6\text{D}_6$ ):  $\delta = 4.66$ - $4.58$  (m,  $\text{CF}_2\text{H}$ );  $1.44$ - $1.39$  (m,  $\text{CH}_2$ ) ppm. The signals were based on the  $^{19}\text{F}$ - $^1\text{H}$  COSY NMR spectrum and  $^1\text{H}$ - $^1\text{H}$  COSY NMR spectrum.

**Formation of  $[\text{Rh}((Z)\text{-CFCFH})(\text{PEt}_3)_3]$  (**25**) and *trans*- $[\text{Rh}(\text{F})(\eta^2\text{-CF}_2\text{CFH})(\text{PEt}_3)_2]$  (**26**)**

In a Young NMR tube  $[\text{Rh}(\text{H})(\text{PEt}_3)_3]$  (**1**) (27.8 mg, 0.061 mmol) was dissolved in 0.5 mL of  $\text{C}_6\text{D}_6$ . CsF (12.5 mg, 0.082 mmol) was added to the solution. The solution was cooled to 77 K, degassed *in vacuo*, and pressurized with trifluoroethylene to 0.2 bar (14 mg, 0.171 mmol). After 10 min at room temperature, the NMR spectra revealed a full conversion of complex **1** to give complex **25**, complex *trans*- $[\text{Rh}(\text{F})(\eta^2\text{-CF}_2\text{CFH})(\text{PEt}_3)_2]$  (**26**) (ratio 1:2.4, based on the  $^{31}\text{P}\{^1\text{H}\}$  NMR spectrum) and compound 1,1-difluoroethylene as well as free phosphine.

Analytical data for **25**:



**$^{31}\text{P}\{^1\text{H}\}$  NMR** (121.5 MHz,  $\text{C}_6\text{D}_6$ ):  $\delta = 20.3$  (dq,  $^1J(\text{P},\text{Rh}) = 122.1$  Hz,  $^3J(\text{P},\text{F}) \approx ^2J(\text{P},\text{P}) = 36.3$  Hz,  $\text{P}_{\text{trans}}$ );  $17.3$  (ddm,  $^1J(\text{P},\text{Rh}) = 147.4$  Hz,  $^2J(\text{P},\text{P}) = 37.1$  Hz,  $\text{P}_{\text{cis}}$ ) ppm.

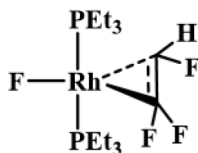
**$^{19}\text{F}$  NMR** (282.4 MHz,  $\text{C}_6\text{D}_6$ ):  $\delta = -128.5$  (dm,  $^3J(\text{F},\text{F}) = 109$  Hz, dddt in the  $^{19}\text{F}\{^1\text{H}\}$  NMR spectrum,  $^3J(\text{F},\text{P}) = 35$  Hz,  $^2J(\text{F},\text{Rh}) = 8$  Hz,  $^3J(\text{F},\text{P}) = 4$  Hz,  $\text{RhCF}$ );



−183.1 (ddm,  $^3J(\text{F},\text{F}) = 109 \text{ Hz}$ ,  $^2J(\text{F},\text{H}) = 90 \text{ Hz}$ , dm in the  $^{19}\text{F}\{^1\text{H}\}$  NMR spectrum, CFH) ppm.

Selected  $^1\text{H}$  NMR data (300.1 MHz,  $\text{C}_6\text{D}_6$ ):  $\delta = 8.21$  (ddm,  $^2J(\text{H},\text{F}) = 89.6 \text{ Hz}$ ,  $^3J(\text{H},\text{F}) = 12.7 \text{ Hz}$ , dd in the  $^1\text{H}\{^{31}\text{P}\}$  NMR spectrum, CFH) ppm.

Analytical data for **26**:



$^{31}\text{P}\{^1\text{H}\}$  NMR (121.5 MHz,  $\text{C}_6\text{D}_6$ ):  $\delta = 32.3$  (ddtd,  $^2J(\text{P},\text{P}) = 368.2 \text{ Hz}$ ,  $^1J(\text{P},\text{Rh}) = 138.9 \text{ Hz}$ ,  $^3J(\text{P},\text{F}) = 47.9 \text{ Hz}$ ,  $^2J(\text{P},\text{F}) = 27.5 \text{ Hz}$ ); 25.9 (dddd,  $^2J(\text{P},\text{P}) = 368.2 \text{ Hz}$ ,  $^1J(\text{P},\text{Rh}) = 133.3 \text{ Hz}$ ,  $^3J(\text{P},\text{F}) = 44.2 \text{ Hz}$ ,  $^2J(\text{P},\text{F}) = 28.6 \text{ Hz}$ ,  $J = 14.8 \text{ Hz}$ ) ppm.

$^{19}\text{F}$  NMR (282.4 MHz,  $\text{C}_6\text{D}_6$ ):  $\delta = -89.4$  (dddd,  $^2J(\text{F},\text{F}) = 109 \text{ Hz}$ ,  $^3J(\text{F},\text{P}) = 47 \text{ Hz}$ ,  $J = 33 \text{ Hz}$ ,  $J = 13 \text{ Hz CFF}$ ); −90.8 (dddm, dddd in the  $^{19}\text{F}\{^1\text{H}\}$  NMR spectrum,  $^3J(\text{F},\text{F}) = 109 \text{ Hz}$ ,  $^3J(\text{F},\text{F}) = 69 \text{ Hz}$ ,  $^3J(\text{F},\text{P}) = 44 \text{ Hz}$ ,  $J = 7 \text{ Hz}$ ,  $J = 4 \text{ Hz, CFF}$ ); −194.9 (m, CFH), −218.3 (m, RhF) ppm.

Selected  $^1\text{H}$  NMR data (300.1 MHz,  $\text{C}_6\text{D}_6$ ):  $\delta = 5.50$  (br dd,  $^2J(\text{H},\text{F}) = 73.3 \text{ Hz}$ ,  $J(\text{H},\text{P}) = 9.1 \text{ Hz}$ , br d in the  $^1\text{H}\{^{31}\text{P}\}$  NMR spectrum, CFH) ppm.

#### Independent synthesis of complex *trans*-[Rh(F)( $\eta^2$ -CF<sub>2</sub>CFH)(PEt<sub>3</sub>)<sub>2</sub>] (**26**)

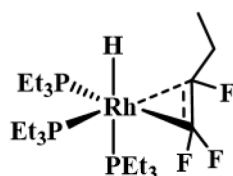
In a Young NMR tube [Rh(F)(PEt<sub>3</sub>)<sub>3</sub>] (**28**)<sup>[59, 120]</sup> (22 mg, 0.046 mmol) was dissolved in 0.5 mL of  $\text{C}_6\text{D}_6$ . The solution was cooled to 77 K, degassed *in vacuo*, and pressurized with trifluoroethylene to 0.2 bar (14 mg, 0.171 mmol). After 10 min at room temperature, the NMR spectra revealed the full conversion of complex **28** to give complex *trans*-[Rh(F)( $\eta^2$ -CF<sub>2</sub>CFH)(PEt<sub>3</sub>)<sub>2</sub>] (**26**) as well as the release of free phosphine.

**Formation of *fac*-[Rh(H)( $\eta^2$ -CF<sub>2</sub>CFC<sub>2</sub>H<sub>5</sub>)(PEt<sub>3</sub>)<sub>3</sub>] (**29**), [Rh(CF<sub>2</sub>CFHC<sub>2</sub>H<sub>5</sub>)(PEt<sub>3</sub>)<sub>3</sub>] (**30**), *mer*-[Rh(H)(FHF)((*Z*)-CFCFC<sub>2</sub>H<sub>5</sub>)(PEt<sub>3</sub>)<sub>3</sub>] (**31**) and [Rh((*Z*)-CFCFC<sub>2</sub>H<sub>5</sub>)(PEt<sub>3</sub>)<sub>3</sub>] (**27**)**

In a Young NMR tube [Rh(H)(PEt<sub>3</sub>)<sub>3</sub>] (**1**) (42 mg, 0.092 mmol) was dissolved in 0.5 mL of *d*<sub>8</sub>-toluene. The solution was cooled to 77 K, degassed *in vacuo*, and pressurized with 1,1,2-trifluorobutene to 0.3 bar (20 mg, 0.182 mmol). The reaction

was monitored by NMR spectroscopy at low temperature. At 233 K, complex *fac*-[Rh(H)( $\eta^2$ -CF<sub>2</sub>CFC<sub>2</sub>H<sub>5</sub>)(PEt<sub>3</sub>)<sub>3</sub>] (**29**) and [Rh(CF<sub>2</sub>CFHC<sub>2</sub>H<sub>5</sub>)(PEt<sub>3</sub>)<sub>3</sub>] (**30**) were trapped. After 2 h at 253 K, the NMR spectra revealed the full conversion of complex **1** to give complex **30**. After warming up the reaction solution to 263 K, complex *mer*-[Rh(H)(FHF)((*Z*)-CFCFC<sub>2</sub>H<sub>5</sub>)(PEt<sub>3</sub>)<sub>3</sub>] (**31**) and [Rh((*Z*)-CFCFC<sub>2</sub>H<sub>5</sub>)(PEt<sub>3</sub>)<sub>3</sub>] (**27**) in a 1:3 ratio were immediately formed. Slowly warming up the reaction solution to 298 K led to full conversion into complex **27**. When the reaction solution was directly warmed up to room temperature, complex **27** was afforded in 5 min.

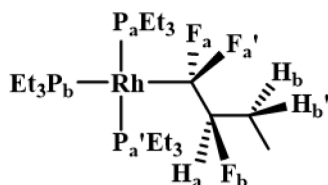
Analytical data for **29**:



<sup>19</sup>F NMR (282.4 MHz, *d*<sub>8</sub>-Tol, 233 K):  $\delta$  = -95.3 (m, CFF); -102.1 (ddm,  $J$  = 145, 67 Hz, CFF); -174.9 (m, CF) ppm.

Selected <sup>1</sup>H NMR data (300.1 MHz, *d*<sub>8</sub>-Tol, 233 K):  $\delta$  = -13.36 (dm, <sup>2</sup> $J$ (H,P) = 149.7 Hz; dtd in the <sup>1</sup>H{<sup>19</sup>F} NMR spectrum, <sup>2</sup> $J$ (H,P) = 23.7 Hz, <sup>1</sup> $J$ (H,Rh) = 17.3 Hz; pseudo t in the <sup>1</sup>H{<sup>31</sup>P} NMR spectrum; RhH) ppm.

Analytical data for **30**:



<sup>31</sup>P{<sup>1</sup>H} NMR (202.5 MHz, *d*<sub>8</sub>-Tol, 253 K):  $\delta$  = 16.1-7.7 (br) ppm.

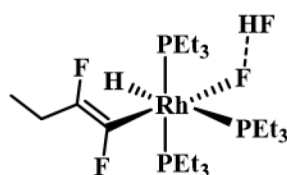
<sup>31</sup>P{<sup>1</sup>H} NMR (202.5 MHz, *d*<sub>8</sub>-Tol, 193 K):  $\delta$  = 15.5 (dddd, <sup>2</sup> $J$ (P<sub>a</sub>,P<sub>a</sub>') = 291.0 Hz, <sup>1</sup> $J$ (P<sub>a</sub>,Rh) = 175.2 Hz, <sup>3</sup> $J$ (P<sub>a</sub>,F<sub>a</sub>') = 96.1 Hz, <sup>2</sup> $J$ (P<sub>a</sub>,P<sub>b</sub>) = 38.1 Hz, 1P, P<sub>a</sub>); 11.7 (dpdm, <sup>1</sup> $J$ (P<sub>b</sub>,Rh) = 111.3 Hz, <sup>3</sup> $J$ (P<sub>b</sub>,F<sub>a</sub>) = 37.3 Hz, <sup>3</sup> $J$ (P<sub>b</sub>,F<sub>a</sub>') = 37.3 Hz, <sup>2</sup> $J$ (P<sub>b</sub>,P<sub>a</sub>) = 38.1 Hz, <sup>2</sup> $J$ (P<sub>b</sub>,P<sub>a</sub>') = 36.1 Hz, <sup>4</sup> $J$ (P<sub>b</sub>,F<sub>b</sub>) = 10.2 Hz, 1P, P<sub>b</sub>); 8.4 (dddtdm, <sup>2</sup> $J$ (P<sub>a</sub>,P<sub>a</sub>') = 291.0 Hz, <sup>1</sup> $J$ (P<sub>a</sub>',Rh) = 166.7 Hz, <sup>2</sup> $J$ (P<sub>a</sub>',P<sub>b</sub>) = 36.1 Hz, <sup>3</sup> $J$ (P<sub>a</sub>',F<sub>a</sub>) = 17.6 Hz, <sup>3</sup> $J$ (P<sub>a</sub>',F<sub>a</sub>') = 17.6 Hz, <sup>4</sup> $J$ (P<sub>a</sub>',F<sub>b</sub>) = 6.2 Hz, 1P, P<sub>a</sub>') ppm.

<sup>19</sup>F NMR (470.7 MHz, *d*<sub>8</sub>-Tol, 253 K):  $\delta$  = -75.6 (br dm, <sup>2</sup> $J$ (F<sub>a</sub>,F<sub>a</sub>') = 248 Hz, 1F, F<sub>a</sub>); -82.2 (br dm, <sup>2</sup> $J$ (F<sub>a</sub>',F<sub>a</sub>) = 248 Hz, 1F, F<sub>a</sub>'); -186.9 (br, 1F, F<sub>b</sub>) ppm.

Selected  $^1\text{H}$  NMR data (500.1 MHz,  $d_8$ -Tol, 253 K):  $\delta = 4.74$  (dddd,  $^2J(\text{H}_a, \text{F}_b) = 52.1$  Hz,  $^3J(\text{H}_a, \text{F}_a') = 19.5$  Hz,  $^3J(\text{H}_a, \text{H}_b') = 10.3$  Hz,  $^3J(\text{H}_a, \text{H}_b) = 2.1$  Hz, 1H,  $\text{H}_a$ ); 2.89 (ddq,  $^3J(\text{H}_b, \text{F}_b) = 40.3$  Hz,  $^2J(\text{H}_b, \text{H}_b') = 15.0$  Hz,  $^3J(\text{H}_b, \text{H}) = 7.5$  Hz, 1H,  $\text{H}_b$ ); 2.28 (dm,  $^3J(\text{H}_b', \text{F}_b) = 20.6$  Hz, ddq in the  $^1\text{H}\{^{19}\text{F}\}$  NMR spectrum,  $^2J(\text{H}_b', \text{H}_b) = 15.0$  Hz,  $^3J(\text{H}_b', \text{H}_a) = 10.3$  Hz,  $^2J(\text{H}_b', \text{H}) = 7.1$  Hz, 1H,  $\text{H}_b'$ ); 1.27 (t,  $^3J(\text{H}, \text{H}) = 7.4$  Hz, 3H,  $\text{CH}_3$ ) ppm.

$^1\text{H}$ - $^{13}\text{C}$  HMQC NMR (500.1/125.8 MHz,  $d_8$ -Tol, 253 K)  $\delta = 98.4$  (m, CFH); 26.8 (m,  $\text{CH}_2$ ) ppm.

Analytical data for **31**:



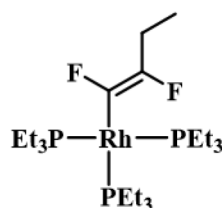
$^{31}\text{P}\{^1\text{H}\}$  NMR (121.5 MHz,  $d_8$ -Tol, 263 K):  $\delta = 20.1$  (dddd,  $^1J(\text{P}, \text{Rh}) = 102.8$  Hz,  $^2J(\text{P}, \text{P}) = 23.2$  Hz,  $^2J(\text{P}, \text{F}) = 15.4$  Hz,  $^3J(\text{P}, \text{F}) = 2.7$  Hz,  $\text{P}_{cis}$  to hydrido ligand); 2.2-0.0 (m,  $\text{P}_{trans}$  to hydrido ligand) ppm.

$^{19}\text{F}$  NMR (282.4 MHz,  $d_8$ -Tol, 263 K):  $\delta = -91.0$  (dddm,  $^3J(\text{F}, \text{F}) = 123$  Hz,  $^3J(\text{F}, \text{F}) = 82$  Hz,  $^3J(\text{F}, \text{P}) = 35$  Hz, dddd in the  $^{19}\text{F}\{^1\text{H}\}$  NMR spectrum,  $^2J(\text{F}, \text{Rh}) = 15$  Hz,  $\text{RhCF}$ ); -146.9 (dq,  $^3J(\text{F}, \text{F}) = 123$  Hz,  $^3J(\text{F}, \text{H}) \approx ^4J(\text{F}, \text{F}) = 22$  Hz, ddm in the  $^{19}\text{F}\{^1\text{H}\}$  NMR spectrum,  $\text{CFCH}_2$ ); -177.0 (br dd,  $^1J(\text{F}, \text{H}) \approx 374$  Hz,  $^2J(\text{F}, \text{F}) = 118$  Hz,  $\text{RhFHF}$ ); -357.2 (br,  $\text{RhFHF}$ ) ppm.

Selected  $^1\text{H}$  NMR data (300.1 MHz,  $d_8$ -Tol, 263 K):  $\delta = 12.91$  (br d,  $^1J(\text{H}, \text{F}) \approx 381$  Hz,  $\text{FHF}$ ); 2.36 (dm,  $^3J(\text{H}, \text{F}) = 21.7$  Hz, q in the  $^1\text{H}\{^{19}\text{F}\}$  NMR spectrum,  $^3J(\text{H}, \text{H}) = 7.3$  Hz,  $\text{CFCH}_2$ ); -9.27 (dm, br t in the  $^1\text{H}\{^{31}\text{P}\}$  NMR spectrum,  $^1J(\text{H}, \text{Rh}) \approx ^2J(\text{H}, \text{F}) = 13.6$  Hz, dq in the  $^1\text{H}\{^{19}\text{F}\}$  NMR spectrum,  $^2J(\text{H}, \text{P}) = 178.3$  Hz,  $^2J(\text{H}, \text{P}) = 13.6$  Hz,  $\text{RhH}$ ) ppm. The other signal of the  $\text{CFCH}_2\text{CH}_3$  moiety was overlapped by other signals.

$^1\text{H}$ - $^{13}\text{C}$  HMQC NMR (300.1/75.5 MHz,  $d_8$ -Tol, 263 K)  $\delta = 21.1$  (m,  $\text{CFCH}_2$ ) ppm.

Analytical data for **27**:



**$^{31}\text{P}\{^1\text{H}\}$  NMR** (121.5 MHz,  $d_8$ -Tol):  $\delta$  = 20.8 (dq,  $^1J(\text{P,Rh})$  = 123.1 Hz,  $^3J(\text{P,F}) \approx ^2J(\text{P,P})$  = 36.5 Hz,  $\text{P}_{\text{trans}}$ ); 17.5 (ddm,  $^1J(\text{P,Rh})$  = 149.2 Hz,  $^2J(\text{P,P})$  = 37.0 Hz,  $\text{P}_{\text{cis}}$ ) ppm.

**$^{19}\text{F}$  NMR** (282.4 MHz,  $d_8$ -Tol):  $\delta$  = -120.5 (ddm,  $^3J(\text{F,F})$  = 102 Hz,  $^3J(\text{F,P})$  = 36 Hz, dddt in the  $^{19}\text{F}\{^1\text{H}\}$  NMR spectrum,  $^2J(\text{F,Rh})$  = 10 Hz,  $^3J(\text{F,P})$  = 5 Hz,  $\text{RhCF}$ ); -155.1 (dtm,  $^3J(\text{F,F})$  = 102 Hz,  $^3J(\text{F,H})$  = 22 Hz, dm in the  $^{19}\text{F}\{^1\text{H}\}$  NMR spectrum,  $\text{CF}$ ) ppm.

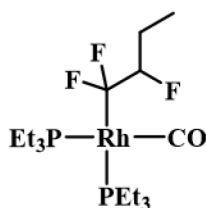
Selected  **$^1\text{H}$  NMR** data (300.1 MHz,  $d_8$ -Tol):  $\delta$  = 2.69 (dm,  $^3J(\text{H,F})$  = 21.7 Hz, q in the  $^1\text{H}\{^{19}\text{F}\}$  NMR spectrum,  $^3J(\text{H,H})$  = 7.3 Hz,  $\text{CFCH}_2$ ); 1.71-1.62 (m,  $\text{PCH}_2\text{CH}_3$ ); 1.45-1.36 (m,  $\text{PCH}_2\text{CH}_3$ ); 1.16-0.96 (m,  $\text{PCH}_2\text{CH}_3$ ) ppm. The other signal of the  $\text{CFCH}_2\text{CH}_3$  moiety was overlapped by the phosphine ligands.

**$^1\text{H}$ - $^{13}\text{C}$  HMQC NMR** (300.1/75.5 MHz,  $d_8$ -Tol, 263 K)  $\delta$  = 21.5 (m,  $\text{CFCH}_2$ ) ppm.

#### Synthesis of *cis*-[Rh(CF<sub>2</sub>CFHC<sub>2</sub>H<sub>5</sub>)(CO)(PEt<sub>3</sub>)<sub>2</sub>] (**32**)

In a Young NMR tube [Rh(H)(PEt<sub>3</sub>)<sub>3</sub>] (**1**) (36 mg, 0.079 mmol) was dissolved in 0.5 mL of  $d_8$ -toluene. The solution was cooled to 77 K, degassed *in vacuo*, and pressurized with 1,1,2-trifluorobutene to 0.2 bar (14 mg, 0.121 mmol). After melting, the solution was immediately cooled to 77 K again, degassed *in vacuo* and introduced CO. After warming up to room temperature, the NMR spectra revealed the formation of complex **32**.

Analytical data for **32**:



**$^{31}\text{P}\{^1\text{H}\}$  NMR** (121.5 MHz,  $d_8$ -Tol):  $\delta$  = 14.5 (br) ppm.

**$^{31}\text{P}\{^1\text{H}\}$  NMR** (121.5 MHz,  $d_8$ -Tol, 243 K):  $\delta = 21.9$  (dtd,  $^1J(\text{P,Rh}) = 73.1$  Hz,  $^3J(\text{P,F}) = 47.8$  Hz,  $^3J(\text{P,P}) = 24.0$  Hz,  $\text{P}_{cis}$  to CO); 8.6 (dm,  $^1J(\text{P,Rh}) = 124.8$  Hz,  $\text{P}_{trans}$  to CO) ppm.

**$^{19}\text{F}$  NMR** (282.4 MHz,  $d_8$ -Tol, 243 K):  $\delta = -59.5$  (br dtm,  $^2J(\text{F,F}) = 226$  Hz,  $^3J(\text{F,P}) = 45$  Hz, CFF);  $-60.9$  (br dtm,  $^2J(\text{F,F}) = 226$  Hz,  $^3J(\text{F,P}) = 45$  Hz, CFF);  $-183.5$  (br tm, pseudo tq in the room temperature spectrum,  $^2J(\text{F,H}) \approx ^3J(\text{F,H}) = 48$  Hz,  $^3J(\text{F,F}) \approx ^3J(\text{F,H}) = 13$  Hz, t in the  $^{19}\text{F}\{^1\text{H}\}$  NMR spectrum, CFH) ppm.

Selected  **$^1\text{H}$  NMR** data (300.1 MHz,  $d_8$ -Tol, 243 K):  $\delta = 4.52$  (dm,  $^2J(\text{H,F}) = 47.7$  Hz, CFH); 2.18 (m, overlapped with other signals, CHH); 2.09 (m, overlapped with other signals, CHH); 1.09 (t,  $^3J(\text{H,H}) = 7.3$  Hz,  $\text{CH}_3$ ) ppm.

**General procedure for the catalytic conversion of pentafluorostyrene**

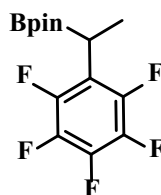
In a NMR tube, the catalyst (mol% based on the amount of pentafluorostyrene) was dissolved in the corresponding solvent (0.5 mL) and HBpin. Then pentafluorostyrene was added to the solution stepwise. After 5 min at room temperature, the  $^1\text{H}$  and  $^{19}\text{F}$  NMR spectroscopic data revealed a full conversion of pentafluorostyrene as well as the formation of the Markovnikov hydroboration compound **33**,<sup>[184]</sup> small amounts of the anti-Markovnikov product **34**,<sup>[184]</sup> the diboryl compound **35**<sup>[184]</sup> as well as the hydrogenation compound **36**.

Entry 1:  $[\text{Rh}(\text{H})(\text{PEt}_3)_3]$  (**1**) (5 mg, 0.011 mmol, 3 mol%) was dissolved in  $\text{C}_6\text{D}_6$ . Then HBpin (70  $\mu\text{l}$ , 0.46 mmol) and pentafluorostyrene (70.3 mg, 0.36 mmol) were added. The mixture of products **33:34:35:36** was obtained in a ratio of 91:6:1:2.

Entry 2:  $[\text{Rh}(\text{Bpin})(\text{PEt}_3)_3]$  (**1**) (7.8 mg, 0.013 mmol, 3.7 mol%) was dissolved in  $\text{Me}_6\text{Si}_2$  in a PFA tube. HBpin (70  $\mu\text{l}$ , 0.46 mmol) and pentafluorostyrene (70.3 mg, 0.36 mmol) were added afterwards. The mixture of products **33:34:35:36** was obtained in a ratio of 81:9:3:3. Additionally, an unidentified product was afforded in 4 % yield.

Entry 3:  $[\text{Rh}(\text{H})(\text{PEt}_3)_3]$  (**1**) (10 mg, 0.022 mmol, 1.5 mol%) was added to a mixture of HBpin (273  $\mu\text{l}$ , 1.79 mmol) and pentafluorostyrene (281.2 mg, 1.42 mmol). The mixture of products **33:34:35:36** was obtained in a ratio of 75:13:4:8.

Analytical data for **33**:

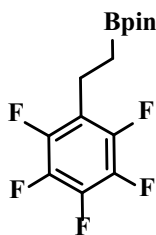


$^{19}\text{F}$  NMR (282.4 MHz,  $\text{C}_6\text{D}_6$ ):  $\delta = -144.8$  (dm,  $^3J(\text{F},\text{F}) = 22$  Hz, *o*-F);  $-160.3$  (t,  $^3J(\text{F},\text{F}) = 22$  Hz, *p*-F);  $-164.4$  (tm,  $^3J(\text{F},\text{F}) = 22$  Hz, *m*-F) ppm.

$^1\text{H}$  NMR data (300.1 MHz,  $\text{C}_6\text{D}_6$ ):  $\delta = 2.63$  (q,  $^3J(\text{H},\text{H}) = 7.7$  Hz,  $\text{CHBpin}$ );  $1.28$  (d,  $^3J(\text{H},\text{H}) = 7.7$  Hz,  $\text{CH}_3$ );  $1.05$  (s,  $\text{CH}_3$  on Bpin moiety) ppm.

GC-MS ( $d_8$ -Tol): Calculated ( $m/z$ ) for  $[\text{C}_{14}\text{H}_{16}\text{BF}_5\text{O}_2]^+$ : 322; found: 322.

Analytical data for **34**:

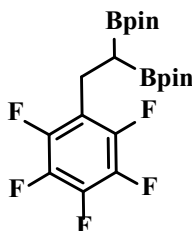


**<sup>19</sup>F NMR** (282.4 MHz, C<sub>6</sub>D<sub>6</sub>):  $\delta = -145.5$  (dm,  $^3J(\text{F},\text{F}) = 22$  Hz, *o*-F);  $-160.2$  (t,  $^3J(\text{F},\text{F}) = 22$  Hz, *p*-F);  $-164.6$  (tm,  $^3J(\text{F},\text{F}) = 22$  Hz, *m*-F) ppm.

The signals for **34** in the <sup>1</sup>H NMR spectrum overlap with these for compound **33**, **35** and **36**.

**GC-MS** (*d*<sub>8</sub>-Tol): Calculated (*m/z*) for [C<sub>14</sub>H<sub>16</sub>BF<sub>5</sub>O<sub>2</sub>]<sup>+</sup>: 322; found: 322. This compound is proposed based on the GC-MS data and literature.<sup>[184]</sup>

Analytical data for **35**:



**<sup>19</sup>F NMR** (282.4 MHz, C<sub>6</sub>D<sub>6</sub>):  $\delta = -143.5$  (dm,  $^3J(\text{F},\text{F}) = 22$  Hz, *o*-F); (the other two signals are overlapped with signals for compound **33**, **34** and **36**) ppm.

**<sup>1</sup>H NMR** data (300.1 MHz, C<sub>6</sub>D<sub>6</sub>):  $\delta = 3.01$  (d,  $^3J(\text{H},\text{H}) = 7.7$  Hz, CH<sub>2</sub>); 1.39 (br, observed in the <sup>1</sup>H-<sup>1</sup>H COSY NMR spectrum, overlapping with signals for compound **33** and unknown compound) ppm.

**GC-MS** (*d*<sub>8</sub>-Tol): Calculated (*m/z*) for [C<sub>20</sub>H<sub>27</sub>B<sub>2</sub>F<sub>5</sub>O<sub>4</sub>]<sup>+</sup>: 448; found: 448.

### **Stoichiometric hydroboration reactions with [Rh(H)(PEt<sub>3</sub>)<sub>3</sub>] (**1**) or [Rh(Bpin)(PEt<sub>3</sub>)<sub>3</sub>] (**3**)**

In a NMR tube [Rh(H)(PEt<sub>3</sub>)<sub>3</sub>] (**1**) (51.0 mg, 0.111 mmol) was dissolved in 0.5 mL of *d*<sub>8</sub>-toluene. HBpin (41  $\mu$ l, 0.269 mmol) was introduced into the solution. After 30 s, pentafluorostyrene (21.1 mg, 0.109 mmol) was added into the solution. The <sup>19</sup>F NMR spectroscopic data revealed after 5 min the full conversion of pentafluorostyrene as well as the formation of Markovnikov hydroboration

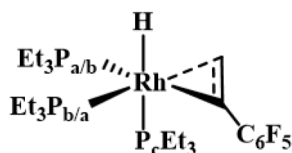
compound  $[\text{C}_6\text{F}_5\text{CH}(\text{Bpin})\text{CH}_3]$  (**33**), small amounts of the *anti*-Markovnikov product  $[\text{C}_6\text{F}_5\text{CH}_2\text{CH}_2(\text{Bpin})]$  (**34**), the diboryl compound  $[\text{C}_6\text{F}_5\text{CH}_2\text{CH}(\text{Bpin})_2]$  (**35**) as well as the hydrogenation compound **36** in a ratio of 92:2:4:2. The rhodium (III) complex *fac*- $[\text{Rh}(\text{Bpin})(\text{H})_2(\text{PEt}_3)_3]$  (**2**)<sup>[61]</sup> was formed as the only rhodium complex.

Alternatively, in a NMR tube equipped with a PFA tube  $[\text{Rh}(\text{Bpin})(\text{PEt}_3)_3]$  (**3**) (36.7 mg, 0.063 mmol) was dissolved in *d*<sub>14</sub>-methylcyclohexane (0.3 mL). Pentafluorostyrene (12.7 mg, 0.065 mmol) was added to the solution. After 30 s, HBpin (12  $\mu\text{l}$ , 0.079 mmol) was introduced to the solution. The <sup>19</sup>F NMR spectroscopic data revealed after 5 min the full conversion of pentafluorostyrene as well as the formation of the same organic products in a ratio of 49:14:22:15 as well as the rhodium (III) complex **2**.

#### Formation of *fac*- $[\text{Rh}(\text{H})(\eta^2\text{-CH}_2\text{CHC}_6\text{F}_5)(\text{PEt}_3)_3]$ (**37**)

In a NMR tube  $[\text{Rh}(\text{H})(\text{PEt}_3)_3]$  (**1**) (40 mg, 0.087 mmol) was dissolved in 0.5 mL of *d*<sub>8</sub>-toluene. Pentafluorostyrene (12 mg, 0.062 mmol) was added to the solution. After 5 min at room temperature, NMR spectra were measured at room temperature and at 213 K revealing the full conversion of pentafluorostyrene and the formation of complex **37**.

Analytical data for **37**:



<sup>31</sup>P{<sup>1</sup>H} NMR (121.5 MHz, *d*<sub>8</sub>-Tol, 213 K):  $\delta$  = 20.3 (ddd, <sup>1</sup>*J*(P<sub>a/b</sub>,Rh) = 139.8 Hz, <sup>2</sup>*J*(P<sub>a</sub>,P<sub>b</sub>) = 42.6 Hz, <sup>2</sup>*J*(P<sub>a/b</sub>,P<sub>c</sub>) = 24.2 Hz, P<sub>a/b</sub>); 13.7 (ddd, <sup>1</sup>*J*(P<sub>b/a</sub>,Rh) = 134.0 Hz, <sup>2</sup>*J*(P<sub>b</sub>,P<sub>a</sub>) = 42.9 Hz, <sup>2</sup>*J*(P<sub>b/a</sub>,P<sub>c</sub>) = 28.8 Hz, P<sub>b/a</sub>); 5.8 (dm, br, <sup>1</sup>*J*(P<sub>c</sub>,Rh) = 95.8 Hz, P<sub>c</sub>) ppm.

<sup>19</sup>F NMR (282.4 MHz, *d*<sub>8</sub>-Tol, 213 K):  $\delta$  = -146.0 (d br, <sup>3</sup>*J*(F,F) = 21 Hz, *o*-F); -146.7 (d br, <sup>3</sup>*J*(F,F) = 21 Hz, *o*-F); -166.3 (t, <sup>3</sup>*J*(F,F) = 21 Hz, *m*-F); -167.0 (t, <sup>3</sup>*J*(F,F) = 21 Hz, *m*-F); -170.9 (t, <sup>3</sup>*J*(F,F) = 21 Hz, *p*-F) ppm.

<sup>1</sup>H NMR (300.1 MHz, *d*<sub>8</sub>-Tol, 213 K):  $\delta$  = 3.32 (br, pseudo t in the <sup>1</sup>H{<sup>31</sup>P} NMR spectrum, <sup>3</sup>*J*(H,H)  $\approx$  8 Hz, *CHC*<sub>6</sub>F<sub>5</sub>); 3.05 (br, d in the <sup>1</sup>H{<sup>31</sup>P} NMR spectrum,



$^3J(\text{H,H}) = 9.5 \text{ Hz}$ ,  $\text{CH}_2\text{CHC}_6\text{F}_5$ ); 1.83 (br, d in the  $^1\text{H}\{^{31}\text{P}\}$  NMR spectrum,  $^3J(\text{H,H}) = 8.1 \text{ Hz}$ ,  $\text{CH}_2\text{CHC}_6\text{F}_5$ ); 1.59–1.43 (m,  $\text{PCH}_2\text{CH}_3$ , overlapping with signals for the rhodium complex **1**); 1.20–1.03 (m,  $\text{PCH}_2\text{CH}_3$ , overlapping with signals for **1**); 0.95–0.86 (m, t in the  $^1\text{H}\{^{31}\text{P}\}$  NMR spectrum  $^3J(\text{H,H}) = 7.2 \text{ Hz}$ ,  $\text{PCH}_2\text{CH}_3$ ); 0.83–0.74 (m, t in the  $^1\text{H}\{^{31}\text{P}\}$  NMR spectrum,  $^3J(\text{H,H}) = 7.2 \text{ Hz}$ ,  $\text{PCH}_2\text{CH}_3$ ); 0.72–0.63 (m, t in the  $^1\text{H}\{^{31}\text{P}\}$  NMR spectrum,  $^3J(\text{H,H}) = 7.2 \text{ Hz}$ ,  $\text{PCH}_2\text{CH}_3$ ); –14.64 (dtd, d in the  $^1\text{H}\{^{31}\text{P}\}$  NMR spectrum,  $^2J(\text{H,P}_c) = 161.8 \text{ Hz}$ ,  $^2J(\text{H,P}_a) = ^2J(\text{H,P}_b) = 19.8 \text{ Hz}$ ,  $^1J(\text{H,Rh}) = 9.2 \text{ Hz}$ ,  $\text{RhH}$ ) ppm.

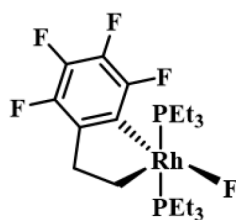
**$^1\text{H}$ - $^{13}\text{C}$  HMQC NMR** (300.1/75.5 MHz,  $d_8$ -Tol, 213 K)  $\delta = 29.2$  (m,  $\text{CHC}_6\text{F}_5$ ); 23.9 (m,  $\text{CH}_2\text{CHC}_6\text{F}_5$ ) ppm.

**Formation of *trans*-[Rh(F)(CH<sub>2</sub>CH<sub>2</sub>(2-C<sub>6</sub>F<sub>4</sub>))(PEt<sub>3</sub>)<sub>2</sub>] (**38**) and *mer*-[Rh(F)(CH<sub>2</sub>CH<sub>2</sub>(2-C<sub>6</sub>F<sub>4</sub>))(PEt<sub>3</sub>)<sub>3</sub>] (**39**)**

In a NMR tube [Rh(H)(PEt<sub>3</sub>)<sub>3</sub>] (**1**) (23 mg, 0.050 mmol) was dissolved in 0.5 mL  $d_8$ -toluene. Pentafluorostyrene (13 mg, 0.067 mmol) was added to the solution. After 1 d at room temperature, NMR spectra were measured at room temperature and at 233 K revealing the full conversion of complex **1**.

The NMR spectra at room temperature showed the formation of complex **38**, free PEt<sub>3</sub>, traces of complex *mer*-[Rh(F)(CH<sub>2</sub>CH<sub>2</sub>(2-C<sub>6</sub>F<sub>4</sub>))(PEt<sub>3</sub>)<sub>3</sub>] (**39**), unreacted complex **37** (36 %), minor amounts of the C–H bond activation complex [Rh(*E*-CHCHC<sub>6</sub>F<sub>5</sub>)(PEt<sub>3</sub>)<sub>3</sub>] (**40**) as well as the hydrogenation product ethylpentafluorobenzene **36**<sup>[190]</sup>. When the sample was cooled down to 233 K, complex **38** converted into complex **39** completely. The low temperature  $^{19}\text{F}$  NMR spectrum shows a ratio of 1:0.07:0.18 for **39**:**40**:**36**. Treatment of the same NMR tube with KPF<sub>6</sub> (30 mg, 0.163 mmol) gave after 14 d a full conversion of complexes **38** and **39** into complex **41** as well as a product of C–D bond activation [Rh(4-C<sub>6</sub>D<sub>4</sub>CD<sub>3</sub>)(PEt<sub>3</sub>)<sub>3</sub>] in a ratio of 5.5:1. In the absence of KPF<sub>6</sub>, complex **41** can also be formed very slowly within weeks.

Analytical data for **38**:



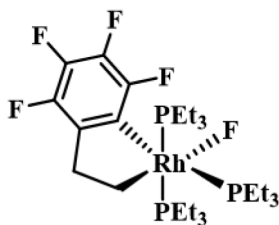
**$^{31}\text{P}\{^1\text{H}\}$  NMR** (121.5 MHz,  $d_8$ -Tol):  $\delta = 18.4$  (dd,  $^1J(\text{P,Rh}) = 114.2$  Hz,  $^2J(\text{P,F}) = 16.6$  Hz) ppm.

**$^{19}\text{F}$  NMR** (282.4 MHz,  $d_8$ -Tol):  $\delta = -130.6$  (m),  $-142.0$  (dd,  $^3J(\text{F,F}) = 20$  Hz,  $J = 16$  Hz);  $-162.5$  (dd,  $^5J(\text{F,F}) = 29$  Hz,  $^3J(\text{F,F}) = 20$  Hz);  $-167.3$  (t,  $^3J(\text{F,F}) = 20$  Hz);  $-290.6$  (m, RhF) ppm.

Selected  **$^1\text{H}$  NMR** data (300.1 MHz,  $d_8$ -Tol):  $\delta = 3.20$  (br,  $\text{RhCH}_2\text{CH}_2$ );  $2.45$  (br,  $\text{C}_6\text{F}_4\text{CH}_2\text{CH}_2$ ) ppm.

Selected  **$^{13}\text{C}\{^1\text{H}\}$  NMR** data (75.5 MHz,  $d_8$ -Tol):  $\delta = 37.3$  (s br,  $\text{C}_6\text{F}_4\text{CH}_2\text{CH}_2$ );  $23.2$  (dm br,  $^2J(\text{C,Rh}) = 32.6$  Hz,  $\text{RhCH}_2\text{CH}_2$ ) ppm.

Analytical data for **39**:



**$^{31}\text{P}\{^1\text{H}\}$  NMR** (121.5 MHz,  $d_8$ -Tol, 233 K):  $\delta = 7.9$  (ddd,  $^1J(\text{P,Rh}) = 103.8$  Hz,  $^2J(\text{P,P}) = 29.7$  Hz,  $^2J(\text{P,F}) = 17.9$  Hz,  $\text{P}_{trans}$  mutually);  $-2.8$  (apparent dm,  $^1J(\text{P,Rh}) \approx 90$  Hz,  $\text{P}_{trans}$  to  $\text{C}_6\text{F}_4$ ) ppm.

**$^{19}\text{F}$  NMR** (282.4 MHz,  $d_8$ -Tol, 233 K):  $\delta = -122.6$  (m),  $-140.6$  (m);  $-161.2$  (m);  $-165.7$  (t,  $^3J(\text{F,F}) = 21$  Hz);  $-385.1$  (m, RhF) ppm.

Selected  **$^1\text{H}$  NMR** data (300.1 MHz,  $d_8$ -Tol, 233 K):  $\delta = 3.04$  (br,  $\text{C}_6\text{F}_4\text{CH}_2\text{CH}_2$ );  $1.42$  (br,  $\text{RhCH}_2\text{CH}_2$ , observed in the  $^1\text{H}$ - $^1\text{H}$  COSY NMR spectrum, overlapping with signals for  $\text{PEt}_3$ ) ppm.

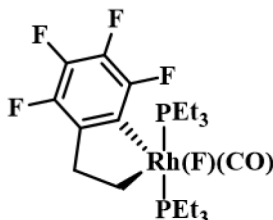
**APT  $^{13}\text{C}$  NMR** (75.5 MHz,  $d_8$ -Tol, 213 K)  $\delta = 37.8$  (m,  $\text{C}_6\text{F}_4\text{CH}_2\text{CH}_2$ );  $23.7$  (dm,  $^2J(\text{C,Rh}) = 16.4$  Hz,  $\text{RhCH}_2\text{CH}_2$ ) ppm.

**Formation of  $trans$ -[Rh(F)(CH<sub>2</sub>CH<sub>2</sub>C<sub>6</sub>F<sub>4</sub>)(CO)(PEt<sub>3</sub>)<sub>2</sub>] (**42**) and  $trans$ -[Rh(F)(CH<sub>2</sub>CH<sub>2</sub>C<sub>6</sub>F<sub>4</sub>)(<sup>13</sup>CO)(PEt<sub>3</sub>)<sub>2</sub>] (**42'**)**

After isolation of complex **38** and applying vacuum, the residue was dissolved in 0.5 mL  $d_8$ -toluene. Then CO (or  $^{13}\text{CO}$ ) was bubbled into the solution for 15 s. The NMR spectra were measured after 5 min at room temperature revealing the full conversion of complex **38** and the formation of complex **42** (or **42'**) as well as

$[\text{Rh}(\text{H})(\text{CO})(\text{PEt}_3)_3]$  (**43**)<sup>[208]</sup> (ratio 3.9:1) (or the isotopologue  $[\text{Rh}(\text{H})(^{13}\text{CO})(\text{PEt}_3)_3]$  (**43'**) (ratio 4.4:1)).

Analytical data for **42**:



**$^{31}\text{P}\{^1\text{H}\}$  NMR** (121.5 MHz,  $d_8$ -Tol):  $\delta = 16.9$  (dd,  $^1J(\text{P},\text{Rh}) = 98.5$  Hz,  $^2J(\text{P},\text{F}) = 17.3$  Hz) ppm.

**$^{19}\text{F}$  NMR** (282.4 MHz,  $d_8$ -Tol, 243 K):  $\delta = -116.3$  (dd,  $^5J(\text{F},\text{F}) = 27$  Hz,  $J = 14$  Hz);  $-139.8$  (dd,  $^3J(\text{F},\text{F}) = 21$  Hz;  $J = 16$  Hz);  $-161.7$  (dd,  $^5J(\text{F},\text{F}) = 27$  Hz,  $^3J(\text{F},\text{F}) = 21$  Hz);  $-165.0$  (t,  $^3J(\text{F},\text{F}) = 21$  Hz);  $-425.3$  (m,  $\text{RhF}$ ) ppm.

Selected  **$^1\text{H}$  NMR** (300.1 MHz,  $d_8$ -Tol):  $\delta = 3.15$  (br t, tt in the  $^1\text{H}\{^{19}\text{F}\}$  NMR spectrum decoupled at -140 ppm,  $^3J(\text{H},\text{H}) = 7.5$  Hz,  $^3J(\text{H},\text{Rh}) \approx ^4J(\text{H},\text{F}) = 1.9$  Hz,  $\text{C}_6\text{F}_4\text{CH}_2\text{CH}_2$ );  $2.56$  (m, ttd in the  $^1\text{H}\{^{19}\text{F}\}$  NMR spectrum decoupled at -400 ppm,  $^3J(\text{H},\text{P}) = 9.3$  Hz,  $^3J(\text{H},\text{H}) = 7.5$  Hz,  $^2J(\text{H},\text{Rh}) = 2.1$  Hz,  $\text{C}_6\text{F}_4\text{CH}_2\text{CH}_2$ ) ppm. Selected  **$^{13}\text{C}\{^1\text{H}\}$  NMR** data (75.5 MHz,  $d_8$ -Tol):  $\delta = 33.4$  (s br,  $\text{C}_6\text{F}_4\text{CH}_2\text{CH}_2$ );  $24.0$  (dq,  $^1J(\text{C},\text{Rh}) = 19.9$  Hz,  $^2J(\text{C},\text{P}) \approx ^2J(\text{C},\text{F}) = 6.6$  Hz,  $\text{RhCH}_2\text{CH}_2$ ) ppm.

**LIFDI-TOF-MS** (toluene): Calculated ( $m/z$ ) for  $[\text{C}_{21}\text{H}_{36}\text{F}_5\text{OP}_2\text{Rh-CO}]^+$ : 534; found: 534.

**IR** (ATR):  $\tilde{\nu}$  (CO)  $2056\text{ cm}^{-1}$ .

Analytical data for **42'**:

**$^{31}\text{P}\{^1\text{H}\}$  NMR** (121.5 MHz,  $d_8$ -Tol):  $\delta = 16.9$  (ddd,  $^1J(\text{P},\text{Rh}) = 98.5$  Hz,  $^2J(\text{P},\text{F}) = 17.3$  Hz,  $^2J(\text{P},\text{C}) = 10.9$  Hz) ppm.

**$^{19}\text{F}$  NMR** (282.4 MHz,  $d_8$ -Tol):  $\delta = -116.5$  (m);  $-140.1$  (dd,  $^3J(\text{F},\text{F}) = 20$  Hz,  $J = 15$  Hz);  $-162.0$  (dd,  $^5J(\text{F},\text{F}) = 26$  Hz,  $^3J(\text{F},\text{F}) = 20$  Hz);  $-165.3$  (t,  $^3J(\text{F},\text{F}) = 20$  Hz);  $-418.2$  (m,  $\text{RhF}$ ) ppm.

Selected  **$^1\text{H}$  NMR** (300.1 MHz,  $d_8$ -Tol):  $\delta = 3.09$  (br t, tq in the  $^1\text{H}\{^{19}\text{F}\}$  NMR spectrum decoupled at -140 ppm,  $^3J(\text{H},\text{H}) = 7.5$  Hz,  $^3J(\text{H},\text{Rh}) \approx ^4J(\text{H},\text{F}) \approx ^4J(\text{H},\text{C}) = 1.9$  Hz,  $\text{C}_6\text{F}_4\text{CH}_2\text{CH}_2$ );  $2.50$  (m, ttt in the  $^1\text{H}\{^{19}\text{F}\}$  NMR spectrum decoupled

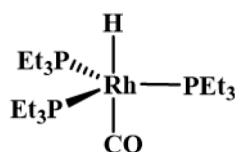
at -400 ppm,  $^3J(\text{H},\text{P}) = 9.3$  Hz,  $^3J(\text{H},\text{H}) = 7.5$  Hz,  $^2J(\text{H},\text{Rh}) \approx ^3J(\text{H},\text{C}) = 2.1$  Hz,  $\text{C}_6\text{F}_4\text{CH}_2\text{CH}_2$ ) ppm.

Selected  $^{13}\text{C}\{^1\text{H}\}$  NMR (75.5 MHz,  $d_8$ -Tol):  $\delta = 189.5$  (ddt,  $^1J(\text{C},\text{Rh}) = 41.3$  Hz,  $^2J(\text{C},\text{F}) = 14.8$  Hz,  $^2J(\text{C},\text{P}) = 10.9$  Hz,  $^{13}\text{CO}$ ) ppm.

**LIFDI-TOF-MS** (Toluene): Calculated ( $m/z$ ) for  $[\text{C}_{20}^{13}\text{CH}_3\text{F}_5\text{OP}_2\text{Rh}-^{13}\text{CO}]^+$ : 534; found: 534.

**IR** (ATR):  $\tilde{\nu}$  ( $^{13}\text{CO}$ )  $2002\text{ cm}^{-1}$ .

Analytical data for **43**:



$^{31}\text{P}\{^1\text{H}\}$  NMR (121.5 MHz,  $d_8$ -Tol):  $\delta = 26.5$  (d,  $^1J(\text{P},\text{Rh}) = 146.7$  Hz) ppm.

Selected  $^1\text{H}$  NMR (300.1 MHz,  $d_8$ -Tol, 243 K):  $\delta = -11.11$  (qd, d in the  $^1\text{H}\{^{31}\text{P}\}$  NMR spectrum,  $^2J(\text{H},\text{P}) = 17.1$  Hz,  $^1J(\text{H},\text{Rh}) = 4.4$  Hz,  $\text{RhH}$ ) ppm.

**IR** (ATR):  $\tilde{\nu}$  (CO)  $1950\text{ cm}^{-1}$ .

Analytical data for **43'**:

$^{31}\text{P}\{^1\text{H}\}$  NMR (121.5 MHz,  $d_8$ -Tol):  $\delta = 26.5$  (ddm,  $^1J(\text{P},\text{Rh}) = 146.0$  Hz,  $^2J(\text{P},\text{C}) = 11.1$  Hz) ppm.

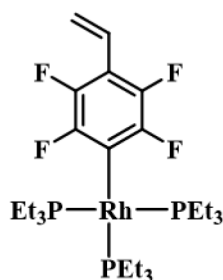
Selected  $^1\text{H}$  NMR (300.1 MHz,  $d_8$ -Tol):  $\delta = -11.17$  (m, dd in the  $^1\text{H}\{^{31}\text{P}\}$  NMR spectrum,  $^2J(\text{H},\text{C}) = 36.3$  Hz,  $^1J(\text{H},\text{Rh}) = 4.4$  Hz,  $\text{RhH}$ ) ppm.

**IR** (ATR):  $\tilde{\nu}$  ( $^{13}\text{CO}$ )  $1902\text{ cm}^{-1}$ .

#### Formation of $[\text{Rh}(\text{4-C}_6\text{F}_4\text{CHCH}_2)(\text{PEt}_3)_3]$ (**44**)

In a NMR tube  $[\text{Rh}(\text{H})(\text{PEt}_3)_3]$  (**1**) (15 mg, 0.033 mmol) was dissolved in 0.5 mL of  $\text{C}_6\text{D}_6$ . Pentafluorostyrene (8.4 mg, 0.043 mmol) was added to the solution. The reaction was monitored by NMR spectroscopy and after 1 d at 333 K, full conversion of complex **1** was observed. Formation of complex  $[\text{Rh}(\text{4-C}_6\text{F}_4\text{CHCH}_2)(\text{PEt}_3)_3]$  (**44**) and the fluoro complex  $[\text{Rh}(\text{F})(\text{PEt}_3)_3]$  (**28**)<sup>[59]</sup> as well as the hydrogenation product ethylpentafluorobenzene **36**<sup>[190]</sup> in a ratio of 1.5:1.6:1 (determined by  $^{19}\text{F}$  NMR spectroscopy) was obtained.

Analytical data for **44**:



$^{31}\text{P}\{^1\text{H}\}$  NMR (121.5 MHz,  $\text{C}_6\text{D}_6$ ):  $\delta = 18.4$  (dm,  $^1J(\text{P},\text{Rh}) = 138.1$  Hz,  $\text{P}_{trans}$  to  $\text{C}_6\text{F}_4$ );  $14.0$  (dd,  $^1J(\text{P},\text{Rh}) = 141.1$  Hz,  $^2J(\text{P},\text{P}) = 40.1$  Hz,  $\text{P}_{cis}$  to  $\text{C}_6\text{F}_4$ ) ppm.

$^{19}\text{F}$  NMR (282.4 MHz,  $\text{C}_6\text{D}_6$ ):  $\delta = -110.7$  (m);  $-147.3$  (m) ppm.

Selected  $^1\text{H}$  NMR data (300.1 MHz,  $\text{C}_6\text{D}_6$ ):  $\delta = 6.98$  (dd,  $^3J(\text{H},\text{H}) = 18.1$  Hz,  $^3J(\text{H},\text{H}) = 12.1$  Hz,  $\text{C}_6\text{F}_4\text{CH}$ );  $6.20$  (d,  $^3J(\text{H},\text{H}) = 18.1$  Hz,  $\text{H}_{cis}$  to  $\text{C}_6\text{F}_4$ );  $5.33$  (d,  $^3J(\text{H},\text{H}) = 12.1$  Hz,  $\text{H}_{trans}$  to  $\text{C}_6\text{F}_4$ ) ppm.

### Reaction of an excess amount of pentafluorostyrene with $[\text{Rh}(\text{Bpin})(\text{PEt}_3)_3]$ (**3**)

In a NMR tube equipped with a PFA inliner  $[\text{Rh}(\text{Bpin})(\text{PEt}_3)_3]$  (**3**) (63 mg, 0.107 mmol) was dissolved in 0.3 mL  $d_{14}$ -methylcyclohexane. Pentafluorostyrene (24 mg, 0.124 mmol) was added to the solution. After 5 min at room temperature, NMR spectra were measured at 213 K. The two complexes  $fac\text{-}[\text{Rh}(\text{H})(\eta^2\text{-CH}_2\text{CHC}_6\text{F}_5)(\text{PEt}_3)_3]$  (**37**) and  $fac\text{-}[\text{Rh}(\text{H})(\eta^2\text{-CH}(\text{Bpin})\text{CHC}_6\text{F}_5)(\text{PEt}_3)_3]$  (**45**) were identified as well as dehydrogenative borylation product **46** in a ratio of 1.8:1:0.6.

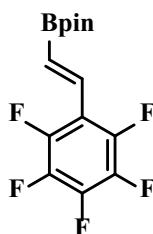
### Reaction of pentafluorostyrene with an excess amount of $[\text{Rh}(\text{Bpin})(\text{PEt}_3)_3]$ (**3**)

In a NMR tube equipped with a PFA inliner  $[\text{Rh}(\text{Bpin})(\text{PEt}_3)_3]$  (**3**) (50 mg, 0.085 mmol) was dissolved in 0.3 mL  $d_{14}$ -methylcyclohexane. Pentafluorostyrene (6.6 mg, 0.034 mmol) was added to the solution. After 5 min at room temperature, NMR spectra were measured at 233 K. Complex  $fac\text{-}[\text{Rh}(\text{H})(\eta^2\text{-CH}(\text{Bpin})\text{CHC}_6\text{F}_5)(\text{PEt}_3)_3]$  (**45**) was identified together with  $[\text{Rh}(\text{H})(\text{PEt}_3)_3]$  (**1**) in a ratio of 1:2 as well as traces of dehydrogenative borylation product **46**.

### Synthesis of *E*- $\text{BpinCH=CHC}_6\text{F}_5$ (**46**)

The synthetic procedure to access compound **46** resembles a literature known method.<sup>[215]</sup> In a NMR tube, a solution of pentafluorophenylacetylene (26.6 mg, 0.14 mmol), MeOH (20  $\mu$ L, 3.6 equiv) and *d*<sub>8</sub>-toluene (0.5 mL) was added to the mixture of B<sub>2</sub>pin<sub>2</sub> (44.9 mg, 0.18 mmol), *t*BuONa (2.8 mg, 0.029 mmol), Xantphos (10.2 mg, 0.018 mmol) and CuCl (2.7 mg, 0.027 mmol). The reaction was followed by NMR spectroscopy and stopped when nearly full conversion of pentafluorophenylacetylene was obtained (between 1.5-2h) and the formation of compound **46** achieved. Then the reaction solution was purified by flash column chromatography on silica gel using a mixture of hexane and diethyl ether (2:1) as eluent to give the pure borylated pentafluorostyrene **46** (20 mg, 0.063 mmol, Yield: 45 %) after removing the solvents by vacuum evaporation.

Analytical data for **46**:



<sup>19</sup>F NMR (282.4 MHz, C<sub>6</sub>D<sub>6</sub>):  $\delta$  = -144.0 (m, <sup>3</sup>*J*(F,F) = 22 Hz, 2F, *o*-F); -155.5 (tm, <sup>3</sup>*J*(F,F) = 22 Hz, 1F, *p*-F); -163.5 (m, <sup>3</sup>*J*(F,F) = 22 Hz, 2F, *m*-F) ppm.

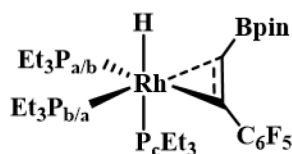
<sup>1</sup>H NMR (300.1 MHz, C<sub>6</sub>D<sub>6</sub>):  $\delta$  = 7.48 (d, <sup>3</sup>*J*(H,H) = 18.8 Hz, 1H, *CHC*<sub>6</sub>F<sub>5</sub>); 6.70 (d, <sup>3</sup>*J*(H,H) = 18.8 Hz, 1H, *CHBpin*); 1.08 (s, 12H, CH<sub>3</sub> on Bpin group) ppm.

GC-MS (*d*<sub>8</sub>-Tol): Calculated (*m/z*) for [C<sub>14</sub>H<sub>14</sub>BF<sub>5</sub>O<sub>2</sub>]<sup>+</sup>: 320; found: 320.

#### Formation of *fac*-[Rh(H)( $\eta^2$ -CH(Bpin)CHC<sub>6</sub>F<sub>5</sub>)(PEt<sub>3</sub>)<sub>3</sub>] (**45**)

In a NMR tube [Rh(H)(PEt<sub>3</sub>)<sub>3</sub>] (**1**) (48 mg, 0.105 mmol) was dissolved in 0.3 mL *d*<sub>8</sub>-toluene and the mixture was cooled in a 193 K bath. Borylated pentafluorostyrene **46** (20 mg, 0.062 mmol) was dissolved in 0.3 mL *d*<sub>8</sub>-toluene and the mixture was cooled down to 193 K. Then, both solutions were combined *via* cannula. After 5 min at 193 K, the reaction solution was warmed up to 213 K revealing the formation of complex **45** with a 40 % consumption of compound **46**.

Analytical data for **45**:



**$^{31}\text{P}\{^1\text{H}\}$  NMR** (121.5 MHz,  $d_8$ -Tol, 213 K):  $\delta$  = 18.2 (ddd,  $^1J(\text{P}_{a/b}, \text{Rh})$  = 142.9 Hz,  $^2J(\text{P}_a, \text{P}_b)$  = 37.6 Hz,  $^2J(\text{P}_{a/b}, \text{P}_c)$  = 28.3 Hz,  $\text{P}_{a/b}$ ); 15.3 (ddd,  $^1J(\text{P}_{b/a}, \text{Rh})$  = 134.3 Hz,  $^2J(\text{P}_b, \text{P}_a)$  = 37.1 Hz,  $^2J(\text{P}_{b/a}, \text{P}_c)$  = 25.3 Hz,  $\text{P}_{b/a}$ ); 3.3 (dm,  $^1J(\text{Rh}, \text{P}_c)$  = 96.7 Hz,  $\text{P}_c$ ) ppm.

**$^{19}\text{F}$  NMR** (282.4 MHz,  $d_8$ -Tol, 213 K):  $\delta$  = -144.2 (d,  $^3J(\text{F}, \text{F})$  = 21 Hz,  $o$ -F) (overlapping with a signal of compound **46**); -145.0 (d,  $^3J(\text{F}, \text{F})$  = 21 Hz,  $o$ -F); -166.5 (t,  $^3J(\text{F}, \text{F})$  = 21 Hz,  $m$ -F); -167.1 (t,  $^3J(\text{F}, \text{F})$  = 21 Hz,  $m$ -F); -170.4 (t,  $^3J(\text{F}, \text{F})$  = 21 Hz,  $p$ -F) ppm.

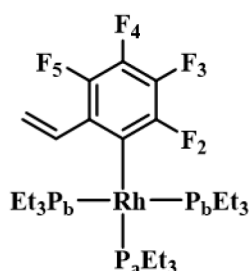
Selected  **$^1\text{H}$  NMR** (300.1 MHz,  $d_8$ -Tol, 213 K):  $\delta$  = 3.97 (br, d in the  $^1\text{H}\{^{31}\text{P}\}$  NMR spectrum,  $^3J(\text{H}, \text{H})$  = 12.0 Hz,  $\text{CHC}_6\text{F}_5$ ); 3.10 (br, d in the  $^1\text{H}\{^{31}\text{P}\}$  NMR spectrum,  $^3J(\text{H}, \text{H})$  = 12.0 Hz,  $\text{CHBpin}$ ); -14.87 (dtd,  $^2J(\text{H}, \text{P}_c)$  = 163.0 Hz,  $^2J(\text{H}, \text{P}_a)$  =  $^2J(\text{H}, \text{P}_b)$  = 18.2 Hz,  $^1J(\text{H}, \text{Rh})$  = 5.5 Hz,  $\text{RhH}$ ) ppm.

**$^1\text{H}$ - $^{13}\text{C}$  HMQC NMR** (300.1/75.5 MHz,  $d_8$ -Tol, 213 K)  $\delta$  = 37.4 (m,  $\text{CHC}_6\text{F}_5$ ); 15.8 (m,  $\text{CHBpin}$ ) ppm.

#### Formation of $[\text{Rh}(\text{2-C}_6\text{F}_4\text{CHCH}_2)(\text{PEt}_3)_3]$ (**41**)

In a NMR tube  $[\text{Rh}(\text{H})(\text{PEt}_3)_3]$  (**1**) (36 mg, 0.078 mmol) was dissolved in 0.5 mL of  $d_8$ -toluene. Borylated pentafluorostyrene **46** (34 mg, 0.106 mmol) was added to the solution. After 30 min at room temperature, the NMR spectra revealed a full conversion of complex **1** to give complex **41** as well as another unidentified complex (ratio 13.5:1, based on the  $^{31}\text{P}\{^1\text{H}\}$  NMR spectrum). The  $^{31}\text{P}$  and  $^{19}\text{F}$  NMR data given below were confirmed by simulation using gNMR software.<sup>[164]</sup>

Analytical data for **41**:



**$^{31}\text{P}\{^1\text{H}\}$  NMR** (121.5 MHz,  $d_8$ -Tol):  $\delta = 15.8$  (dtddd,  $^1J(\text{P}_a, \text{Rh}) = 123.3$  Hz,  $^2J(\text{P}_a, \text{P}_b) = 38.0$  Hz,  $^4J(\text{P}_a, \text{F}_2) = 14.6$  Hz,  $^5J(\text{P}_a, \text{F}_5) = 9.8$  Hz,  $^5J(\text{P}_a, \text{F}_3) = 6.6$  Hz,  $\text{P}_a$ ); 10.5 (dd,  $^1J(\text{P}_b, \text{Rh}) = 143.3$  Hz,  $^2J(\text{P}_b, \text{P}_a) = 38.0$  Hz,  $\text{P}_b$ ) ppm.

**$^{19}\text{F}$  NMR** (282.4 MHz,  $d_8$ -Tol):  $\delta = -105.7$  (dq,  $^5J(\text{F}_2, \text{F}_5) = 43.8$  Hz,  $^3J(\text{F}_2, \text{F}_3) \approx ^3J(\text{F}_2, \text{Rh}) \approx ^4J(\text{F}_2, \text{P}_a) = 14.6$  Hz,  $\text{F}_2$ );  $-143.4$  (dddd,  $^3J(\text{F}_3, \text{F}_4) = 20.3$  Hz,  $^3J(\text{F}_3, \text{F}_2) = 14.6$  Hz,  $^5J(\text{F}_3, \text{P}_a) = 6.6$  Hz,  $^4J(\text{F}_3, \text{Rh}) = 4.0$  Hz,  $\text{F}_3$ );  $-160.5$  (dddd,  $^5J(\text{F}_5, \text{F}_2) = 43.8$  Hz,  $^3J(\text{F}_5, \text{F}_4) = 20.3$  Hz,  $^5J(\text{F}_5, \text{P}_a) = 9.8$  Hz,  $^4J(\text{F}_5, \text{Rh}) = 5.2$  Hz,  $\text{F}_5$ );  $-165.7$  (t,  $^3J(\text{F}_4, \text{F}_3) = ^3J(\text{F}_4, \text{F}_5) = 20.3$  Hz,  $\text{F}_4$ ) ppm.

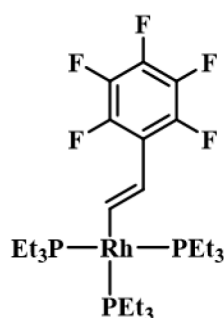
Selected  **$^1\text{H}$  NMR** data (300.1 MHz,  $d_8$ -Tol):  $\delta = 8.16$  (dd,  $^3J(\text{H}, \text{H}) = 18.4$  Hz,  $^3J(\text{H}, \text{H}) = 11.8$  Hz,  $\text{CHC}_6\text{F}_4$ ); 6.38 (d,  $^3J(\text{H}, \text{H}) = 18.1$  Hz,  $\text{CH}_2=\text{CHC}_6\text{F}_4$ ); 5.40 (d,  $^3J(\text{H}, \text{H}) = 11.5$  Hz,  $\text{CH}_2=\text{CHC}_6\text{F}_4$ ) ppm.

**LIFDI-TOF-MS** (Toluene): Calculated ( $m/z$ ) for  $[\text{C}_{26}\text{H}_{48}\text{F}_4\text{P}_3\text{Rh}]^+$ : 632; found: 632.

### Synthesis of $[\text{Rh}(\text{E}-\text{CHCHC}_6\text{F}_5)(\text{PEt}_3)_3]$ (**40**)

In a Schlenk tube  $[\text{Rh}(\text{Me})(\text{PEt}_3)_3]$  (**47**) (44 mg, 0.093 mmol) was dissolved in 0.7 mL of THF. Pentafluorostyrene (14.2  $\mu\text{L}$ , 0.10 mmol) was added to the solution. After 30 min at room temperature the volatiles were removed in vacuum, and complex **40** as a brown oil was obtained. Yield: 87% (54 mg).

Analytical data for **40**:



**$^{31}\text{P}\{^1\text{H}\}$  NMR** (202.5 MHz,  $d_8$ -THF):  $\delta = 19.4$  (dt,  $^1J(\text{P}, \text{Rh}) = 115.7$  Hz,  $^2J(\text{P}, \text{P}) = 36.1$  Hz,  $1\text{P}$ ,  $\text{P}_{\text{trans}}$ ); 16.6 (dd,  $^1J(\text{P}, \text{Rh}) = 156.7$  Hz,  $^2J(\text{P}, \text{P}) = 36.1$  Hz,  $2\text{P}$ ,  $\text{P}_{\text{cis}}$ ) ppm.

**$^{19}\text{F}$  NMR** (282.4 MHz,  $d_8$ -THF):  $\delta = -155.3$  (dm,  $^3J(\text{F}, \text{F}) = 22$  Hz,  $2\text{F}$ ,  $o\text{-F}$ );  $-171.0$  (m,  $2\text{F}$ ,  $m\text{-F}$ );  $-172.1$  (tm,  $^3J(\text{F}, \text{F}) = 22$  Hz,  $1\text{F}$ ,  $p\text{-F}$ ) ppm.



**$^1\text{H}$  NMR** data (300.1 MHz,  $d_8$ -THF):  $\delta$  = 9.18 (dm, d br in the  $^1\text{H}\{^{31}\text{P}\}$  NMR spectrum, dtt in the  $^1\text{H}\{^{19}\text{F}\}$  NMR spectrum,  $^3J(\text{H},\text{H}) = 18.6$  Hz,  $^3J(\text{H},\text{P}_{cis}) = 4.4$  Hz,  $^3J(\text{H},\text{P}_{trans}) \approx ^2J(\text{H},\text{Rh}) = 1.9$  Hz, 1H,  $\text{CHRh}$ ); 6.42 (ddq br, d br in the  $^1\text{H}\{^{31}\text{P}\}$  NMR spectrum, ddq in the  $^1\text{H}\{^{19}\text{F}\}$  NMR spectrum,  $^3J(\text{H},\text{H}) = 18.6$  Hz,  $^3J(\text{H},\text{P}_{trans}) = 6.7$  Hz,  $^3J(\text{H},\text{P}_{cis}) \approx ^2J(\text{H},\text{Rh}) = 1.7$  Hz, 1H,  $\text{CHC}_6\text{F}_5$ ); 1.70-1.53 (m, 18H,  $\text{PCH}_2\text{CH}_3$ ); 1.21-1.05 (m, 27H,  $\text{PCH}_2\text{CH}_3$ ) ppm.

**APT  $^{13}\text{C}$  NMR** (75.5 MHz,  $d_8$ -THF):  $\delta$  = 198.0 (dqm,  $^1J(\text{C},\text{Rh}) = 75.7$  Hz,  $^2J(\text{C},\text{P}) = 27$  Hz,  $\text{RhCH}$ ); 144.3 (dm,  $^1J(\text{C},\text{F}) = 242.7$  Hz,  $o\text{-CF}$ ); 138.7 (dm,  $^1J(\text{C},\text{F}) = 246.9$  Hz,  $m\text{-CF}$ ); 137.3 (dm,  $^1J(\text{C},\text{F}) = 245.1$  Hz,  $p\text{-CF}$ ); 117.4 (m,  $\text{C}_{ipso}\text{F}$ ); 115.7 (s br,  $\text{CHC}_6\text{F}_5$ ); 21.5 (dt,  $^1J(\text{C},\text{P}_{trans}) = 15.8$  Hz,  $^1J(\text{C},\text{P}_{cis}) = 2.9$  Hz,  $\text{P}_{trans}\text{CH}_2\text{CH}_3$ ); 19.1 (t br,  $^1J(\text{C},\text{P}) = 11.5$  Hz,  $\text{P}_{cis}\text{CH}_2\text{CH}_3$ ); 9.7 (s,  $\text{P}_{trans}\text{CH}_2\text{CH}_3$ ); 9.3 (s,  $\text{P}_{cis}\text{CH}_2\text{CH}_3$ ) ppm

**LIFDI-TOF-MS** (Toluene): Calculated ( $m/z$ ) for  $[\text{C}_{26}\text{H}_{47}\text{F}_5\text{P}_3\text{Rh}]^+$ : 650; found: 650.



## 7. Reference

- [1] K. D. Sen, M. C. Böhm, P. C. Schmidt, in *Electronegativity of atoms and molecular fragments*, Vol. 66 (Eds.: K. D. Sen, C. K. Jorgensen), Springer-Verlag Berlin Heidelberg, Berlin, Heidelberg, **1987**, pp. 99-123.
- [2] P. Kirsch, in *Modern Fluoroorganic Chemistry*, **2013**, pp. 1-24.
- [3] P. Jeschke, *ChemBioChem* **2004**, *5*, 570-589
- [4] K. Müller, C. Faeh, F. Diederich, *Science* **2007**, *317*, 1881-1886
- [5] Y. Zhou, J. Wang, Z. Gu, S. Wang, W. Zhu, J. L. Aceña, V. A. Soloshonok, K. Izawa, H. Liu, *Chem. Rev.* **2016**, *116*, 422-518
- [6] M. Jaccaud, R. Faron, D. Devilliers, R. Romano, in *Ullmann's Encyclopedia of Industrial Chemistry*, Weinheim: Wiley-VCH, **2000**, pp. 381-395.
- [7] T. Okazoe, *Proc Jpn Acad Ser B Phys Biol Sci* **2009**, *85*, 276-289
- [8] R. E. Banks, J. C. Tatlow, *J. Fluorine Chem.* **1986**, *33*, 71-108
- [9] J. N. Dahanayake, C. Kasireddy, J. P. Karnes, R. Verma, R. M. Steinert, D. Hildebrandt, O. A. Hull, J. M. Ellis, K. R. Mitchell-Koch, in *Annual Reports on NMR Spectroscopy*, Vol. 93 (Ed.: G. A. Webb), Academic Press, **2018**, pp. 281-365.
- [10] E. P. Gillis, K. J. Eastman, M. D. Hill, D. J. Donnelly, N. A. Meanwell, *J. Med. Chem.* **2015**, *58*, 8315-8359
- [11] J.-D. Hamel, J.-F. Paquin, *Chem. Commun.* **2018**, *54*, 10224-10239
- [12] H. Amii, K. Uneyama, *Chem. Rev.* **2009**, *109*, 2119-2183
- [13] J. E. Huheey, E. A. Keiter, R. L. Keiter, *Inorganic chemistry : principles of structure and reactivity*, HarperCollins College Publishers, New York, NY, **1993**.
- [14] T. Fujita, K. Fuchibe, J. Ichikawa, *Angew. Chem. Int. Ed.* **2019**, *58*, 390-402; *Angew. Chem.* **2019**, *131*, 396-408.
- [15] O. Eisenstein, J. Milani, R. N. Perutz, *Chem. Rev.* **2017**, *117*, 8710-8753
- [16] T. Ahrens, J. Kohlmann, M. Ahrens, T. Braun, *Chem. Rev.* **2015**, *115*, 931-972
- [17] J. Weaver, S. Senaweera, *Tetrahedron* **2014**, *70*, 7413-7428
- [18] J. L. Kiplinger, T. G. Richmond, C. E. Osterberg, *Chem. Rev.* **1994**, *94*, 373-431
- [19] T. Braun, F. Wehmeier, *Eur. J. Inorg. Chem.* **2011**, *2011*, 613-625
- [20] E. Clot, O. Eisenstein, N. Jasim, S. A. Macgregor, J. E. McGrady, R. N. Perutz, *Acc. Chem. Res.* **2011**, *44*, 333-348
- [21] M. Talavera, T. Braun, *Synlett* **2020**
- [22] M. Aizenberg, D. Milstein, *Science* **1994**, *265*, 359-361
- [23] S. T. Belt, M. Helliwell, W. D. Jones, M. G. Partridge, R. N. Perutz, *J. Am. Chem. Soc.* **1993**, *115*, 1429-1440
- [24] M. Ballhorn, M. G. Partridge, R. N. Perutz, M. K. Whittlesey, *Chem. Commun.* **1996**, 961-962
- [25] W. D. Jones, M. G. Partridge, R. N. Perutz, *J. Chem. Soc., Chem. Commun.* **1991**, 264-266
- [26] M. Arisawa, T. Suzuki, T. Ishikawa, M. Yamaguchi, *J. Am. Chem. Soc.* **2008**, *130*, 12214-12215
- [27] D. Noveski, T. Braun, B. Neumann, A. Stammler, H.-G. Stammler, *Dalton Trans.* **2004**, 4106-4119
- [28] R. J. Lindup, T. B. Marder, R. N. Perutz, A. C. Whitwood, *Chem. Commun.* **2007**, 3664-3666
- [29] A. L. Raza, J. A. Panetier, M. Teltewskoi, S. A. Macgregor, T. Braun, *Organometallics* **2013**, *32*, 3795-3807
- [30] M. Teltewskoi, J. A. Panetier, S. A. Macgregor, T. Braun, *Angew. Chem. Int. Ed.* **2010**, *49*, 3947-3951; *Angew. Chem.* **2010**, *122*, 4039-4043.

- [31] M. Schäfer, J. Wolf, H. Werner, *Dalton Trans.* **2005**, 1468-1481
- [32] M. Schäfer, J. Wolf, H. Werner, *Organometallics* **2004**, 23, 5713-5728
- [33] M. J. Cowley, J. M. Lynam, J. M. Slattery, *Dalton Trans.* **2008**, 4552-4554
- [34] J. M. Lynam, *Chem. Eur. J.* **2010**, 16, 8238-8247
- [35] J. Berger, T. Braun, T. Ahrens, P. Kläring, R. Laubenstein, B. Braun-Cula, *Chem. Eur. J.* **2017**, 23, 8886-8900
- [36] J. Kohlmann, T. Braun, R. Laubenstein, R. Herrmann, *Chem. Eur. J.* **2017**, 23, 12218-12232
- [37] L. M. Milner, N. E. Pridmore, A. C. Whitwood, J. M. Lynam, J. M. Slattery, *J. Am. Chem. Soc.* **2015**, 137, 10753-10759
- [38] F. Y. Pétillon, J. L. L. Quéré, F. L. Floch-Pérennou, J. E. Guerchais, M. B. Gomes De Lima, L. Manojlović-Muir, K. W. Muir, D. W. A. Sharp, *J. Organomet. Chem.* **1983**, 255, 231-244
- [39] M. Knorr, I. Jourdain, F. Villafañe, C. Strohmann, *J. Organomet. Chem.* **2005**, 690, 1456-1466
- [40] T. Hanamoto, K. Yamada, *J. Org. Chem.* **2009**, 74, 7559-7561
- [41] J.-C. Kizirian, N. Aiguabella, A. Pesquer, S. Fustero, P. Bello, X. Verdaguer, A. Riera, *Org. Lett.* **2010**, 12, 5620-5623
- [42] T. Konno, K. Moriyasu, R. Kinugawa, T. Ishihara, *Org. Biomol. Chem.* **2010**, 8, 1718-1724
- [43] L. M. Milner, L. M. Hall, N. E. Pridmore, M. K. Skeats, A. C. Whitwood, J. M. Lynam, J. M. Slattery, *Dalton Trans.* **2016**, 45, 1717-1726
- [44] L. Ferrand, Y. Lyu, A. Rivera-Hernández, B. J. Fallon, M. Amatore, C. Aubert, M. Petit, *Synthesis* **2017**, 49, 3895-3904
- [45] K. Nakajima, T. Kato, Y. Nishibayashi, *Org. Lett.* **2017**, 19, 4323-4326
- [46] L. M. Hall, D. P. Tew, N. E. Pridmore, A. C. Whitwood, J. M. Lynam, J. M. Slattery, *Angew. Chem. Int. Ed.* **2017**, 56, 7551-7556; *Angew. Chem.* **2017**, 129, 7659-7664.
- [47] S. Schweizer, C. Tresse, P. Bissleret, J. Lalevée, G. Evano, N. Blanchard, *Org. Lett.* **2015**, 17, 1794-1797
- [48] J. T. Mague, M. O. Nutt, E. H. Gause, *J. Chem. Soc., Dalton Trans.* **1973**, 2578-2587
- [49] C. Sun, P. U. Thakker, L. Khulordava, D. J. Tobben, S. M. Greenstein, D. L. Grisenti, A. G. Kantor, P. S. Wagenknecht, *Inorg. Chem.* **2012**, 51, 10477-10479
- [50] Y. Jiao, J. Morris, W. W. Brennessel, W. D. Jones, *J. Am. Chem. Soc.* **2013**, 135, 16198-16212
- [51] D. Huang, J. C. Bollinger, W. E. Streib, K. Folting, V. Young, O. Eisenstein, K. G. Caulton, *Organometallics* **2000**, 19, 2281-2290
- [52] M. S. Kirkham, M. F. Mahon, M. K. Whittlesey, *Chem. Commun.* **2001**, 813-814
- [53] S. A. Strazisar, P. T. Wolczanski, *J. Am. Chem. Soc.* **2001**, 123, 4728-4740
- [54] L. A. Watson, D. V. Yandulov, K. G. Caulton, *J. Am. Chem. Soc.* **2001**, 123, 603-611
- [55] B. M. Kraft, W. D. Jones, *J. Am. Chem. Soc.* **2002**, 124, 8681-8689
- [56] G. Ferrando-Miguel, H. Gérard, O. Eisenstein, K. G. Caulton, *Inorg. Chem.* **2002**, 41, 6440-6449
- [57] P. L. Watson, T. H. Tulip, I. Williams, *Organometallics* **1990**, 9, 1999-2009
- [58] L. Schwartsburd, M. F. Mahon, R. C. Poulten, M. R. Warren, M. K. Whittlesey, *Organometallics* **2014**, 33, 6165-6170
- [59] T. Braun, D. Noveski, B. Neumann, H.-G. Stammmler, *Angew. Chem. Int. Ed.* **2002**, 41, 2745-2748; *Angew. Chem.* **2002**, 114, 2870-2873.

- [60] N. Bramanathan, M. Carmona, J. P. Lowe, M. F. Mahon, R. C. Poulten, M. K. Whittlesey, *Organometallics* **2014**, 33, 1986-1995
- [61] T. Braun, M. Ahijado Salomon, K. Altenhöner, M. Teltewskoi, S. Hinze, *Angew. Chem. Int. Ed.* **2009**, 48, 1818-1822; *Angew. Chem.* **2009**, 121, 1850-1854.
- [62] G. J. Irvine, M. J. G. Lesley, T. B. Marder, N. C. Norman, C. R. Rice, E. G. Robins, W. R. Roper, G. R. Whittell, L. J. Wright, *Chem. Rev.* **1998**, 98, 2685-2722
- [63] H. Braunschweig, *Angew. Chem. Int. Ed.* **1998**, 37, 1786-1801
- [64] S. Aldridge, D. L. Coombs, *Coord. Chem. Rev.* **2004**, 248, 535-559
- [65] H. Braunschweig, C. Kollann, D. Rais, *Angew. Chem. Int. Ed.* **2006**, 45, 5254-5274; *Angew. Chem.* **2006**, 118, 5380-5400.
- [66] K. Hiromichi, I. Kazushi, N. Yoichiro, *Chem. Lett.* **1975**, 4, 1095-1096
- [67] R. T. Baker, J. C. Calabrese, S. A. Westcott, P. Nguyen, T. B. Marder, *J. Am. Chem. Soc.* **1993**, 115, 4367-4368
- [68] T. B. Marder, N. C. Norman, C. R. Rice, E. G. Robins, *Chem. Commun.* **1997**, 53-54
- [69] K. S. Cook, C. D. Incarvito, C. E. Webster, Y. Fan, M. B. Hall, J. F. Hartwig, *Angew. Chem. Int. Ed.* **2004**, 43, 5474-5477; *Angew. Chem.* **2004**, 116, 5590-5593.
- [70] S. I. Kalläne, PhD thesis, Humboldt Universität zu Berlin (Berlin, Germany), **2014**.
- [71] S. G. Curto, M. A. Esteruelas, M. Oliván, E. Oñate, A. Vélez, *Organometallics* **2018**, 37, 1970-1978
- [72] C. N. von Hahmann, M. Talavera, C. Xu, T. Braun, *Chem. Eur. J.* **2018**, 24, 11131-11138
- [73] S. G. Curto, M. A. Esteruelas, M. Oliván, E. Oñate, *Organometallics* **2019**, 38, 2062-2074
- [74] W. Clegg, F. J. Lawlor, T. B. Marder, P. Nguyen, N. C. Norman, A. Guy Orpen, M. J. Quayle, C. R. Rice, E. G. Robins, A. J. Scott, F. E. S. Souza, G. Stringer, G. R. Whittell, *J. Chem. Soc., Dalton Trans.* **1998**, 301-310
- [75] S. J. Geier, C. M. Vogels, S. A. Westcott, in *Boron Reagents in Synthesis*, Vol. 1236, American Chemical Society, **2016**, pp. 209-225.
- [76] A. Suzuki, *Heterocycles* **2010**, 80, 15-43
- [77] C. M. Crudden, B. W. Glasspoole, C. J. Lata, *Chem. Commun.* **2009**, 6704-6716
- [78] A. J. J. Lennox, G. C. Lloyd-Jones, *Chem. Soc. Rev.* **2014**, 43, 412-443
- [79] J. R. Coombs, J. P. Morken, *Angew. Chem. Int. Ed.* **2016**, 55, 2636-2649; *Angew. Chem.* **2016**, 128, 2682-2696.
- [80] M. Zaidlewicz, in *Kirk-Othmer Encyclopedia of Chemical Technology*, Vol. 13, **2005**, pp. 631-684.
- [81] H. C. Brown, *Hydroboration*, W. A. Benjamin Inc., New York, **1962**.
- [82] H. C. Brown, G. Zweifel, *J. Am. Chem. Soc.* **1960**, 82, 4708-4712
- [83] H. DeFrancesco, J. Dudley, A. Coca, in *Boron Reagents in Synthesis*, Vol. 1236, American Chemical Society, **2016**, pp. 1-25.
- [84] D. T. Hurd, *J. Am. Chem. Soc.* **1948**, 70, 2053-2055
- [85] K. Burgess, M. J. Ohlmeyer, *Chem. Rev.* **1991**, 91, 1179-1191
- [86] J. V. Obligation, P. J. Chirik, *Nat. Rev. Chem.* **2018**, 2, 15-34
- [87] R. Wilczynski, L. G. Sneddon, *J. Am. Chem. Soc.* **1980**, 102, 2857-2858
- [88] J. D. Hewes, C. W. Kreimendahl, T. B. Marder, M. F. Hawthorne, *J. Am. Chem. Soc.* **1984**, 106, 5757-5759
- [89] I. Beletskaya, A. Pelter, *Tetrahedron* **1997**, 53, 4957-5026
- [90] D. Männig, H. Nöth, *Angewandte Chemie International Edition in English* **1985**, 24, 878-879; *Angew. Chem.* **1985**, 97, 854-855.

- [91] C. M. Crudden, Y. B. Hleba, A. C. Chen, *J. Am. Chem. Soc.* **2004**, *126*, 9200-9201
- [92] H. Yoshida, *ACS Catal.* **2016**, *6*, 1799-1811
- [93] K. Wang, R. W. Bates, *Synthesis* **2017**, *49*, 2749-2752
- [94] H. Ben-Daat, C. L. Rock, M. Flores, T. L. Groy, A. C. Bowman, R. J. Trovitch, *Chem. Commun.* **2017**, *53*, 7333-7336
- [95] T. Konno, J. Chae, T. Tanaka, T. Ishihara, H. Yamanaka, *J. Fluorine Chem.* **2006**, *127*, 36-43
- [96] T. Ishiyama, N. Matsuda, N. Miyaoura, A. Suzuki, *J. Am. Chem. Soc.* **1993**, *115*, 11018-11019
- [97] C. N. Iverson, M. R. Smith, *J. Am. Chem. Soc.* **1995**, *117*, 4403-4404
- [98] C. N. Iverson, M. R. Smith, *Organometallics* **1996**, *15*, 5155-5165
- [99] J. B. Morgan, S. P. Miller, J. P. Morken, *J. Am. Chem. Soc.* **2003**, *125*, 8702-8703
- [100] S. Trudeau, J. B. Morgan, M. Shrestha, J. P. Morken, *J. Org. Chem.* **2005**, *70*, 9538-9544
- [101] F. Zhao, X. Jia, P. Li, J. Zhao, Y. Zhou, J. Wang, H. Liu, *Org. Chem. Front.* **2017**, *4*, 2235-2255
- [102] P. Nguyen, G. Lesley, N. J. Taylor, T. B. Marder, N. L. Pickett, W. Clegg, M. R. J. Elsegood, N. C. Norman, *Inorg. Chem.* **1994**, *33*, 4623-4624
- [103] R. T. Baker, P. Nguyen, T. B. Marder, S. A. Westcott, *Angewandte Chemie International Edition in English* **1995**, *34*, 1336-1338; *Angew. Chem.* **1995**, *107*, 1451-1452.
- [104] C. Dai, T. B. Marder, E. G. Robins, D. S. Yufit, J. A. K. Howard, T. B. Marder, A. J. Scott, W. Clegg, *Chem. Commun.* **1998**, 1983-1984
- [105] P. Nguyen, R. B. Coapes, A. D. Woodward, N. J. Taylor, J. M. Burke, J. A. K. Howard, T. B. Marder, *J. Organomet. Chem.* **2002**, *652*, 77-85
- [106] H. Chen, S. Schlecht, T. C. Semple, J. F. Hartwig, *Science* **2000**, *287*, 1995-1997
- [107] J. M. Murphy, J. D. Lawrence, K. Kawamura, C. Incarvito, J. F. Hartwig, *J. Am. Chem. Soc.* **2006**, *128*, 13684-13685
- [108] N. R. Council, *Climate Intervention: Reflecting Sunlight to Cool Earth*, The National Academies Press, Washington, DC, **2015**.
- [109] N. R. Council, *Climate Intervention: Carbon Dioxide Removal and Reliable Sequestration*, The National Academies Press, Washington, DC, **2015**.
- [110] B. O. Bolaji, Z. Huan, *Renew. Sust. Energ. Rev.* **2013**, *18*, 49-54
- [111] P. Arora, A. Tyagi, G. Seshadri, *Curr. Sci.* **2018**, *115*, 1497-1503
- [112] I. V. Stepanov, A. I. Burmakov, B. V. Kunshenko, L. A. Alekseeva, L. M. Yagupo'skii, *J. Org. Chem. USSR (Engl. Trans.)* **1983**, *19*, 244-248
- [113] V. Montanari, D. D. DesMarteau, *J. Org. Chem.* **1992**, *57*, 5018-5019
- [114] R. Eric Banks, M. G. Barlow, M. Nickkho-Amiry, *J. Fluorine Chem.* **1997**, *82*, 171-174
- [115] V. N. M. Rao, A. C. Sievert, M. J. Nappa (E. I. du Pont de Nemours and Company, USA), WO 2008030440, **2008**.
- [116] Y. Li, D.-H. Tu, Y.-J. Gu, B. Wang, Y.-Y. Wang, Z.-T. Liu, Z.-W. Liu, J. Lu, *Eur. J. Org. Chem.* **2015**, *2015*, 4340-4343
- [117] H. Sakaguchi, Y. Uetake, M. Ohashi, T. Niwa, S. Ogoshi, T. Hosoya, *J. Am. Chem. Soc.* **2017**, *139*, 12855-12862
- [118] G. Meißner, K. Kretschmar, T. Braun, E. Kemnitz, *Angew. Chem. Int. Ed.* **2017**, *56*, 16338-16341; *Angew. Chem.* **2017**, *129*, 16556-16559.
- [119] C. Bakewell, A. J. P. White, M. R. Crimmin, *Angew. Chem. Int. Ed.* **2018**, *57*, 6638-6642; *Angew. Chem.* **2018**, *130*, 6748-6752.

- [120] M. Talavera, C. N. von Hahmann, R. Müller, M. Ahrens, M. Kaupp, T. Braun, *Angew. Chem. Int. Ed.* **2019**, 58, 10688-10692; *Angew. Chem.* **2019**, 131, 10798–10802.
- [121] R. N. Haszeldine, *J. Chem. Soc.* **1952**, 3490-3498
- [122] B. M. Kraft, R. J. Lachicotte, W. D. Jones, *J. Am. Chem. Soc.* **2001**, 123, 10973-10979
- [123] J. Burdon, L. Garnier, R. L. Powell, *J. Chem. Soc., Perkin Trans. 2* **1996**, 625-631
- [124] M. Hanack, J. Ullmann, *J. Org. Chem.* **1989**, 54, 1432-1435
- [125] M. K. Whittlesey, E. Peris, *ACS Catal.* **2014**, 4, 3152-3159
- [126] R. Kojima, K. Kubota, H. Ito, *Chem. Commun.* **2017**, 53, 10688-10691
- [127] M. Teltewskoi, S. I. Kalläne, T. Braun, R. Herrmann, *Eur. J. Inorg. Chem.* **2013**, 2013, 5762-5768
- [128] S. I. Kalläne, T. Braun, *Angew. Chem. Int. Ed.* **2014**, 53, 9311-9315; *Angew. Chem.*, **2014**, 126, 9465-9469.
- [129] S. I. Kalläne, M. Teltewskoi, T. Braun, B. Braun, *Organometallics* **2015**, 34, 1156-1169
- [130] Honeywell, "Solstice® ze Refrigerant (HFO-1234ze)", can be found under <https://www.fluorineproducts-honeywell.com/refrigerants/wp-content/uploads/2017/03/Solstice-ze-hfo-1234ze-brochure.pdf> (accessed: 11.03.2020).
- [131] H. Lu, H. B. Friedrich, D. J. Burton, *J. Fluorine Chem.* **1995**, 75, 83-86
- [132] M. F. Kühnel, D. Lentz, *Dalton Trans.* **2009**, 4747-4755
- [133] A. D. Jaeger, R. Walter, C. Ehm, D. Lentz, *Chem. Asian J.* **2018**, 13, 2908-2915
- [134] H. Mizuno, J. Takaya, N. Iwasawa, *J. Am. Chem. Soc.* **2011**, 133, 1251-1253
- [135] P. Tomar, T. Braun, E. Kemnitz, *Chem. Commun.* **2018**, 54, 9753-9756
- [136] S. A. Westcott, H. P. Blom, T. B. Marder, R. T. Baker, *J. Am. Chem. Soc.* **1992**, 114, 8863-8869
- [137] S. A. Westcott, T. B. Marder, R. T. Baker, *Organometallics* **1993**, 12, 975-979
- [138] A. D. Ibrahim, S. W. Entsminger, A. R. Fout, *ACS Catal.* **2017**, 7, 3730-3734
- [139] J.-F. Li, Z.-Z. Wei, Y.-Q. Wang, M. Ye, *Green Chem.* **2017**, 19, 4498-4502
- [140] SciFinder, can be found under <https://scifinder.cas.org/scifinder/view/scifinder/scifinderExplore.jsf> (accessed: 12.03.2020).
- [141] V. F. Cardoso, D. M. Correia, C. Ribeiro, M. M. Fernandes, S. Lanceros-Méndez, *Polymers* **2018**, 10, 161
- [142] M. Ohashi, H. Shirataki, K. Kikushima, S. Ogoshi, *J. Am. Chem. Soc.* **2015**, 137, 6496-6499
- [143] T. Kawashima, M. Ohashi, S. Ogoshi, *J. Am. Chem. Soc.* **2018**, 140, 17423-17427
- [144] M. Ohashi, R. Kamura, R. Doi, S. Ogoshi, *Chem. Lett.* **2013**, 42, 933-935
- [145] S. P. Diefenbach US 4704377, **1987**.
- [146] M. F. Kuehnel, P. Holstein, M. Kliche, J. Krüger, S. Matthies, D. Nitsch, J. Schutt, M. Sparenberg, D. Lentz, *Chem. Eur. J.* **2012**, 18, 10701-10714
- [147] C. S. Cundy, M. Green, F. G. A. Stone, *J. Chem. Soc. A* **1970**, 1647-1653
- [148] K. A. Giffin, L. A. Pua, S. Piotrkowski, B. M. Gabidullin, I. Korobkov, R. P. Hughes, R. T. Baker, *J. Am. Chem. Soc.* **2017**, 139, 4075-4086
- [149] J. Browning, C. S. Cundy, M. Green, F. G. A. Stone, *J. Chem. Soc. A* **1969**, 20-23
- [150] M. E. Slaney, M. J. Ferguson, R. McDonald, M. Cowie, *Organometallics* **2012**, 31, 1384-1396
- [151] M. Tamura, H.-d. Quan, A. Sekiya, *Eur. J. Org. Chem.* **1999**, 1999, 3151-3153

- [152] D. J. Blair, C. J. Fletcher, K. M. P. Wheelhouse, V. K. Aggarwal, *Angew. Chem. Int. Ed.* **2014**, *53*, 5552-5555; *Angew. Chem.* **2014**, *126*, 5658-5661.
- [153] N.-C. Yang, T.-C. Shieh, E. D. Feit, C. L. Chernick, *J. Org. Chem.* **1970**, *35*, 4020-4024
- [154] K. Endo, M. Hirokami, T. Shibata, *J. Org. Chem.* **2010**, *75*, 3469-3472
- [155] N. A. Phillips, A. J. P. White, M. R. Crimmin, *Adv. Synth. Catal.* **2019**, *361*, 3351-3358
- [156] X.-B. Li, Z.-F. Xu, L.-J. Liu, J.-T. Liu, *Eur. J. Org. Chem.* **2014**, *2014*, 1182-1188
- [157] D. A. Ellis, K. A. Denkenberger, T. E. Burrow, S. A. Mabury, *J. Phys. Chem. A* **2004**, *108*, 10099-10106
- [158] R. W. Cockman, E. A. V. Ebsworth, J. H. Holloway, *J. Am. Chem. Soc.* **1987**, *109*, 2194-2195
- [159] A. Conkie, E. A. V. Ebsworth, R. A. Mayo, S. Moreton, *J. Chem. Soc., Dalton Trans.* **1992**, 2951-2954
- [160] R. P. Hughes, P. R. Rose, A. L. Rheingold, *Organometallics* **1993**, *12*, 3109-3117
- [161] T. Ahrens, M. Ahrens, T. Braun, B. Braun, R. Herrmann, *Dalton Trans.* **2016**, *45*, 4716-4728
- [162] T. Ahrens, M. Teltewskoi, M. Ahrens, T. Braun, R. Laubenstein, *Dalton Trans.* **2016**, *45*, 17495-17507
- [163] M. Talavera, R. Müller, T. Ahrens, C. N. von Hahmann, B. Braun-Cula, M. Kaupp, T. Braun, *Faraday Discuss.* **2019**, *220*, 328-349
- [164] P. H. M. Budzelaar, gNMR, Version 4.1, Adept Scientific plc, Letchworth, 2001
- [165] C. Xu, M. Talavera, S. Sander, T. Braun, *Dalton Trans.* **2019**, *48*, 16258-16267
- [166] G. Meier, T. Braun, *Angew. Chem. Int. Ed.* **2011**, *50*, 3280-3284; *Angew. Chem.* **2011**, *123*, 3338-3342.
- [167] D. Noveski, T. Braun, S. Krückemeier, *J. Fluorine Chem.* **2004**, *125*, 959-966
- [168] Z. Li, T. W. Yokley, S. L. Tran, J. Zong, N. D. Schley, T. P. Brewster, *Dalton Trans.* **2019**, *48*, 8782-8790
- [169] S. I. Källäne, T. Braun, M. Teltewskoi, B. Braun, R. Herrmann, R. Laubenstein, *Chem. Commun.* **2015**, *51*, 14613-14616
- [170] G. P. Ford, *Correl. Anal. Chem.: Recent Adv.* **1978**, 269-311
- [171] D. F. Harvey, E. M. Grenzer, P. K. Gantzel, *J. Am. Chem. Soc.* **1994**, *116*, 6719-6732
- [172] B. M. Schmidt, D. Lentz, *Chem. Lett.* **2014**, *43*, 171-177
- [173] G. S. Remya, C. H. Suresh, *Phys. Chem. Chem. Phys.* **2016**, *18*, 20615-20626
- [174] T. Fuchikami, M. Yatabe, I. Ojima, *Synthesis* **1981**, *1981*, 365-366
- [175] H. Li, K.-H. He, J. Liu, B.-Q. Wang, K.-Q. Zhao, P. Hu, Z.-J. Shi, *Chem. Commun.* **2012**, *48*, 7028-7030
- [176] J. P. Collman, Z. Wang, A. Straumanis, M. Quelquejeu, E. Rose, *J. Am. Chem. Soc.* **1999**, *121*, 460-461
- [177] A. T. Normand, C. G. Daniliuc, B. Wibbeling, G. Kehr, P. Le Gendre, G. Erker, *J. Am. Chem. Soc.* **2015**, *137*, 10796-10808
- [178] X. Xu, G. Kehr, C. G. Daniliuc, G. Erker, *J. Am. Chem. Soc.* **2015**, *137*, 4550-4557
- [179] I. Ojima, K. Kato, M. Okabe, T. Fuchikami, *J. Am. Chem. Soc.* **1987**, *109*, 7714-7720
- [180] H. C. Brown, G.-M. Chen, M. P. Jennings, P. V. Ramachandran, *Angew. Chem. Int. Ed.* **1999**, *38*, 2052-2054
- [181] P. V. Ramachandran, M. P. Jennings, H. C. Brown, *Org. Lett.* **1999**, *1*, 1399-1402
- [182] A. M. Segarra, C. Claver, E. Fernandez, *Chem. Commun.* **2004**, 464-465
- [183] A. Black, J. M. Brown, C. Pichon, *Chem. Commun.* **2005**, 5284-5286



- [184] D. I. McIsaac, S. J. Geier, C. M. Vogels, A. Decken, S. A. Westcott, *Inorg. Chim. Acta* **2006**, 359, 2771-2779
- [185] P. V. Ramachandran, M. P. Jennings, *J. Fluorine Chem.* **2007**, 128, 827-831
- [186] S. Kisan, V. Krishnakumar, C. Gunanathan, *ACS Catal.* **2017**, 7, 5950-5954
- [187] R. Xu, G.-p. Lu, C. Cai, *New J. Chem.* **2018**, 42, 16456-16459
- [188] W. A. Herrmann, S. J. Eder, *Chem. Ber.* **1993**, 126, 31-37
- [189] L. Cronin, C. L. Higgitt, R. Karch, R. N. Perutz, *Organometallics* **1997**, 16, 4920-4928
- [190] Y. Sun, H. Sun, J. Jia, A. Du, X. Li, *Organometallics* **2014**, 33, 1079-1081
- [191] M. Kidwai, P. Mothra, *Indian J. Chem., Sect B* **2006**, 45B, 2330-2336
- [192] P. T. Anastas, J. C. Warner, *Green Chemistry: Theory and Practice*, Oxford University Press, Oxford, **1998**.
- [193] K. Burgess, W. A. Van der Donk, S. A. Westcott, T. B. Marder, R. T. Baker, J. C. Calabrese, *J. Am. Chem. Soc.* **1992**, 114, 9350-9359
- [194] X. He, J. F. Hartwig, *J. Am. Chem. Soc.* **1996**, 118, 1696-1702
- [195] T. G. Appleton, H. C. Clark, L. E. Manzer, *Coord. Chem. Rev.* **1973**, 10, 335-422
- [196] B. J. Coe, S. J. Glenwright, *Coord. Chem. Rev.* **2000**, 203, 5-80
- [197] J. A. Hatnean, M. Shoshani, S. A. Johnson, *Inorg. Chim. Acta* **2014**, 422, 86-94
- [198] M. W. Drover, L. L. Schafer, J. A. Love, *Dalton Trans.* **2015**, 44, 19487-19493
- [199] T. Piou, F. Romanov-Michailidis, M. Romanova-Michaelides, K. E. Jackson, N. Semakul, T. D. Taggart, B. S. Newell, C. D. Rithner, R. S. Paton, T. Rovis, *J. Am. Chem. Soc.* **2017**, 139, 1296-1310
- [200] S. A. Johnson, E. T. Taylor, S. J. Cruise, *Organometallics* **2009**, 28, 3842-3855
- [201] B. Procacci, Y. Jiao, M. E. Evans, W. D. Jones, R. N. Perutz, A. C. Whitwood, *J. Am. Chem. Soc.* **2015**, 137, 1258-1272
- [202] H. Baumgarth, G. Meier, T. Braun, B. Braun-Cula, *Eur. J. Inorg. Chem.* **2016**, 2016, 4565-4572
- [203] N. Pfister, T. Braun, P. Wittwer, M. Ahrens, *Z. Anorg. Allg. Chem.* **2018**, 644, 1064-1070
- [204] M. Wozniak, T. Braun, M. Ahrens, B. Braun-Cula, P. Wittwer, R. Herrmann, R. Laubenstein, *Organometallics* **2018**, 37, 821-828
- [205] J. Cámpora, P. Palma, E. Carmona, *Coord. Chem. Rev.* **1999**, 193-195, 207-281
- [206] J. Cámpora, J. A. López, P. Palma, D. del Rio, E. Carmona, P. Valerga, C. Graiff, A. Tiripicchio, *Inorg. Chem.* **2001**, 40, 4116-4126
- [207] J. Cámpora, M. a. del Mar Conejo, K. Mereiter, P. Palma, C. Pérez, M. L. Reyes, C. Ruiz, *J. Organomet. Chem.* **2003**, 683, 220-239
- [208] J. K. MacDougall, M. C. Simpson, M. J. Green, D. J. Cole-Hamilton, *J. Chem. Soc., Dalton Trans.* **1996**, 1161-1172
- [209] S. I. Kalläne, T. Braun, B. Braun, S. Mebs, *Dalton Trans.* **2014**, 43, 6786-6801
- [210] J. Rankin, A. C. Benyei, D. J. Cole-Hamilton, A. D. Poole, *Chem. Commun.* **1997**, 1835-1836
- [211] A. L. Raza, T. Braun, *Chem. Sci.* **2015**, 6, 4255-4260
- [212] T. Braun, J. Izundu, A. Steffen, B. Neumann, H.-G. Stammer, *Dalton Trans.* **2006**, 5118-5123
- [213] X. Zhang, S. Fan, C.-Y. He, X. Wan, Q.-Q. Min, J. Yang, Z.-X. Jiang, *J. Am. Chem. Soc.* **2010**, 132, 4506-4507
- [214] A. Singh, C. J. Fennell, J. D. Weaver, *Chem. Sci.* **2016**, 7, 6796-6802
- [215] G. He, S. Chen, Q. Wang, H. Huang, Q. Zhang, D. Zhang, R. Zhang, H. Zhu, *Org. Biomol. Chem.* **2014**, 12, 5945-5953
- [216] T. Beweries, L. Brammer, N. A. Jasim, J. E. McGrady, R. N. Perutz, A. C. Whitwood, *J. Am. Chem. Soc.* **2011**, 133, 14338-14348

- [217] Z. Chen, C.-Y. He, Z. Yin, L. Chen, Y. He, X. Zhang, *Angew. Chem. Int. Ed.* **2013**, 52, 5813-5817; *Angew. Chem.* **2013**, 125, 5925-5929.
- [218] P. Zhao, J. F. Hartwig, *Organometallics* **2008**, 27, 4749-4757
- [219] T. Braun, D. Noveski, M. Ahijado, F. Wehmeier, *Dalton Trans.* **2007**, 3820-3825
- [220] R. T. Price, R. A. Andersen, E. L. Muetterties, *J. Organomet. Chem.* **1989**, 376, 407-417
- [221] G. W. T. M. J. Frisch, H. B. Schlegel, G. E. Scuseria, M. A. Robb, J. R. Cheeseman, G. Scalmani, V. Barone, G. A. Petersson, H. Nakatsuji, X. Li, M. Caricato, A. Marenich, J. Bloino, B. G. Janesko, R. Gomperts, B. Mennucci, H. P. Hratchian, J. V. Ortiz, A. F. Izmaylov, J. L. Sonnenberg, D. Williams-Young, F. Ding, F. Lipparini, F. Egidi, J. Goings, B. Peng, A. Petrone, T. Henderson, D. Ranasinghe, V. G. Zakrzewski, J. Gao, N. Rega, G. Zheng, W. Liang, M. Hada, M. Ehara, K. Toyota, R. Fukuda, J. Hasegawa, M. Ishida, T. Nakajima, Y. Honda, O. Kitao, H. Nakai, T. Vreven, K. Throssell, J. A. Montgomery, Jr., J. E. Peralta, F. Ogliaro, M. Bearpark, J. J. Heyd, E. Brothers, K. N. Kudin, V. N. Staroverov, T. Keith, R. Kobayashi, J. Normand, K. Raghavachari, A. Rendell, J. C. Burant, S. S. Iyengar, J. Tomasi, M. Cossi, J. M. Millam, M. Klene, C. Adamo, R. Cammi, J. W. Ochterski, R. L. Martin, K. Morokuma, O. Farkas, J. B. Foresman, and D. J. Fox, Gaussian 09, Revision D.01, Gaussian, Inc., Wallingford CT, 2016
- [222] D. Andrae, U. Häußermann, M. Dolg, H. Stoll, H. Preuß, *Theor. Chim. Acta* **1990**, 77, 123-141
- [223] F. Weigend, R. Ahlrichs, *Phys. Chem. Chem. Phys.* **2005**, 7, 3297-3305
- [224] S. Grimme, J. Antony, S. Ehrlich, H. Krieg, *J. Chem. Phys.* **2010**, 132, 154104
- [225] S. Grimme, S. Ehrlich, L. Goerigk, *J. Comput. Chem.* **2011**, 32, 1456-1465
- [226] G. M. Sheldrick, SHELXT-2014, Program for the Solution of Crystal Structures from X-Ray Data, University of Göttingen, Göttingen (Germany), 2013
- [227] G. M. Sheldrick, SHELXL-2013, Program for the Refinement of Crystal Structures from X-Ray Data, University of Göttingen, Göttingen (Germany), 2013
- [228] G. M. Sheldrick, SADABS, Program for Empirical Absorption Correction of Area Detector Data, University of Göttingen, Göttingen (Germany), 1996

## 8. Appendix

### 8.1 Abbreviations

Å	Angstrom ( $10^{-10}$ m)
Atm	Standard atmosphere
Bcat	1,3,2-benzodioxaboryl
Bpin	4,4,5,5-tetramethyl-1,3,2-dioxaboryl
br	Broad
Bu	Butyl
$\delta$	Chemical shift (ppm)
cat*	Cat-4- <i>t</i> Bu
cod	1,5-cyclooctadiene
COSY	Homonuclear correlation spectroscopy
Cp*	Pentamethylcyclopentadiene
Cy	Cyclohexyl
d	Day (s) (time); doublet (NMR)
depm	Bis(diethylphosphino)methane
DFT	Density functional theory
dppb	1,4-bis(diphenylphosphino)butane
$\eta^n$	hapticity of ligand with n as the number of coordinating atoms
Et	Ethyl
eq	Equivalents
h	Hour
GC	Gas chromatography
GWP	Global warming potential
HFC	Hydrofluorocarbon
HFO	Hydrofluoroolefin
HMBC	Heteronuclear multiple bond correlation spectroscopy
HMQC	Heteronuclear multiple quantum correlation spectroscopy
IMes	1,3-dimesitylimidazol-2-ylidene
IPr	1,3-bis(2,6-diisopropylphenyl)imidazol-2-ylidene
IR	Infrared spectroscopy
<i>i</i>	<i>iso</i>
<i>J</i>	Coupling constant (Hz)
K	Kelvin (temperature)

kJ/mol	Kilojoule per mole
LIFDI	Liquid injection field desorption ionization
m	Multiplet (NMR)
[M] <sup>+</sup>	Molecular ion peak
<i>m/z</i>	Mass-to-charge ratio
Me	Methyl
mg	Milligram
ml	Milliliter
mmol	Millimole
MHz	Megahertz
min	Minute
MS	Mass spectroscopy
6-NHC	1,3-dialkyltetrahydropyrimidin-2-ylidene; alkyl = Me, Et, <i>i</i> Pr
NMR	Nuclear magnetic resonance
$\tilde{\nu}$	Wavenumber (cm <sup>-1</sup> )
ODP	Ozone depletion potential
Ph	Phenyl
PFA	Perfluoroalkoxy alkanes
pm	Picometer
ppm	Part per million
Pr	Propyl
PTFE	Polytetrafluoroethylene
q	Quartet
rt	Room temperature
s	Singlet (NMR)
<i>t</i>	<i>tert</i>
t	triplet
THF	Tetrahydrofuran
Tol	Tolyl
Tp'	Tris-(3,5-dimethylpyrazolyl)borate

## 8.2 Data for *mer*-[Rh(F)(CH<sub>2</sub>CH<sub>2</sub>(2-C<sub>6</sub>F<sub>4</sub>))(PEt<sub>3</sub>)<sub>3</sub>] (39)

Crystal data and structural refinement details for complex **39** are given in the table below. CCDC 1956127 contains the crystallographic data.

Crystal data and structure refinement for complex **39**

Empirical formula	C <sub>26</sub> H <sub>49</sub> F <sub>5</sub> P <sub>3</sub> Rh
Formula weight	652.47
Temperature	100(2) K
Wavelength	0.71073 Å
Crystal system	Orthorhombic
Space group	Pbca
Unit cell dimensions	a = 19.5336(18) Å b = 13.3846(12) Å c = 22.1579(19) Å
Volume	5793.2(9) Å <sup>3</sup>
Z	8
Density (calculated)	1.496 Mg/m <sup>3</sup>
Absorption coefficient	0.802 mm <sup>-1</sup>
F(000)	2720
Crystal size	0.320 x 0.284 x 0.217 mm <sup>3</sup>
Theta range for data collection	2.582 to 26.434°.
Index ranges	-24 ≤ h ≤ 24, -16 ≤ k ≤ 16, -27 ≤ l ≤ 27
Reflections collected	222646
Independent reflections	5956 [R(int) = 0.0554]
Completeness to theta = 25.242°	99.9 %
Absorption correction	Semi-empirical from equivalents
Max. and min. transmission	0.7454 and 0.6695
Refinement method	Full-matrix least-squares on F <sup>2</sup>
Data / restraints / parameters	5956 / 0 / 325
Goodness-of-fit on F <sup>2</sup>	1.050
Final R indices [I > 2σ(I)]	R1 = 0.0199, wR2 = 0.0426
R indices (all data)	R1 = 0.0256, wR2 = 0.0446
Largest diff. peak and hole	0.395 and -0.339 e.Å <sup>-3</sup>

## 8.3 Selbstständigkeitserklärung

Ich erkläre, dass ich die Dissertation selbstständig und nur unter Verwendung der von mir gemäß § 7 Abs. 3 der Promotionsordnung der Mathematisch-Naturwissenschaftlichen Fakultät, veröffentlicht im Amtlichen Mitteilungsblatt der Humboldt-Universität zu Berlin Nr. 42/2018 am 11.07.2018, angegebenen Hilfsmittel angefertigt habe.

Berlin, den 28.07.2020

.....

Conghui Xu

## 8.4 List of figures of all complexes

